

# **Hydrothermal Processing of Microalgae**

Patrick Biller

Submitted in accordance with the requirements for the degree of

Doctor of Philosophy

The University of Leeds

Energy Research Institute

April 2013



The candidate confirms that the work submitted is his own, except where work which has formed part of jointly-authored publications has been included. The contribution of the candidate and the other authors to this work has been explicitly indicated below. The candidate confirms that appropriate credit has been given within the thesis where reference has been made to the work of others.

Following jointly authored publications are part of the thesis:

1. Biller, P., Ross, A.B. 2012. Hydrothermal processing of algal biomass for the production of biofuels and chemicals. *Biofuels*, 3(5), 603-623.
2. Ross, A.B., Biller P., Kubaki, M.L., Lea-Langton, A., Jones, J.M. Hydrothermal processing of microalgae using alkali and organic acids. *Fuel*, 2010. 89(9): p. 2234-2243.
3. Biller, P., R. Riley, and A.B. Ross, Catalytic hydrothermal processing of microalgae; Decomposition and upgrading of lipids. *Bioresource Technology* 102(7): 4841-4848.
4. Biller, P. and A.B. Ross, Potential yields and properties of oil from the hydrothermal liquefaction of microalgae with different biochemical content. *Bioresource Technology*, 2011. 102(1): p. 215-225.
5. Biller, P., Ross, A.B., Skill, S.C., Lea-Langton, A., Balasundaram, B., Hall, C., Riley, R., Llewellyn, C.A. 2012. Nutrient recycling of aqueous phase for microalgae cultivation from the hydrothermal liquefaction process. *Algal Research*, 1(1), 70-76.
6. Biller, P., Friedman, C., Ross, A.B., Hydrothermal microwave processing of microalgae as a pre-treatment and extraction technique for bio-fuels and bio-products. *Bioresource Technology*, 2013. 136, 188-195

Details of contributions from the candidate and co-authors are listed below:

1. The candidate wrote the review and his supervisor Dr. Ross contributed with comments, guidance and proof reading.
2. The candidate performed the majority of the experimental work. Dr. Ross performed the majority of the write up. Lea-Langton and Kubaki performed some experiments which were included. Prof. Jones proof read.
3. The candidate performed all the experiments, analysis and write up. Riley was a MEng student helping in the laboratory with analysis. Dr. Ross contributed with comments, guidance and proof reading.

4. The candidate performed all the experiments, analysis and write up. Dr. Ross contributed with comments, guidance and proof reading.
5. The candidate performed the majority of the experiments, analysis and write up. Dr. Ross contributed with comments, guidance and proof reading. Skill, Llewellyn and Balasundaram performed some experiments, proof read and provided guidance and comments throughout the course of the work.
6. C. Friedman helped with experimental work in the laboratory during her MEng project. The candidate performed the majority of the experimental and analytical work and write up. Dr. Ross contributed with comments, guidance and proof reading.

This copy has been supplied on the understanding that it is copyright material and that no quotation from the thesis may be published without proper acknowledgement.

## I. ACKNOWLEDGMENTS

First and foremost I would like to thank my supervisor Andy Ross for the guidance and support he provided throughout the course of this work. Andy was a great supervisor and I am very grateful for all the hard work and guidance he has provided throughout my PhD! I would also like to thank my co-supervisors Jenny Jones and Hu Li for their support over the years. I would especially like to thank our technician Simon Lloyd who was always there to help me with any query I had. This work would not have been possible without the help of numerous people in the laboratory and the office. Therefore I would like to thank my colleagues Amanda Lea-Langton, Konstantinos Anastasakis, Abby Saddawi, Gaurav Nahar, Rob Johnson, Adrian Cunliff, Stuart Micklethwaite, Sara Dona, Leilani Darvell, Surjit Singh, Bijal Gudka, Femi Akinrinola, Thomas Robin, Philippa Usher, Ramzi Cherad, Pete Riley, Heather Strachan, Sheilagh Ogden, Dave Haynes, Bob Boreham and Ed Woodhouse. I would also like to thank the Master students Cerri Friedman, Callum Hall and Richard Riley for their excellent work in the laboratory. I would like to express my gratitude to the EPSRC for the PhD scholarship and the WUN network for providing funding to work at the University of Sydney. At this institution I would like to thank my supervisor Brian Haynes and Chris Jazrawi as well as Alejandro Montoya and Sergio Londono. Gratitude is also expressed to the technical staff of the Civil Engineering department of the University of Leeds, Sheena Bennett, Dave Elliot and Karen Stevens. I would also like to thank Steve Skill and Carol Llewellyn from the Plymouth Marine Laboratory. Finally I would like to thank my parents and my brother for the support over the years.

## II. ABSTRACT

Microalgae are regarded as a promising biomass resource for the production of biofuels and chemicals which does not compete with food production. Microalgae contain large amounts of lipids and have faster growth rates than terrestrial biomass. One of the current technological bottlenecks of biofuels conversion is the economic extraction and processing of microalgae components. Due to their aquatic nature microalgae contain large amounts of water when harvested. Hydrothermal liquefaction (HTL) involves processing the algae as a slurry in hot compressed water, avoiding drying of the wet feedstock. This is a major energy benefit compared to dry microalgae processing methods.

A detailed characterisation of the microalgae feedstocks investigated for the current work is provided. The main differences between marine, fresh water and cyanobacteria strains are presented. The microalgae strains are investigated for biochemical composition, proximate and ultimate analysis, thermo-gravimetric analysis, pyrolysis GC-MS, metal content, pigment analysis and by scanning electron microscopy. The results from the characterisation work are employed throughout the thesis for mass balance calculations and investigation of reaction chemistry.

HTL for bio-crude production is investigated both on laboratory batch systems and a continuous pilot scale facility. Processing at mild conditions results in mainly the lipids of microalgae being extracted resulting in a high quality bio-crude. Higher temperatures are shown to result in higher yields of bio-crude as carbohydrates and proteins increasingly contribute to bio-crude formation. This allows processing of low lipid containing microalgae which are associated with higher growth rates. Maximum bio-crude yields of around 50 wt.% can be achieved but can contain significant amounts of nitrogen and oxygen. A total of 11 microalgae strains is investigated leading to an average bio-crude yield of 34 %, a heating value of 36 MJ/kg, a nitrogen content of 4.7 wt.% and an oxygen content of 13.6 wt.%.

The use of homogeneous and heterogeneous catalysts is investigated to increase bio-crude quality and yields. Model compounds of protein, lipid and carbohydrates are processed individually to shed light on the HTL behaviour of microalgae components and the reaction pathways involved in bio-crude formation. The effect of sodium carbonate and formic acid as homogeneous catalysts is investigated on various microalgae strains with changing biochemical composition and on model compounds separately. It is shown that biochemical

components of microalgae behave additively in respect to bio-crude formation. The trends of bio-crude formation follow lipids>protein>carbohydrates. It is further shown that carbohydrates are best processed in alkali conditions while protein and lipids are best processed without the use of catalysts. The same effect is demonstrated for algae high in carbohydrates or proteins and lipids respectively. Heterogeneous catalysts are shown not to increase the bio-crude significantly but result in additional decarboxylation of the bio-crude to reduce the oxygen level by a further 10%.

The process water composition from HTL is investigated for common nutrients required for algae cultivation. It is shown that nutrients are present in higher concentrations than comparable standard algae growth media. The process water also contains large amounts of organic carbon which is considered a loss, unavailable for bio-crude formation. Growth trials in dilutions of the process water to grow fresh algae demonstrate that growth is sustainable. The organic carbon in the process water is shown to act as a substrate for mixotrophic growth resulting in increased growth rates and carbon efficiency.

For analysis of the algae obtained from small scale growth trials a new analysis technique for microalgae composition analysis is introduced. This involves Py-GC-MS of model compounds and comparisons to algae pyrolysis products. Promising results are presented, showing the feasibility of detecting protein, carbohydrate and lipid levels of microalgae directly from growth cultures. Additionally the methodology is expanded to detect phytochemical concentrations such as astaxanthin and chlorophyll *a*.

An alternative to direct hydrothermal liquefaction involving removal of valuable compounds from microalgae by hydrothermal microwave processing (HMP) is investigated. HMP is shown to remove protein and large amounts of nutrients from the algae biomass which could be used as a source of nutrients for microalgae cultivation. The cells walls are shown to be disrupted, leading to increased recovery of lipids by solvent extraction while the lipids' degree of saturation is not affected. This allows effective extraction of high value poly-unsaturated fatty acids. The residue from HMP is processed using flash pyrolysis and HTL for bio-crude production. The results show that bio-crudes of increased quality are produced. The technique appears especially suitable for marine microalgae strains as the salt content acts as microwave absorbers, reducing energy consumption and increasing reaction rates.

Overall, the experimental work shows that hydrothermal processing is a low energy intensive wet processing technique for microalgae to produce bio-fuels and chemicals.

### III. TABLE OF CONTENTS

I.	ACKNOWLEDGMENTS .....	III
II.	ABSTRACT.....	IV
III.	TABLE OF CONTENTS.....	VI
IV.	PUBLICATIONS.....	XI
V.	LIST OF FIGURES .....	XIII
VI.	LIST OF TABLES .....	XVIII
1.	CHAPTER I - Introduction.....	1
1.1	Biofuel.....	1
1.2	Microalgae .....	5
1.3	Microalgae Cultivation .....	7
1.4	Processing of Microalgae.....	9
1.5	Hydrothermal processing .....	10
1.5.1	Introduction.....	10
1.5.2	Hydrothermal Carbonisation (HTC).....	16
1.5.3	Hydrothermal Liquefaction (HTL) .....	18
1.5.4	Catalytic HTL .....	24
1.5.5	Hydrothermal Gasification (HTG).....	27
1.5.6	Energy Balances.....	31
1.5.7	Nutrient Recycling .....	36
2.	CHAPTER II - Aims and Outline of the Thesis .....	39
3.	CHAPTER III - Methodology.....	43
3.1	Biomass characterisation.....	43
3.1.1	Microalgae strains .....	43
3.1.2	Proximate and ultimate analysis .....	45
3.1.3	Elemental Analysis .....	45
3.1.4	Biochemical Analysis .....	46
3.1.5	Scanning Electron Microscopy .....	48
3.1.6	Pigment Analysis .....	48
3.1.7	Metal Analysis .....	50
3.1.8	Pyrolysis GC-MS .....	50



3.1.9	Lipid Analysis .....	51
3.1.10	Thermo-gravimetric analysis .....	52
3.2	Hydrothermal processing.....	53
3.2.1	Parr batch processing.....	53
3.2.2	Swagelok reactor batch processing.....	53
3.2.3	Continuous processing.....	55
3.2.4	Microwave processing.....	58
3.3	Sample Workup.....	60
3.3.1	Bio-crude Analysis .....	60
3.3.2	Water Analysis .....	61
3.3.3	Solid residue Analysis .....	62
3.4	Microalgae Cultivation.....	62
4.	CHAPTER IV - Characterisation .....	66
4.1.	Introduction .....	66
4.2.	Proximate and ultimate analysis.....	67
4.3.	Biochemical Analysis.....	69
4.4.	Thermo gravimetric Analysis .....	70
4.5.	Pyrolysis GC-MS Analysis.....	73
4.6.	Metal Analysis.....	76
4.7.	Pigment Analysis.....	78
4.8.	SEM Analysis.....	79
5.	CHAPTER V - Microalgae HTL.....	81
5.1	Introduction .....	81
5.2	Methodology .....	81
5.3	Results .....	82
5.3.1	Microalgae HTL at standard conditions .....	82
5.3.2	Effect of HTL Temperature.....	84
5.3.3	Effect of HTL Residence Time .....	86
5.3.4	Analysis of the Process Water .....	87
5.4	Conclusions .....	89
6.	CHAPTER VI - Catalytic HTL .....	90
6.1	Introduction .....	90
6.2	Methodology .....	92

6.3	Homogenous Catalysis.....	92
6.3.1	Liquefaction yields.....	92
6.3.2	Bio-crude Analysis.....	93
6.3.3	Aqueous phase analysis .....	100
6.3.4	Nitrogen balance in product streams.....	102
6.3.5	Role of catalyst.....	103
6.4	Heterogeneous Catalysis.....	106
6.4.1	Lipid Profiles .....	106
6.4.3	HTL Results .....	111
6.4.4	Influence of hydrothermal treatment on lipids.....	112
6.4.5	Elemental analysis of bio-crude.....	117
6.5	Conclusions.....	118
7.	CHAPTER VII - Investigation of bio-crude formation pathways .....	120
7.1	Introduction.....	120
7.2	Methodology .....	121
7.3	Results and Discussion .....	121
7.3.1	Liquefaction Results .....	121
7.3.2	Elemental analysis of bio-crude.....	127
7.3.3	Energy Balance .....	130
7.3.4	Nitrogen balance in product streams.....	133
7.3.5	Carbon balance in product streams .....	136
7.3.6	GC/MS analysis of the bio-crude.....	138
7.4	Conclusions.....	141
8.	CHAPTER VIII - Nutrient Recycling from HTL process water .....	143
8.1	Introduction.....	143
8.2	Methodology .....	144
8.3	Results and Discussion .....	144
8.3.1	HTL Results .....	144
8.3.2	Analysis of Process Water .....	147
8.3.3	Cultivation Trials .....	150
8.3.4	Analysis of process water after cultivation.....	154
8.5	Conclusions.....	156
9.	CHAPTER IX - Py-GC-MS for analysis of microalgae .....	158

9.1	Introduction .....	158
9.2	Methodology .....	160
9.2.1	Sample preparation.....	160
9.2.2	Microalgae and growth trial analysis.....	161
9.3	Results .....	162
9.3.1	Py-GC-MS of Model Compounds.....	162
9.3.2	Py-GC-MS of microalgae.....	167
9.4	Conclusions .....	175
10.	CHAPTER X - HTL Reactor Systems .....	177
10.1	Introduction .....	177
10.2	Methodology .....	178
10.3	Continuous reactor HTL.....	178
10.3.1	Microalgae Feedstock Analysis.....	178
10.3.2	Reactor Performance .....	180
10.3.3	HTL Results .....	183
10.3.4	SEM Analysis.....	185
10.3.5	Bio-crude Analysis .....	187
10.3.6	Carbon Balance in the product phase .....	190
10.4	Comparison of reactor types.....	192
10.5	Conclusions .....	194
11.	CHAPTER XI - Hydrothermal Microwave processing.....	196
11.1	Introduction .....	196
11.2	Methodology .....	197
11.3	Results and Discussion.....	198
11.3.1	Microwave processing.....	198
11.3.2	Lipid Extraction.....	206
11.3.3	Hydrothermal processing of pre-treated algae.....	210
11.3.4	Pyrolysis behaviour .....	211
11.4	Conclusions .....	217
12.	CHAPTER XII – Conclusions, Implication and Future Work .....	218
12.1	Experimental studies .....	218
12.2	Implications for process development.....	222
12.3	Future Work .....	225

13. References.....	227
14. Nomenclature.....	235
APPENDIX A.....	<b>Error! Bookmark not defined.</b>

## IV. PUBLICATIONS

### Journal Papers

1. Biller, P., Friedman, C., Ross, A.B. Hydrothermal microwave processing of microalgae as a pre-treatment and extraction technique for bio-fuels and bio-products. *Bioresource Technology*, In Press, 2013.
2. Li, H., Biller, P., Hadavi, S.A., Andrews, G.E., Przybyla, G., Lea-Langton, A. Assessing combustion and emission performance of direct use of SVO in a diesel engine by oxygen enrichment of intake air method. *Biomass and Bioenergy* 2013 (0).
3. Budarin, V., Ross, A.B., Biller, P., Riley, R., Clark, J.H., Jones, J.M., Gilmour, D.J., Zimmerman, W. 2012. Microalgae biorefinery concept based on hydrothermal microwave pyrolysis. *Green Chemistry*, 14(12), 3251-3254.
4. Biller, P., Ross, A.B. 2012. Hydrothermal processing of algal biomass for the production of biofuels and chemicals. *Biofuels*, 3(5), 603-623.
5. Biller, P., Ross, A.B., Skill, S.C., Lea-Langton, A., Balasundaram, B., Hall, C., Riley, R., Llewellyn, C.A. 2012. Nutrient recycling of aqueous phase for microalgae cultivation from the hydrothermal liquefaction process. *Algal Research*, 1(1), 70-76.
6. Hadavi, S., Li, H., Biller, P., Lea-Langton, A. 2012. Rape Seed Oil B100 Diesel Engine Particulate Emissions: The Influence of Intake Oxygen on Particle Size Distribution. *SAE Technical Paper*, 01-0435.
7. Biller, P. and A.B. Ross, *Potential yields and properties of oil from the hydrothermal liquefaction of microalgae with different biochemical content*. *Bioresource Technology*, 2011. 102(1): p. 215-225.
8. Biller, P., R. Riley, and A.B. Ross, *Catalytic hydrothermal processing of microalgae: Decomposition and upgrading of lipids*. *Bioresource Technology*, 2011. 102(7): p. 4841-4848.
9. Ross, A.B., Biller P., Kubaki, M.L., Lea-Langton, A., Jones, J.M. *Hydrothermal processing of microalgae using alkali and organic acids*. *Fuel*, 2010. 89(9): p. 2234-2243.
10. Lea-Langton A., Hu Li, Andrews G.E., Biller P. *The Influence of Fuel Pre-Heating on Combustion and Emissions with 100% Rapeseed Oil for a DI Diesel Engine*. Leeds, UK: SAE International, 2009. SAE 2009-01-0486. Also published in: "CI engine Performance for use with Alternative Fuels, 2009". SAE International SP-2237 pp. 87-98. ISBN 978-0-7680-2133-2, SAE International, 2009.
11. Hu Li, Lea-Langton A., Biller P., Andrews G.E., Richards P. *Effect of Fuel Detergent Package on Fuel Injector Deposit, Combustion and Emissions using Pure Rape Seed Oil for a DI Diesel*. Leeds, UK: Society of Automotive Engineers International, 2009. SAE 09FFL-0222

## Conference Papers and Posters

1. Biller, P. *Lessons from Nature: Renewable Biofuels from Microalgae*. SHOWCASE 2012 – The 3rd annual University of Leeds postgraduate research conference, Leeds, UK
2. Jazrawi C., Biller P., Ross A.B., Montoya A., Maschmeyer T., Haynes B.S. *Hydrothermal Processing of Microalgae on a Continuous Flow Pilot Scale Reactor*. 2<sup>nd</sup> International Conference on Algal Biofuels, Biomass and Bioproducts, 2012. San Diego, USA
3. Biller P., Ross A.B., *Using Py-GC-MS to investigate the influence of growth conditions on production of biochemical components from microalgae*. 2<sup>nd</sup> International Conference on Algal Biofuels, Biomass and Bioproducts, 2012. San Diego, USA
4. Biller P., Ross A.B., *Using Py-GC-MS to study the change in composition of the microalgae Chlorella vulgaris in different growth Media*. 19th International Symposium on Analytical and Applied Pyrolysis, Linz, Austria (2012)
5. Ross, A. B., Biller, P., Hall, C. *Catalytic hydrothermal processing of microalgae with integrated nutrient recycling*. 18th European Biomass Conference and Exhibition, Berlin, Germany (2011)
6. Biller P., Ross A.B., Skill S., Llewellyn, C.A. *Nutrient Recycling of Aqueous Phase for Microalgae Cultivation from the Hydrothermal Liquefaction Process*. 1<sup>st</sup> International Conference on Algal Biofuels, Biomass and Bioproducts 2011, St. Louis, USA
7. Ross, A.B., Biller, P. *Catalytic Hydrothermal Liquefaction of Microalgae*. 1<sup>st</sup> International Conference on Algal Biofuels, Biomass and Bioproducts 2011, St. Louis, USA
8. Biller P, Riley .R., Ross A. B., *Decomposition of Lipids from Microalgae and Oil Seeds using Hydrothermal Processing*, in BioTen Conference 2010, T. Bridgewater, Editor. 2010: Birmingham, UK.
9. Budarin, A.B. Ross, P. Biller, R. Riley, J. Clark, J.M. Jones, D.J.Gilmour, W. Zimmerman., *Hydrothermal Microwave Pyrolysis of Microalgae*, in Bioten Conference 2010, T. Bridgewater, Editor. 2010: Birmingham, UK.
10. Hadavi, S., Li, H., Lea-Langton, A., Biller, P., Altaher, M.A., Andrews, G. *Effect of Multifunctional Fuel Additive Package on Particulate Number Concentration and Size Distribution Using Pure Rape Seed Oil in a Diesel Engine* 18th European Biomass Conference and Exhibition, Berlin, Germany (2011)

## V. LIST OF FIGURES

**Figure 1.1:** Hydrothermal processing conditions in the water phase diagram; data from *Perry's Chemical Engineers' Handbook* [1]

**Figure 1.2:** Density [2], static dielectric constant [3] at 30MPa and ionic product [4] of water at 25 MPa

**Figure 1.3:** Schematics of an integrated HT process with nutrient and CO<sub>2</sub> recycle

**Figure 3.1:** Schematic of the Parr 75 ml reactor layout

**Figure 3.2:** Schematic of the Swagelok reactor used at the University of Sydney with nitrogen purge.

**Figure 3.3:** Swagelok reactor set-up at the University of Leeds with thermocouple and without nitrogen purge.

**Figure 3.4:** Schematic of the continuous reactor at Sydney University.

**Figure 3.5:** Continuous reactor configuration.

**Figure 3.6:** Schematic of the HMP process and sample workup.

**Figure 3.7:** Schematic of the HTL sample workup.

**Figure 3.8:** Images of the cultivation trials and bulk algae cultivation.

**Figure 3.9:** Schematic layout of the HTL reactions, sample workup and cultivation trials.  
DCM= *dichloromethane*, HT=*hydrothermal*

**Figure 4.1:** TGA/DTG plot of *Haematococcus pluvialis* in N<sub>2</sub> at 10°C/min heating rate.

**Figure 4.2:** TGA/DTG plot of *Nannochloropsis* in N<sub>2</sub> at 10°C/min heating rate.

**Figure 4.3:** TGA/DTG plot of *Pseudochoricystis ellipsoidea* in N<sub>2</sub> at 10°C/min heating rate.

**Figure 4.4:** Total ion chromatogram of Py-GC-MS of *Chlorogloeopsis fritschii* at 500°C

**Figure 4.5:** Total ion chromatogram of Py-GC-MS of *Navicula sp.* at 500°C

**Figure 4.5:** Total ion chromatogram of Py-GC-MS of *Pseudochoricystis ellipsoidea* at 500°C

**Figure 4.6:** Analysis of pigments by HPLC in selected microalgae strains, units in mg/kg (daf).

**Figure 4.7:** SEM image of (a) *Chlorogloeopsis fritschii* and (b) *Spirulina OZ* at 1500 magnification

**Figure 5.1:** Bio-crude yields from HTL of *Chlorella vulgaris OZ* at varying temperature for 15 min.

**Figure 5.2:** Effect of residence time on the HTL bio-crude yields at 250°C and 350°C.

**Figure 6.1:** Yields of products from hydrothermal processing for (a) *Spirulina* at 300°C (b) *Spirulina* at 350°C (c) *Chlorella* at 300°C (d) *Chlorella* at 350°C.

**Figure 6.2:** GC/MS of bio-crude from *Chlorella* at 350°C for (a) 1M Na<sub>2</sub>CO<sub>3</sub> (b) 1M KOH (c) 1M acetic acid and (d) 1M formic acid.

**Figure 6.3:** GC/MS of bio-crude from *Spirulina* at 350°C for (a) 1M Na<sub>2</sub>CO<sub>3</sub> (b) 1M KOH (c) 1M acetic acid and (d) 1M formic acid.

**Figure 6.4:** Distribution of nitrogen in the product streams from (a) *Spirulina* at 300°C, (b) *Spirulina* at 350°C, (c) *Chlorella* at 300°C, (d) *Chlorella* at 350°C.

**Figure 6.5:** Carbon balance between product phases for (a) *Spirulina* at 300°C, (b) *Spirulina* at 350°C, (c) *Chlorella* at 300°C, (d) *Chlorella* at 350°C.

**Figure 6.6:** TAG HPLC chromatograms of (a) Soya oil, (b) *Chlorella* and (c) *Nannochloropsis*

**Figure 6.7:** GC-MS chromatograms of (a) soya oil processed in water only and (b) processed with Ni/Al<sub>2</sub>O<sub>3</sub> catalyst.

**Figure 6.8:** HPLC-SEC chromatograms of soya oil hydrothermally processed in Ni/Al<sub>2</sub>O<sub>3</sub>, Pt/Al<sub>2</sub>O<sub>3</sub>, Co/Mo/Al<sub>2</sub>O<sub>3</sub>, Water and unprocessed soya oil.

**Figure 6.9:** TGA boiling point profiles of lipids and bio-crudes without catalyst and Ni/Al catalyst of (a) soya oil and (b) *Chlorella*.

**Figure 7.1:** Yields of products from hydrothermal processing under (a) water, (b) sodium carbonate, (c) formic acid



**Figure 7.2:** Distribution of nitrogen in the product streams from hydrothermal processing under (a) water, (b) sodium carbonate, (c) formic acid

**Figure 7.3:** Distribution of carbon in the product streams from hydrothermal processing under (a) water, (b) sodium carbonate, (c) formic acid

**Figure 8.1:** Product distribution from the hydrothermal liquefaction of the different microalgae strains at 300°C and 350°C

**Figure 8.2:** Growth of algae in process water dilutions of (a) *Spirulina* 300°C (b) *Chlorella* 300°C determined by chlorophyll a absorbance

**Figure 8.3:** Growth of algae in process water dilutions of (a) *Chlorella* 350°C (b) *Scenedesmus* 350°C determined by cell count

**Figure 9.1:** Image of an empty pyro tube and a tube with trapped algae cells

**Figure 9.2:** Schematic methodology of the wet Py-GC-MS analysis technique.

**Figure 9.3:** Total ion chromatogram of bovine serum at 500°C

**Figure 9.4:** Total ion chromatogram of the model lipid compound palmitic acid.

**Figure 9.5:** Total ion chromatogram of the Chlorophyll *a* extract.

**Figure 9.6:** Chromatogram of *Chlorella vulgaris* with marker compounds indicated.

**Figure 9.7:** Calculated protein, lipid and chlorophyll *a* content of *Chlorella* strains grown in different dilutions of process water from HTL/HTG.

**Figure 9.8:** Protein content of the different *Chlorella* strains by analysis of *Indole* peak areas and by the nitrogen to protein conversion factor of 6.25.

**Figure 9.9:** Peak areas and percentage standard deviation of three peaks of triplicate repeats of *Chlorella* OZ pyrolysis products.

**Figure 9.10:** Py-GC-MS analysis of *Navicula* sp. strains for Chlorophyll a, protein, lipid and starch grown in different concentration of silicate.

**Figure 9.11:** Photograph of *Navicula* sp. grown in 100% silicate for 10 days, 13 days, 15 days, 50% silicate 10 days and 25 % silicate 10 days.

**Figure 9.12:** Astaxanthin levels detected in *Haematococcus pluvialis* grown in different media by Py-GC-MS and HPLC.

**Figure 9.13:** Analysis of *B. braunii* grown in ½ N BBM+V media over 20 days by Py-GC-MS.

**Figure 10.1:** Size distribution of dehydrated microalgae.

**Figure 10.2:** Pressure control for *Spirulina* at 150 bar (a) varying experimental temperatures for a residence time of 3 minutes (b) varying residence times of 3 and 5 minutes at 300°C.

**Figure 10.3:** Yields of products for the different hydrothermal liquefaction experiments.

**Figure 10.4:** SEM images of *Chlorella* (a) dry unprocessed (b) processed at 250°C 3 min (c) processed at 275°C 3 min (d) processed at 300°C 3 min.

**Figure 10.5:** Sim-dis by TGA for bio-crudes derived from (a) *Chlorella* and (b) *Spirulina*.

**Figure 10.6:** Carbon balance from the continuous HTL of (a) *Chlorella* and (b) *Spirulina*.

**Figure 10.7:** Heat profiles of different reactor types on HTL of 10 wt% *Chlorella* OZ.

**Figure 11.1:** SEM images of untreated *Chlorogloeopsis* (a) Mag=2320, processed at 120°C (b) Mag=1500 and 140°C (c) Mag=1500.

**Figure 11.2:** SEM images of untreated *Nannochloropsis* (a) Mag=5430, processed at 120°C (b) Mag=4660 and 140°C (c) Mag=4660.

**Figure 11.3:** SEM images of *Pseudochoricystis* (a) Mag=4660, processed at 120°C (b) Mag=4660 and 140°C (c) Mag=4660.

**Figure 11.4:** HPLC-SEC chromatogram of *P.ellipsoidea* indicating the triglyceride and free fatty acid fractions

**Figure 11.5:** Distribution of fatty acid methyl esters from unprocessed and HMP samples of *P. ellipsoidea* at 80°C, 100°C and 140°C.

**Figure 11.6:** Energy requirement to heat samples to desired temperature at constant heating rate and residence time.

**Figure 11.7:** DTG pyrolysis plots of pre-treated and raw algae in nitrogen at 50-750°C of (a) *Chlorogloeopsis*, (b) *Nannochloropsis*, (c) *Pseudochoricystis* and (d) *Pseudochoricystis* in 0.1M NaCl.

**Figure 11.8:** Relative amounts of Nitrogen and Sulphur present in the bio-crude from flash pyrolysis detected by Py-GC-AED.

## VI. LIST OF TABLES

**Table 1.1:** Algae cost, productivity and concentration comparison between open ponds and photobioreactors. Adapted from Draaisma et al. [26].

**Table 1.2:** Summary of HTL studies using only water, no catalyst

**Table 1.3:** Summary of published literature on Catalytic HTL

**Table 1.4:** Summary of research published on the HTG of algae

**Table 1.5:** Energy recovery and heating energy for different HT studies

**Table 3.1:** Name, source, strain code and growth media of the microalgae strains investigated with Chapter reference

**Table 3.2:** HPLC gradient program with A: 85% methanol/water (v/v) buffered with 0.5 M ammonium acetate, B: 90% acetonitrile/water (v/v) and C: ethyl acetate

**Table 3.3:** Concentration of nutrients in different algae grown media.

**Table 4.1.** Proximate, ultimate analysis and HHV of selected microalgae strains.

**Table 4.2.** Protein, carbohydrate and lipid contents of selected microalgae strains.

**Table 4.3:** Compounds identified form Py-GC-MS of *Chlorogloeopsis fritschii* at 500°C

**Table 4.4:** Compounds identified form Py-GC-MS of *Navicula sp.* at 500°C

**Table 4.5:** Compounds identified form Py-GC-MS of *Pseudochoricystis ellipsoidea* at 500°C

**Table 4.6:** Concentration of metals and P present in selected microalgae strains in mg/kg.

**Table 5.1:** Hydrothermal liquefaction yields, elemental analysis and HHV of bio-crude of selected microalgae species.

**Table 5.2:** Effect of operating temperature on elemental composition and HHV of bio-crudes from HTL.

**Table 5.3:** Effect of residence time on elemental composition and HHV of bio-crudes from HTL.

**Table 5.4:** Effect of temperature on anion, cation, TOC, TN concentration (in mg/l) and pH

**Table 6.1:** Ultimate Analysis in % and HHV of bio-crude at 300°C

**Table 6.2:** Ultimate Analysis in % and HHV of bio-crude at 350°C

**Table 6.3:** Compounds identified in bio-crude from HTL of microalgae

**Table 6.4:** Boiling point distribution of bio-crudes at 350°C

**Table 6.5:** TOC, pH, ammonium, phosphate and potassium content of the aqueous phase.

**Table 6.6:** Retention times, PN, quantification and structures of FFA and TAG of the lipid samples

**Table 6.7:** Bio-crude yields from hydrothermal liquefaction

**Table 6.8:** Average Molecular weight of bio-crudes and Soya oil

**Table 6.9:** Elemental analysis in wt.% of the bio-crudes and HHV

**Table 7.1:** Proximate and ultimate analysis, HHV of the model compounds and microalgae

**Table 7.2:** Ultimate analysis, HHV and energy balances of the bio-crudes of model compounds and microalgae

**Table 7.3:** Most abundant GC-MS identified compounds in the bio-crudes from liquefaction at different conditions

**Table 8.1:** Influence of temperature and biomass species on bio-crude composition, higher heating value, and yield.

**Table 8.2:** Nutrient analysis of the process water compared to standard growth media 3N-BBM+V

**Table 8.3:** dry weights of harvested algae at the end of growth trials in dilutions of process water and standard media (mg/l)

**Table 8.4:** Nutrient analysis of the culture medium before and after cultivation trials in different dilutions of process water. All units in mg/l, no replicates carried out

**Table 9.1:** Pyrolysis marker compounds identified from pyrolysis of microalgae model compounds.

**Table 9.2:** Elemental Analysis of *Navicula* sp. strains.

**Table 10.1:** Analysis of microalgae feedstock.

**Table 10.2:** Elemental analysis (wt%) and Higher Heating Value (HHV) of bio-crudes from hydrothermal liquefaction of *Chlorella* and *Spirulina* at different processing conditions.

**Table 10.3:** Comparison of bio-crude yields and composition from *Chlorella OZ* at 350°C.

**Table 11.1:** Proximate, ultimate, biochemical and metal analysis of microalgae feedstock.

**Table 11.2:** Ash content and wt.% carbon and nitrogen recovered to the solid microalgae residue following HMP.

**Table 11.3:** Analysis of water phase after microwave treatment.

**Table 11.4:** Lipid extraction yields from solvent extraction using DCM

**Table 11.5:** Bio-crude yields, elemental composition and HHV from the hydrothermal liquefaction of pre-treated algae.

**Table 11.6:** Flash Pyrolysis volatiles yields on a dry ash free basis.

## **1. CHAPTER I - Introduction**

### **1.1 Biofuel**

Biofuels are by no means a new technology, wood and charcoal has been burned by humans for thousands of years as a source of heat for food preparation and comfort. With the onset of the industrial age fossil fuels such as coal and petroleum became more popular due to their higher energy density, affordability and availability. In the 20<sup>th</sup> century petroleum became the dominant energy carrier for the industrialised world, associated with cheap prices and a huge industry developing around petroleum products. Only towards the end of the century in 1973 when the OPEC chose to proclaim an oil embargo and in 1979 when the Iranian revolution occurred, did the West realise that the days of cheap oil are not endless. This was the period when the first real governmental research into alternative fuels started. Especially the US was concerned about their dependency on oil from the politically unstable regions of the Middle East. In 1978 President Jimmy Carter started the first research program into the use of algae as a source of bioenergy called the Aquatic Species Program [2]. This program was set for two decades and was concluded in 1996. The dependency of foreign oil is still a big driver into the development of alternative biologically sourced fuels. However, since around 1980 concern over global warming has become an increasingly important driver for advances in biofuels.

Biofuels offer a possible route for the mitigation of CO<sub>2</sub> emissions as the carbon emitted during combustion is taken from the atmosphere during the growth of the biomass. For the mitigation of climate change, biofuels will play a significant role as the transport sector has seen less development than the electricity generation industry concerning renewable solutions. Even though the development of electric cars has seen considerable development in recent years, powering heavy good vehicles, planes and ships by renewable electricity is not viable in the near future due to cost, weight and safety concerns of lithium-ion based batteries. Therefore, for the transport sector, the development of sustainable biofuels is necessary to reduce its CO<sub>2</sub> emissions.

Traditional biofuels from corn or rape seed as they are popular in the US and Europe respectively, are known as first generation biofuels. These first generation fuels are no longer regarded as environmentally friendly and CO<sub>2</sub> mitigating. The Gallagher review published in 2008 was set up by the UK Government to assess the climate benefits, effects on food prices and possible deforestation due to first generation biofuels. It was concluded that biofuels do indeed contribute to

rising food prices and a slow down on first generation biofuel growth is required to avoid detrimental effects. Biofuel production on agricultural land was shown to displace existing food production causing land-use change with increased net greenhouse gas emissions [3]. To date the sources of biofuels on the market are mostly first or second generation derived fuels, mainly from food crops. Second generation, or advanced biofuels, are defined as biofuels made from lignocellulosic biomass. However these have also been shown to potentially replace agricultural land for the dedicated production of energy crops, with aforementioned detrimental effects. Corn and sugar cane are commonly converted to bioethanol by fermentation in the US and Brazil respectively. In the European Union biodiesel production is more common by extracting the oils from rape seed and subsequent transesterification.

In 2009 a total of 29.0 Gt of anthropogenic CO<sub>2</sub> were emitted of which 23 wt.% arose from the transportation sector, this amount could be reduced significantly with the use of sustainably grown biofuels in road, marine and aviation transport [4]. The European Union has recognised this and issued the Directive 2003/30/EC which forced all member countries to add 2 vol.% biofuels to transport fuels from 2005, this amount was increased to 5.75 % by volume in 2010. A further increase to 10 vol.% by 2020 has been agreed by the directive 2009/28/EC but is subject to biofuels being produced sustainably without the abovementioned detrimental effects of first and second generation fuels.

The UK Government supports the EU position on the basis of a sustainable production path and are hoping for the commercialisation of sustainable next generation biofuels [5]. The RTFO (2011) requires fossil fuel suppliers to produce evidence showing that a percentage of fuels for road transport supplied in the UK come from renewable sources and are sustainable, or that a substitute amount of money is paid [6]. Destruction of biodiversity especially in bio-diversely rich areas such as rain forests is of concern because local farmers will potentially destroy woodland area to grow monocultures for biofuel production such as palm oil. This leads to increased atmospheric pollution since forests are regarded as a carbon sink which are consequently lost. The issue of monocultures has also been raised in the US and Europe where farmers are increasingly growing corn and rape seed for bioenergy applications rather than employing the traditional farming methods of crop rotation. This practice of growing different crops in different seasons prevents over replenishment of nutrients from the soil. Growing merely energy crops consequently leads to increased use of fertilizers which is associated with an increase of greenhouse gas emissions.



The rising popularity of biofuels has led to large price increases for the staple foods worldwide. From 2001 to 2011 the worldwide biofuels production increased from 10 to 60 million tonnes of oil equivalent [7]; going hand in hand with increases in food crop prices. The use of terrestrial plants also puts considerable strains on the natural resource base which is being exploited for its nutrients and water. Currently 1% of the world's arable land is used for the production of biofuels, providing 1% of the world's transport fuel demand [8]. Clearly increasing the proportion of biofuels from terrestrial plants to anywhere near 100 % would have disastrous effects on the world food supply.

The concept behind advanced generation biofuels is to use biomass which is usually discarded; such as stems, forestry waste, fast growing trees, switch grass and more recently algae. The potential of reducing greenhouse gas emissions with these biofuels is greatly improved. It is generally agreed that the development of next generation liquid biofuels are required that are not derived from biomass competing with food supplies. Second generation biofuels are produced from lignocellulosics, while microalgae are seen as being a future source of third generation biofuels and chemicals. Next generation biofuels can be produced by a variety of pathways from different sources and processes. The different processes are classed mainly into biochemical and thermochemical processes.

The most established technologies are the biological processes; fermentation and anaerobic digestion. Fermentation for the production of biofuels is the most common and established process to produce liquid fuels. The fermentation process is well understood and has been used for thousands of years to produce alcoholic beverages. Simple sugars such as glucose are converted to ethanol and carbon dioxide by the biological activity of yeast. The process requires anaerobic conditions to avoid cellular respiration of pyruvate breaking down to water and CO<sub>2</sub>; pyruvate is an intermediate product of the fermentation of sucrose. Industrially the process converts sugars from sugar cane, sugar beet or corn to ethanol. Especially in Brazil the technology is well established, stemming from an almost 40 year running ethanol program making them one of the world's largest producers of bioethanol. Bioethanol can be blended with conventional gasoline up to 10 vol.% without modifications to the engine. Bioethanol is regarded as a first generation biofuel but there is considerable research into producing ethanol from more complex carbohydrates from non food crops by pre-treatment (hydrolysis) or biological breakdown to simpler carbohydrates which can be fermented.

The other biological pathway commonly employed is known as anaerobic digestion (AD). During AD bacteria break down organic fragments to smaller molecules by hydrolysis. Proteins are

hydrolysed to amino acids, lipids to fatty acids and carbohydrates to sugars. Acidogenic bacteria then convert these molecules to carbonic acids, alcohols, ammonia,  $H_2$  and  $CO_2$ . Different, acetogenic, bacteria are able to further break the organic acids down to acetic acid. In the final step of methanogenesis, microbes form  $CH_4$  by anaerobic respiration of  $H_2$  and  $CO_2$ . The produced gas from AD hence contains  $CH_4$ ,  $CO_2$  and small amounts of trace gases. AD is used for digestion of organic waste, or purpose grown energy crops such as corn, to a biogas. It is also the process occurring in landfill sites to produce landfill gas. The produced biogas is commonly combusted to generate electricity and heat. The process results in a by-product of dead bacteria and indigestible material, known as digestate, which is high in nutrients and can be used as fertiliser.

Biomass and microalgae can also be converted to biofuels by thermochemical processes. These include gasification, pyrolysis and hydrothermal processing. Gasification involves the partial controlled oxidation of organic material to a syngas (sometimes referred to as producer gas). Syngas contains  $CO$ ,  $H_2$  and  $CO_2$ . Apart from direct combustion, the other promising application of syngas is the conversion to a synthetic fuel, so called “gas to liquid fuel” (GTL), by the Fisher-Tropsch process. This converts  $H_2$  and  $CO$  to straight chain liquid hydrocarbons which are a suitable renewable substitute to petroleum derived diesel fuel.

Pyrolysis refers to the thermal decomposition of feedstocks in the absence of air. Products from pyrolysis vary depending on processing temperature, heating rate and residence time. Generally lower temperatures lead to the formation of a solid biochar product. This is very similar to traditional charcoal manufacture and is still performed especially in developing countries. The process drives off the moisture and volatiles, improves the handling properties and increases the carbon content of the fuel. At temperatures up to  $300^\circ C$  the process is known as torrefaction which is being increasingly used to process biomass to a more suitable solid fuel for co-combustion with coal. At higher temperatures ( $>500^\circ C$ ) the product distribution favours the production of a liquid bio-oil. This is a highly oxygenated, acidic liquid resembling crude oil. It is not suitable for blending with diesel or gasoline but can be combusted for power generation or upgraded by hydrogenation/ hydro-cracking to green diesel.

One of the drawbacks of the thermochemical routes mention above is that the biomass feedstock needs to be dry while biomasses, and especially algae, typically have a high moisture content. Therefore, wet thermochemical routes are more suited to process biomass with high moisture content such as algae. Only anaerobic digestion and hydrothermal processing allow processing feedstocks with significant water content. Dry biomass processing is associated with a large energy

input to drive off water. Hydrothermal processing involves treating a water-biomass slurry in hot compressed water to produce biofuels. A detailed introduction and literature review on hydrothermal processing is covered in **Section 1.5**.

## 1.2 Microalgae

The development of third generation biofuels from microalgae has seen increasing research efforts over the last decade. The advantages of these biomass technologies are that they do not stand in direct competition to food production and potentially have a better energy balance. Microalgae are microscopic organisms that can grow in fresh, brackish or salt water. There are two functional groups of microalgae; phototrophic and heterotrophic. Phototrophic means that the algae use CO<sub>2</sub> and sunlight via photosynthesis while heterotrophic algae require an organic source of carbon for their growth. Both phototrophic and heterotrophic algae also require nutrients and water. The advantage of microalgae compared to terrestrial biomass is its much higher photosynthetic efficiency which results in higher growth rates and improved CO<sub>2</sub> mitigation [8]. Switch grass, one of the fastest growing terrestrial plants, is estimated to convert no more than 1W/m<sup>2</sup> sunlight at a yearly rate, that is equivalent to 0.5 % of the irradiation at medium latitude [9]. It must be taken into account that only the photosynthetic active radiation can be utilised during basic carbohydrate production by photosynthesis. This active radiation represents 42.3 % of the total radiation [8]. Other factors such as photosaturation, photorespiration and poor light absorption further decrease the photosynthetic efficiency of plants. Microalgae have been found to have much higher theoretical photosynthetic efficiencies, compared to terrestrial plants, ranging between 10-20 % [9]. In practice however efficiencies of around 5-10 % are more likely [8, 10]. Microalgae are primitive plants (thallophytes), lacking stems, roots and leaves; their structure is primarily for energy conversion without any development beyond cells, therefore higher growth rates and photosynthetic efficiencies are achieved [11].

The photosynthetic efficiency is a very important factor to consider and has a large impact on the economic feasibility of microalgae systems. If the photosynthetic efficiency is doubled, the land area required for the same amount of biomass is halved. This is one of the reasons why microalgae have a larger potential than terrestrial biomass for providing significant amounts of our energy demand. Only 3.9% of the world surface is arable land, while 25.3% are non arable and the rest is aquatic [12]. An estimation by Stephens *et al.* states that with a photosynthetic efficiency of 3 or 10%

at tropical and subtropical regions, would require 0.4 or 0.1 % of the world's non-arable land respectively to fully supply the world's fuel demand by microalgae. It is also stated that an efficiency of 4% is achieved routinely in conventional open pond systems [12]. Microalgae can contain up to 80% lipids by weight which strongly affects the suitability of a strain for biofuel production. The lipid content of microalgae can vary widely and has a major impact on the economics and energy balances of microalgae for bio-diesel systems. Wijffels et al. state in their review on microalgae for biofuels and chemicals that potential oil yields of 8,000 to 32,000 l ha<sup>-1</sup> year<sup>-1</sup> could be possible, with current technology achieving a maximum productivity of around 8,000 l year<sup>-1</sup> [13]. This is higher than the best performing terrestrial oil producing plants [14]; palm and rapeseed oils can be produced at 6,000 and 1,500 l ha<sup>-1</sup> year<sup>-1</sup> respectively [13]. This is also due to the fact that microalgae can be harvested all year around and double their cell count every few days, while terrestrial plants are usually seasonal and often only allow one harvest per year. Therefore a more uniform biofuel production throughout the year is achievable which is closer to the actual market demand of liquid fuels. Another advantage of microalgae over terrestrial plants is that they use less fresh water for their growth.

By converting CO<sub>2</sub>, H<sub>2</sub>O and sunlight to biomass, microalgae effectively capture carbon from the atmosphere. Upon combustion there is therefore no additional carbon added to the atmosphere, unlike fossil fuels which are regarded as a carbon sink which have stored carbon for millions of years. Alternatively CO<sub>2</sub> from flue gases can be used for enhanced algal growth and is available at little or no cost from fossil fuel power plants. Natural CO<sub>2</sub> levels in the atmosphere are quite low (~360 ppm v/v); therefore the growth by capturing CO<sub>2</sub> from the atmosphere is limited by the mass transfer from the atmospheric CO<sub>2</sub> to the growing medium. Fossil fuel powered power plants often have CO<sub>2</sub> concentrations of 15% which can greatly improve the photosynthetic efficiency and therefore the growth rate of microalgae [15]. One problem associated with this approach is that many algal species are not tolerant to high levels of NO<sub>x</sub> and SO<sub>x</sub>, therefore careful strain selection is necessary. Microalgae are estimated to sequester around 1.8 kg of CO<sub>2</sub> per kg of algae produced, by bio-fixation [16].

All microalgae produce, lipids, proteins, carbohydrates and nucleic acids in varying compositions for different strains. The compositions also vary depending on culturing conditions. The lipid content is the primary component for biodiesel production and this fraction can make up anywhere between approximately 5 wt.% and 80 wt.% [17]. There are also valuable bi-products that can be harvested from microalgae which can significantly increase the economics of biofuel production. Some algal strains can produce polyunsaturated fatty acids (omega-3) in the form of EPA and DHA

which are popular and expensive food supplements and are essential for human development and physiology [14]. Usually omega-3 fats are extracted from fish but this is not suitable for vegetarians and is associated with unpleasant odour and taste. The cyanobacteria *Spirulina* has been a successful food supplement for years due to its high protein content and essential oils. *Chlorella* is produced for its medicinal value as it is claimed to protect against renal failure and growth promotion of intestinal lactobacillus. There are also a number of valuable recombinant proteins found in microalgae as well as valuable pigments such as  $\beta$ -carotene, astaxanthin and C-phyococyanin [18-19]. *Dunalliella salina* with a production rate of 1200 t a year is exploited for its  $\beta$ -carotene content of 14 wt.% due to its current market value of  $\sim$  2000 €/kg [19].

### 1.3 Microalgae Cultivation

It is advantageous to use natural sunlight but this has the disadvantage of diurnal cycles and seasons resulting in a limiting factor on available light. A location with high solar irradiation therefore is beneficial for algal growth. Artificial light is commonly used for laboratory scale applications but is too expensive and would be detrimental for GHG saving reasons if employed at a larger scale. Higher growth rates can be achieved if CO<sub>2</sub> flue gas circulation is employed from power plants or industrial installations. Ideally the algae cultivation facility should be in close proximity to such an installation to avoid expensive CO<sub>2</sub> transportation. Inorganic nutrients have to be present in the aqueous growing media and include nitrogen and phosphorus. Grobbelaar (2007) presented a formula for nutrient requirements based on the molecular composition of typical algae; CO<sub>0.48</sub>H<sub>1.83</sub>N<sub>0.11</sub>P<sub>0.01</sub> but this varies for different algae strains [20]. From this formula it can be seen that not much phosphorus is necessary but Chisti (2007) states that this element should be provided in excess as phosphate ions bond with metal ions and are therefore not available for algal growth [17]. One way of providing nutrients to microalgae being researched is the use of wastewater or nutrient rich agricultural run-off. Pittman et al. (2011) conclude in their review that algae cultivation based on current technologies is unlikely to provide a positive energy return or to be economically viable unless it is combined with waste water treatment, as this reduces the energy cost, GHG emissions and the nutrient and freshwater resource costs [21].

Algae cultivation can be achieved either in open pond or photo-bioreactor systems. Open pond systems can be implemented into natural water systems such as lakes, lagoons and ponds but it is more common to use artificial systems such as raceway ponds. These structures are usually

arranged in a closed loop of various designs with a paddle wheel for circulation and mixing. This is important as turbulent flow maximises algal growth and prohibits microalgae from settling on the raceway floor. The floor is lined with a plastic liner and usually painted white to increase reflectance which increases the light received by the cells. The culture is fed continuously in front of the paddlewheel and the algae broth is harvested just behind the paddlewheel.

Open raceway ponds are advantageous due to cheap construction, low energy input during operation, easy maintenance and the fact that they can be built on non arable land. But one of the biggest problems with raceway ponds is the contamination of other algae and protozoa. To achieve monoculture cultivation it is therefore necessary to have quite extreme growing environments. For example *Chlorella* can grow in extremely nutrient rich media, *Dunaliella salina* is adaptable to very high salinity and *Spirulina* can withstand high alkalinity [22].

A more sophisticated culturing system is the use of photobioreactors. This incorporates the use of transparent tubes or plates which act as the culturing environment. The most common design is the tubular design but flat plate and column photobioreactors are also used, each with different advantages and limitations. The broth is circulated from a reservoir where the pump is located (typically air-lift or mechanical pumps); the air-lift pump has the advantage of being able to introduce CO<sub>2</sub> and degas the accumulated O<sub>2</sub>. Degassing of O<sub>2</sub> is important as too much oxygen in the culture will inhibit algal growth. The main advantage of closed systems is that culturing of a monoculture species without contamination is possible for a substantial period without cleaning or other maintenance. CO<sub>2</sub> and light usage is also much higher than with open systems which drastically increases the biomass production per volume. This has the effect that harvesting also becomes much cheaper as the biomass concentration is up to 30 times higher than in open systems [17]. The major drawback is that the more sophisticated system has a much higher unit construction cost and therefore increases the cost of biomass. Demirbas (2011) states that photobioreactors require 10 times the capital cost compared to open raceway ponds, this leads to an estimated algae production cost of \$10/kg and \$30-70/kg for open pond and photobioreactor cultivation respectively [14]. A more recent evaluation of algae production costs and productivity by Draaisma et al. (2013) comes to a different conclusion [23]. The data presented in **Table 1.1** is based on growing the strain *Thalassiosira pseudonana* in Southern Europe with the photobioreactor being of the stacked horizontal tubular design. The algae production cost for open pond systems is in the same range as the estimates by Demirbas (2011) however the photobioreactor algae production cost is shown to be lower than the open pond system with a price of 8 €/kg. The Table demonstrates that the algae productivity and algae concentrations are much higher in the photobioreactors. In this current

opinion in Biotechnology it is also stated that the price achieved with current technology of 5.5 €/kg could be reduced to 0.68 €/kg if the technology develops. It is apparent that there are large uncertainties in estimations in literature and this is an area where additional research efforts should focus on.

**Table 1.1:** Algae cost, productivity and concentration comparison between open ponds and photobioreactors. Adapted from Draaisma et al. [23], DW=dry weight.

	Open Ponds	Photobioreactor
Algae production cost (€/kg DW)	12.7	8
Algae productivity (t/ha/year)	14.9	56.6
Algae concentration (g/l)	0.1	1.1

#### 1.4 Processing of Microalgae

One of the challenges for producing microalgal derived biofuels is performing economic extraction of the lipids from the wet biomass before conversion to biodiesel. The lipids can be extracted by solvent extraction or by physical extraction following rupture of the cell wall. These lipids can then be further transesterified to biodiesel in the same manner as terrestrial seed oils [24-25]. One of the problems of this approach is that the wet aquatic biomass requires drying before it can be processed. This is major cost factor and it is unlikely that economic biodiesel production is possible if drying is necessary [26]. The three most common techniques to extract the algal oil are using an expeller/press, solvent extraction and supercritical CO<sub>2</sub> extraction. Mechanical extraction is very simple and can achieve oil extraction of 70-75 wt.% of the total algal oil [14]. The most common chemical solvents used include hexane or chloroform/MeOH mix which is the basis of the total lipid determination method, Bligh and Dyer established in 1959 [27]. The associated problem of solvents is that they are relatively expensive, flammable, harmful and dangerous to the environment. Supercritical CO<sub>2</sub> extraction is more efficient than the former two methods as it can extract almost 100 wt.% of the lipids [14]. Lee et al. investigated possible pre-treatment methods for microalgae before solvent extraction. They investigated autoclaving, bead-beating, microwaves, sonication and an osmotic shock. They found that the most simple, easy and effective pre-treatment method was the use of microwaves. An increase of 20 wt.% lipid extraction by this pre-treatment could be shown [28]. Alternative processing by thermo-chemical methods include liquefaction, gasification

and pyrolysis. Gasification is a process of partial oxidation in high temperatures to produce a syngas. Pyrolysis involves the production of a bio-oil, syngas and charcoal in the absence of air at moderate to high temperatures, although pyrolysis is limited to feedstocks with a maximum of 20 wt.% moisture content. Because of the high water content of microalgae, wet conversion routes offer clear advantages and can result in significant reductions in energy consumption. Wet conversion routes include anaerobic digestion and hydrothermal processing routes. Anaerobic digestion is an approach for delivering gaseous products, and hydrothermal liquefaction is a promising route for delivering liquid products.

### **1.5 Hydrothermal processing**

#### **1.5.1 Introduction**

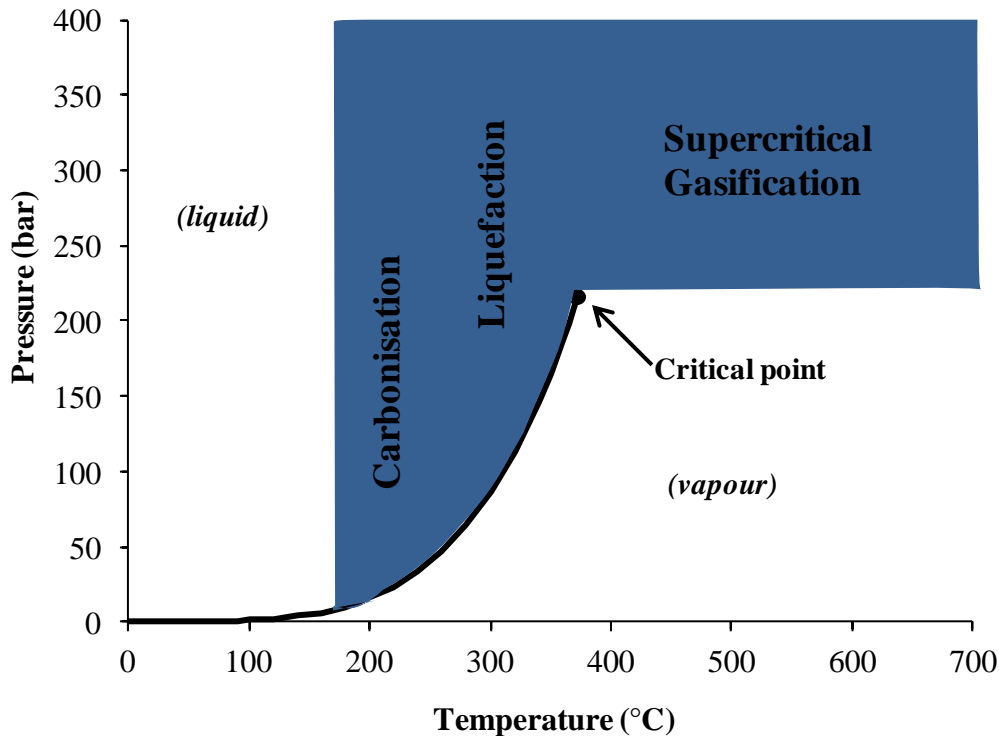
One of the economic and energetic drawbacks in the processing of microalgae is the dewatering stage as microalgae typically only grow to a solids concentration of 1-5 g/l [8]. This makes concentration and drying challenging and energy intensive. Microalgae biofuel is most commonly produced by the extraction of lipids and subsequent transesterification to bio-diesel. Most common lipid extraction techniques require a dry biomass feedstock before transesterification as does conversion to thermal energy or syngas by combustion or gasification. This can account for as much as 25 % of the energy contained in the algae [29]. Hydrothermal processing avoids this step as the algae is processed as a slurry in hot compressed water and does not require drying. Operating conditions vary depending on the desired product. At low temperatures  $<200^{\circ}\text{C}$ , the process is referred to as hydrothermal carbonisation (HTC) and predominantly produces a char. At intermediate temperatures  $\sim 200\text{-}375^{\circ}\text{C}$  the process is referred to as hydrothermal liquefaction (HTL) and predominantly produces an oil. At high temperatures  $>375^{\circ}\text{C}$  hydrothermal gasification (HTG) reactions occur, predominantly producing a syngas. The aim of these hydrothermal processing routes is to generate a product with higher energy density than the feedstock by removal of oxygen. The char produced from HTC can be co-fired with coal or used as a biochar for soil amendment [30], the bio-crude from HTL can be upgraded to a variety of fuels and chemicals while the syngas from HTG can be used for combustion or converted to hydrocarbons by either biological or catalytic processing e.g. Fisher Tropsch synthesis.



Hydrothermal processing essentially simulates the natural processes which have taken place in nature in the production of fossil fuel reserves. All fossil fuel reserves have been created by the transformation of organic matter under pressure and heat over long periods of time. Coal is mainly formed from terrestrial plants while oil and gas is mainly the product of decaying phytoplankton and zooplankton. The process of applying high pressures and temperatures to organic matter in modern hydrothermal processing is therefore a way of speeding up nature's natural pathways to form a renewable fossil fuel. Just as in nature, the state and quality of the resulting fossil reserve is dependent on the severity of the environmental conditions. The products of hydrothermal processing are consequently often referred to as green coal, bio-coal, bio-crude and syngas. Research has been carried out in all of these synthetic hydrothermal pathways and is discussed in the following sections.

Apart from the above mentioned hydrothermal processes, there are some additional wet processing methods which have been used for algal biomass as it is realized that wet extraction techniques offer a distinct energy requirement advantage. Levine et al. for example proposed the in situ lipid hydrolysis of wet algal biomass followed by supercritical transesterification with ethanol [31]. Alternatively Patil et al. have suggested the wet transesterification to fatty acid methyl esters in supercritical methanol [32]. There have also been limited studies on the co-liquefaction of algal biomass with coal or organic solvents to improve the yields and quality of bio-crude [33-34]. However this review will focus on the hydrothermal routes.

Water as a reaction medium has several advantages over chemicals as it is ecologically safe, cheap and readily available. When water is heated and compressed, the hydrogen bonds are weakened resulting in a change in dielectric content, acidity and polarity, each of which can increase opportunities for water to take part in reactions. This leads to water acting as a catalyst, lowering activation energies and allowing reaction pathways which would not occur at ambient conditions. The critical point of water is at 374°C and 22.1 MPa, below this point the vapour pressure curve separates the liquid from the gaseous phase. Approaching the critical point, the density of the two phases become more and more alike and finally identical at the critical point [35]. Above this point, the density of supercritical water is interchangeable without any phase transitions over a wide range of conditions. Depending where in the phase diagram the process conditions are placed determines if HTC, HTL or HTG reaction conditions are met as can be seen in **Figure 1.1**.



**Figure 1.1:** Hydrothermal processing conditions in the water phase diagram; data from *Perry's Chemical Engineers' Handbook* [1]

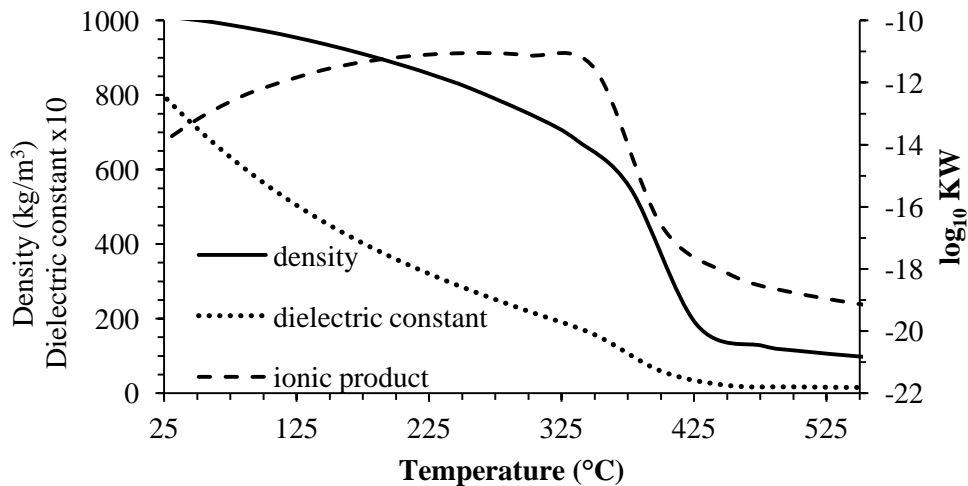
During the carbonisation stage, the carbon concentration of the biomass is increased and the oxygen and mineral matter content are reduced, the gaseous product is low and a biochar is produced by carbonisation reactions. During liquefaction, biomass feedstocks are decomposed to smaller molecules which are reactive and can re-polymerize into oily compounds [36]. The main reaction steps during liquefaction have been summarised by Garcia Alba et al. as follows [37];

1. Hydrolysis of macromolecules (lipids, proteins and carbohydrates) into smaller fragments;
2. Conversion of these fragments by, for example, dehydration into smaller compounds;
3. Rearrangement via condensation, cyclisation, and polymerization producing new larger, hydrophobic macro-molecules.

The products from hydrothermal liquefaction consist of a bio-crude fraction, a water fraction containing some polar organic compounds, a gaseous fraction and a solid residue fraction. At the more severe conditions in HTG, the desired product is a syngas and depending on reaction

conditions, consists of varying amounts of  $H_2$ ,  $CO$ ,  $CO_2$ ,  $CH_4$  and light hydrocarbons. The initial reaction steps are the same as during liquefaction but the more severe conditions lead to the small fragments decomposing even further to low molecular weight gaseous compounds. At high temperatures  $>500^\circ C$   $H_2$  production is favoured while  $CH_4$  production is favoured at  $350$  to  $500^\circ C$  although all these conversion pathways can be influenced with the use of catalysts and pressure [38].

At ambient conditions, the miscibility of water for hydrocarbons and gases is poor but it is a good solvent for salts due to its high dielectric constant of 78.5 [39]. Just below the critical point, the miscibility for hydrocarbons is improved as the dielectric constant is in the range of 10, which would be equivalent to that of dichloromethane, decreasing further in the supercritical region. The change in dielectric constant can be seen in **Figure 1.2** over a range of temperatures at 30 MPa pressure. It can be seen that even at HTC conditions of around  $250^\circ C$ , the dielectric constant has more than halved, increasing the solubility of organics and opening new reaction pathways. The reaction rates in hydrothermal media can be adjusted by means of temperature and pressure as this affects the dielectric constant which influences the activation energy of reactions. Above the supercritical point of water, the miscibility for hydrocarbons and gases is very high making it a good reaction medium for organics and gases. Below the supercritical point, miscibility of these compounds is not complete but increased compared to ambient conditions. When the process products cool back down to ambient conditions, the water and the organic compounds will separate as they are not soluble anymore; this makes distillation or other costly separation techniques unnecessary.



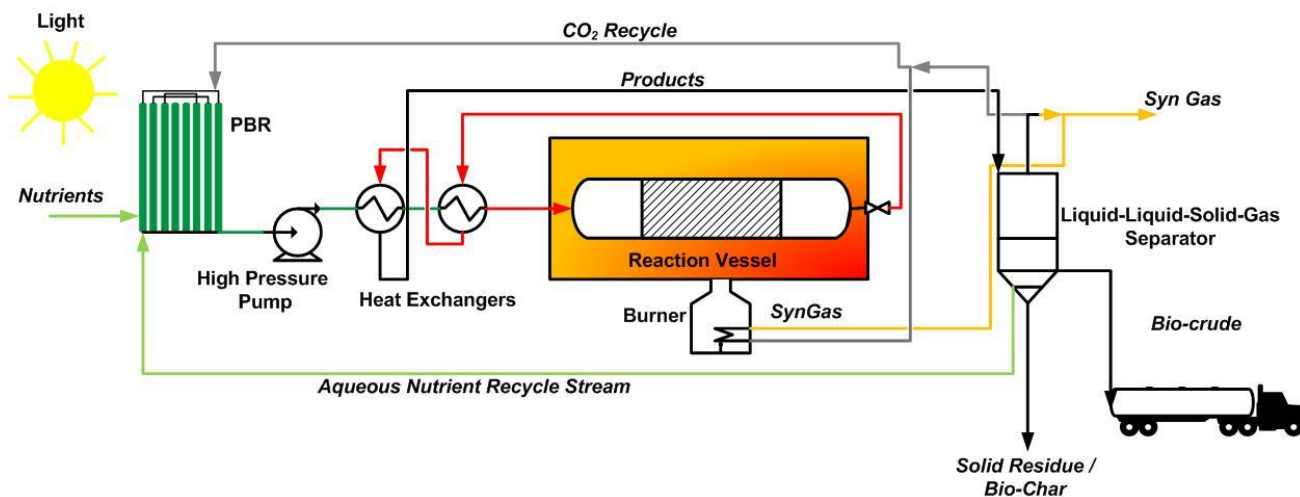
**Figure 1.2:** Density [40], static dielectric constant [41] at 30 MPa and ionic product [42] of water at 25 MPa

At high temperature and pressure below the supercritical point, the ionic product is up to three orders of magnitude higher than under ambient conditions and is plotted on a logarithmic scale in **Figure 1.2**. The high ionic product supports acid or base catalysed reactions and can act as an acid/base catalyst precursor because of the relative high concentrations of  $\text{H}_3\text{O}^+$  and  $\text{OH}^-$  ions from the self-dissociation of water [39]. The advantage of this is that the addition of acid or base catalysts can be avoided. The concentration of ions is at its maximum at  $275^\circ\text{C}$  which is therefore the optimum temperature for acid/base catalysed reactions. Above  $350^\circ\text{C}$  the ionic product decreases rapidly by 5 orders of magnitude or more above  $500^\circ\text{C}$  [43]. The density of water at 30 Mpa over the hydrothermal temperature is plotted in **Figure 1.2** and it can be seen that the most dramatic change takes place in the region of the critical point ( $375^\circ\text{C}$ ). Between  $300$  and  $450^\circ\text{C}$ , the density at 30 MPa changes from a liquid like  $750\text{ kg/m}^3$  to a gas-like  $150\text{ kg/m}^3$ ; however there is no phase change taking place. This change in density directly correlates with properties such as solvation power, degree of hydrogen bonding, polarity, dielectric strength, diffusivity and viscosity [35].

Some of the earliest work on hydrothermal processing was carried out at the Pittsburgh Energy Research Centre in the 1970s-1980s. Their process of biomass liquefaction was based on technology used for lignite coal liquefaction. Some early research into HTL of biomass was performed at the Royal Institute of Technology, Stockholm, the University of Arizona and the University of Toronto. All the early research investigated terrestrial biomass only and algal biomass was first investigated in the '90s. Hydrothermal gasification of biomass is first reported in the USA, at the Massachusetts Institute of Technology. More information about the history of the process development can be found in D.C. Elliott's recent chapter of Robert C. Brown's book "*Thermochemical Processing of Biomass*" [44].

Hydrothermal processing of lignocellulosic biomass has received much more attention than algal biomass and has been extensively reviewed by Peterson et al. and Toor et al. [35, 45]. Terrestrial biomass consists mainly of cellulose, hemi-cellulose and lignin while algae consist of varying amounts of protein, starch like carbohydrates and lipids. If the algae is from a marine origin it typically contains large amounts of ash as salts and other mineral matter, some strains can have ash contents as high as 60 wt.% on a dry basis. Macroalgae are typically higher in carbohydrate and much lower in lipid content compared to microalgae, and if from a marine environment can be very high in ash content [46]. This can affect hydrothermal reactions and presents a significant difference to terrestrial biomass which is typically low in ash content. The different biochemical components undergo different reaction pathways in hydrothermal media and have previously been reviewed [35, 45].

**Figure 1.3** describes an idealized closed loop HT concept with integrated nutrient recycling for algae cultivation. **Figure 1.3** depicts a photo-bio reactor for microalgae cultivation where nutrients, water, light and CO<sub>2</sub> are the only required inputs. A similar concept could be described for open pond cultivation or for macroalgae where the cultivation layout could include growth in marine environments. It is important to note that whilst the algal biomass is processed wet in hydrothermal processing, some dewatering is still required. Low cost dewatering is more challenging for microalgae than macroalgae but many processes are available such as flocculation. Algae is grown, harvested and dewatered to produce a slurry with a higher solid content. Subsequently the slurry is processed in hot compressed water to produce the desired primary energy product. The product phases include a gaseous fraction, process water, solid residue and a bio-crude. The amounts of each fraction depend on both the temperature and pressure of operation and the amount of biomass in the slurry. The solids:water ratio of the feedstock can be altered to the specific requirements and capabilities of the processing facility. When the solids content of the slurry is higher, the amount of water per mass of algae to be heated is less; reducing the energy requirements but at the same time more energy is spent in dewatering. One advantage of hydrothermal processing of algal biomass is that nutrients such as nitrogen, which are concentrated in the process water, can potentially be recycled [47-48]. The amount of nutrients in the process water varies with hydrothermal conditions and feed composition. In HTC and HTL, the gaseous fraction contains predominantly CO<sub>2</sub> and can potentially be recycled to the cultivation step. In HTG, the syngas could be converted to a liquid fuel by Fischer-Tropsch after separation of CO<sub>2</sub> and clean up or burnt in a gas turbine directly. The bio-crude produced by HTL can be further upgraded to produce fuels and chemicals. The solid residue, which still contains some nitrogen and minerals depending upon processing conditions, may be used as a fertilizer, as a fuel or as a biochar. Most of the current research and development into hydrothermal processing of algal biomass fits somewhere into this idealized concept. The technology is still very much in the research stages, most of which are still based on a laboratory scale and there are still many uncertainties and challenges associated with each of these process options. The following sections summarise the current state of research on the hydrothermal processing of micro and macro algae. Process conditions, feedstock, products, energy balance considerations and nutrient recycling possibilities are all discussed.



**Figure 1.3:** Schematics of an integrated HT process with nutrient and CO<sub>2</sub> recycle

### 1.5.2 Hydrothermal Carbonisation (HTC)

Hydrothermal carbonisation is the mildest of the three routes, processing temperatures range from 150-250°C but often the residence time can be significantly longer (>1 hr). The principle aim of HTC is to concentrate the carbon in a stable, easy to handle material; therefore upgrading poor fuels into higher energy density solid fuels. The char material is reported to have good nutrient properties for terrestrial plants and has been proposed as a source of biochar for soil amendment but could also potentially be co-fired with coal [49-50]. The applications of char from hydrothermal carbonisation for novel materials is also of interest and many studies have produced functionalized carbons with applications in water purification, fuel cell catalysis, energy storage, CO<sub>2</sub> sequestration, bio-imaging, drug delivery and gas sensors. The different applications of HTC biochar have been summarised in a recent review by Bo Hu et al. [51]. The first reported experiments on HTC were performed in 1913 by Bergius who processed cellulose with the aim of producing a coal like material [52]. Interest in HTC of lignocellulosic materials has received increased interest in recent years [53-55] while there are only limited reports of HTC of algal biomass. Heilmann et al. have recently published their research in two separate papers on the subject [56-57]. Three types of microalgae; *Chlamydomonas reinhardtii*, *Dunaliella* and an undisclosed algae from Inspired Fuels, Inc (Austin, TX) were processed in a batch 450 ml stirred reactor. Operating conditions were 5-25 wt.% solids, 190-210°C for 0.5-2 hours. It was found that the lipids of microalgae were adsorbed on the char product and could be separated by solvent extraction for further processing. Carbon recovery yields

in the char ranged from 20-60 wt.% depending on algae strain and operating conditions. It was shown that cyanobacteria produce higher carbon containing chars but lower yields while blue green algae with less strong cell walls enhanced char formation. The char produced was of similar energy content to a bituminous coal although the nitrogen content was found to be 5-7 wt.% which would be problematic in terms of NO<sub>x</sub> emissions. The authors highlighted the advantages of the process wherein no extensive concentration of the algae is necessary, the oil fraction is obtained by simple solvent extraction and the aqueous co-products can be used for nutrient recycling. Yu et al. processed *Chlorella pyrenoidosa* for bio-crude production but also investigated low processing temperatures of 100-250°C giving insight into carbonisation behaviour as the water insoluble fraction was analysed prior to bio-crude separation using toluene [58]. It was found that below 180°C, the residue appeared as green algal cake and only above this temperature did the char appear as a black solid, indicating the onset of carbonisation. The carbon recoveries at these temperatures were very high reaching 70-80 wt.% while already around 30 wt.% of the nitrogen was partitioned to the water phase. This could be beneficial for recycling of nutrients for algae cultivation. When the solid residue was separated from the bio-crude using solvents it was shown that the carbon distribution to the bio-crude surpasses that of the char at around 210°C.

A significant factor to consider is that under HTC conditions, the protein breakdown to bio-crude will not have occurred resulting in concentration of nitrogen in the char rather than the oil fraction. The drawback of HTC of microalgae is that the primary product, char is currently of low commercial value although new applications of this char may make this process more attractive. To date microalgae are still expensive to cultivate and potentially demand the extraction of high value chemicals and fatty acids before processing [8, 19]. Therefore the authors are of the opinion that carbonisation of the entire microalgae without prior extraction of valuable components is less feasible but processing of residues, lower lipid algae such as macroalgae or problematic algal blooms could be more feasible. Results regarding the potential of algal biochar in soil amendment or as a carbon sink are not available and should be the focus of future research.

The hydrothermal carbonization of macroalgae has received less attention however the work reported by Anastasakis et al. operating at the higher end of the HTC temperature range of 250°C shows some insight into its behaviour [59]. A char yield of 25 wt.% is achieved at 250°C with a heating value of 15.9 MJ kg<sup>-1</sup>, indicating slight upgrading. Increasing the processing temperature, decreases the carbon content and increases the ash content, resulting in chars with lower heating value. Lower biomass and water feeds favour char formation and ash removal, a char with a heating value of 22.8 MJ kg<sup>-1</sup> was produced at 350°C with a 52 wt.% carbon content and 26 wt.% ash

content indicating removal of mineral matter. Macroalgae contain many water soluble components such as laminarin and mannitol and the water phase is typically high in soluble organic carbon after hydrothermal processing.

### 1.5.3 Hydrothermal Liquefaction (HTL)

The vast majority of research into hydrothermal processing of algae has been conducted in the intermediate temperature range (HTL) where the primary product is bio-crude. A summary of the published results on HTL without the presence of a catalyst are presented in **Table 1.2**. Bio-crude is a viscous, black crude oil like material with a heating values of around 30-38 MJ/kg. The bio-crude or bio-oil is thought to be suitable to process in conventional crude oil refineries either mixed with crude or separately. This would reduce the tail end emissions of the whole product range of the refining process, as the CO<sub>2</sub> emitted was previously taken from the atmosphere by photosynthesis of the algae. There have been some attempts at upgrading the bio-crude by hydro-treating/hydrogenation followed by cracking and distillation and also some work on supercritical catalytic upgrading; however these areas have not been investigated as much as the initial bio-crude production stage [60-62]. Alternatively the bio-crude could be directly combusted in boilers as a heavy fuel although the NO<sub>x</sub> emissions due to the fuel bound nitrogen in the bio-crude would likely pose a problem. The liquefaction process was first extensively researched in the 1970-80s at the Pittsburgh Energy Research Centre and more recently Shell in the Netherlands tried to develop the commercialization of the hydrothermal upgrading process (HTU) with the aim of producing liquid biofuels from terrestrial biomass [35].

The earliest reported HTL of microalgae was carried out in the early '90s at the National Institute for Resources and Environment in Tsubaka, Japan. The group led by Prof. Minowa published four papers in this period which laid the foundations of microalgae HTL research [63-66]. In their first publication in 1993, *Botryococcus braunii* was processed in a stirred reactor for 1 hr at 200-340°C [63]. This strain exhibits a very high oil content of 50 wt. % dry basis resulting in a yield of bio-crude as high as 58 wt. % at 300°C without the use of a catalyst. The bio-crude yield was found to be higher than the lipid content leading to the conclusion that bio-crude was being formed also from the carbohydrate and protein fraction. At 300°C, the elemental composition was found to be most favourable. There was no oxygen and only 0.9 % nitrogen in the bio-crude leading to a Higher Heating Value (HHV) of 50 MJ/kg exceeding that of crude oil. This HHV value and the H/C ratio



of 2.1 is extremely high and is not typical of the studies performed since, which are usually between 30-40 MJ/kg and H/C 1.3-1.6 respectively. At higher temperatures, the nitrogen content increases suggesting the onset of protein breakdown. *B. braunii* exhibits an extremely high oil content and a low protein content, resulting in 2.8 wt.% nitrogen in the algae. Following their initial research results, the group published a paper focusing on the analysis of the bio-crude derived from *B. braunii* [64]. The maximum recovery of hydrocarbons (botryococenes) from the algae was observed at 200°C while at higher temperatures, the hydrocarbons started to degrade to smaller molecular weight hydrocarbons. At the highest temperature (350°C), higher molecular weight oxygenated hydrocarbons were observed which were attributed to the formation of bio-crude from non lipid fractions of the algae. In two further studies, the authors processed a marine microalgae strain, *Dunaliella tertiolecta*. This strain exhibits a high protein content on an ash free basis of 64 wt.% but still contains a relatively high lipid content of 20.5 wt.%. The bio-crude yield was found to be much lower than that of *B. braunii*, with less favourable nitrogen and oxygen contents of around 7 wt.% and 11 wt.% respectively. This consequently led to a lower HHV.

The effect of operating conditions on the HTL of microalgae has been the focus of several studies [37, 59, 67-70]. Jena et al. investigated the effect of operating conditions on the HTL of *Spirulina platensis* [67]. Experiments were carried out in a 1.8 l stirred batch reactor. Operating temperatures were varied from 200 to 380°C with holding times up to 120 min and solids concentrations of 10-50 wt.%. It was found that the highest bio-crude yield could be achieved at 350°C, 60 min holding time and 20 wt.% solids. This led to a bio-crude yield of 39.9 wt.% and a HHV value of 35.3 MJ/kg. Increasing the temperature resulted in additional de-oxygenation of the bio-crude, however the nitrogen content increased. The holding time and the solid loading had less effect on the oxygen and nitrogen content. The bio-crude yield increased with holding time by around 10% from 0 to 60 min. The solid loading had almost no effect on any of the parameters. Reactions with higher solid loading have an improved energy balance as less water to be heated although this must be offset against the additional energy invested to achieve the high solids concentration. This will be discussed in more detail in **Section 1.5.6**. In a similar study, Yu et al. investigated the HTL of the low lipid microalgae *Chlorella pyrenoidosa* (0.1 wt.% lipids) as the biomass productivity of low lipid algae is often much higher than that of high lipid strains [69]. The effect of reaction temperature and holding time on the bio-crude yield was studied at a 20 wt.% solids concentration. It was found that the highest refined oil yield was achieved at 280°C and a reaction time of 120 min. The elemental composition of the oil is not discussed but the HHV at the above process conditions was 35.4 MJ/kg; however at 300°C and 30 min reaction time, the HHV increased to 38.5 MJ/kg

suggesting a lower oxygen content in the oil. Brown et al. (2010) investigated the effects of temperature on the bio-crude and gas formation of *Nannochloropsis sp.* at a constant residence time of 60 min. Temperatures of 200-500°C with 50°C steps were investigated [68]. The highest bio-crude yield was observed at 350°C while higher temperatures favoured gasification reactions. At 350°C, the bio-crude yield was found to be 43 wt.% with a heating value of 39 MJ/kg, the gas yield was 1.8 mmol/g and HHV of 4.2 MJ/kg leading to a maximum energy recovery of 78%. Similarly, Jena et al. (2011) also observed that de-oxygenation increases at higher temperatures but the levels of nitrogen in the bio-crude increases due to the onset of protein breakdown; there is therefore a trade-off between high O and high N in the bio-crude. This decision is most likely dependant on the desired end product and its use.

Garcia Alba et al. (2011) published a detailed study of the hydrothermal treatment of microalgae (*Desmodesmus sp.*) in two separate publications. The first focuses on the HT processing conditions with varying temperature (175-450°C) and reaction times (0-60 min) [37] while the second investigates the molecular characterization of the obtained bio-crude in detail for different process conditions [71]. It was concluded that a maximum bio-crude yield is achieved at 375°C and 5 min reaction time, achieving a bio-crude yield of 49 wt.%. The bio-crude exhibited a HHV of 35 MJ/kg, corresponding to an energy recovery of 75%. Garcia Alba et al. are the first to visually inspect the microalgae cells pre and post HTL by scanning electron microscopy. This allowed the extent of cell rupture at respective conditions to be investigated. The largest step change in bio-crude yield was achieved from 225 to 250°C which was shown to coincide with a major visual breakage of cells after 5 min. The cells at 175°C appeared virtually intact with some clustering, at 200°C, additional clustering and some solid residue/precipitate was observed but the cells still remain largely intact. At 225°C a strong cell clustering effect could be observed with deformed cells, above 250°C no individual cells were recognisable. It was concluded that the thermal breakage of cells at 250°C allows additional bio-crude to be formed and extracted leading to a large decrease in solid residue. In this study, the elemental composition and product fractionation as a function of operating conditions was also investigated. The largest step change in N content in the bio-crude for shorter reaction times (5 min) occurred at 200-225°C while at the longer reaction residence times (60 min) it was at the lower temperature of 175-200°C. This indicates the conditions where the onset of protein breakdown begins. The nitrogen content continues to increase with increasing operating temperature, while the oxygen content decreases in agreement with previous work [67-68]. Garcia Alba et al. conclude that operating conditions are largely dependent on the desired product; if a lipid rich oil is preferred, operating temperatures should not exceed 250°C but if crude-like oil is desired,

temperatures as high as 375°C could be used. In an accompanying publication the bio-crude fraction was investigated in detail by a number of analytical techniques giving insight into reaction pathways involved at different operating conditions and their resulting molecular bio-crude compounds. In brief, it was shown that below 250°C, the bio-crude consist mainly of lipids and some short chain algaenan and hydrophobic protein fragments. At harsher conditions, the onset of protein and carbohydrate breakdown results in increased amounts of cyclic dipeptides, furans and asphaltene like material. Full discussion of the molecular characterization of the bio-crudes is beyond the scope of this review but the publication provides more information [71].

Whilst the main focus has been directed towards microalgae, some notable investigations have been performed on macroalgae. Anastasakis and Ross (2011) investigated the influence of reaction conditions on the HTL of the brown macro-algae *Laminaria saccharina* [59]. Macro-algae generally exhibit a low lipid content, and higher carbohydrate content but they typically have a lower HHV due to the high ash content [46]. HTL was performed in a 75ml batch reactor; reaction variables included temperature (250-370°C), residence time (15-120 min) and biomass/water ratio. Optimum reaction conditions were found to be 350°C and 15 min with a 1:10 biomass water ratio (19.3 wt.% bio-crude yield). The bio-crude was described to be similar to heavy crude oil with a HHV of 36.5 MJ/kg but contains higher nitrogen and oxygen contents of 4.9 and 5.4 wt.% respectively. The oxygen content in the bio-crude was lowest at shorter residence times (15min) and increased with increasing residence time in agreement with the observations of Brown et al. and Jena et al. [67, 72]. An elemental balance on C, N, Ca, Mg, Na and K was made on the different product streams. It was shown that around 50 wt.% of elemental C results in the bio-crude with the rest distributed almost equally in the solids, water and gas phase. Elemental N was found to be predominantly present in the aqueous phase but still 40 wt.% in the bio-crude. The metals Na and K almost entirely resulted in the aqueous phase while Ca and Mg resulted in the residue. It was concluded that the dissolved sugars in the aqueous phase could be further utilized by fermentation and the large amounts of K and other minerals dissolved in the water could be a source of fertilizer. In a similar study, Zhou et al. investigated the macroalgae *Enteromorpha prolifera* [70]. The temperature was varied from 220-320°C and the reaction time adjusted between 5 and 60 min. The highest bio-crude yield without the use of catalyst was measured at 300°C and a reaction time of 30 min. This is 50°C cooler and 15 min longer than the optimum conditions Anastasakis and Ross observed. The discrepancy is most likely due to the different feedstock. There is also a notable difference in the oxygen content of the bio-crudes between the two studies. Zhou et al. found the

bio-crude to contain 22.5 wt.% oxygen leading to a HHV of only 28 MJ/kg compared to 36.5 MJ/kg for Anastasakis and Ross.

Recently Prof. Chen's research group at the University of Washington has developed a novel two-step sequential HTL technology (SEQHTL) for the extraction of value-added polysaccharides followed by bio-crude production [73-74]. This is an interesting approach as the extraction of high-value compounds from algal biomass is an aspect that could favourably distinguish it from terrestrial biomass. The first step involved mild hydrothermal processing (160°C) and removal of the polysaccharides rich water extract and precipitation with ethanol. The residue was subsequently processed at 300°C to produce a bio-crude. It was found that polysaccharides could efficiently be extracted at mild hydrothermal conditions of 160°C and 20 min, yielding 32 wt.% polysaccharides from a total of 46 wt.% polysaccharides present in the *Spirulina* biomass. The subsequent yield of bio-crude was found to be 5 wt.% higher than with direct HTL and the bio-char yield was reduced by 50 wt.%. Additionally the second step HTL required lower temperatures (240°C) to achieve similar maximum yields observed from direct HTL at 300°C. Although there is an additional step involved, and the use of an organic solvent to recover the polysaccharides is required, this technique appears promising as the energy input was calculated to be 15 MJ less, per kg bio-crude produced, than for direct HTL. The only other study where an attempt was made to extract high value compounds was by Vardon et al. who extracted the lipid content of *Scenedesmus* prior to HTL and compared the results from defatted and raw algal biomass [75]. The lipids were recovered by Soxhlet extraction of the dry biomass with hexane and the residue subsequently hydrothermally processed. Especially polyunsaturated fatty acids have high value but alternatively the lipids could also be used for biodiesel production. The liquefaction yield from the defatted algae was found to be around 10% lower and also exhibited a higher nitrogen content; nevertheless the extraction of fatty acids prior to HTL or HTG is an attractive approach.

Summarizing the published papers on HTL of algae show that a high bio-crude yield (~35 wt. %) is obtained which is a highly viscous oil with relatively high nitrogen content (~5 wt %) and HHV of around 35 MJ/kg (see **Table 1.2**). It appears that the optimum operating conditions for maximum bio-crude yield lie somewhere between 300-350°C and around 15 min. However the operating conditions are highly strain and system specific. If a bio-crude of lower nitrogen and higher lipid content is desired, lower operating conditions should be used or the protein fraction removed prior to HTL in a biorefinery concept. Alternatively value-added compounds can be extracted as demonstrated by Miao et al. and Vardon et al. and bio-crude produced subsequently [73-75]. All results to date are on batch systems and unfortunately no data is available on continuous reaction

systems. The majority of studies have used organic solvents to recover the bio-crude fraction which is perhaps not necessary in a continuous process. The use of solvents increases the bio-crude recovery and will affect the water phase composition. Therefore the batch experiments only give limited insight into a continuous process; despite this, the studies are useful as the optimum operating conditions and reaction pathways are reported.

**Table 1.2:** Summary of HTL studies using only water, no catalyst

Reference	Algae Species	Temp. (°C)	Time (min)	Biomass conc. (%wt)	Max Bio-crude Yield (%)	Comments
<i>Biller &amp; Ross</i> [76-77]	<i>Chlorella</i> , <i>Spirulina</i> , <i>Nanno.</i> , <i>Proph.</i> , <i>CX68</i> , <i>Scene.</i>	300, 350	60	10	35	Effect of biochemical composition on bio-crude is discussed. High lipid >protein>carbohydrate favourable.
<i>Brown et al.</i> [72]	<i>Nannochloropsis</i> sp.	200- 500	60	5.5	43	Max oil yield at 350°C, 75% C in bio-crude and 90% total energy recovery.
<i>Jena et al.</i> [48]	<i>Spirulina platensis</i>	100- 380	0-120	10-50	40	Highest yields at 350°C and 60 min holding time
<i>Vardon et al.</i> [75, 78]	<i>Spirulina</i> , <i>Scendesmus</i>	300	30	20	45	Focus on composition of bio-crude, compared to sewage sludge, swine manure and defatted algae. Algae found to be the favourable feedstock.
<i>Yu et al.</i> [58, 69]	<i>Chlorella pyrenoidosa</i>	200- 300	0-120	20	39	Max bio-crude yield at 280°C for 120 min
<i>Anastasakis and Ross</i> [59]	<i>Laminaria Saccharina</i>	250- 375	15-120	2-20	19	Max bio-crude yield at 350°C and 15 min
<i>Zhou et al.</i> [70]	<i>Enteromorpha prolifera</i>	220- 320	5-60	13	20	Max bio-crude yield at 300°C 30 min
<i>Minowa et al.</i> [63-66]	<i>Botryococcus braunii</i> , <i>Dunaliella tertiolecta</i>	250- 340	5-60	20	57	Yields of 57% for <i>B. braunii</i> and 37% for <i>D. tertiolecta</i>
<i>Yang et al.</i> [79]	<i>Microcystis viridis</i>	300- 340	30-60	5	28	30 min and 340°C suggested optimum operating conditions
<i>Li et al.</i> [80]	<i>Sargassum patens</i>	320- 380	5-90	3-17	32	Max yield at 340°C and 15 min, HHV of 27 MJ/kg
<i>Yu et al.</i> [58, 69]	<i>Chlorella pyrenoidosa</i>	200- 300	0-120	20	39	Max yield at 280°C and 120 min
<i>Garcia Alba et</i>	<i>Desmodesmus sp</i>	175-	5-60	7-8	49	375°C, 5 min max yield.

al. [37, 71]		450				Detailed analysis and discussion on cell wall ruptures, bio-refinery concept and oil characterization
Zou et al. [81]	<i>D. tertiolecta</i>	280-380	10-90	10	25	Most severe conditions gave highest yield
Miao et al. [73-74]	<i>Chlorella sorokiniana</i>	220-300	5-60	8-33	31	Two step sequential HTL with extraction of polysaccharides was investigated and gave promising results.

#### 1.5.4 Catalytic HTL

The idea of incorporating catalysts in HTL rests on the potential of increasing yields and reducing oxygen and nitrogen content and viscosity. The majority of research into catalytic HTL was performed using homogenous catalysts, i.e. catalysts soluble in water. The most widely investigated homogeneous catalyst is  $\text{Na}_2\text{CO}_3$  with six different groups investigating its effect on HTL. Only three articles have been published using heterogeneous catalysts. A summary of the published research on catalytic HTL of algae is presented in **Table 1.3**.

The group of T. Minowa again performed the earliest work using homogenous catalysis in HTL. They used concentrations of 5 wt.% sodium carbonate in their studies on *B. braunii* and *D. tertiolecta* [64-65]. It was observed that the bio-crude yield of *B. braunii* was increased with the use of catalyst by around 5 wt.% at 300°C but decreased by around 10 wt.% at 200 and 340°C. Additionally the oxygen content was decreased at 200°C with the use of sodium carbonate but increased at the higher temperatures of 300 and 340°C. The authors highlighted that the effect of the catalyst was not very strong although it was quite distinct when processing wood and sewage sludge. In a further study, these results were confirmed with the algae *D. tertiolecta* which also exhibited a 5 wt.% increase in yield with addition of sodium carbonate. Yang et al. also investigated 5 wt.%  $\text{Na}_2\text{CO}_3$  at 300°C, 340°C and 30 and 60 min holding times [79]. It was found that the effect of the catalyst was stronger at the lower temperature and especially at the shorter residence time. Zhou et al. observed similar results using sodium carbonate with slight increases in bio-crude yield and decreases in solid residue, a slight decrease in oxygen content of the bio-crude was also observed [70].

The results from Anastasakis and Ross on the HTL of *Laminaria saccharina* showed that the use of potassium hydroxide in concentrations of 0-100 wt.% loading consistently decreased the bio-crude yield and increased the amount of water soluble products [59]. A further study by Zou et al. obtained similar results to previous researchers with the use of different sodium carbonate loadings on the HTL of *D. tertiolecta*; the increase in bio-crude was < 5 wt.%, parameters such as temperature and holding time were shown to have much larger effects [81-82]. A recent study by Jena et al. investigated the use of Na<sub>2</sub>CO<sub>3</sub>, Ca<sub>3</sub>(PO<sub>4</sub>)<sub>2</sub> and NiO on the HTL of *Spirulina platensis* [83]. This paper shows the largest increase in yield with the use of Na<sub>2</sub>CO<sub>3</sub> of 10 wt.% which has previously not been reported before by other groups. The use of the calcium and nickel catalysts both increased the gas yields and decreased the bio-crude formation. The discrepancy of the high yields using sodium carbonate compared to other studies is not clear but could be due to the high carbohydrate and protein content of the algae strain investigated.

It appears that the use of homogeneous catalysts do not have a particularly beneficial effect on bio-crude yields and properties especially if the additional cost is taken into consideration. Recovery of the homogenous catalysts also poses a problem. Therefore two groups have performed research on heterogeneous catalysts. These could potentially have advantages over homogeneous catalysts as they are easily recoverable although stability and poisoning of catalysts under hydrothermal conditions pose a challenge [84]. On the other hand, the mass transfer of reactants with the catalyst is more difficult to achieve with heterogeneous than homogeneous catalysts. The most extensive report on the influence of heterogeneous catalysis on HTL was published by Duan and Savage (2010) who investigated six different catalysts supported on carbon, Al<sub>2</sub>O<sub>3</sub> support and a zeolite [85]. Palladium, Platinum and Ruthenium on carbon as well as Nickel and Cobalt-Molybdenum on alumina and a zeolite were investigated in a helium and a hydrogen atmosphere. It was shown that the bio-crude yields from *Nannochloropsis sp.* at 350°C for 1 hour were increased by all catalysts. The maximum yield was achieved for the Pd/C; 57% compared to 37 wt.% with the use of water alone. The bio-crude yields of all the other catalysts were essentially the same ranging from 45-50 wt.%. It was highlighted that the bio-crude catalysed by Pt, Pd, Ru and CoMo exhibited an apparent lower viscosity and lighter colour than the un-catalysed or zeolite-catalysed samples. The bio-crude from Ni catalysed HTL had a dark red colour. The effect on heating value and heteroatom removal was negligible, although the H/C ratio was increased with the use of the noble metal catalysts while the presence of Nickel, Pt and CoMo decreased the O/C ratio. It was concluded that catalytic deoxygenation or hydrodeoxygenation is being promoted. Processing the microalgae in a reducing atmosphere (H<sub>2</sub>) did not result in significant hydrogenation of the bio-crude; from the results

presented by Duan and Savage this route does not seem particularly beneficial. Analysis showed that the different catalysts had different effects on gas yields and composition. H<sub>2</sub> and CH<sub>4</sub> yields were increased with the use of Ni and Ru while zeolite was the only catalyst to produce N<sub>2</sub> which was attributed to the catalytic decomposition of NH<sub>3</sub>. The potential of heterogeneous catalysis in HTL of algae appears very promising especially when the carbon recoveries reported by Duan and Savage are considered; the elemental carbon recovery in the bio-crude using a heterogeneous catalyst exceeds 90 wt.% compared to 62 wt.% without catalysts. However there are still significant challenges that need to be addressed. Research on the recovery, stability and reusability of heterogeneous catalysts has not been reported and is an area where further work is required [84]. Moreover none of the catalysts were able to significantly reduce the amount of N in the bio-crude.

**Table 1.3:** Summary of published literature on Catalytic HTL

Reference	Algae Species	Catalyst	Cat. Conc. (wt.%)	Atmos	Bio-crude Yield (wt.%)	Comments
Minowa et al. [63, 65]	<i>B. braunii</i> , <i>D. tertiolecta</i>	Na <sub>2</sub> CO <sub>3</sub>	0-5	N <sub>2</sub>	22-64	Yield increased with cat loading from 0- 5% Na <sub>2</sub> CO <sub>3</sub> .
Yang et al.[79]	<i>Microcystis v.</i>	Na <sub>2</sub> CO <sub>3</sub>	5	N <sub>2</sub>	25-34	Best results at 340°C 30 min 5% with alkali catalyst
Zhou et al. [70]	<i>Enteromorpha prolifera</i>	Na <sub>2</sub> CO <sub>3</sub>	5		25	A moderate T=300°C with 5 wt % Na <sub>2</sub> CO <sub>3</sub> and reaction time of 30 min led to the highest bio-oil yield of 25 wt %.
Zou et al. [81]	<i>D. tertiolecta</i>	Na <sub>2</sub> CO <sub>3</sub>	0-10	Air	26	A maximum bio-crude yield of 26% is obtained at a reaction T= 360°C, t= 50 min using 5% Na <sub>2</sub> CO <sub>3</sub>
Ross et al. [47, 77]	<i>Chlorella</i> , <i>Spirulina</i> , <i>Nannochloropsis</i> , <i>Prophydridium</i>	Formic acid, Acetic acid, KOH, Na <sub>2</sub> CO <sub>3</sub>	1M	Air	~20	Higher yields with organic acids but additional HV added. Organic acids give better quality oil.
Biller et al. [76]	<i>Nannochloropsis</i> , <i>Chlorella</i>	Pt/Al, CoMo/Al, Ni/Al,	20	Air	18-40	Yields increased slightly with catalysts but HHV increased by 10%. Different catalysts affect proteins, carbohydrates and lipids differently
Anastasakis and Ross [59]	<i>Laminaria Saccharina</i>	KOH		0-100 Air		Very small effect of KOH, slight increase in water soluble fraction.
Duan and Savage [85]	<i>Nannochloropsis sp.</i>	Pd/C, Pt,C, Ru/C, Ni/SiO <sub>2</sub> -Al <sub>2</sub> O <sub>3</sub> , CoMo/y-Al <sub>2</sub> O <sub>3</sub> , Zeolite	50	He/H <sub>2</sub>	35-58	No hydrogenation by high pressure H <sub>2</sub> , highest yields with Pd>CoMo>Ni>Ru>zeolite>H <sub>2</sub> O



Jena et al. [83]	<i>Spirulina platensis</i>	Na <sub>2</sub> CO <sub>3</sub> , Ca <sub>3</sub> (PO <sub>4</sub> ) <sub>2</sub> , NiO	5%	N <sub>2</sub>	30- 52	Na <sub>2</sub> CO <sub>3</sub> increased the yield by 10 %, Ni and Ca <sub>3</sub> (PO <sub>4</sub> ) <sub>2</sub> increased gasification.
---------------------	----------------------------	--	----	----------------	-----------	---

### 1.5.5 Hydrothermal Gasification (HTG)

Hydrothermal gasification occurs in the higher temperature region above the supercritical point where water is in the supercritical state. The primary product now becomes a syngas high in combustible gases such as H<sub>2</sub>, CH<sub>4</sub>, CO and light hydrocarbons (C<sub>2</sub>-C<sub>3</sub>); however there is also CO<sub>2</sub> produced. The energy requirements to obtain the water in its supercritical state are higher than the subcritical due to the higher operating temperatures required. Calzavara et al. evaluated the thermodynamic energy yield based on their experimental results for corn starch and on thermodynamic calculations and concluded that with integrated heat recovery an energy yield of 76% could be achieved [86]. This however assumes no heat losses.

To date there are a total of seven studies on the HTG of algal biomass which are summarised in **Table 1.4**. HTG has a number of advantages over HTL, namely the produced fuel is nitrogen free allowing the use of high protein microalgae. The organic carbon found in the water phase is also much lower than for HTL, which could increase the carbon efficiency [87-88]. However the larger energy requirements to reach higher temperatures are a drawback. The foundation work on HTG of algae was carried out by Minowa and Sawayama who took a visionary approach in 1999 when they first investigated the possibility of recycling the aqueous phase to supply the nutrients required for algae cultivation [89]. *Chlorella vulgaris* was gasified with a nickel catalyst at 350°C, the gas phase was analysed and the water phase was used to grow the algae strain in the recovered aqueous phase. The most favourable results were achieved with a maximum catalyst loading of 50 wt%; the carbon conversion to gas was found to be 70% with a methane yield of 50 vol.%. Lower catalysts loadings were shown to produce larger amounts of H<sub>2</sub> and less methane.

Stucki et al. from the Paul-Scheerer Institute in Switzerland proposed an elegant theoretical continuous process for hydrothermal gasification of microalgae. The concept is to preheat the algae slurry to supercritical conditions whereby the salts have a very low solubility in water so that they are precipitated and separated in a kind of reverse-flow gravity separator [90]. The organics and water then pass to the catalytic reactor where gasification and methanation occurs over different ruthenium catalysts. The concept of the salt separator is that the organic sulphur does not produce

hydrogen sulphide (which is a strong catalyst poison) but to precipitate to sulphide salts in its appropriate pH range. The approach is to recover all nutrients as ammonium, sulphide and phosphate before the organic fraction enters the catalytic reactor and can be used to feed algae cultivation. Results from the proposed novel continuous process are not presented but a series of batch experiments with varying loadings of Ru on activated coconut carbon and zirconia, varying feed concentrations and retention times was presented and discussed. Complete gasification was achieved with both Ru/C and Ru/ZrO<sub>2</sub> at a catalyst to biomass ratio of 8. Many of the batch experiments came close to the chemical equilibrium calculations concerning the methane yield (43.5 vol.%), however this was only achieved with high catalyst loadings. The highest yields of C<sub>1</sub>-C<sub>3</sub> products was achieved with the Ru/ZrO<sub>2</sub> catalyst of around 32 wt.%. It was shown that complete gasification of the algae was possible with 60-70% of the chemical energy in the algae recovered as methane. It was also highlighted that there are still challenges concerning catalyst poisoning and excess catalyst loadings were necessary to achieve complete gasification. In another study by the Swiss group the microalgae *Phaeodactylum tricornutum* was gasified over a Ru/C catalyst [88]. Again it was shown that algae-released sulphur, adversely affected the catalyst performance. The carbon gasification efficiencies were lower, only reaching a maximum of 74% with a low feed concentration. Higher feed concentrations resulted in lower carbon gasification efficiencies and this was attributed to the higher ratio of free sulphur to ruthenium sites on the catalysts. In the batch system, a number of catalyst sites had to effectively be sacrificed for the poisonous sulphur heteroatoms. The possibility for recycling nutrients for algae growth is also discussed in this concept.

Chakinala et al. investigated the catalytic gasification of *Chlorella vulgaris* and the influence of temperature and residence time [38]. The catalysts investigated included Ru/TiO<sub>2</sub>, NiMo/Al<sub>2</sub>O<sub>3</sub>, PtPd/Al<sub>2</sub>O<sub>3</sub>, CoMo/Al<sub>2</sub>O<sub>3</sub>, Inconel powder and nickel wire. The reaction temperature was varied between 400 and 700°C while the retention time was changed from 1 to 15 min. The experiments were carried out in quartz capillaries of 0.5 ml volume which could be charged with catalysts, this method allows high throughput when screening experimental conditions. The reaction temperature was investigated at 2 min residence time and was shown to have a large influence on the gasification efficiency. It was shown to increase from 14 to 82 % from 400 to 700°C. Additionally the gas composition is more favourable at higher temperatures; at 400°C CO<sub>2</sub> formation is predominant while above 600°C H<sub>2</sub>, CO, CH<sub>4</sub> and C<sub>2</sub>-C<sub>3</sub> hydrocarbons were produced. At the highest temperature of 700°C the H<sub>2</sub> yield was the highest and the amount of CO was reduced compared to 600°C. The reaction time was shown to have no effect on the gasification efficiency

after 5 min when gasification reached its maximum, however the gas composition changed after this. The amount of H<sub>2</sub> and CH<sub>4</sub> were shown to increase further while the amounts of CO and C<sub>2</sub>-C<sub>3</sub> were reduced, this was attributed to the reforming of C<sub>2</sub>-C<sub>3</sub> components to methane and hydrogen via the water-gas shift reaction. The experiments using catalysts showed that the gasification efficiency was highest using Inconel and Nickel, while the highest hydrogen yields were achieved using the Ruthenium catalyst. It was further demonstrated that complete gasification could be achieved using Ru catalysts at 700°C and 2 min reaction time as well as 600°C with excess amounts of catalyst. The incomplete conversion at the lower temperature was attributed to poor contact of the catalyst with the biomass and catalyst poisoning.

Guan et al. investigated the hydrothermal gasification of *Nannochloropsis sp.* in supercritical water [91]. As well as investigating temperature, holding time and algae loading; this is the first study that examined the effect of water density on the gasification behaviour. The water density is a function of the water loading in the batch reactor and temperature at supercritical conditions. The temporal variations at 500°C largely agree with the results published by Chakinala et al. [38], gasification is complete after about 5-10 min however the gas composition is still affected by increases in H<sub>2</sub> and CH<sub>4</sub> and reductions in CO<sub>2</sub> and CO. Interestingly, these results show half the CO content and 2-3 times the H<sub>2</sub> content compared to similar reaction conditions of Chikinala et al. This was attributed to the catalytic wall effects of the metal reactor wall in Guan et al.'s study (compared to quartz reactors) catalysing the water-gas shift reaction. Previously, Resende and Savage had shown that metal surfaces begin affecting gasification behaviour at ratios higher than 15 mm<sup>2</sup>/mg [92]. The effect on the carbon yield was examined for varying temperature and residence times. The yields were shown to rapidly increase up to 10 min after which only a gradual increase occurs up to 75 min. The temperature also showed favourable effects on the carbon yields; yields of 20, 45 and 60 % were reached at 450, 500 and 550°C respectively. It was suggested that these would increase even more at higher temperatures. Another parameter investigated was the algae loading as it was highlighted that it would be more economical to gasify biomass at high loadings. It was shown that the energy recovery and carbon recovery are largely unaffected by algae loading; however the H<sub>2</sub> yield was halved when the loading was increased from 1 to 5 wt.%. The water density was also investigated in this study. Previously it was shown that carbon recovery and energy recovery was largely unaffected during gasification of cellulose and lignin and a pronounced reduction in CO and increase in H<sub>2</sub> mole fraction was observed as the water density increased [93]. Gasification of *Nannochloropsis* however showed that the gas composition is largely independent of the water density [91]. The carbon recovery and energy recovery on the other hand almost doubled when

increasing the water density from 0.02 to 0.13 g/cm<sup>3</sup>. This also means that the yield of each gas fraction doubled over this range of water densities. The discrepancy of terrestrial model compounds to algae was attributed to the catalysing effects of metal reactor walls and mineral matter of the algae on the water gas shift reaction hence leaving no opportunity for the higher water densities influencing un-catalysed water gas shift rates. Concluding, it was stated that the supercritical water gasification variation in carbon yields and gas composition appear to be largely system specific.

The only study on hydrothermal gasification of macroalgae was published by Schumacher et al. in 2011 [94]. Four species of seaweed were processed (*Fucus serratus*, *Laminaria digitata*, *Alaria esculenta* and *Bifurcaria bifucata*). Gasification experiments were carried out in an Inconel tumbling batch autoclave charged with 140 ml of 5 wt.% algae for one hour at 500°C. Process conditions were not the focus of this study, only the gas yields and compositions of the different species were investigated. A maximum gasification efficiency of 50% was achieved for the *Bifurcaria* strain with all other strains exhibiting a gasification efficiency of around 31-37%. These gasification yields were higher than comparable results on terrestrial biomass and the char yields were lower [95]. This was partially attributed to the reduced cell wall strength of macroalgae and the increased amount of inorganic salts promoting gasification. The gas composition was shown to be almost the same for all strains apart for *Bifurcaria* which exhibited a larger CH<sub>4</sub> and H<sub>2</sub> fraction. The amount of H<sub>2</sub> produced from gasification was found to be considerably higher (2-3 fold) than experiments by the authors on lignocellulosic biomass which was suggested to be due to the different in composition of algae compared to terrestrial biomass [95].

Summarising, it can be concluded that hydrothermal gasification of algae is mostly complete after around 10 min and gasification efficiencies can be increased by increasing temperature. Higher reaction temperatures also increase the amount of H<sub>2</sub> produced over CH<sub>4</sub> while at lower temperatures, the CO<sub>2</sub> fraction is more prominent. The studies on catalytic HTG of algae show that the reaction temperatures can be reduced to achieve similar high gasification efficiencies observed at higher temperature non-catalytic reactions. In several studies, it was shown that more or less complete conversion can be achieved with the use of catalysts; however the catalysts were usually provided in excess due to catalyst poisoning. Finding catalysts that are not adversely affected by algae released sulphur is one of the most challenging issues associated with catalytic HTG of algal biomass. Continuous HTG systems of algae have been proposed in the literature but to date no experimental data has been published which would be required to evaluate the feasibility of HTG of algal biomass.

**Table 1.4:** Summary of research published on the HTG of algae

Reference	Algae	Temp (°C)	Res. Time (min)	Biomass Conc. (%)	Catalyst	Carbon conv. (%)	Comments
Guan et al. [91]	<i>Nanno. sp</i>	450-550	0-80	1-15		30-60	Increasing temp, time and water density increased C yield and energy recovery
Stucki et al. [90]	<i>Spirulina platensis</i>	400	60-360	2.5-20	Ru/C, Ru/ZrO <sub>2</sub>	20-100	With 8/1 cat./algae 90-100 % carbon conversion
Chakinala et al. [38]	<i>Chlorella vulgaris</i>	400-700	1-15	7	Ru/TiO <sub>2</sub> , NiMo/Al <sub>2</sub> O <sub>3</sub> , PtPd/Al <sub>2</sub> O <sub>3</sub> , CoMo/Al <sub>2</sub> O <sub>3</sub> , Ni wire	15-100	At 600°C 4 min +. Ru/TiO <sub>2</sub> in excess > complete gasification
Schumacher et al. [94]	<i>4 seaweed species</i>	500	60	5			Higher gasification efficiency and H <sub>2</sub> yields than terrestrial biomass observed
Haiduc et al. [88]	<i>Phaeodactylum tricornutum</i>	400	12-67	2.5-13	Ru/C	68-74	Sulphur shown to adversely affect Ru cat., nickel leaching investigated
Minowa et al. [89]	<i>Chlorella vulgaris</i>	350	0	12	Ni/SiO <sub>2</sub> /Al <sub>2</sub> O <sub>3</sub>	35-70	N recycle to algae cultivation investigated

### 1.5.6 Energy Balances

The energy requirements to process the algal slurry during hydrothermal processing are a major factor when considering the feasibility of the different process routes. Only limited studies on entire energy balance for the production of biofuels from hydrothermal processing of algae are available in the literature. This is an area where additional research is required and is hindered by the lack of data for continuously operating reactor systems. The data presented in this section therefore only presents a comparison of the energy considerations derived from batch processes on a laboratory scale. Despite this some useful insight can be made. When comparing the different hydrothermal routes, the energy for nutrients, cultivation and harvesting of algae are the same. Differences are largely associated with the amount of heat required to reach reaction conditions and residence times.

The construction and specifications of materials required for reactors is another important factor. The specifications for a supercritical reactor to perform HTG potentially operating at up to 700°C and 400 bar is higher than a reactor for HTC operating at 200°C and 20 bar. It is expected that a continuous process is necessary to make hydrothermal processing energetically feasible. Heat recovery can be integrated in a continuous system for preheating of the feedstock. Since all the results of published research discussed herein are based on batch systems, there is uncertainty in estimating the energetics of the different process routes. Calzavara et al. estimated that the energy efficiency of hydrothermal gasification reaches 60% and can be increased to 90% if energy recovery of the water is included [86]. It is assumed that similar performance could be obtained for HTL and HTC. Xu et al. have reported the most relevant estimate of the energy balance of hydrothermal processing of microalgae [29]. In their approach, a dry and a wet processing route were compared. The dry route involves the removal of water by mechanical and thermal drying down to 80 wt% solids with subsequent lipid extraction using hexane to produce biodiesel and glycerol. The residue in their model is pyrolysed to pyrolysis oil, bio-gas and char. The wet route involves mechanical drying down to 30 wt.% solids and a wet lipid extraction using the *Bligh and Dyer method* in a stirred ball mill. The wet residues are then hydrothermally gasified to produce H<sub>2</sub> and other gases; the H<sub>2</sub> is subsequently used to hydro-treat the lipid extract to green diesel. This wet extraction process differs from most research discussed in this review as the lipids are extracted with solvents in the aqueous phase while most HT techniques process the entire algae to produce bio-crude or syngas. Nevertheless the results by Xu et al. show that the difference in dewatering to 15 or 80 wt.% solids requires approximately five times more energy while the energy requirements for flocculation, centrifuge and mechanical dryers are the same and insignificant compared to the thermal drying required for the dry route. The wet lipid extraction however requires significantly more energy than the dry route which overall resulted in the conclusion that the dry route has more favourable energy balance while the wet route has more potential in producing high value biofuels. The method described in the process gives detailed insight into the energy required for drying and processing but is not entirely applicable to the HT routes described in the current literature review. The wet lipid extraction by Xu et al. was the largest single energy input for the wet extraction method and even exceeded the energy required to hydrothermally gasify the residue. The research papers discussed herein process the entire algae so that this energy input would not be applicable which would result in the wet route performing favourably over the dry route presented by Xu et al.. On the other hand, a high value green diesel is produced by hydro-treating the lipids in their approach, which is a possible scenario. As can be seen, the energy balance assessment of hydrothermally processing algae is not straight forward and requires additional work.

One method of comparing the different HT approaches is by a comparison of the *Energy recovery*. This is an expression of how much chemical energy of the algae is recovered in the form of gas, bio-crude or char. It is calculated by:

$$\text{Energy recovery (\%)} = \frac{\text{HHV product} \left(\frac{\text{MJ}}{\text{kg}}\right) \times \text{mass product (kg)}}{\text{HHV biomass} \left(\frac{\text{MJ}}{\text{kg}}\right) \times \text{mass biomass (kg)}} \times 100 \quad \text{Eqn. 1.1}$$

**Table 1.4** presents some selected energy recoveries of different research papers using different algae and process conditions. The energy recoveries presented are the chemical energy in the primary product and excludes the energy in the char for HTL and HTG. For HTC it excludes the energy in the gas and bio-crude while for HTG it excludes the energy in the char and bio-crude fraction. These excluded products are typically low. The energy recoveries range from 58~100%, these values are a function of the yields and heating values of the primary products as seen in **Eqn. 1.1**. HTG energy recoveries range from 58-70 %, the highest value reached by Guan et al. was achieved at 550°C [91] the higher results by Stucki et al. were achieved with the use of ruthenium catalysts [90]. In general, the use of catalysts increase carbon conversion and gasification efficiency hence increasing the yields of syngas. For HTG, the gas composition is just as important as the gas yield as it affects the HHV.

The only available report for the energy recovery for HTC of algae is by Heilmann et al. and indicates a slightly higher efficiency than HTG but only by 6% [56]. It could be argued that a syngas is more valuable than a char as an energy carrier and can be more efficiently used; therefore a complete life cycle balance would be more favourable for HTG. Heilmann et al. describe their HTC char as a “product of bituminous coal quality” and the bio-crude is often compared to petroleum crude [56]. Therefore comparisons of HT products are often made to coal and crude oil. Gas powered power stations usually have a considerably higher thermal efficiency compared to coal powered stations hence favouring HTG over HTC. Another aspect to consider is the emissions; the HTG syngas is nitrogen free and therefore exhibits no fuel bound NO<sub>x</sub> emissions upon combustion. The oils and chars from HTL and HTC respectively, typically have a nitrogen content of around 5 % which would increase pollutant formation and require expensive post combustion NO<sub>x</sub> clean up. CO<sub>2</sub> emissions are typically also higher for oils and coal powered processes compared to natural gas.

The highest energy recoveries reported for HTL are using heterogeneous catalysts. Duan and Savage report values exceeding 100 % [85], possibly due to incorporation of hydrogen from the water increasing the energy content of the oil. The energy recoveries are very high in this study and are increased from 74 to around 100% with the use of catalysts. Garcia Alba al. achieve energy

recoveries of around 70%, and found that the highest energy recovery was exhibited at the lower residence time. This has implications for a continuous system suggesting throughput could be higher [37]. Brown et al. achieved the highest energy recovery without the use of catalysts of 88 % [72]. For comparison, a study on macroalgae HTL resulted in a lower energy recovery of 59%.

Taking into account the energy recovery, it would appear that HTL is favoured over HTC and HTG, however as discussed earlier, this is not the only factor to consider. The energy required to heat the reactants to the process temperature vary significantly for HTC, HTL and HTG. **Table 1.5** presents data based on heating 1 kg of pure water (not an algae slurry) to the respective reaction temperatures. In all three processes, the latent heat of vaporisation is avoided by the pressures remaining above the water saturation line (see **Figure 1.1**). Beyond the critical point (374°C, 22 MPa) the phases become alike and the latent heat of vaporization is zero. It can be seen that the energy required for HTG is around double that of HTL and triple that of HTC. HTG at 400°C with the aid of catalysts requires 2.1 MJ while non-catalytic gasification at 550°C requires ~35% more energy. For HTL, an increase of 50°C results in an additional energy input of 20%. These are significant margins when assessing hydrothermal processes. Another factor affecting the energy balance is the solid concentration of algae in the slurry. If more algae is heated per unit mass of water, more product is formed hence increasing the energy efficiency. Heilmann et al. estimated the heat capacity of algae to be around 50% compared to water [56] which also results in less energy being required to heat a higher solids concentration slurry. The pumping requirements for a continuous HT system are also a factor to consider. Pumping slurries to high pressures is an engineering challenge which has posed problems on previous work on terrestrial biomass [44]. Microalgae are generally smaller in size and do not require grinding which would be required for macroalgae.

Sawayama et al. tried to perform an energy balance on the HTL of *B. braunii* and *D. tertiolecta* which included the energy required from liquefaction, fertilizers, cultivation and harvesting denoted as the energy consumption ratio (ECR) [66]. It was shown that a net energy production was possible with the use of *B. braunii* but not for *D. tertiolecta*. This was mainly due to *D. tertiolecta* requiring a much higher energy demand during cultivation largely for supplying nutrients. The use of wastewater as a source of fertilizers was also included in the calculation which reduced the energy conversion ratio from 0.45 to 0.40. Biller and Ross adapted the same ECR calculations with the same assumptions but left out the energy requirements for cultivation, fertilizers and harvesting and incorporated it with their results on four different algae species and model compounds [77]. It was shown that only *Chlorella* was able to produce net energy while *Spirulina* had an ECR of 1 and



*Nannochloropsis* and *Porphyridium* over 1. It was demonstrated however that higher lipid containing algae would perform more favourably and that protein content is favourable over carbohydrates.

**Table 1.5:** Energy recovery and heating energy for different HT studies

Reference	HT process	Temp. (T <sub>2</sub> ) (°C)	Energy recovery (%)	ΔE (T <sub>2</sub> -T <sub>1</sub> ) 1 kg H <sub>2</sub> O (MJ)
Heilmann et al. [56]	Carbonisation	203	76	0.8
Guan et al. [91]	Gasification	550	58	3.2
Stucki et al. [90]	Gasification	400	70	2.1
Brown et al. [68]	Liquefaction	350	88	1.6
Anastasakis and Ross [59]	Liquefaction	350	59	1.6
Duan et al. [85]	Liquefaction	350	~100	1.6
Garcia Alba et al.[37]	Liquefaction	300	71	1.3

Recently two studies were published comparing the LCA for different renewable diesel production pathways from microalgae. The first study by Frank et al. (2012) compares hydrothermal liquefaction with subsequent upgrading of bio-crude to solvent extraction and transesterification [96]. It was concluded that HLT offers advantages compared to lipid extraction regarding the efficient use of algal biomass. 1.8 fold less algae was required to achieve the same amount of biodiesel. On the other hand the nitrogen in the bio-crude was identified as one of the major bottlenecks. If the nitrogen in bio-crude is removed via hydro-denitrogenation as ammonia the recyclability of N could become an issue. Therefore the authors conclude that the nitrogen should be fractionated to the process water for process optimisation.

The second recent LCA study by De Boer et al. (2012) compares four different biodiesel production pathways:

1. Pulsed electrical field-assisted extraction followed by transesterification of dry algae
2. In situ acid catalysed esterification of dry algae
3. In situ hydrolysis and esterification of wet algae
4. Hydrothermal liquefaction of wet algae

De Boer et al. conclude that energetically feasible methods for biodiesel production from microalgae exist but further research is required to achieve commercial scale application [97]. Each

scenario in this LCA includes anaerobic digestion of the residues for biogas production for heat and power. The first scenario was shown to consume 42 % of energy for mechanical dehydration, 32 % for transesterification and 26 % for cell lysing. This led to a final surplus of energy in the form of biodiesel and biogas of 7.8 MJ from 1 ton of algae (dry weight). The second scenario involving dry biomass required 45% of total energy for thermal drying and 41 % for methanol recovery. This scenario was shown to have an overall energy deficit of 7.1 MJ for the same system boundaries. Similarly the third scenario was not able to produce net energy due to the high energy consumption of ethanol recovery (46 %), supercritical ethanolysis (28 %) and in situ hydrolysis (21 %). The net energy deficit was calculated as 7.9 MJ but 9 MJ was created in the form of biodiesel. The hydrothermal liquefaction scenario had an overall energy surplus of 9.2 MJ. The majority of energy was required for the hydrothermal processing (85 %). It is highlighted that HTL is energetically feasible but requires a high capital cost for the HT processing facility and only 4.7 MJ are available in the form of biodiesel.

### 1.5.7 Nutrient Recycling

The recycling of nutrients from the process water from hydrothermal processing has been investigated in several studies and proposed as an advantage of hydrothermal routes over other alternative routes such as biodiesel production. Macroalgae is usually cultured in marine environments where nutrient recycling would be more of a challenge. Significant amounts of the feed nitrogen, phosphorous and potassium have been shown to concentrate in the process water after hydrothermal processing. This is the case for HTC, HTL and HTG [56-58, 88]. Minowa and Sawayama were the first to recognize this potential and attempted to cultivate microalgae in the process water from the HTG of *Chlorella vulgaris* [89]. It was found that all of the nitrogen in the algae was converted to ammonia which was distributed in the water phase. Cultivation trials were performed in the process water after dilution and compared to standard media, it was found that algal growth in the undiluted process water was a fraction compared to the standard media; however blending standard growth media with HTL process water showed good growth rates. It was concluded that cultivation in standard media without nitrogen plus process water was possible and therefore a saving on nutrients could be achieved. The same group later performed similar experiments but going into more detail concerning ammonia, micro-elements and nickel concentrations [98]. It has previously been shown that nickel can inhibit algae growth due to accumulation on the cell surface by adsorption and thus acting as a selective barrier for nutrient

uptake by the cells [99]. *Chlorella vulgaris* growth was shown by Spencer et al. to be inhibited by nickel levels as low as 0.85 mg/l [100]. Sawayama et al. tried to determine the optimum culture conditions using the recovered aqueous phase supplemented with necessary nutrients. The effects of nickel and ammonium ions were also investigated. The nitrogen in the algae was converted to ammonium and nickel was leached from the nickel catalyst [98]. It was shown that *Chlorella vulgaris* was able to grow in ammonium concentrations of 0.22 to 1.11 g/l but became toxic above 16.6 g/l. Therefore it was concluded that the recovered process water would have to be diluted at least 30 fold to avoid ammonium toxicity. The nickel concentrations found in the water phase from the nickel catalysts used were found to be very high (240 mg/l) although a 30 fold dilution would be sufficient to avoid nickel growth inhibition. Using a 75-300 fold dilution of the recovered water phase with supplementation of phosphorous and magnesium was shown to yield growth rates similar to the standard medium.

Jena et al. (2011) performed growth trials using the process water from the HTL of *Spirulina* to grow a strain of *Chlorella* [48]. It was shown that growth was possible in dilutions of the process water. When using a dilution factor of 10, no growth occurred and this was attributed to the presence of growth inhibition, possibly by nickel, phenols or fatty acids. These have all previously been shown to adversely affect algae growth [88, 100-102] and are likely constituents of the water phase. The growth in the 100, 300 and 500 fold dilutions was higher. The highest growth was observed in the 500 times dilution, reaching a maximum of around 80% compared to a standard BG11 growth medium. A mass balance on an integrated HTL system with nutrient recycling was performed and the results suggest that from 1 t of dry biomass 0.4 t of bio-crude could be produced. The process water would contain 3.4 kg of P and 70 kg of N and significant amounts of mineral nutrients. Part of this could be used to grow more algae and the rest concentrated to valuable fertilizer high in NPK, additionally the 0.18 t of CO<sub>2</sub> produced could be used to enhance algae growth [48].

The potential issues occurring from nickel either from Ni catalyst leaching, from reactor wall corrosion or from the algae itself (minor amounts) has been highlighted in a study by Haiduc et al. [88]. They realized that when using a continuous closed loop system integrating nutrient recycling, the process water would become progressively enriched in contaminants such as nickel. In their research paper they therefore evaluated the growth of four green microalgae strains and a cyanobacteria in standard BG11 media doped with 0, 1, 5, 10 and 25 mg/l nickel [88]. It was found that 10 mg/l had significant detrimental effects on the growth of all algae strains. *Scenedesmus v.* was able to grow in BG11 doped with 1 and 5 mg/l Ni but 10 mg/l reduced the growth by around

half while 25 mg/l inhibited growth entirely. It was concluded that if nutrient recycling is incorporated into a hydrothermal system, nickel concentrations in the effluent need to be monitored closely and if required, the stream should be diluted if the concentration approaches 25 mg/l or removed .

The potential of recycling of nutrients to cultivate algae is significant due the cost associated with supplying large amounts of nutrients. The fossil energy input for the production of growth nutrients is significant and would reduce the life cycle energy balance. Especially for phosphorous which is a finite non-renewable resource extracted from phosphate rock and requires high energy inputs. Current estimates predict peak phosphorous reserves may be depleted in 50-100 years [103]. The limited studies on recycling of nutrients for algae cultivation are promising but additional research needs to be performed to identify problems occurring with progressive build up of growth inhibitors. A wider range of algae strains and mixed strains should also be investigated as some species are expected to endure harsher cultivation conditions than others.

## 2. CHAPTER II - Aims and Outline of the Thesis

The overall aim of the thesis is to investigate the production of bio-crude from microalgae via hydrothermal liquefaction in a sustainable way. It is desirable for the bio-crude to be of a quality which will allow direct combustion as a heavy fuel or upgrading in conventional refineries. Therefore, a low nitrogen content is favourable as this will decrease NO<sub>x</sub> emissions upon combustion and require less hydrogen for upgrading via hydrogenation. Additionally a low boiling point range is favourable over high molecular weight fractions as these are of higher commercial value and are associated with better pour behaviour. In order to achieve this aim of producing bio-crude from microalgae a number of objectives with associated goals are outlined below and were investigated in this thesis.

The first chapter provides an introduction to the subject area covered within this thesis. The concept of biomass for bioenergy is explained and the general aspects of biomass and its associated advantages and disadvantages are discussed. The conversion routes available for processing and utilisation of biomass and current research and development are briefly presented. Microalgae as a source of third generation biofuels is introduced. There are a number of different options in cultivation, extraction and processing microalgae which are covered in **Chapter 1**. The introduction shows the relevance of the work covered in this thesis and the concept of hydrothermal processing of microalgae is introduced. A detailed study of the literature on hydrothermal liquefaction, carbonisation and gasification was performed for the purpose of this thesis. The published literature allows a deeper understanding of the work carried out, identifies areas of research that have been covered and the bottlenecks that require further investigation.

**Chapter 3** describes the methodology used. The main objective of this chapter is to describe the methods used allowing others to replicate the experiments. Further, it is important for readers to have an understanding of the sample workup and analysis for the same reason. Each instrument used is described with the manufacturers name and model code. The chemical and physical operation of the instruments is not covered in this chapter as this would be beyond the scope of this thesis. Additionally this information is publicly available and most readers interested in the current work are expected to have some initial knowledge of the technologies involved.

The microalgae feedstocks used in this thesis are presented in **Chapter 4**. Due to the large number of different microalgae strains and properties investigated, not every parameter is presented for each strain. All the data is however attached in separate data sheets in **APPENDIX A**. The data in

**Chapter 4** is presented in such a way that the main distinctions in different types of microalgae become apparent. The significance of this is then discussed. The objective of the characterisation is to lay the groundwork of the thesis which is referred back to throughout the thesis. The characterisation of the feedstock is fundamental to the understanding of all the experiments carried out in the subsequent chapters.

**Chapter 5** describes the hydrothermal processing of microalgae in water without catalyst. The objective of this chapter was to assess different microalgae strains and operating conditions. In order to achieve this objective the majority of microalgae strains were processed at standard conditions to allow a comparative study of their hydrothermal liquefaction behaviour. Following this, the influence of residence time and operating temperature on hydrothermal liquefaction is investigated. This parametric study determines the optimum operating conditions for maximum bio-crude yield. The bio-crude was additionally analysed for its elemental composition and HHV to assess the bio-crude quality. The process waters resulting from the HTL of microalgae are also analysed in this chapter for common anions, cations, TN, TOC, TIC and pH. This is later referred to in **Chapter 8** which investigates nutrient recycling from the process water for microalgae cultivation.

**Chapter 6** describes the HTL of microalgae in the presence of catalysts. The objective of this chapter was to increase yields and/or improve the quality of bio-crudes. The chapter is split in two sections; the first includes the use of homogeneous catalysts while the second includes the use of heterogeneous catalysts. The homogeneous catalysts include alkali or organic acids. The heterogeneous catalysts include transition metals and precious metals adsorbed on silica and alumina. The effects on yields and bio-crude quality are assessed for both types of catalysts and discussed. The effect of homogeneous catalysts on the nitrogen and carbon distribution in the product fractions was investigated. Analysis of the process water was carried out to evaluate if the homogeneous catalysts affect the concentration of nutrients. The effect of heterogeneous catalysts on the lipid fraction degradation was examined in detail. The fate of triglycerides and free fatty acids and the potential of deoxygenating these to straight chain hydrocarbons was investigated. The yields and composition of bio-crudes produced was investigated and conclusions could be drawn concerning the bio-crude quality by elemental analysis and GC-MS.

**Chapter 7** the mechanistic pathways of bio-crude production from microalgae are investigated in detail in order to understand bio-crude formation pathways in more detail. 4 microalgae strains and 7 model compounds were hydrothermally processed in water alone and sodium carbonate and

formic acid. The 7 model compounds include several protein, carbohydrate, lipid and amino acid samples as these are the main constituents of microalgae. By processing these and analysing the bio-crude, conclusions could be drawn on the HTL of microalgae. The four selected microalgae differ in biochemical composition; this facilitated comparative examination with results from the model compounds and sheds light on the bio-crude formation and composition from microalgae. The bio-crudes were analysed for total yield and oil composition and by GC-MS so that typical compounds present in microalgae bio-crudes could be linked to their biochemical origin. The effect of the catalysts was studied on the model compounds and microalgae. Conclusions were drawn on the effects of alkali and acidic catalysts on the HTL behaviour of model compounds and microalgae.

The objective of **Chapter 8** was to investigate the use of process water as a source of nutrients for microalgae cultivation. For the purpose of these experiments, the process waters produced at different operating conditions and using different microalgae strains were analysed for its concentration of nutrients. Growth trials of 4 different microalgae were performed using the process water derived from HTL. Growth was assessed by various methods such as chlorophyll a absorbance and cell count and the results compared to growth in standard growth media. The influence of common growth inhibitors such as phenols and nickel are investigated and discussed.

During the cultivation trial used to investigate the nutrient recycling a drawback in the analytical methodologies was identified. The small scale growth trials used result in small amounts of harvested microalgae. This makes analysis by the previously employed techniques (described in **Chapter 3**) impossible. Therefore, in **Chapter 9**, a new analytical technique based on Pyrolysis GC-MS was developed to analyse the microalgae allowing analysis of small amounts of sample. The technique involves pyrolysing less than 1 mg of microalgae and separating the pyrolysis products by GC-MS. By fingerprinting common model compounds of microalgae, marker compounds could be identified for each biochemical component. This has allowed comparison of the chromatograms from microalgae grown under different conditions and sheds light on the composition of the different strains. The new analysis technique was also assessed as a means to determine concentrations of specific high value compounds found in microalgae.

**Chapter 10** includes research carried out in collaboration with the University of Sydney, Australia. Here a state of the art continuous hydrothermal pilot plant processing facility has been used. This allowed experiments to be performed on a large scale (20-40 l/h) for two microalgae strains over the course of the ten week collaborative visit through the WUN network. This was the first time continuous processing has been employed for microalgae on a hydrothermal liquefaction reactor.

The reactor performance was investigated in regard to feedstock and operating conditions. The results concerning the yields and bio-crude quality are compared to experiments of the same feedstock processed in batch reactors. The objective of this work was to assess the feasibility of continuous processing of microalgae in a HTL reactor in order to make bio-crude production possible on an industrial scale.

In **Chapter 11** the use of hydrothermal microwave processing as a pre-treatment method is investigated. The technique is expected to be especially suited for high ash containing marine microalgae samples as the metals in the ash act as microwave absorbers, lowering the activation energy and reducing the energy consumption. Microwave irradiation was assessed as a technique for extraction of protein, polysaccharides and other valuable phytochemicals. Additionally, the technique was evaluated as a pre-treatment for bio-fuel production by hydrothermal processing and flash pyrolysis. The fate of nitrogen during pre-treatment and during bio-fuel production was of particular interest.

The conclusions of the experimental sections are presented in **Chapter 12**. The overall conclusions of each chapter are discussed separately even though an overall summary on the feasibility of hydrothermal processing for biofuels and chemicals is presented. The limitations of the research performed in this thesis are identified and further work is discussed.



### 3. CHAPTER III - Methodology

#### 3.1 Biomass characterisation

##### 3.1.1 Microalgae strains

The microalgae samples investigated during the course of this research originate from various sources which are summarised in **Table 3.1**. The different strains were used for various experiments throughout this piece of work and their location within the thesis is indicated in **Table 3.1**. Additionally, each algae strain is presented using a separate data sheet containing the main physical and chemical characteristics in **APPENDIX A**.

Four algae samples were obtained from commercial sources where they are traded as health food supplements; namely *Spirulina sp.* and *Chlorella sp.* which were bought from Naturally Green Ltd. (Reading, UK) and the *Spirulina sp. OZ* and *Chlorella vulgaris OZ* samples which were obtained from Synergy Natural Ltd. (Prymont, Australia). For these samples the exact strains and growth media are unknown. Five strains of microalgae were supplied by partnering institutions and provided freeze-dried. *Porphyridium cruentum* was provided by the University of Almaria, the strain and growth media are unknown. *Porphyridium* is a marine red algae of the *Porphyridiaceae* family. Two strains of *Dunaliella salina* (19/18 and 19/30 strains) were provided by the University of Sheffield. These strains were grown in a modified f/2 media with adjustments made to the NaCl concentration. *Navicula sp.* was also provided by the University of Sheffield, the strain code and growth media are unknown. However, this is a known silica containing diatom which requires Si in its media to sustain growth. The cyanobacteria *Chlorogloeopsis fritschii* was grown in JM media by the Plymouth Marine Laboratory and provided dry after lyophilisation. Following strains were cultured in the University of Leeds laboratories; *Scenedesmus dimorphus* (276/48); *Chlorella vulgaris* (211/52); *Spirulina platensis* (85.79); *Nannochloropsis oculata* (849/1); *Botryococcus braunii* (807/1, Guadeloupe, race B); *Dunaliella tertiolecta* (19/27); *Haematococcus pluvialis* (34/1D); *Tetraselmis chuii* (8/6). More information on the culturing conditions is provided in **Section 3.4**. Three strains of microalgae were provided by the DENSO CORPORATION (Kariya, Japan). Two of the strain names are not known and are therefore referred to by their origin; *Miyako* and *Zenmyo*. The *Pseudochorocystis ellipsoidea* strain (*P.*

*ellipsoidea*) was also isolated by the DENSO CORPORATION and has the unique ability to synthesise and accumulate aliphatic hydrocarbons [104].

**Table 3.1:** Name, source, strain code and growth media of the microalgae strains investigated with Chapter reference

<b>Name</b>	<b>Source</b>	<b>Strain</b>	<b>Growth Media</b>	<b>Referred to in Chapter</b>
<i>Scenedesmus dimorphus</i>	CCAP	276/48	3N-BBM+V	4, 5, 8
<i>Chlorella vulgaris</i>	CCAP	211/52	3N-BBM+V	4, 5, 8, 9
<i>Chlorella sp.</i>	Naturally Green Ltd	unknown	3N-BBM+V	4, 5, 6, 7, 8
<i>Chlorella vulgaris OZ</i>	Synergy Natural Ltd	unknown	3N-BBM+V	4, 5, 10
<i>Spirulina platensis</i>	SAG	85.79	modified BG11	8
<i>Spirulina sp.</i>	Naturally Green Ltd	unknown	unknown	4, 5, 6, 7, 8
<i>Spirulina sp. OZ</i>	Synergy Natural Ltd	unknown	unknown	4, 5, 10
<i>Porphyridium cruentum</i>	Almeria University	unknown	unknown	4, 5, 7
<i>Nannochloropsis oculata</i>	CCAP	849/1	f/2	4, 5, 6, 7, 11
<i>Pseudochorocystis ellipsoidea</i>	Denso Corp.	MBIC11204	unknown	4, 5, 11
<i>Miyako</i>	Denso Corp.	unknown	unknown	4, 5
<i>Zenmyo</i>	Denso Corp.	unknown	unknown	4, 5
<i>Botryococcus braunii</i>	CCAP	807/1 Guadeloupe (race B)	3N-BBM+V	4, 9
<i>Dunaliella salina</i>	Sheffield University/CCAP	19/18	modified f/2 and f/2	4
<i>Dunaliella salina</i>	Sheffield	19/30	modified f/2	4

	University/CCAP		and f/2	
<i>Dunaliella tertiolecta</i>	CCAP	19/27	f/2	4
<i>Navicula sp.</i>	Sheffield University	unknown	f/2+Si	4, 9
<i>Haematococcus pluvialis</i>	CCAP	34/1D	3N-BBM+V	4, 9
<i>Tetraselmis chuii</i>	CCAP	8/6	f/2	4
<i>Chlorogloeopsis fritschii</i>	Plymouth Marine Laboratory	1411/1	JM	4, 5, 8, 9, 11

---

### 3.1.2 Proximate and ultimate analysis

To determine the amount of water contained in samples, proximate analysis was carried out. The water content affects mass balance calculations and therefore requires consideration to allow for a consistent base to be set amongst samples. Water content determination was performed in an oven at 105°C for 2 hours; approximately 3 g of biomass were weighed in a ceramic crucible and the moisture content expressed as a percentage by weighing the dried biomass. The ash content was determined by placing 3 g of dry sample in a ceramic crucible in a muffle furnace for 3 hours at 550°C. To determine the amount of total organic material the ash and water contents were combined to express a *dry ash free* fraction. Alternatively, if only very little biomass was available, the samples were analysed by TGA for ash and moisture content on a Stanton Redcroft TGA or TA Instruments IR5000Q TGA in air. The TGA oven temperature was increased to 105°C and held for 15 min, subsequently ramped to 550°C and held for 60 min to determine the moisture and ash content respectively.

### 3.1.3 Elemental Analysis

Ultimate analysis was determined by the C, H, N, S content of the samples using a CE Instruments Flash EA 1112 series elemental analyser. The results from the proximate analysis were used to calculate the elemental composition on a dry ash free basis. The instrument was calibrated using a BBOT standard (2,5-Bis (5-tert-butyl-benzoxazol-2-yl) thiophene) which contains 72.53 wt.%

carbon, 6.09 wt.% hydrogen, 6.51 wt.% nitrogen, 7.44 wt.% sulphur and 7.43 wt.% oxygen. The second standard used was oat meal (C=47.76 wt.%; H=5.72 wt.%; N=2.09 wt.%; S=0.16 wt.%). Approximately 2.5-3.5 mg of samples and standards were weighed out in duplicate in tin capsules. These were combusted in excess oxygen by the elemental analyser. The analyser automatically calculated the elemental composition of samples by analysing CO<sub>2</sub>, NO<sub>x</sub> and SO<sub>2</sub> concentrations in the product gas. The elemental composition was used to calculate the HHV using the *DuLong formula* [105] according to:

$$HHV \left( \frac{MJ}{kg} \right) = 0.3383 \times C + 1.443 \times \left( H - \frac{O}{8} \right) + 0.0942 \times S \quad \text{Eqn. 3.1}$$

Variables C, H, O and S are the mass fractions carbon, hydrogen, oxygen and sulphur in wt.% on a dry basis.

### 3.1.4 Biochemical Analysis

The biochemical composition of the microalgae strains was determined colorimetrically; for the protein analysis the J. Waterborge method was used [106] which involves the use of a folin reagent, subsequent absorbance measurements at 720 nm and comparison to a bovine standard absorbance at the same wavelength. For this procedure 0.05 g of sample were weighed and mixed with 5 ml 2M NaOH in a sample tube and placed in a breaker of boiling water for 10 min. Subsequently the tube was centrifuged for 5 min and 2.5 ml of the supernatant was pipette into a fresh tube with 7.5 ml 2M NaOH and mixed. 0.5 ml of this solution was mixed with 5 ml of a complexing reagent made up of a copper sulphate and sodium potassium tartrate solutions and left for 10 min. Finally 0.5 ml of Folin reagent was added to the sample and absorbance measured at 750 nm after zeroing with a reagent blank. The sample procedure was carried out with a bovine standard and the total protein content calculated by:

$$\text{wt. \% total Protein} = \frac{(A1-B) \times V \times C \times d}{A2 \times W \times 10000} \quad \text{Eqn. 3.2}$$

A1=Absorbance of sample

A2= Absorbance of standard

W= weight in g

C = Concentration of standard in µg/ml

V=initial Volume

D= dilution factor

B= sample blank

Carbohydrates were determined by a sulphuric acid hydrolysis method developed by Sol M. Gerchakov [107]. This involved weighing approximately 0.05 g of sample (and glucose as a standard) into a 10 ml sample tube. 3 ml of 72 wt.% sulphuric acid was added, mixed and placed into a oven at 40°C for 30 min. After hydrolysis samples were diluted to 100 ml and spun at 3000 rpm for 5 min. 1ml of sample was added to two separate tubes, one with 1 ml 5 wt.% phenol solution and one with 1 ml distilled water (sample blank). To all tubes 5 ml of conc. Sulphuric acid was added, mixed and left for 1 hour. The spectrophotometer was set to 485 nm and zeroed with a reagent blank and absorbance was measured for sample blanks and samples. The following formula was used to calculate the carbohydrate concentration:

$$\text{wt. \% Total Carbohydrate} = \frac{(A1-B) \times V \times C \times d \times Q2}{A2 \times W \times Q1 \times 10000} \quad \text{Eqn. 3.3}$$

A1 = Absorbance of sample

A2 = Absorbance of standard

W = Weight in g

C= Concentration of standard µg/ml

V = Initial volume

d = Dilution factor

B = Sample blank

Q1= aliquot of sample ml

Q2= aliquot of standard ml

Lipid extraction was performed using the Bligh and Dyer method employing a 2:1 methanol/chloroform extraction at room temperature [27]. This entailed 3 subsequent solvent extractions and filtrations of approximately 1 g of algae with aliquots of 15 ml solvent mixture.

Samples were weighed into sample tubes, solvent added and shaken continuously for 20 min using a mechanical shaker. The solvent was subsequently evaporated, the residue weighed and the lipid fraction expressed as a weight fraction. Additionally, the lipids were extracted by the same method using hexane.

### 3.1.5 Scanning Electron Microscopy

Microalgae samples were freeze dried in a Christ Alpha 1-2 LDPlus (Christ, Germany) for 8 hours then coated with a thin gold layer before analysis by scanning electron microscopy (SEM) on a Zeiss EVO MA 15 (Carl Zeiss Microscopy, Germany). SEM of the solid residue after hydrothermal processing was carried out by air drying the residue and then solvent washing with acetone to remove any residual bio-crude. Subsequently the solids were freeze dried and analysed by SEM.

The particle size distribution of selected algae cells was measured using a Malvern Mastersizer S analyser series 2600 (Malvern Instruments, UK). Approximately 5 g of dry sample were placed in the analyser and blown with a fan through a laser beam, the resulting light scattering by particles was analysed by the instrument and a particle size distribution plotted.

### 3.1.6 Pigment Analysis

Algal pigments were analysed by a method based on the method by Wright et al. 1992 and slightly modified based on M.A. van Leeuwe et al.'s work [108-109]. Pigments were extracted in 90 vol.% acetone; 0.5 g of biomass were mixed with the solvent solution and agitated with a mechanical shaker for 30 min. Subsequently the solution was centrifuged and the supernatant analysed by HPLC. The pigments were analysed on a Dionex Ultimate 3000 HPLC system with a C-18 column. 100 µl of sample were injected and the pigments eluted with the mobile phase ramp program specified in **Table 3.2**. The solvents A, B and C correspond to 85% methanol/water (v/v) buffered with 0.5 M ammonium acetate, 90% acetonitrile/water (v/v) and ethyl acetate respectively. The flow rate was kept at 0.8 ml/min constantly. Absorbance was recorded at 450 nm and a scan between 400 and 700 nm was also recorded to allow absorbance/wavelength plots of selected peaks. Peaks were identified by comparing published retention times and absorbance

spectra of known pigments. Additionally, standards of chlorophyll a, astaxanthin and beta-carotene were run to allow semi-quantitative analysis of these pigments. The cell wall of *Chlorogloeopsis fritschii* is very strong; therefore acetone extraction did not release all of the pigments. Consequently, extraction was performed in the same manner but with pure dimethylformamide. Peak areas were measured and divided by the initial mass of algae to calculate peaks in units of “area/mg”. The area of beta carotene was used as a one-point calibration standard using the chromatograms peak area of the purchased beta carotene standard. This was the only pure standard available due to the high cost of pure pigments. Therefore the pigment analysis is of a qualitative nature to identify which pigments are present. The analysis should not be regarded as fully quantitative even though the results are presented in mg/kg. The results are used solely for the purpose of comparing between the same pigment within different samples. The main application of the data is in **Chapter 9** where it is discussed in more detail.

**Table 3.2:** HPLC gradient program with A: 85% methanol/water (v/v) buffered with 0.5 M ammonium acetate, B: 90% acetonitrile/water (v/v) and C: ethyl acetate

Time (min)	% A	% B	% C
0	60	40	0
2	0	100	0
7	0	80	20
17	0	50	50
21	0	30	70
28.5	0	30	70
29.5	0	100	0
30	60	40	0
35	60	0	0

### 3.1.7 Metal Analysis

Metal analysis was carried out by digesting 200 mg of sample in HNO<sub>3</sub> in a closed vessel. This was performed in 50 ml conical flasks with reflux funnels. The samples were mixed with 10 ml of conc. HNO<sub>3</sub> and placed in a hot plate heater filled with sand. The digestion was performed at 220°C for 2 hours. After cooling of the samples they were diluted to 100 ml and sent to the Department of Geography at the University of Leeds for analysis. Metal concentrations were determined using an Optima 5300 DV inductively coupled plasma spectrometer (ICP) with optical emission spectrometry (Perkin Elmer, Cambridge, UK). The instrument was calibrated for the elements Al, B, Ba, Ca, Co, Cu, Fe, K, Mg, Mn, Na, Ni, Pb, Si, Zn with concentrations of 0.1, 0.25, 0.5, 1, 5, 10, 25 and 50 mg/l.

### 3.1.8 Pyrolysis GC-MS

Pyrolysis–GC-MS analysis was performed using a CDS 5000 series pyrolyser connected to a Shimadzu 2010 GC-MS. Samples of approximately 2 mg were weighed into a pre-weighed quartz tube with quartz wool at one end. Subsequently the other end of the tube was filled with quartz wool to keep the sample in place. The tube was reweighed before pyrolysis. Pyrolysis was performed at a temperature of 500°C with a ramp rate of 20°C per millisecond with a hold time of 20 seconds. The volatiles were trapped on a trap before being desorbed at 300°C onto a heated transfer line (300°C). The purge flow to remove any oxygen prior to pyrolysis was set to 20 ml/min. The heated transfer line was connected to the split/splitless injector of the GC inlet port which was set to 280°C. Split ratios were chosen depending on sample type and mass of sample, for very small amounts of sample (>0.5 mg) splitless injection was used, the highest split ratio used was 30:1. The products were separated on an Rtx 1701 60m capillary column, 0.25 id, 0.25 µm film thickness, using a temperature program of 40°C, hold time 2 minutes, ramped to 280°C, hold time 30 minutes and a constant column head pressure of 2.07 bar. After pyrolysis the tube was reweighed to determine the amount of sample pyrolysed. This allowed calculation of peaks as an area per mg sample pyrolysed. The split ratio was adjusted for data analysis to allow comparison of different samples. The mass spec ion source was set to 230°C and the interface to 280°C, scanning to place once per second in the range of 50 to 550 *m/z*. Peaks were identified using the NIST mass spectral database.



Alternatively, the same pyrolysis unit was connected to a jas-Agilent G2350A Atomic Emission Detector connected to an Agilent GC 6890N with the same column and GC program. AED detectors work with a plasma source exciting elements to higher energy states from which they emit light once they return to their original energy state. This emitted light is of a different wavelength for each element. This therefore allows identification of all elements apart from the carrier gas (He). The same Pyrolysis, transfer line, inlet and GC temperatures and flow rates were employed as for GC-MS analysis. The AED's purge vent was set to 30 ml/min He and the cavity vent to 60 ml/min. The spectrophotometer was purged for 2 days at 3.45 bar N<sub>2</sub> and set to 1.38 bar during analysis. The AED was set up to detect nitrogen (N, wavelength 174 nm), sulphur (S wavelength 181 nm) and carbon (C wavelength 179 nm). The chromatograms were integrated to obtain a total chromatogram area. This was divided by the mg of sample pyrolysed and adjusted for the split ratio. The total chromatograms were compared to each other to calculate the changes in total nitrogen and sulphur in the pyrolysis volatiles.

### 3.1.9 Lipid Analysis

The microalgal triglycerides were analysed on a Dionex Ultimate 3000 HPLC system with a C-18 column. The method used is known as "non-aqueous reverse phase high-pressure liquid chromatography" with acetonitrile (ACN) and iso-propanol as the mobile phase [110-111]. The samples were dissolved in DCM and the mobile phase gradient flow was 0.5 ml/min with 100% ACN for 2 min, ramped to 30% iso-propanol at t=6 min, ramped to 80% iso-propanol at t=60 min, isocratic flow for 10 min and finally 15 min of 100% ACN re-equilibration time. UV-Vis detection was used at 210-255 nm and full wavelength scanning to allow 3-D plot comparisons of selected peaks. The lipids were additionally transesterified to FAME using methanol and sulphuric acid. Approximately 2 ml methanol were added to 200 mg of extracted lipids with one drop of sulphuric acid and agitated for 1 hour at 55°C in a shaking water bath. 3 ml of pentane and water were added to the reaction mixture. After 1 hour the two distinct layers were separated using a glass syringe, the pentane was left to evaporate resulting in the final FAME extract. The FAME extract was analysed on an Agilent 5890 GC-MS using a RTX-1701 capillary column. The split (10:1) inlet was set to 280°C with an initial column temperature of 60°C held for 2 min, ramped to 280°C at 6°C/min, held for 15 min with a constant column pressure of 2.07 bar. The instrument was calibrated using an external FAME standard purchased from Sigma-Aldrich (F.A.M.E. Mix, C8-C24).

Size exclusion chromatography of the lipids was carried out on a Perkin Elmer Series 200 HPLC instrument with a Varian PGel column of 30 cm length, 7.5 mm diameter, 3µm particle size and a THF mobile phase flow rate of 0.8 ml/min. Approximately 100 mg of lipids were dissolved in 1.5 ml THF and detection was achieved with a refractive index detector. The chromatograms were divided by the sample mass injected for comparison. The instrument was calibrated using a polystyrene molecular weight standard.

### 3.1.10 Thermo-gravimetric analysis

Thermo-gravimetric analysis (TGA) was performed on a Stanton Redcroft DTA or a TA Instruments IR5000Q TGA from 40-900°C in 50 ml min<sup>-1</sup> N<sub>2</sub> at a heating rate of 10°C min<sup>-1</sup>. The corresponding 1<sup>st</sup> derivative of the TGA curve was plotted at various points in the thesis to investigate the volatilisation rate in units of wt.%/°C and is referred to as the DTG curve or derivative mass loss. This can show the temperature of highest volatilisation rate.

The TGA profile was set up to reach 105°C at a rate of 10°Cmin<sup>-1</sup> and held for 10 min, this gives information about the water content of biomass by measuring the weight loss at 105°C. Routinely TGA analysis was carried out using in a constant flow of N<sub>2</sub>. This allows determination of moisture content, the volatile fraction and the non-volatile fraction which consists of the fixed carbon and ash fractions. By switching the gas flow from N<sub>2</sub> to air at high temperature (900°C) the ash fraction can be determined in the same analysis although some ash volatilisation at these temperatures is likely. The fixed carbon content can be calculated by difference from the ash and volatile fraction. Equations 3.4 to 3.7 determine the different proximate fractions:

$$\text{wt. \% Moisture} = \frac{\text{Mass}_{\text{Initial}} - \text{Mass}_{105^{\circ}\text{C}}}{\text{Mass}_{\text{Initial}}} \times 100 \quad \text{Eqn. 3.4}$$

$$\text{wt. \% Volatile} = \frac{\text{Mass}_{105^{\circ}\text{C}} - \text{Mass}_{900^{\circ}\text{C N}_2}}{\text{Mass}_{\text{Initial}}} \times 100 \quad \text{Eqn. 3.5}$$

$$\text{wt. \% Ash} = \frac{\text{Mass}_{900^{\circ}\text{C Air}}}{\text{Mass}_{\text{Initial}}} \times 100 \quad \text{Eqn. 3.6}$$

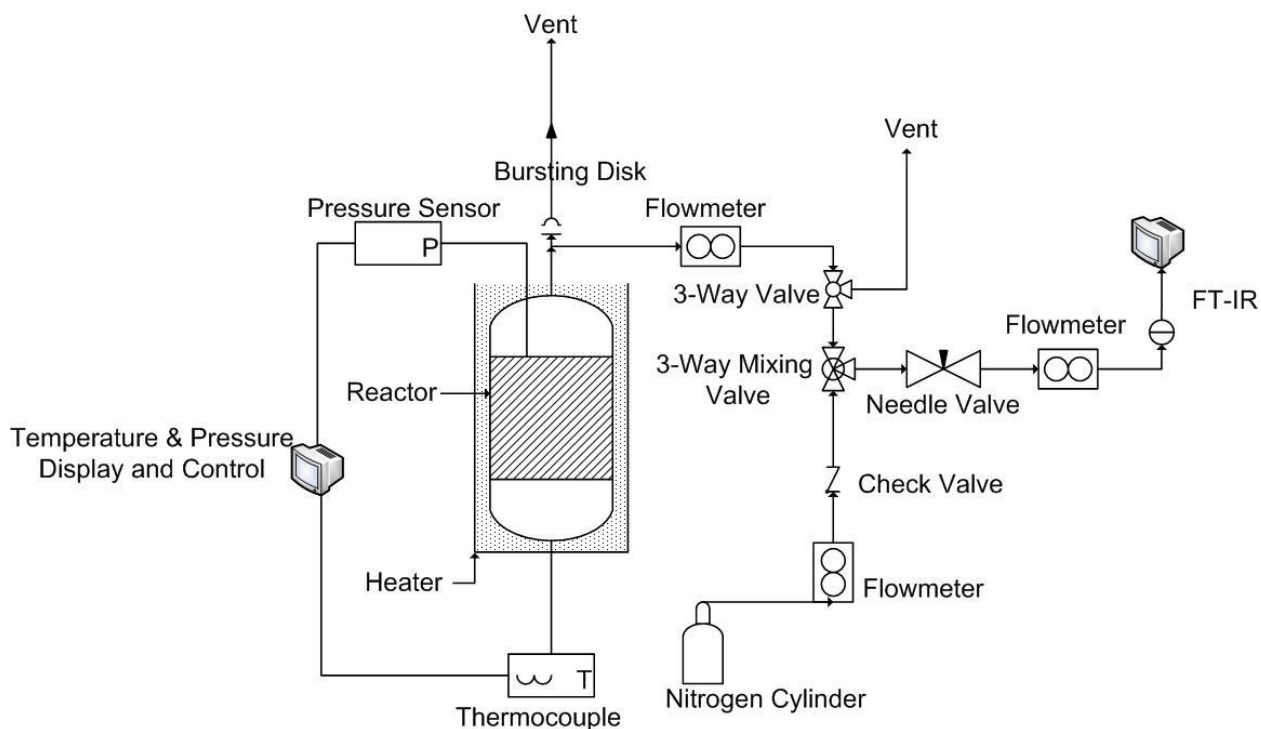
$$\text{wt. \% Fixed Carbon} = 100 - (\text{wt. \% Ash} + \text{wt. \% Volatile} + \text{wt. \% Moisture}) \quad \text{Eqn. 3.7}$$

For bio-crude samples the analysis using TGA to 900°C in N<sub>2</sub> is referred to as *simulated distillation*.

## 3.2 Hydrothermal processing

### 3.2.1 Parr batch processing

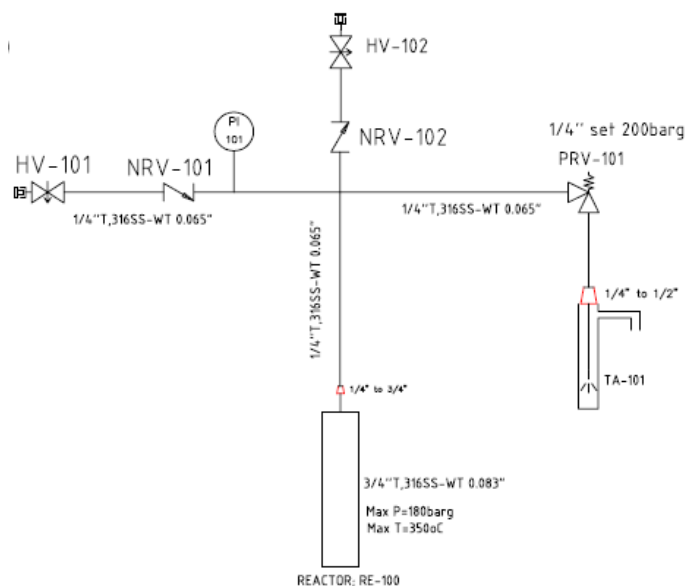
Hydrothermal liquefaction was performed in a batch reactor (75 ml, Parr, USA), charged with biomass and pure distilled water (single distilled, electrical conductivity  $<0.05 \mu\text{S/cm}$ ) or containing either 1 M  $\text{Na}_2\text{CO}_3$  and KOH or 1M of an organic acid ( $\text{CH}_3\text{COOH}$  and  $\text{HCOOH}$ ). The reactor designs are of bomb type and made of either 316 stainless steel or Hastelloy steel. The reactors are unstirred. Standard liquefaction experiments were performed at two temperatures,  $300^\circ\text{C}$  and  $350^\circ\text{C}$  for 1 hour, the heating rate of the reactor is approximately  $9\text{-}13^\circ\text{C min}^{-1}$ . The residence time was taken from the point the reactor reaches temperature. The reactors were cooled at approximately  $6^\circ\text{C min}^{-1}$  by removing the heating mantle and exposing the reactor to ambient air. In each case approximately 3 g of microalgae was mixed with 27 ml of catalyst solution or distilled water. Microalgae was added to the reactor premixed as a slurry. The batch reactor layout is illustrated in **Figure 3.1**.



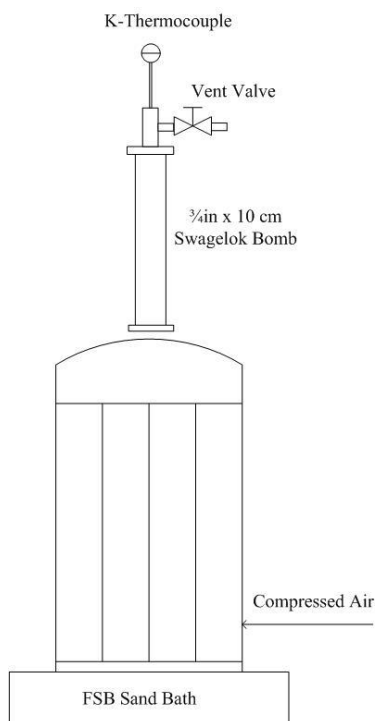
**Figure 3.1:** Schematic of the Parr 75 mL reactor layout

### 3.2.2 Swagelok reactor batch processing

The Swagelok reactors were constructed from 316 stainless steel 1.905 cm x 10 cm Swagelok pipes and are essentially closed bomb type reactor tubes. The first set-up of Swagelok reactors had one reactor end capped and the other connected to a 1.905-0.635 cm reducer. The 0.635 cm pipe was connected to a quick fitting so that the reactor could be purged and pressurised with nitrogen. There was also a pressure release valve connected to a 0.635 cm cross which was set to 200 bar as a safety precaution. The layout of the first reactor set up is shown in **Figure 3.2**. The second set-up was designed with the same reactor size of 1.905 cm pipe and 10 cm length leading to a volume of 25 ml; however for this set-up no nitrogen purge was set up but a thermocouple was added to measure the temperature inside the reactor. Using this internal K-Type thermocouple the time to reach reaction temperature of the reactants was measured to be 2 min. The second setup including the sand bath is shown in **Figure 3.3**. The reactors were submerged completely into a fluidised sand bath (FSB-3, OMEGA Engineering Ltd, Manchester, UK) at the desired temperature and residence time. Once the desired residence time was reached the reactor was quenched in a cold water bath. Reactors were charged with approximately 1 g of microalgae and 10 ml of distilled water. The resulting products were separated and analysed as described in **Section 3.3.1**.



**Figure 3.2:** Schematic of the Swagelok reactor used at the University of Sydney with nitrogen purge.



**Figure 3.3:** Swagelok reactor set-up at the University of Leeds with thermocouple and without nitrogen purge.

### 3.2.3 Continuous processing

A slurry concentration of 1 wt.% was made up by mixing the dried microalgae with 50 litres of distilled water. The slurry viscosity was measured using an Anton Parr SVM 3000 viscometer (Anton Parr GmbH, Austria). The algal feedstock solution was processed in the continuous flow pilot plant at the *University of Sydney* in duplicate for all process conditions and average values are reported. The reactor design and performance are discussed in **Chapter 10**. Following liquefaction, the product stream was collected in 500 ml Duran flasks. Since the biomass to water ratio was so low in this study the amount of bio-crude floating on the water was very small. Therefore, dichloromethane (DCM) was used in order to quantify the bio-crude yields gravimetrically. After addition of DCM, the mixture was separated and filtered to isolate the bio-crude, solids and aqueous phase fraction.

The continuous flow hydrothermal biomass plant was designed and built in-house at the *University of Sydney*. The upper design temperature and pressure of the system are 350 °C and 250 bar which fall in the sub-critical region of water.

The process flow diagram of the plant is presented in **Figure 3.4**. Biomass slurry is pumped in two stages from stirred atmospheric-pressure batch tanks (Pumps 1 and 2 in **Figure 3.4**). Pump 1 is a low pressure screw pump (Range MD, Seepex, Germany) which provides the necessary suction pressure (2-6 bar) for the high pressure stage. Pump 2 is a GEA Niro Soavi model Ariete NS3006P triplex piston pump capable of delivering high viscosity fluids and slurries at pressures up to 600 bar and flowrates in the range 15 – 90 L/hr. The pumping rate is adjusted through the use of a variable speed drive; a mass flow meter (F in **Figure 3.4**) is used to measure the actual slurry feed rate.

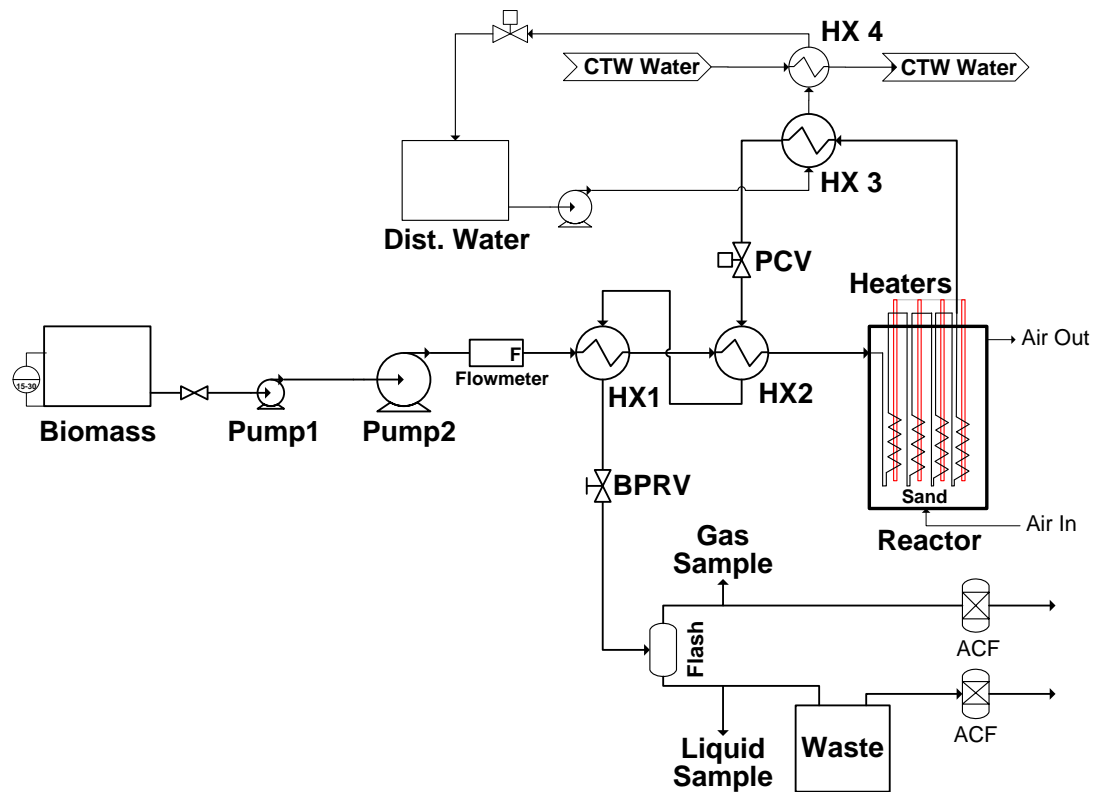
The pressurised slurry (up to 250 bar) is partially preheated in feed-effluent exchangers HX1 and HX2 which capture some of the heat of the product stream leaving the reactor. The heat exchangers HX1 and HX2 are coil-in-shell devices (FLF series sample cooler, Sentry Equipment Corp, USA) in which only the coils are rated for the maximum design pressure of the plant – for this reason, the hot products leaving the reactor are let down to ~10 bar downstream pressure control valve PCV (Type 1711 needle valve, Badger Meter Inc, Germany) before passing to the heat recovery section. In order to maintain the process water in the liquid state during this pressure let-down, the products are first cooled to ~170 °C via contact with a clean circulating water stream in heat exchanger HX3, the temperature of this circulating stream in turn being maintained by contact with cooling tower water in HX4. Back-pressure regulating valve BPRV (KPB series, Swagelok Company, USA) is utilised to keep this line above the saturation pressure. After BPRV, the products are nominally at atmospheric pressure and are separated into gaseous and liquid streams for sampling and analysis. Gases and vapours are vented to atmosphere via activated carbon filters (ACF).

In order to alter the residence times of the experiments, the pump speed was changed and the overall residence times through the reactor coils were calculated based on the flow rate, density, pipe diameter and length.

The reactor is shown schematically in **Figure 3.5**. The reactor comprises of four stainless steel (grade 316) coils immersed into a heated fluidized bed. Depending on the reactor coils

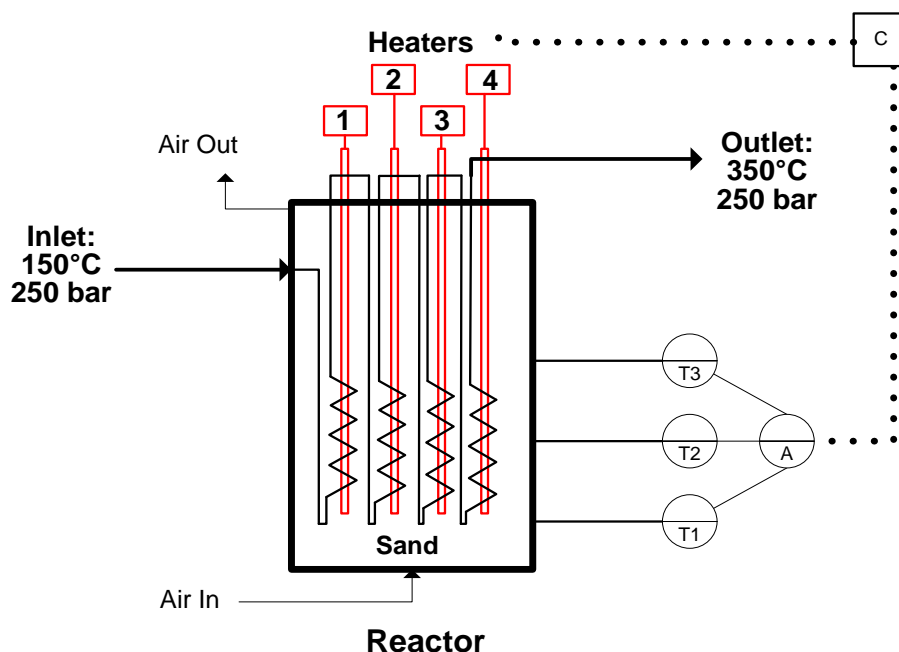
configuration, the plant can provide residence times between  $<1$  and 30 minutes; for this study, the coils (each 16 m in length, outer diameter 9.5 mm and wall thickness of 1.65 mm, total reaction volume  $\sim 2$  L) are connected in series to enable reaction times between 2 and 8 minutes to be studied. Approximately 200 kg of alumina is fluidized by compressed air within the vessel. Heating is provided by  $4 \times 6$  kW electric heating elements inserted into the fluidized bed.

The entire plant is controlled via a distributed supervisory control and data acquisition (SCADA) system supplied by Yokogawa Australia Pty Ltd. Process variables including temperature, pressure and flow rate are specified by the operators through Yokogawa's FAST/TOOLS SCADA software. As illustrated in **Figure 3.5**, the average bed temperature is used to control the power input from the heaters into the system.



**Figure 3.4:** Schematic of the continuous reactor at Sydney University. \*HX=Heat Exchanger; CTW=Cooling Tower Water; ACF=Activated Carbon Filter; PCV=Pressure Control Valve; BPRV=Back Pressure Regulating Valve.

Pressure relief valves are utilised in the process as a safety measure in the case of a pressure build-up due to blocking or poor control resulting in a pressure overshoot. The control system has also been programmed to ensure that set pressures always exceed the saturation pressure of water at the temperature at which the system is operating at each point in time.



**Figure 3.5:** Continuous reactor configuration.

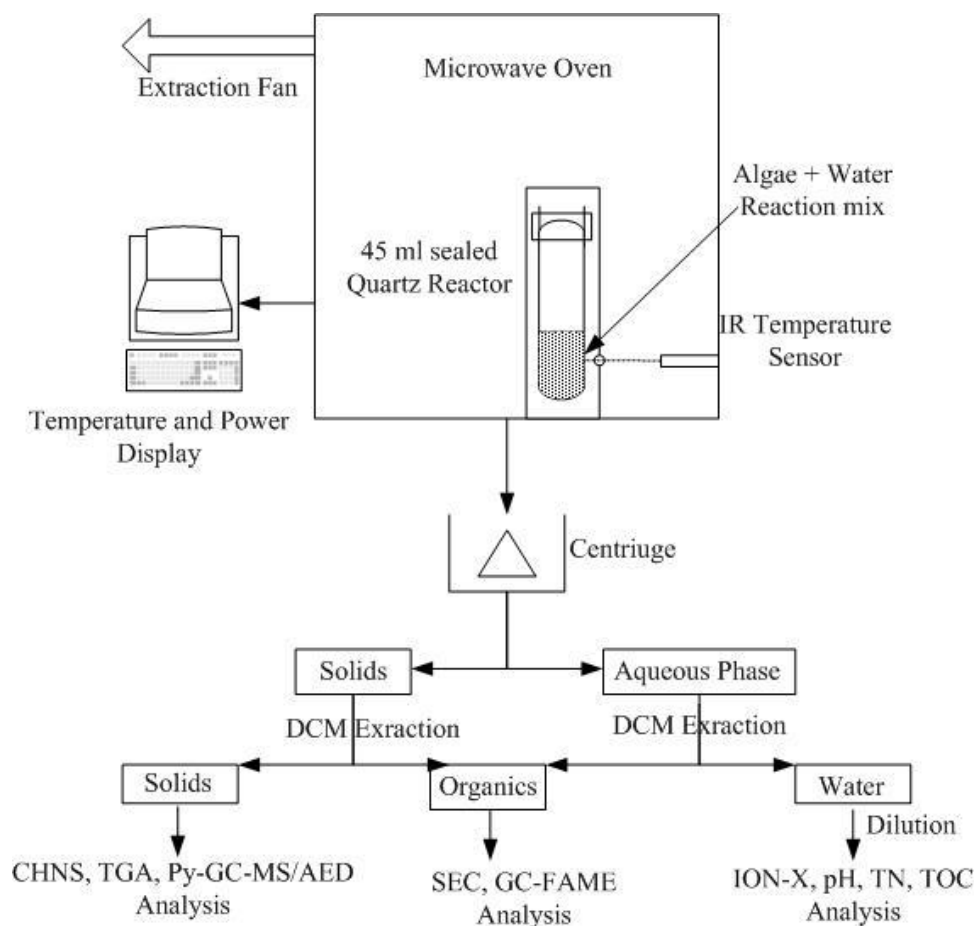
\* C= Control unit; T1-3=Thermocouple; A=Average bed temperature.

### 3.2.4 Microwave processing

Algal slurries were processed individually in a 45 ml sealed quartz reaction vessel within a 1.2 kW Milestone StartSynth microwave oven. Samples were heated to 80, 100, 120 and 140°C within 3 min, the temperature was then kept constant for 12 min before a fan was operated to cool the samples. Internal temperatures of the microalgal samples during processing were measured by an IR thermometer and logged on the control display. The energy used during microwave heating was determined through the integration of the power profiles using the computer's inbuilt Energy consumption/time function. These values were then converted from Wh to MJ/kg to determine the energy required to process 1 kg of dry algae.



After the samples had been cooled, they were centrifuged for 15 minutes at 3500 rpm, equivalent to a  $g$  force of 2264. This was performed to separate the solid biomass sediment from the liquid phases to enable lipid extraction and compositional analysis. The liquid phase was then diluted to 250 ml with deionised water. After centrifugation and freeze drying of the microwaved samples 25 ml of dichloromethane was added in a sealed sample container and shaken continuously for 45 min. Subsequently Whatman type 3 filters were used to separate the DCM soluble fraction from the defatted solids. Yields of lipids were determined gravimetrically after evaporation of the DCM at room temperature. 10 ml of DCM was also added to the supernatant of the centrifuging step to assess if there were any lipids dissolved in the aqueous phase. Water and dichloromethane were separated in a separation funnel and the mass of lipids dissolved in the water were assessed gravimetrically after evaporation of the dichloromethane fraction. The entire processing and sample workup flow diagram is presented schematically in **Figure 3.6**.



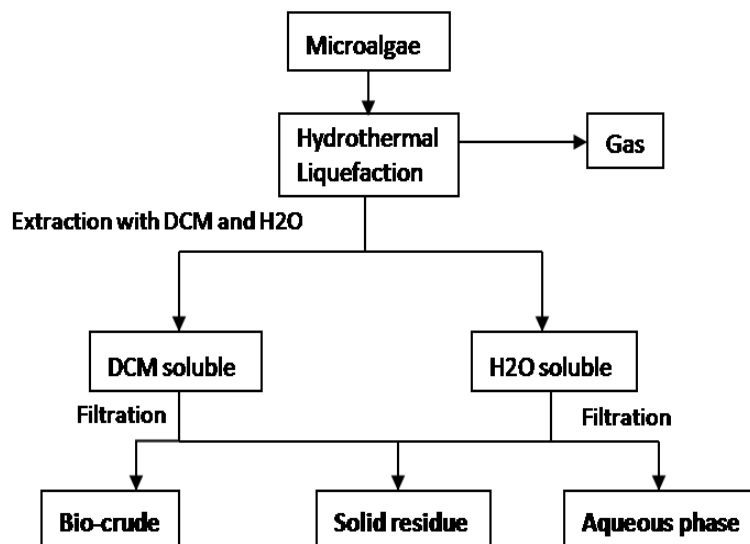
**Figure 3.6:** Schematic of the HMP process and sample workup.

Approximately 1 g of freeze dried unprocessed and microwave processed algae biomass was mixed with 10 ml of deionised water and sealed in a  $\frac{3}{4}$  in x 13.5 cm Swagelok sealed reactor, the remaining headspace contained ambient air. The sealed reactor was submerged to a preheated fluidised sand bath (FSB-3, OMEGA Engineering Ltd, Manchester, UK) at 300°C for a constant residence time of 15 min (see **Figure 3.3**). Using an internal K-Type thermocouple the time to reach reaction temperature of the reactants was measured to be 2 min. Subsequently the reactor was quenched in cold water, once cooled to room temperature the gases were vented. The reactor contents were decanted and the reactor washed using DCM and deionised water (30 ml each in 15 ml aliquots). The resulting mixture was separated in a separating funnel and filtration to a bio-crude, solids and water phase. The solids and bio-crude were weighed and the water phase diluted to 100 ml with deionised water. Yields of bio-crude and solids were determined and analysed as described in the next section.

### 3.3 Sample Workup

#### 3.3.1 Bio-crude Analysis

A schematic of procedures carried out post HTL reactions is presented in **Figure 3.7**. Following liquefaction, 50 ml of dichloromethane (DCM) and 50 ml of water was added to the reaction mixture and the two phases separated in a separation funnel. The DCM phase was separated and filtered following which the solvent was removed by evaporation to determine the mass of bio-crude. The insoluble residue was weighed and then analysed for C, H, N, S content. A portion of the evaporated DCM solubles was analysed for C, H, N, S content and a portion by GC/MS and thermal gravimetric analysis (TGA). The bio-crude was analysed by GC/MS on an Agilent 5975B inert MSD. Separation was achieved on an Rtx 1701 60m capillary column, 0.32 id, 0.25  $\mu\text{m}$  film thickness, using a temperature program of 40°C, hold time 2 minutes, ramped to 250°C, hold time 30 minutes, column head pressure of 30 psi. TGA was performed on a Stanton Redcroft DTA or a TA Instruments IR5000Q TGA from 40-900°C in 50 ml min<sup>-1</sup> N<sub>2</sub> at 10°C min<sup>-1</sup>.



**Figure 3.7:** Schematic of the HTL sample workup.

The HHV of the bio-crude was calculated from their ultimate analysis using the *DuLong* formula [105]. The bio-crude yields were calculated according to **Eqn. 3.8**.

$$\text{Yield} = \frac{\text{Oil Mass}}{\text{Sample Mass} \times (100 - \text{Mois} - \text{Ash})/100} \times 100 \quad \text{Eqn. 3.8}$$

### 3.3.2 Water Analysis

The aqueous phase following hydrothermal processing was diluted to 1 litre with distilled water. Using a Buchner funnel, and a Buchner flask the diluted water phase was filtered through Whatman Type 3 filter papers (10 cm diameter). The retained residue on the filter paper was air dried for 24 hours and weighed by difference of the previously pre-weighed filter paper. 10 ml aliquots of the aqueous phase were analysed by ion chromatography (Dionex, USA) to identify and quantify the main anions and cations present. Total organic and inorganic carbon (TOC, TIC) in the aqueous phase was determined using a TOC analyser (HACH- IL 550 TOC, Hach-Lange, Germany) using a differential method. Total Nitrogen concentrations were determined using HACH-LANGE colorimetry test cuvettes (LCK338, Hach-Lange, Germany). The trace metal concentration in the aqueous phase was measured using an Optima 5300 DV inductively coupled plasma spectrometer (ICP) with optical emission spectrometry (Perkin Elmer, Cambridge, UK) as described previously.

### 3.3.3 Solid residue Analysis

The solid residues were analysed for moisture and ash content by thermo gravimetric analysis on a STANTON Redcroft TGA/ TA Instruments IR5000Q TGA. 5-10 mg of sample was heated in 50 ml/min of air to 650°C at 50°C/min. The residue was also analysed for C, H, N, S content by elemental analysis. A fraction of the solid residue was also digested and analysed by ICP-OES to determine the metal content by the same method described in **Section 3.1.7**.

## 3.4 Microalgae Cultivation

*Chlorella vulgaris*, *Scenedesmus dimorphus* and *Spirulina platensis* were grown and harvested in respective standard growth medium in the University of Leeds, UK laboratory. The cyanobacteria *Chlorogloeopsis fritschii* was cultured and harvested by the Plymouth Marine Laboratories, UK.

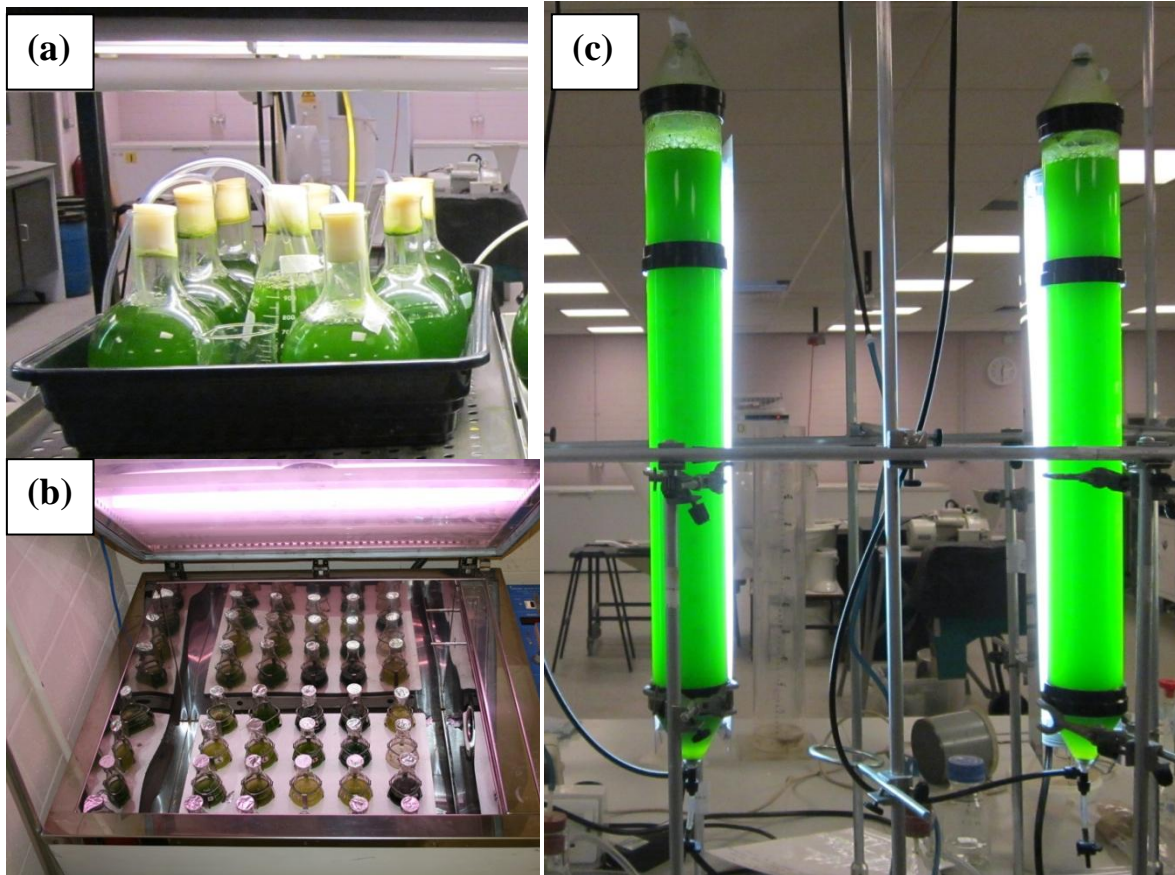
Bulk samples of *Chlorella vulgaris*, *Spirulina* and *Scenedesmus* were cultivated in 10 litre bioreactors using axenic strains obtained from the *Culture Collection of Algae and Protozoa* (SAMS Research Services Ltd, Scottish Marine Institute, Oban, Scotland). The photobioreactors used to grow bulk samples is depicted in **Figure 3.8 (c)**. *Scenedesmus* and *Chlorella* were grown in 3N-BBM+V and *Chlorogloeopsis fritschii* in BG 11 standard media. *Spirulina* was grown in a specially prepared media, the concentrations of nutrients of the different media are presented in **Table 3.3**.

**Table 3.3:** Mass of nutrients made up to 1 litre of distilled water for different algae growth media.

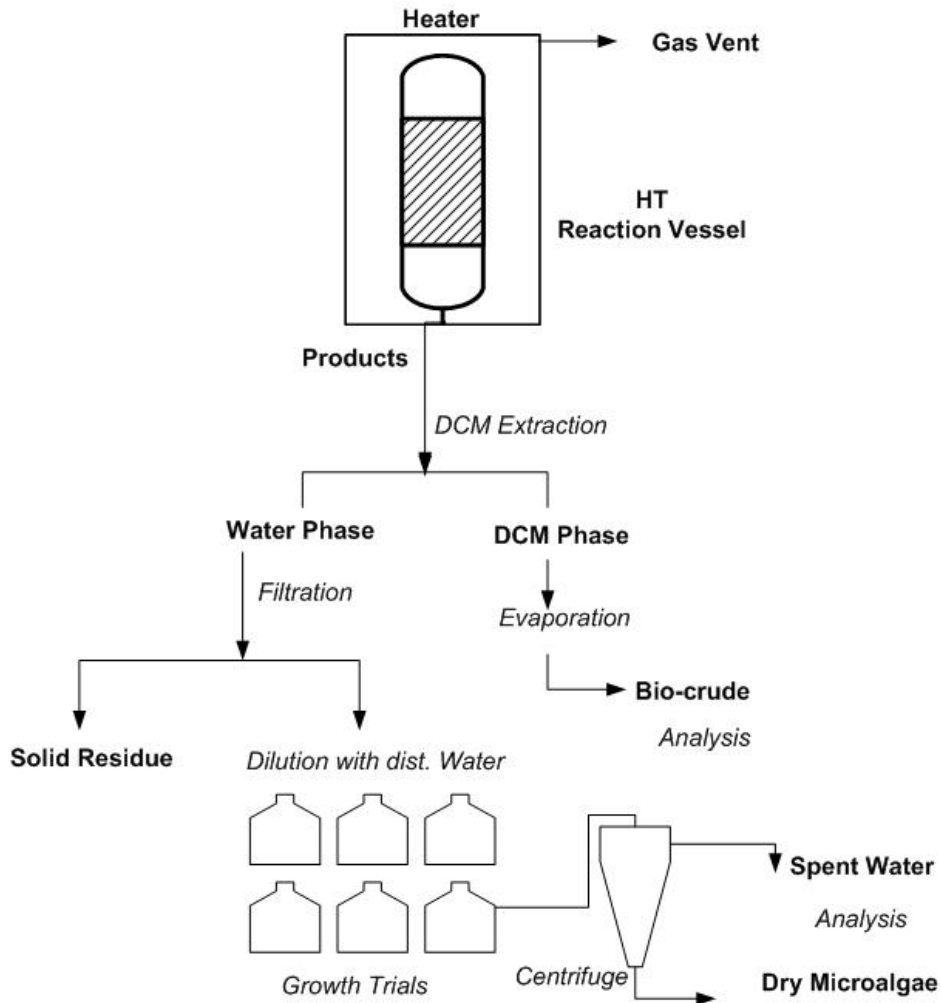
<b>3N-BBM+V</b>		<b>BG11</b>		<b>Spirulina medium</b>	
<i>NaNO<sub>3</sub></i>	750 mg	<i>NaNO<sub>3</sub></i>	1500 mg	<i>NaNO<sub>3</sub></i>	2500 mg
<i>CaCl<sub>2</sub>·2H<sub>2</sub>O</i>	25 mg	<i>CaCl<sub>2</sub>·2H<sub>2</sub>O</i>	36 mg	<i>CaCl<sub>2</sub>·2H<sub>2</sub>O</i>	40 mg
<i>MgSO<sub>4</sub>·7H<sub>2</sub>O</i>	75 mg	<i>MgSO<sub>4</sub>·7H<sub>2</sub>O</i>	75 mg	<i>MgSO<sub>4</sub>·7H<sub>2</sub>O</i>	200 mg
<i>K<sub>2</sub>HPO<sub>4</sub>·3H<sub>2</sub>O</i>	75 mg	<i>Citric Acid</i>	6 mg	<i>K<sub>2</sub>HPO<sub>4</sub>·3H<sub>2</sub>O</i>	500 mg
<i>KH<sub>2</sub>PO<sub>4</sub></i>	175 mg	<i>NH<sub>4</sub> Fe citrate</i>	6 mg	<i>K<sub>2</sub>SO<sub>4</sub></i>	1000 mg
<i>NaCl</i>	25 mg	<i>Na<sub>2</sub>EDTA</i>	1 mg	<i>NaCl</i>	1000 mg
<i>Na<sub>2</sub>EDTA</i>	4500 µg	<i>Na<sub>2</sub>CO<sub>3</sub></i>	20 mg	<i>Na<sub>2</sub>EDTA</i>	80 mg
<i>FeCl<sub>3</sub>·6H<sub>2</sub>O</i>	582 µg	<i>H<sub>3</sub>BO<sub>3</sub></i>	2860 µg	<i>FeSO<sub>4</sub>·7H<sub>2</sub>O</i>	10 mg
<i>MnCl<sub>2</sub>·4H<sub>2</sub>O</i>	246 µg	<i>MnCl<sub>2</sub>·4H<sub>2</sub>O</i>	1810 µg	<i>NaHCO<sub>3</sub></i>	15000 mg
<i>ZnCl<sub>2</sub>·6H<sub>2</sub>O</i>	30 µg	<i>ZnSO<sub>4</sub></i>	222 µg		
<i>CoCl<sub>2</sub>·6H<sub>2</sub>O</i>	12 µg	<i>Na<sub>2</sub>MoO<sub>4</sub></i>	390 µg		
<i>Na<sub>2</sub>MoO<sub>4</sub>·2H<sub>2</sub>O</i>	24 µg	<i>CuSO<sub>4</sub></i>	79 µg		
<i>Vitamin B1</i>	1200 µg	<i>Co(NO<sub>3</sub>)<sub>2</sub></i>	49.4 µg		
<i>Vitamin B12</i>	1 µg				

Growth trials of 300°C HTL process waters were carried out at the Plymouth Marine Laboratories and the trials of 350°C HTL process waters at the University of Leeds. In Leeds, 10 ml of approximately 150 mg/l concentrated media culture was used to inoculate the cultivation trials in 500 ml conical flasks in a media consisting of diluted process water or fresh standard cultivation media (see **Figure 3.8 (a)**). The trials in Plymouth were inoculated at higher concentrations of around 85 mg biomass dry matter in 250 ml conical growth flasks (see **Figure 3.8 (b)**). The process water was diluted (50×, 100×, 200×, 400× and 600×) and the growth rate compared to standard media measured over a 11-12 day period. Each growth trial was carried out in duplicate and the standard deviation is plotted using error bars for each respective growth data point. Ambient air was supplied to the reactors to provide agitation and CO<sub>2</sub>; the reactors were continuously illuminated. The cell count was estimated using a haemocytometer each day and the final biomass produced was separated and dried to obtain a final yield. Biomass accumulation was determined by chlorophyll a absorbance at 660 nm; for each sample, 1.5 ml culture was recovered from each growth flask, the cells were pelleted with a micro centrifuge and the supernatant decanted into a separate tube. 1.5 ml of acetone was added to the pelleted biomass, mixed and incubated overnight in a fridge. Subsequently the biomass was centrifuged again and the supernatant scanned in a UV/Vis spectrophotometer to provide a relative biomass concentration.

Relative chlorophyll a absorbance was measured by a spectrophotometer scan at 660 nm. The growth trials were carried out in duplicate and average measurements of growth are reported. The remaining spent media was analysed by ion exchange chromatography and photometry to assess the uptake of different nutrients. A schematic diagram of the HTL procedure and the growth trials is presented in **Figure 3.9**.



**Figure 3.8:** Images of the cultivation trials and bulk algae cultivation.



**Figure 3.9:** Schematic layout of the HTL reactions, sample workup and cultivation trials. DCM= dichloromethane, HT=hydrothermal

## 4. CHAPTER IV - Characterisation

### 4.1. Introduction

A thorough understanding of the original feedstock is vital in all areas of microalgae research. If the algae strains are grown for a specific extractable compound, compositional analysis allows the determination of its concentration. A typical application of microalgae is the production of bio-diesel for which the total lipid content of the algae is the most important factor. However, the composition of the lipids is just as important; neutral-, polar, phospho-, saturated- and unsaturated lipids are not equally suitable for the production of biodiesel. The characterisation of microalgae lipid fractions is beyond the scope of this Chapter but is addressed for two strains in **Chapter 6**. The other biochemical components analysed, apart from total lipids, are the protein and carbohydrate content. The protein content is significant as this is the main source of nitrogen in the biomass. A high level of nitrogen in algae can lead to complications during thermochemical conversion. Alternatively, if algae is grown as a food supplement, a high protein content is desirable. The carbohydrates contained in microalgae are a source of polysaccharides which are valuable in a range of applications. The composition of carbohydrates can vary between mono-, di- and polysaccharides. A high proportion of monosaccharides can improve the microalgae's suitability as a feedstock for fermentation to ethanol, however many microalgae strains contain carbohydrates such as amylose and starch.

The algae strains were subjected to proximate analysis either by the conventional method in a muffle furnace (see **Section 3.1.2**) or, when only small amounts of biomass was available, by TGA. The moisture content is mainly used for mass balance calculations and to determine chemical composition on a dry ash free basis for characterisation. The ash content is the main source of inorganics in microalgae and can range from very low (<1 wt.%) to very high levels (>60 wt.%). This is significant when performing mass balances and dry ash free calculations. The mineral matter is high in metals which were analysed for the majority of the algae strains by ICP-OES. Some metals are essential for microalgae growth while some are toxic, the fate of these is therefore important during cultivation. Elements such as Cl are additionally of concern due to corrosion. In general, marine strains are high in NaCl and other inorganic salts making them less suitable for combustion due to the high potential for slagging and fouling as shown by Anastasakis et al. [112].



One of the most important parameters investigated is the ultimate analysis, used to determine the carbon, hydrogen, nitrogen, sulphur and oxygen content of the feedstock. The elemental composition was used to calculate the HHV using the *DuLong formula* [105]. The HHV was calculated when not enough biomass (>3 g) was available for analysis using bomb calorimetry. The nitrogen content determined by ultimate analysis also provides the basis of the nitrogen to protein conversion factor as described by Laurens et al. [113]. High carbon and low oxygen contents are generally desirable as these increases the HHV which is beneficial in energy applications. Even small amounts of sulphur in the biomass are undesirable as these can lead to complications during catalytic thermochemical processing since sulphur is known to be a strong catalyst poison.

The analysis of the microalgae feedstocks considered was carried out by multiple techniques to determine their structural composition. Determining feedstock compositions is often essential to ensure more accurate predictions in terms of the chemistry of different algal conversion processes. The characterisation of the feedstock is the basis of all mass balance calculations in subsequent chapters. The current chapter provides a selected overview of the parameters investigated and the main differences amongst microalgae strains.

The analysis methods used in this section are described in **Chapter 3**. Complete data sheets for each microalgae strain are attached in **APPENDIX A**. Parameters analysed include: Proximate and ultimate analysis, biochemical analysis, thermo gravimetric analysis, pyrolysis GC-MS analysis, metal analysis, pigment analysis and scanning electron microscopy (SEM) analysis. There are gaps in the analysis for some strains in the data sheets, mainly due to insufficient masses of microalgae being available for the entire set of analyses. This is indicated in the data sheets as appropriate.

## 4.2. Proximate and ultimate analysis

Five microalgae species were selected to demonstrate the difference in proximate and ultimate composition and are presented in **Table 4.1**. *Haematococcus* is a quite standard green phototrophic microalgae strain with an ash content of 5.7 wt.%, which is typical for this type of microalgae. The two selected marine strains *Porphyridium* and *Nannochloropsis* have a much higher ash content of 24 and 26 wt.% respectively, due to the high levels of inorganic salts originating from the high salinity of the media. This has a detrimental effect on the HHV value, shown in **Table 4.1**. The cyanobacteria *Spirulina* is grown in fresh water but has a slightly higher ash content than the

microalgae *Haematococcus*. The high lipid microalgae *Pseudochoricystis* has a very low ash content of 1 wt.% resulting in a high HHV of 29.4 MJ/kg. The measure ash values in **Table 4.1** are specific to the samples analysed and could vary significantly depending on harvesting and drying techniques; drying off salt water results in higher salt concentrations than for example centrifuging. The ash fraction, which is high in salt, is not differentiated between intra- and extracellular salts therefore the values are unique to the current samples and not the algae strains itself. In addition to the HHV, the nitrogen content is also significant as thermochemical processing of a feed high in nitrogen often results in increased levels of nitrogen in the resulting fuels. The cyanobacteria, *Spirulina*, contains the largest proportion of nitrogen. Cyanobacteria typically have high protein contents, which lead to high nitrogen levels. The high lipid strain *Pseudochoricystis* has the lowest nitrogen content of 2.1 wt.% indicating a low protein content while the other three strains have nitrogen contents of around 8 wt.%, which is a typical value for microalgae. The carbon contents vary between 50 and 60 wt.% with the high lipid strain exhibiting the highest amount. The oxygen contents of the strains investigated range from approximately 25 to 30 wt.%. Strains of algae containing high proportions of carbohydrates tend to have higher oxygen contents, which lower the HHV values. This can be a significant drawback in terms of biofuel processing, as a deoxygenation step might be required to produce the desired fuel compositions.

**Table 4.1.** Proximate, ultimate analysis and HHV of selected microalgae strains.

Name	Proximate (wt.%)		Ultimate Analysis (wt.% daf)					HHV (MJ/kg)
	Ash	Moisture	C	H	N	S	O	
<i>Haematococcus pluvialis</i>	5.7	8.1	53	7.5	7.8	<0.2	31.6	23.9
<i>Porphyridium cruentum</i>	24.4	5.1	51	7.6	8	<0.2	33.1	14.7
<i>Nannochloropsis oculata</i>	26.4	7.2	58	8	8.6	<0.2	25.7	17.9
<i>Pseudochoricystis ellipsoidea</i>	1.0	1.2	61.3	9.1	2.1	<0.2	27	29.4
<i>Spirulina sp. OZ</i>	7.6	5.7	54	7.7	12	0.6	25.9	24.9

### 4.3. Biochemical Analysis

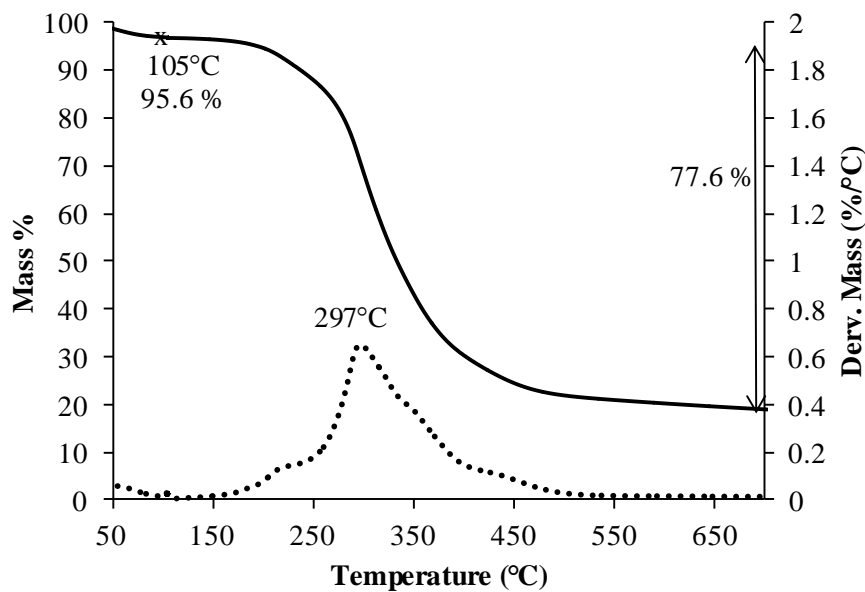
Microalgae are used for a number of applications and depending on the desired use they require different biochemical compositions. For biodiesel production and hydrothermal processing, high lipid contents are favoured. As a feedstock for nutrition, high levels of protein are favoured while this is detrimental for biofuel production. Carbohydrates are generally only required for the extraction of polysaccharides as phytochemicals or fermentation into ethanol. The biochemical composition of selected microalgae strains is presented in **Table 4.2**. The highest lipid content is observed for *Pseudochoricystis* as determined by the Bligh and Dyer method [27]. It has to be mentioned however that this strain also exhibits some aliphatic hydrocarbons which are included in the total lipids [104]. Primarily microalgae only produce triglycerides and free fatty acids. The selected strains exhibit lipid contents in the range of 5 to 67 wt.% leading to varying suitability as a feedstock for biofuel production. The lowest lipid content are observed for the two cyanobacteria; *Spirulina* and *Chlorogloeopsis*. The remaining three green algae: *Chlorella*, *Nannochloropsis* and *Scenedesmus*, have relatively high lipid content ranging from 18 to 35 wt.%. *Spirulina* has a particularly high protein content (65 wt.%) and has commercial applications as a nutritional supplement. The high lipid strain *Pseudochoricystis* has the lowest protein content, which is the reason for the low nitrogen content presented in **Table 4.1**. The other cyanobacteria *Chlorogloeopsis* has a protein content of 50 wt.% which is lower than typical cyanobacteria but this specific strain exhibits an unusually high carbohydrate content of 44 wt.%. The biochemical composition of microalgae is strongly influenced by growth conditions such as nitrogen limitation which leads to higher lipid accumulation. Stress due to nutrient availability or exposure to light can also affect biochemical composition [114]. The required composition can be influenced by growth conditions and is determined by the desired application. Aspects concerning this are covered in more detail in **Chapter 8** and **9**. The current analysis in **Table 4.2** only refers to the specific algae samples analysed for which the growth conditions are unknown and should therefore not be regarded as microalgae species specific.

**Table 4.2.** Protein, carbohydrate and lipid contents of selected microalgae strains.

<i>Microalgae Strain</i>	(wt.% daf)		
	<b>Protein</b>	<b>Carbohydrate</b>	<b>Lipid</b>
<i>Pseudochoricystis ellipsoidea</i>	25	7	67
<i>Chlorella sp.</i>	55	9	36
<i>Spirulina sp. OZ</i>	65	20	5
<i>Nannochloropsis oculata</i>	57	8	35
<i>Scenedesmus dimorphus</i>	43	16	18
<i>Chlorogloeopsis fritschii</i>	50	44	7

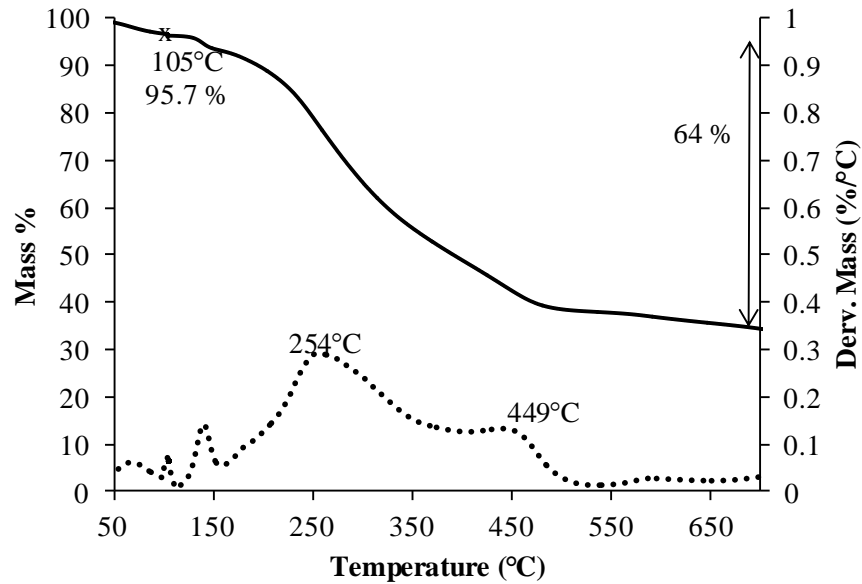
#### 4.4. Thermo gravimetric Analysis

Thermo gravimetric analysis (TGA) is a quick and simple analysis technique which is especially useful when only very small amounts of sample are available (< 10 mg). It gives information about the water content of biomass by measuring the weight loss at 105°C. The data presented in the current section is from analysis in a constant flow of N<sub>2</sub>. This allows determination of moisture content, the volatile fraction and the non-volatile fraction which consists of the fixed carbon and ash fractions. By switching the gas flow from N<sub>2</sub> to air at high temperature (900°C) the ash fraction can be determined in the same analysis as described in **Section 3.1.10**. The 1<sup>st</sup> derivative of the weight loss curve indicated in **Figures 4.1-4.3** as *Deriv. Mass*, shows the main devolatilisation temperatures of microalgae components. This is discussed in more detail in **Chapter 6** and in a journal article [76]. **Figure 4.1** shows the TGA/DTG plot of *Haematococcus* in N<sub>2</sub> between 50 and 750°C. It is shown that the largest weight loss occurs at around 300°C with the DTG curve exhibiting a shoulder towards 400°C. The final mass remaining is around 20 wt.%. In **Table 4.1** it is shown that the ash content is around 6 wt.%, suggesting the algae strain exhibits around 14 wt.% fixed carbon. The weight difference between the temperatures at 105°C and the final temperature is the volatile fraction; this is shown to be around 78 wt.%.



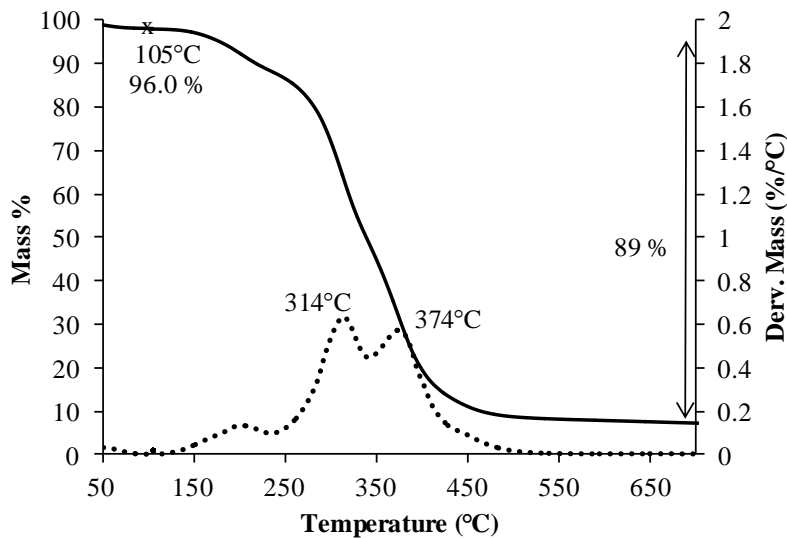
**Figure 4.1:** TGA / 1<sup>st</sup> Derivative Mass loss plot of *Haematococcus pluvialis* in N<sub>2</sub> at 10°C/min heating rate.

**Figure 4.2** shows the TGA/DTG plot of *Nannochloropsis* at the same conditions as **Figure 4.1**. It is observed that the main devolatilisation peak occurs at 250°C with an additional peak at 450°C. The first peak represents the majority of the organic fraction and is likely to be the carbohydrate and protein fraction while the secondary peak at around 450°C corresponds to the volatilising fraction of the triglycerides. This assumption is based on analysing model compounds of protein, starch and lipids which showed that triglycerides volatilise later than the other biochemical components. By integration of DTG peaks around 450°C or comparison of different TGA plots a comparison of the microalgae's lipid content can be estimated as demonstrated by Kebelmann et al. (2013) [115]. This is helpful when comparing different microalgae strains or different growth conditions of the same strain when only limited amounts of sample are available. This is not a fully quantitative method but allows quick and easy comparison; accurate lipid content analysis is carried out by the Bligh & Dyer method but requires around 3 g of biomass. The ash fraction of *Nannochloropsis* is very high; around 25 wt.% as shown in **Table 4.1**, therefore over % of the mass is still remaining at 750°C. The volatile content of *Nannochloropsis* is consequently only 64 wt.% compared to 76 wt.% for *Haematococcus*.



**Figure 4.2:** TGA / 1<sup>st</sup> Derivative Mass loss plot of *Nannochloropsis* in N<sub>2</sub> at 10°C/min heating rate.

The final TGA/DTG selected is of the high lipid strain *Pseudochoricystis*. **Figure 4.3** clearly shows two distinct peaks on the DTG curve. The second peak at 374°C exhibits the lipid fraction volatilising which is known from comparison with model lipid compounds (see **Chapter 6**). The ash content of *Pseudochoricystis* is only 1 wt.%, therefore this strain exhibits a fixed carbon content of 5.7 wt.% and a volatile content of 90 wt.%.

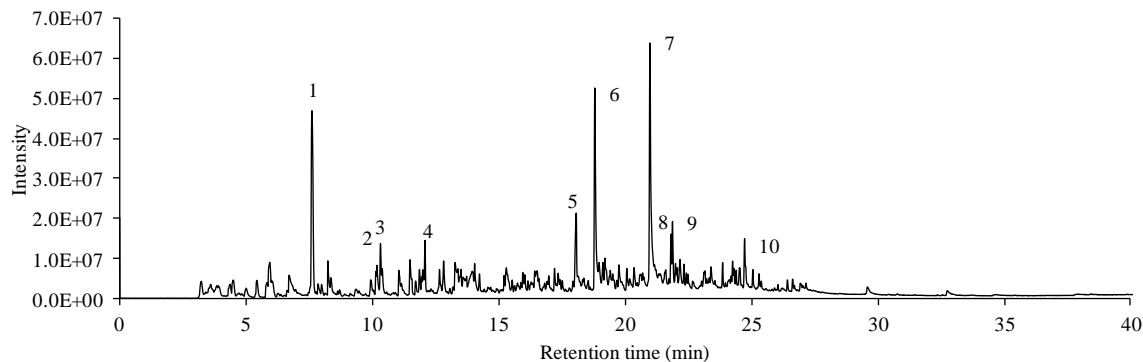


**Figure 4.3:** TGA / 1<sup>st</sup> Derivative Mass loss plot of *Pseudochoricystis ellipsoidea* in N<sub>2</sub> at 10°C/min heating rate.

#### 4.5. Pyrolysis GC-MS Analysis

Pyrolysis GC-MS is a powerful technique for the characterisation of biomass such as microalgae. Only very small amounts of sample (<3 mg) are required for analysis, making it suitable for characterisation of microalgae from small growth trials. Applications of the technique are covered in more detail in **Chapter 9**. Py-GC-MS was used to investigate the flash pyrolysis products formed at 500°C which were separated on a RTX 1701 GC column. Different strains of microalgae produce a “fingerprint” chromatogram unique to the specific sample. The individual peaks are identified by comparison with mass spectral libraries. The origin of peaks is unique to specific biochemical components of microalgae. Pyrolysis products from different model compounds of microalgae components were identified. Lipids generally produce straight chain hydrocarbons and fatty acids, while protein produces nitrogen containing heterocycles and amides. More information on the pyrolysis of model compounds is presented in **Chapter 9**.

The total ion chromatograms of *Chlorogloeopsis*, *Navicula sp.* and *Pseudochorocystis* are plotted in **Figures 4.4, 4.5 and 4.6** respectively. Basic observations of the chromatograms show that, although they differ significantly, certain peaks can be found in all chromatograms. The 10 largest peaks by area are presented in **Tables 4.3, 4.4 and 4.5** with the corresponding identified compound names and retention times. It is shown that *Chlorogloeopsis* produces a number of phenolic compounds and cyclopentadione which are common pyrolysis products of the carbohydrate fraction. Toluene is mainly produced from the pyrolysis of protein and is found in all three chromatograms indicating the presence of protein in all samples. The absolute area of e.g. toluene can be compared to other algae chromatograms' toluene area and a comparison drawn on protein content of the different microalgae strains. *Chlorogloeopsis* is shown to produce mainly carbohydrate and protein derived products which are due to its high protein, carbohydrate and low lipid content. The only lipid derived compound observed within the 10 largest peaks is 2-methyl-1-Hexene.



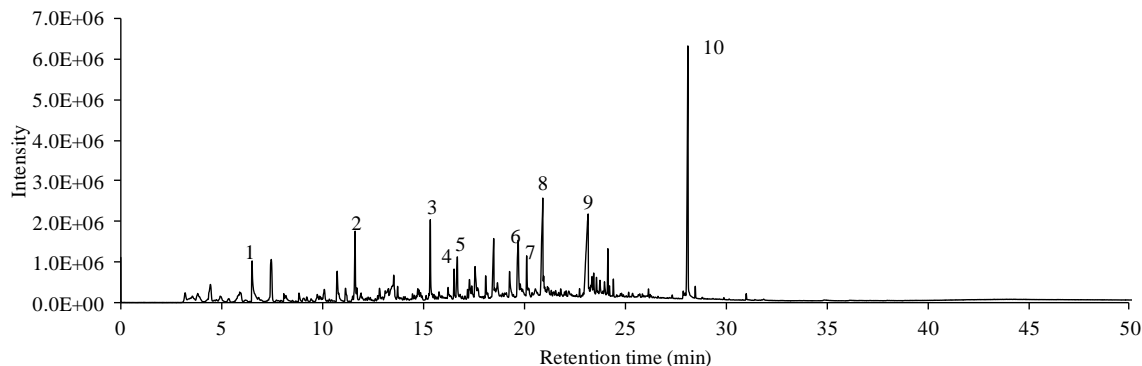
**Figure 4.4:** Total ion chromatogram of Py-GC-MS of *Chlorogloeopsis fritschii* at 500°C

**Table 4.3:** Compounds identified form Py-GC-MS of *Chlorogloeopsis fritschii* at 500°C

Peak number	Retention time	Area %	Compound
1	7.6	24.9	Toluene
2	10.1	3.1	Ethylbenzene
3	10.3	2.7	Pyrrole
4	12.1	2.9	<i>NI</i>
5	18.1	7.4	3-methyl-1,2-Cyclopentanedione
6	18.8	20.8	Phenol
7	20.9	27.1	4-methyl-Phenol,
8	21.8	3.5	2-methyl-1-Hexene
9	21.9	4.9	Benzyl nitrile
10	24.7	2.5	Benzenepropanenitrile

The chromatogram of the diatom *Navicula sp.* (**Figure 4.5**) looks distinctly different to that of *Chlorogloeopsis*. Only two protein derived, nitrogen-containing compounds are present, indicating a low concentration of protein in the microalgae. The largest peak, with 35 % of total chromatogram area, is an alcohol derived from the lipid fraction of the algae. There is also the straight chain hydrocarbon pentadecane observed. This indicates that the microalgae strain exhibits a high lipid level. The majority of the remaining compounds are derived from carbohydrates such as furfural, maltol, levoglucosenone and the furan and phenol compounds. This leads to the conclusion that the most abundant biochemical fractions present in the microalgae are carbohydrates and lipids.



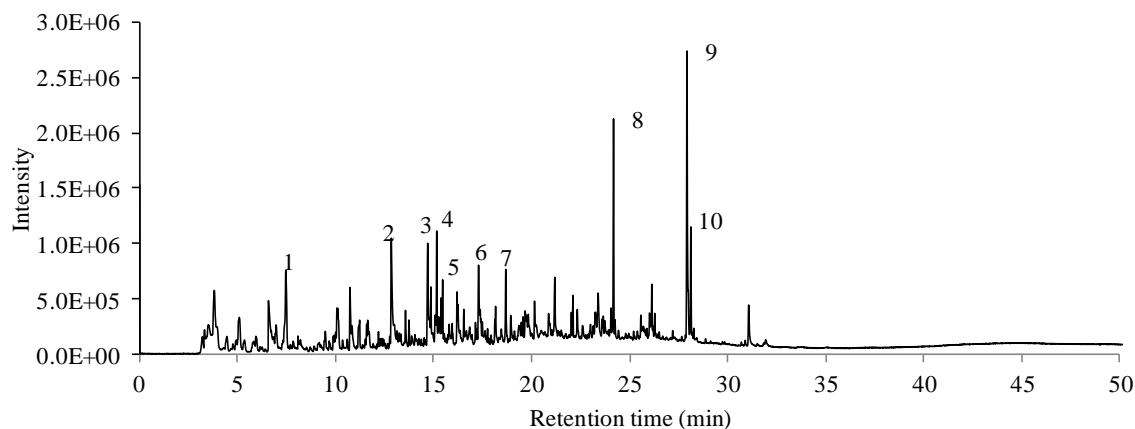


**Figure 4.5:** Total ion chromatogram of Py-GC-MS of *Navicula sp.* at 500°C

**Table 4.4:** Compounds identified form Py-GC-MS of *Navicula sp.* at 500°C

Peak Number	Retention time	Area %	Compound
1	7.5	8.9	Toluene
2	11.6	7.2	Furfural
3	15.3	7.8	5-methyl-2-Furancarboxaldehyde
4	16.5	2.6	4-Amino-2(1H)-pyridinone
5	16.7	5.6	2,2-diethyl-3-methyl-Oxazolidine,
6	19.7	10.7	Maltol
7	20.1	3.8	4-methyl-Phenol
8	20.9	14.2	Levogluosenone
9	24.1	3.9	Pentadecane
10	28.1	35.4	2-(octadecyloxy)-Ethanol,

The total ion chromatogram of *Pseudochorocystis* is shown in **Figure 4.5**. For this algae strain no nitrogen-containing compounds were identified in the 10 largest peaks due to its low protein content. The largest peaks are produced from the lipid fraction, such as the three straight chain hydrocarbons and the alcohol compound present. Cyclopentanedione and furanmethanol are produced from the carbohydrate fraction of the algae. This is known from the pyrolysis of starch as a model compound which also produced these compounds. The only protein-derived compound present is toluene although this is also produced from chlorophyll *a*.



**Figure 4.5:** Total ion chromatogram of Py-GC-MS of *Pseudochoricystis ellipsoidea* at 500°C

**Table 4.5:** Compounds identified from Py-GC-MS of *Pseudochoricystis ellipsoidea* at 500°C

Peak Number	Retention time	Area %	Compound
1	7.4	7.1	Toluene
2	12.8	11.6	2-Furanmethanol
3	14.7	11.2	1,2-Cyclopentanedione
4	14.8	5.0	ND
5	15.1	5.7	3-Undecene, (E)-
6	17.3	6.0	1,2-Cyclopentanedione, 3-methyl-
7	18.7	4.6	5-Decen-1-ol, (Z)-
8	24.1	13.4	Pentadecane
9	27.9	28.0	3-Heptadecene, (Z)-
10	28.1	7.5	Heptadecane

#### 4.6. Metal Analysis

The concentration of metals present in selected microalgae strains is presented in **Table 4.6**. The metal concentration is a significant factor to consider in applications of bioenergy. The metals mainly originate from salts and are typically much higher when the algae originate from a marine environment. High concentrations of metals cause problems when the biomass is combusted as they

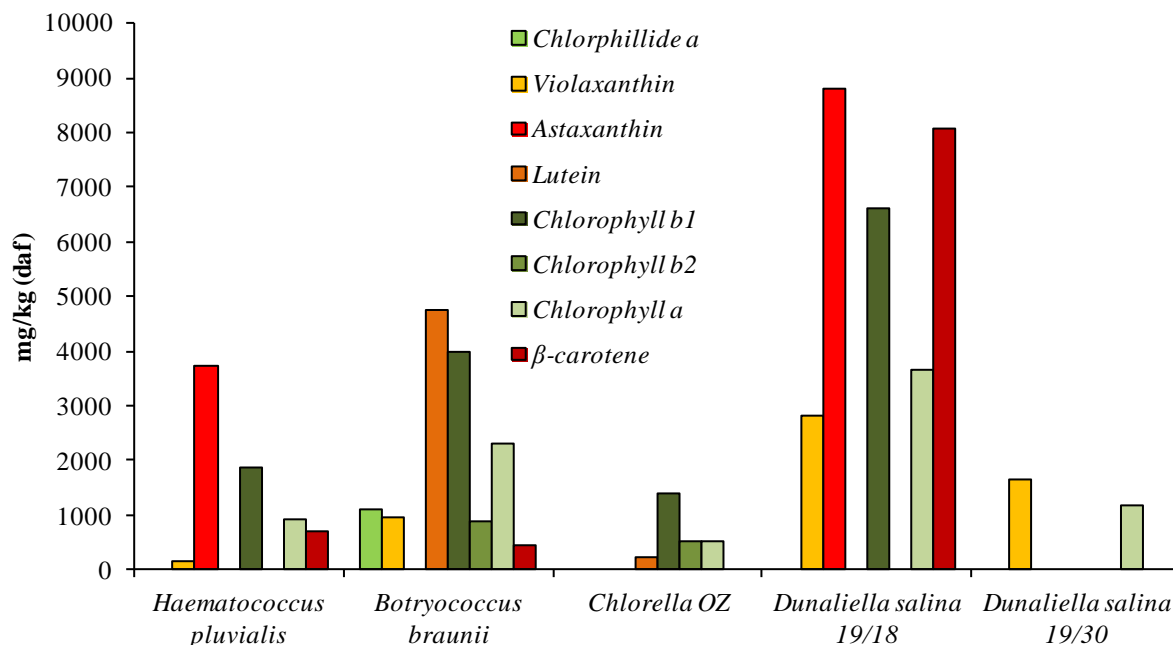
cause fouling of heat exchangers and slagging in the furnace due to ash melting [112]. Additionally chloride can cause corrosion in both combustion and hydrothermal processing. Nutrients required for algae growth include metals: K, Ca, Fe, Na and the non-metal P. The fate of these compounds throughout hydrothermal processing is important if nutrient recycling is to be incorporated. Ni on the other hand is toxic to microalgae growth. Microalgae have been suggested as a technique of recuperating and recycling nutrients from waste water. This could result in accumulation of heavy metals which requires consideration and monitoring. The analysis of common metals and P was carried out by ICP-OES and the results of five selected strains are presented in **Table 4.6**. The concentration of metals is influenced by the harvesting technology. If the initial solids concentration contains significant amounts of salt water, evaporation will lead to increased levels of metals in the dry biomass and extracellular salts are present. The current analysis was performed regardless of the harvesting technology employed as further processing was carried out on the samples as presented below. It is shown that the marine strains *Nannochloropsis* and *Porphyridium* have much higher concentrations of most metals and especially of Na and Cl due to their high ash and salt contents. Typical Cl values of a marine strain range from approximately 25-80,000 mg/kg while the fresh water strains only contain around 4000 mg/kg and *Pseudochoricystis* only 10 mg/kg. The levels of potassium are in the range of 15-20,000 mg/kg for all strains except *Pseudochoricystis*, this strain exhibits extremely low concentrations of all metals, and only the level of P is comparable to the other strains. Phosphorus concentrations are very similar for all strains at around 6-9,000 mg/kg. This is an element essential for microalgae growth but world resources are limited. There is considerable interest in recycling of this element as it is essential for all biomass growth.

**Table 4.6:** Concentration of metals and P present in selected microalgae strains in mg/kg.

(mg/kg db)	Al	Ca	Cl	Cu	Fe	K	Mg	Mn	Na	Ni	P	Zn
<i>Chlorella sp.</i>	13	3141	3893	6	1179	14899	4028	44	1108	1	7954	135
<i>Porphyridium cruentum</i>	ND	39852	25348	16	1815	19009	5085	116	80400	3	8889	99
<i>Nannochloropsis occulata</i>	ND	700	76955	10	714	14989	3295	53	189271	ND	7806	18
<i>Pseudochoricystis ellipsoidea</i>	ND	209	10	11	48	2899	244	7	124	ND	6256	11
<i>Spirulina OZ</i>	402	7782	4433	8	879	13899	4256	56	4732	3	8817	27

## 4.7. Pigment Analysis

Pigment analysis was performed by HPLC and selected results are presented in **Figure 4.6**. Pigments are commonly extracted from microalgae due to their high concentrations and high commercial value.  $\beta$ -carotene and astaxanthin have been produced commercially from *Dunaliella salina* and *Haematococcus* respectively. Both these pigments are beneficial for human health and have a commercial value of up to 10,000 €/kg [18]. Violaxanthin is an orange coloured pigment which is used as a food colouring agent. Lutein is the carotenoid responsible for the yellow coloration in egg yolks and acts as an antioxidant. The analysis of pigments is helpful when microalgae is grown for the production of phytochemicals. Pigment analysis is also addressed in **Chapter 9**. **Figure 4.6** shows that all strains have chlorophyll *a* present which is expected as the presented strains are all phototrophic. Chlorophyll *a* is the main pigment responsible for light absorption for photosynthesis. The levels of different chlorophyll compounds vary from strain to strain. Astaxanthin is only produced by *Haematococcus* and *Dunaliella salina 19/18*; the two strains used commercially for extraction of this compound. *Dunaliella salina 19/18* is also grown commercially for the production of  $\beta$ -carotene. The level of this pigment is 8000 mg/kg while the other *Dunaliella* strain (19/30) does not produce any  $\beta$ -carotene. It appears that *Botryococcus* and *Dunaliella 19/18* have the most diverse profile of different pigments while *Dunaliella 19/30* only exhibits violaxanthin and chlorophyll *a*. It should be noted that the results presented in **Figure 4.6** are not fully quantitative and are to be regarded as a means of comparing pigment levels in different strains of microalgae. This is the purpose of the pigment analysis in the current work and especially for the topics covered in **Chapter 9**. Full quantification of each pigment is beyond the scope of this study.

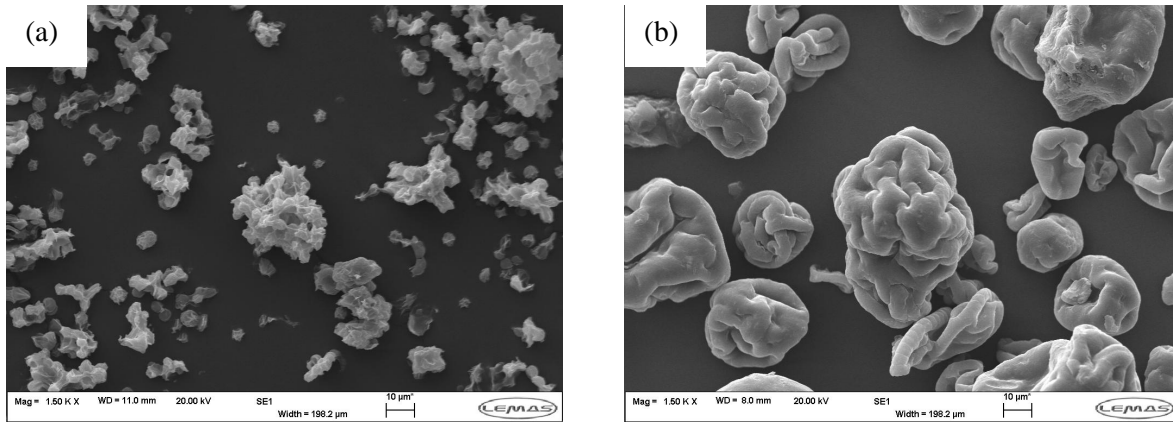


**Figure 4.6:** Analysis of pigments by HPC in selected microalgae strains, units in mg/kg (daf).

#### 4.8. SEM Analysis

Scanning electron microscopy (SEM) was employed to obtain visual images of the microalgae strains. This was mainly performed to assess the effects of processing techniques on the structure and damage to algae cells (see **Chapter 10** and **11**). However SEM also gives information on the size of individual cells which is valuable when filtration is used to harvest microalgae. Additionally, dried microalgae can be investigated to examine if individual cells agglomerate to larger structures or appear as separate cells. This can be significant during processing, grinding, combustion and when consumed as a food product. SEM images of lyophilised *Chlorogloeopsis fritschii* and *Spirulina OZ* samples are shown in **Figure 4.7 (a-b)** at a magnification of 1500. It is shown that *Chlorogloeopsis* cells are extremely small ranging from 1-4  $\mu\text{m}$  in diameter. Individual cells are surrounded by extracellular material called hormogonia, leading to larger structures of cell clusters ranging from 3-50  $\mu\text{m}$ . Some cells do however appear individually while other structures only exhibit hormogonia and no cells. This extracellular material is not as strong as the cell walls and is therefore easily removed during processing. The cells of *Spirulina* on the other hand, appear as

tubes, spiralled into each other. This leads to individual structures of around 20-70  $\mu\text{m}$ . The spiralling effect is the origin of the cyanobacteria's name; *Spirulina*. The characteristic elongated spiral structures often presented elsewhere are not as apparent in **Figure 4.7b** due to freeze drying of the algae under vacuum. SEM images are available for some of the microalgae strains investigated and are included in the data sheets of each microalgae in **APPENDIX A**.



**Figure 4.7:** SEM image of (a) *Chlorogloeopsis fritschii* and (b) *Spirulina OZ* at 1500 magnification

## 5. CHAPTER V - Microalgae HTL

### 5.1 Introduction

In the current chapter, a variety of different algae are investigated to provide insight into how different properties can affect liquefaction behaviour. A total of 11 strains were processed at standard hydrothermal liquefaction conditions and the yields and compositions of resulting bio-crudes compared. Samples used include strains cultivated in marine and freshwater, cyanobacteria, green algae, red algae and diatoms. This research currently represents the single largest database in the literature comparing different microalgae strains processed by HTL.

Experiments were carried out in a Parr 75 ml batch reactor at a constant residence time of 1 hour and temperature of 350°C. Effects of residence time and temperature were separately investigated on one selected strain, *Chlorella vulgaris* OZ, in order to determine the optimum residence time and operating temperature for maximum bio-crude yield and quality. The effect of operating temperature on the concentration of nutrients, total organic carbon (TOC) and total nitrogen (TN) in the process water was also investigated. Factors such as reactor loading and biomass/water ratio were not investigated, however, these parameters have previously been shown to have minor effects on liquefaction performance [116].

### 5.2 Methodology

The 11 strains were all subjected to hydrothermal liquefaction at 350°C for one hour residence time. The residence time was taken from the time the reactor reached temperature (30 min, heating rate 9-13 °C min<sup>-1</sup>). Detailed procedures of the hydrothermal liquefaction experiments are described in **Chapter 3**. Initial screening of different algae strains was carried out in the 75 ml high-pressure Parr reactor. The effect of temperature and residence time was studied on the custom built Swagelok reactor submerged in a fluidised sand bath. More details are found in **Chapter 3**. Analyses of the microalgae strains before processing can be found in **APPENDIX A**.

## 5.3 Results

### 5.3.1 Microalgae HTL at standard conditions

**Table 5.1** shows the results from the hydrothermal liquefaction of microalgae at 350°C for 1 hour. The bio-crude yields are presented along with their elemental composition and calculated HHV. Yields of bio-crude range from 21 to 51 wt.% on a dry ash free basis for all strains of microalgae investigated. The average lies at 33.7 wt.%, which is higher than the average lipid content of the microalgae strains investigated. The lowest yield is obtained from the red algae *Porphyridium*, this microalgae is high in carbohydrates and ash as it is from a marine origin (see **Table 4.1**). On the other side of the spectrum, the high lipid strain *Pseudochoricystis* exhibits the highest bio-crude yield of 50.5 wt.%. The cyanobacteria *Chlorogloeopsis* also exhibits a particularly high bio-crude yield (44 wt.%). The reason for this is unclear as *Chlorogloeopsis* has a low lipid content of 7 wt.% and a high carbohydrate content of 44 wt.%. The majority of strains result in a bio-crude yield of around 30-35 wt.%. The two strains of *Chlorella* investigated, from different sources, showed a similar bio-crude yield of 32 and 36 wt.%. The two strains of the cyanobacteria, *Spirulina*, were also found to have a similar bio-crude yield of 26 and 29 wt.%. Not every result presented in **Table 5.1** was carried out in duplicate but a number of experiments were carried out in duplicate/triplicate and an average repeatability of 1.6 % was calculated for all Parr reactor hydrothermal liquefaction experiments.

The bio-crude samples were analysed for elemental composition using a CHNS Analyser and oxygen content was determined differentially as presented in **Table 5.1**. From elemental analysis results, the HHV value was calculated using the *Dulong formula* [105]. The average elemental composition of a bio-crude produced at 350°C is 72 wt.% carbon, 9 wt.% hydrogen, 4.7 wt.% nitrogen, 0.1 wt.% sulphur and 13.6 wt.% oxygen. This leads to a HHV of 36 MJ/kg, representing a good quality bio-crude compared to bio-crude from pyrolysis. There are only small amounts of water present in bio-crudes from HTL (> 1 wt.%) [117] compared to around 20 wt.% for pyrolysis oils. HTL processing significantly upgrades the original biomass (see **Table 4.1**) resulting in a HHV close to that of crude oil [75]. The sulphur content of 0.1 wt.% is acceptable but also a factor to consider as it can cause catalyst poisoning. The average oxygen content of 14 wt.% is significantly lower than that of pyrolysis oils but still high when comparing to crude oils (>5 wt.%) [75]. The highest oxygen content found in the bio-crudes is produced from *Chlorogloeopsis*, it represents approximately double the average at 28 wt.%. This is most likely due to the formation of a large



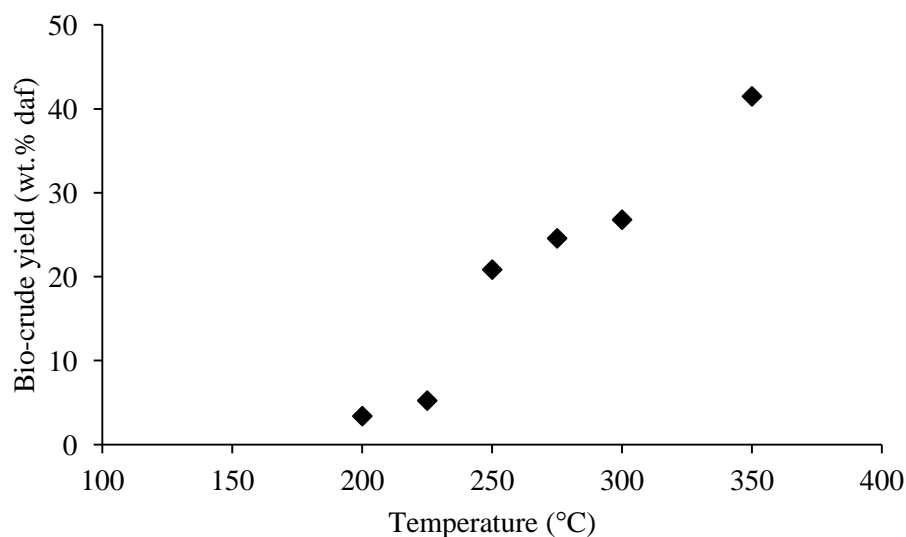
proportion of bio-crude from the carbohydrate fraction. More details on bio-crude formation pathways from biochemical components in are given in **Chapter 7**. The lowest oxygen contents are found for *Chlorella OZ*, *Miyako* and *Zenmyo*, all below 10 wt.%, leading to elevated HHVs of >38 MJ/kg. Although the oxygen content of *Chlorella OZ* is lower, the HHVs of the two samples from the DENSO Corp. (*Miyako* and *Zenmyo*) are higher due to the lower nitrogen content: 2.5 wt.% compared to 6.5 wt.%. The lower nitrogen content of the bio-crude is due to the lower nitrogen/protein content of the microalgae feedstock (see **APPENDIX A**). The nitrogen content of the bio-crudes varies from 1.2 to 6.5 wt.% for *Pseudochoricystis* and *Chlorella vulgaris OZ*, respectively and is directly related to the protein content of the original microalgae. One of the major drawbacks of HTL of microalgae is the high nitrogen content of the bio-crudes. This is problematic during combustion of the bio-crude due to fuel-bound NO<sub>x</sub> emissions. Further problems may be encountered if the fuel is to be upgraded by hydrogenation as large amounts of hydrogen are required to remove nitrogen as ammonia. An obvious solution to overcome these issues would be to grow high-lipid, low-protein feedstocks, however these are more difficult to grow and are associated with lower growth rates. Other possible routes to overcome the high nitrogen content in bio-crudes include pre-treatments and the use of catalysts. These options are investigated in **Chapters 11** and **6** respectively.

**Table 5.1:** Hydrothermal liquefaction yields, elemental analysis and HHV of bio-crude of selected microalgae species.

<b>Strain</b>	<b>Bio-crude yield (wt.% daf)</b>	<b>C</b>	<b>H</b>	<b>N</b>	<b>S</b>	<b>O</b>	<b>HHV (MJ/kg)</b>
<i>Scenedesmus dimorphus</i>	27.1	73.0	8.2	5.7	0.5	12.6	33.6
<i>Chlorella sp.</i>	35.8	70.7	8.6	5.9	0	14.8	35.1
<i>Chlorella OZ</i>	32.3	75.7	9.8	6.5	0	7.8	38.2
<i>Spirulina sp.</i>	29.2	73.3	9.2	7	0	10.4	36.8
<i>Spirulina sp. OZ</i>	25.9	74.6	9.0	5.4	0	10.9	36.9
<i>Porphyridium cruentum</i>	21.2	72.8	8.5	5.4	0.3	13.3	35.7
<i>Nannochloropsis oculata</i>	34.3	68.1	8.8	4.1	0	18.9	34.5
<i>Pseudochoricystis</i>	50.5	74.3	10.8	1.2	0	13.7	36.6
<i>Miyako</i>	37.4	77.4	10.1	2.5	0	9.9	39.2
<i>Zenmyo</i>	32.9	77.5	10.6	2.5	0	9.4	39.9
<i>Chlorogloeopsis fritschii</i>	44.2	59.5	6.9	5.5	0	28.1	29.1
<b>Average</b>	<b>33.7</b>	<b>72.4</b>	<b>9.1</b>	<b>4.7</b>	<b>0.1</b>	<b>13.6</b>	<b>36.0</b>

### 5.3.2 Effect of HTL Temperature

*Chlorella OZ* was used to study the effect of temperature on the HTL of microalgae. A constant residence time of 15 min was employed; measured from time of submersion of the Swagelok reactor into the sand bath until the reactor is quenched with cold water. **Figure 5.1** shows the yields of bio-crude produced at 200, 225, 250, 275, 300 and 350°C. The yields are very low at temperatures below 250°C. The yields were measured to be 3.5 and 5.3 % at 200 and 225°C, respectively. This leads to the conclusion that mainly the lipids are extracted from the algal biomass and that no significant bio-crude formation from other biochemical components occurs. A step change in bio-crude yield is observed at 250°C when the yield increases to 20.8 %. From 250°C to 300°C the yield increases by no more than 6 wt.%. At 350°C however, the yield is increased to 41.5 wt.%. Due to the design of the reactor, temperatures above 350°C could not be investigated, however, it is known that above 350°C, gasification reactions start to predominate, resulting in lower bio-crude yields [68]. It is apparent that increasing temperatures lead to higher bio-crude yields with step changes at 250°C and 350°C; this is most likely due to increased bio-crude formation from non-lipid components of the microalgae.



**Figure 5.1:** Bio-crude yields from HTL of *Chlorella vulgaris OZ* at varying temperature for 15 min.

The elemental analysis of the bio-crudes as a function of temperature at 15 min residence time is presented in **Table 5.2**. The results show that the nitrogen content generally increases at higher temperatures to a maximum of 7 wt.% at 350°C from a minimum of 3.9 wt.% at 225°C. The

nitrogen content observed at 300°C is uncharacteristic for liquefaction behaviour of microalgae at similar conditions; a general increase is observed when higher HTL temperatures are employed [67-68]. The nitrogen increase with higher temperatures is attributed to the protein fraction increasingly breaking down to small molecules and repolymerising to bio-crude compounds. This specific strain is very high in chlorophyll *a*, which also contains nitrogen (see data sheet in **APPENDIX A**). The fate of chlorophyll *a* during HTL has not yet been reported in literature; therefore the fate of nitrogen from chlorophyll *a* during HTL is unknown. This is one possible explanation for the uncharacteristic result at 300°C. Another factor supporting this hypothesis is the relatively high nitrogen content of the bio-crude processed at low temperatures. Similar results by Alba et al. show lower nitrogen contents at these conditions [37].

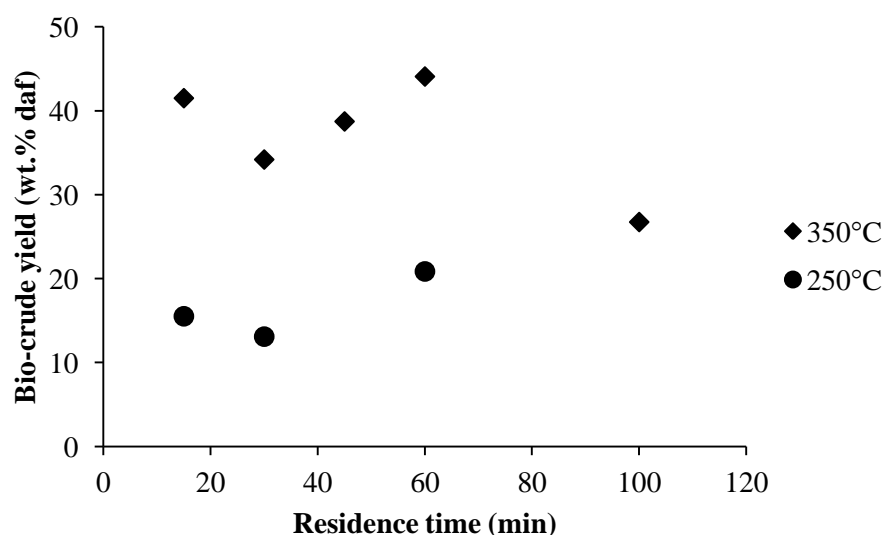
The oxygen content of the bio-crudes initially decreases to 12% as temperatures are increased to 275°C. As the temperatures are raised further, the oxygen contents increase significantly to 25 wt.%. This also appears to contradict the trends reported in published data on HTL of microalgae. Alba et al., Brown et al. and Jena et al. showed constantly decreasing oxygen contents in bio-crude from various strains of microalgae when increasing the HTL temperature [37, 67-68]. The reason for the contradicting results in this study are unclear, but as highlighted in **Chapter 1**, liquefaction behaviour of microalgae is very strain and system specific [116]. The current results are processed using high heating and cooling rates which could affect decarboxylation. More details on the effects of this on oxygen contents of bio-crude from HTL are covered in **Chapter 10**.

**Table 5.2:** Effect of operating temperature on elemental composition and HHV of bio-crudes from HTL.

	<b>C</b>	<b>H</b>	<b>N</b>	<b>S</b>	<b>O</b>	<b>HHV</b>
15 min residence time	<b>(wt.% daf)</b>					<b>(MJ/kg)</b>
<b>200°C</b>	68.2	8.8	4.6	0.5	17.9	32.5
<b>225°C</b>	67.8	8.4	3.9	0.4	19.5	31.4
<b>250°C</b>	68.5	8.7	5.2	0.6	17.0	32.6
<b>275°C</b>	71.1	8.8	7.0	0.7	12.4	34.5
<b>300°C</b>	62.8	7.8	5.7	0.6	23.1	28.3
<b>350°C</b>	60.1	7.3	7.0	0.7	24.9	26.4

### 5.3.3 Effect of HTL Residence Time

The effect of the residence time at constant temperature on the liquefaction yields is plotted in **Figure 5.2** for 250 and 350°C. The results show maximum bio-crude yields at 60 minutes for both temperatures. Higher temperatures are associated with higher yields as shown in the previous section. The yields are initially relatively high at 15 min and then decrease before starting to increase again. This is most likely due to further breakdown of molecules to polar organics, which become soluble in the water phase. At 350°C, the yield of bio-crude at 15 min is 41.5 wt.%, increasing to 44.1 wt.% at 60 min. From an energy input perspective, this slight increase suggests it would be beneficial to process algae for only 15 min. These results are in agreement with results reported by Anastasakis and Ross who observed the highest bio-crude yields from *Laminaria saccharina* at a 15 min residence time [59].



**Figure 5.2:** Effect of residence time on the HTL bio-crude yields at 250°C and 350°C.

The effect of residence time on the composition of the bio-crudes and their HHV is presented in **Table 5.3** for 250 and 350°C. At 250°C, the carbon contents of bio-crudes range from 70.3 to 74.3 wt.% and were found to increase with residence time. The nitrogen content shows an increase at 30 min and a slight decrease at 60 min. The sulphur content is shown to be fairly constant. Oxygen content consistently decreases with increasing residence time (10% from 15%) thus increasing the HHV of the bio-crudes.

At 350°C, similar trends are observed with increasing residence time; carbon content is increased from 60 to 72 wt.% while oxygen content is reduced from 25 to 14 wt.%. This results in the highest HHV of 34 MJ/kg being reached at 100 min. The sulphur content at 350°C is reduced from 0.7 to 0.4% at the longest reaction time. The nitrogen content does not show a clear trend, initially it decreases from 7 to 5.4 wt.% at 45 min, then increases at 60 min before it reducing to 5.7 wt.% at 100 min. The cause of these fluctuations is unclear but the observations are similar to the results from investigating the operating temperature.

**Table 5.3:** Effect of residence time on elemental composition and HHV of bio-crudes from HTL.

	<b>C</b>	<b>H</b>	<b>N</b>	<b>S</b>	<b>O</b>	<b>HHV</b>
	<b>(wt.% daf)</b>					<b>(MJ/kg)</b>
<b>250°C</b>						
15 min	70.3	8.9	5.2	0.7	15.0	33.8
30 min	72.4	9.2	6.3	0.5	11.6	35.6
60 min	74.3	9.3	5.8	0.7	9.9	36.7
<b>350°C</b>						
15 min	60.1	7.3	7.0	0.7	24.9	26.4
30 min	67.4	8.4	5.7	0.6	18.0	31.7
45 min	69.4	8.5	5.4	0.6	16.1	32.8
60 min	70.4	8.5	6.2	0.5	14.3	33.5
100 min	71.7	8.5	5.7	0.4	13.7	34.0

#### 5.3.4 Analysis of the Process Water

The process water produced from the HTL of *Chlorella OZ* at a constant residence time of 15 min was analysed for anions, cations, total organic and inorganic carbon (TOC and TIC), total nitrogen (TN) and pH at temperatures of 250, 300 and 350°C. The concentrations of phosphate, potassium, ammonium and total nitrogen are significant if the process water is used to recycle nutrients for further microalgae cultivation. This aspect is investigated in detail in **Chapter 8**. The amount of carbon in the process water is also significant as it represents a loss if it is in the organic form, making it unavailable for bio-crude formation. If it is removed as inorganic CO<sub>2</sub> from the biomass

by decarboxylation this is beneficial as it reduces the oxygen content of bio-crudes. **Table 5.4** shows that phosphate and sulphate concentrations in the process water are highest at the lowest HTL temperature. Recovery of phosphates into the water phase is generally considered desirable unless the solid residue is to be used as bio-char fertiliser, for this application, phosphates should fractionate preferentially to the solid residue.

The concentration of ammonium is increased three-fold at 350°C compared to 250°C, due to further decomposition of proteins at more severe conditions. The same trend is observed for TN values, which increase at higher temperatures. Levels of potassium increase significantly with increasing temperature from 225 to 1280 mg/l. The pH of the process water changes from slightly acidic at 250°C to alkali at 350°C. This is most likely due to formation of organic acids from carbohydrates at 250°C and high levels of ammonium present at the higher temperatures. Acetate concentrations at 250 and 300°C are 11,000 mg/l reducing to 8,200 mg/l at 350°C. The reductions are likely caused by additional carbon being fractionated to the bio-crude. The TOC levels, on the other hand, are highest at 250°C and about half the level at 300°C, the value at 350°C is in-between the other two (16,000 mg/l). Inorganic carbon is highest at 350°C and reduced at the lower temperatures due to reduced decarboxylation.

**Table 5.4:** Effect of temperature on anion, cation, total organic carbon (TOC), total nitrogen (TN) concentration in mg/l and pH

	Acetate	Cl <sup>-</sup>	PO <sub>4</sub> <sup>3-</sup>	SO <sub>4</sub> <sup>2-</sup>	NH <sub>4</sub> <sup>+</sup>	K	TOC	TIC	TN	pH
<b>250°C</b>	10971	45	3266	354	3556	225	21054	896	5324	6.1
<b>300°C</b>	11045	513	2535	225	7923	986	10465	1679	5600	8.7
<b>350°C</b>	8227	75	2793	260	11400	1280	16461	2557	5912	9.3

## 5.4 Conclusions

Data obtained from the HTL of 11 microalgae strains at constant operating conditions currently represents the single largest data set available for different algal strains and their liquefaction performance. The average bio-crude yield was shown to be 33.7 wt.% with a nitrogen content of 4.7 wt.% and an oxygen content of 13.6 wt.%, leading to a HHV of 36.0 MJ/kg. It is apparent that the main area requiring improvements in HTL of microalgae is the reduction of nitrogen from the resulting bio-crude. The HHV, oxygen content and yields are of acceptable quality for upgrading. Possible options for decreasing the nitrogen content include the use of catalysts or pre-treatment of the feedstock, investigated in **Chapter 6** and **Chapter 11** respectively.

Analyses of aqueous process phases confirmed the presence of high levels of algal nutrients and provided an incentive to investigate the potential for nutrient recycling (**Chapter 8**). The process water was found to contain high concentrations of organic carbon, which is undesirable as this represents a carbon loss which is not available for bio-crude formation.

It appears that the optimum operating temperature and residence time lies at around 15 min and 300°C. However, as highlighted by several researchers and in the current study, operating conditions are highly dependent on the algae strains and processing systems used.

## 6. CHAPTER VI - Catalytic HTL

### 6.1 Introduction

Hydrothermal processing of lignocellulosic biomass has received extensive research over the last two decades for the production of liquid fuels and is extensively reviewed by Peterson et al [35]. Several studies have shown that alkali catalysts can improve liquefaction yields for terrestrial biomass. Catalytic hydrothermal liquefaction of microalgae was first reported by Dote et al. for the high lipid strain *Botryococcus braunii*. Some of the most productive microalgae in terms of biomass production are lower in lipid and contain larger amounts of protein and carbohydrate. Growing these algae for biodiesel is unlikely to be economical and alternative processing routes would be advantageous. The conversion of low lipid content microalgae and cyanobacteria by hydrothermal processing is an alternative route to produce bio-fuels and chemicals from algae; involving the production and subsequent upgrading of the bio-crude. Due to their high nitrogen content these strains result in a bio-crude with high nitrogen content. The main aim of the current Chapter is removing the nitrogen from the bio-crude by catalysis and improving the quality and yields of bio-crude.

This first part of this Chapter is focused towards the production and nature of the bio-crude produced from homogenous catalytic hydrothermal liquefaction of a microalgae (*Chlorella vulgaris*) and a cyanobacteria (*Spirulina*), containing relatively low lipid content and high protein. The influences of process variables such as temperature and catalyst type have been studied. The influences of potential in-situ hydrogen donors or hydrogenating agents such as formic acid are compared to the conventional alkali catalysts. The bio-crudes produced have been analysed by proximate and ultimate analysis and by GC/MS and thermal gravimetric analysis. The aqueous fraction has been analysed by ion exchange chromatography (IEC) and for total organic carbon (TOC). The influence of process variables on the yield and quality of the bio-crude is discussed including the carbon balance and the nitrogen partitioning between the product phases.

The second part of the Chapter investigates the use of heterogeneous catalysts for HTL of microalgae. Previous results in **Chapter 5** show that the bio-crudes from hydrothermal liquefaction of microalgae contain significant amounts of nitrogen and oxygen, and while this is lower than those in pyrolysis oils, it is undesirable in the final bio-crude [47, 77]. During hydrothermal processing, the lipids have been shown to decompose to fatty acids although the full



decarboxylation to hydrocarbons is relatively small [77]. The effect of heterogeneous catalysts on the lipid fraction of the algae is studied in detail in this part of the Chapter and its potential of deoxygenating the lipids to a green diesel type fuel.

Watanabe et al. investigated the effect of supercritical water treatment on the fatty acid stearic acid for 30 minutes and found that the decomposition products were CO<sub>2</sub> and C<sub>16</sub> alkene [118]. The addition of alkali hydroxides increased decarboxylation but the main product was a C<sub>17</sub> alkane. Other studies by Holliday et al. show that subcritical water treatment of triglycerides (soybean, linseed and coconut oils) resulted in free fatty acids at temperatures of 260-280°C [119-120]. The hydrolysis reaction of triglycerides was presented by Mills and McClain in 1949 and is described as a step wise hydrolysis of triglycerides to diglycerides and fatty acid, with the diglyceride reacting with water to form a monoglyceride and a fatty acid which in turn reacts to another fatty acid and glycerol [121]. Alenezi et al. state that the fatty acids can act as a catalyst in hydrolysis reactions and experimentally showed that sunflower oil is converted to fatty acids at 350°C with a yield of 93 % [122].

The second part of the current Chapter investigates the possibility of further de-oxygenating the fatty acids from microalgae and plant oils to produce alkanes using heterogeneous catalysts under hydrothermal conditions. Duan and Savage conducted similar research on the microalgae *Nannochloropsis* and six different heterogeneous catalysts. They found that the bio-crude yields increased for each catalyst although there was a higher (50 wt.%) catalyst loading employed than in this research [85]. The fate of lipids and the effect of their composition on the liquefaction behaviour during catalytic hydrothermal processing has not been reported before. In the current research different strains of microalgae containing different biochemical compositions have been investigated as well as the lipids derived from soybean oil. A comparison of the lipid composition before and after hydrothermal processing is presented with and without the presence of heterogeneous catalysts. In this work, three catalysts have been investigated included an alumina supported Co/Mo catalyst, an alumina/silica supported Ni catalyst and an alumina supported Pt catalyst. Cobalt-Molybdenum catalysts are typical hydrotreatment catalysts and are used for hydrodesulphurisation of petroleum and could therefore be effective in removing heteroatoms S, N and O from bio-crude. The Pt catalyst was chosen due to its high activity in reducing oxygenates to hydrocarbons and the Ni catalyst has previously been shown to be a strong catalyst in hydrothermal gasification [85]. All catalysts were introduced in stainless steel baskets in concentrations of 50 wt.% based on algae loading.

## 6.2 Methodology

The hydrothermal liquefaction experiments in this chapter were performed in a 75 ml Parr high pressure reactor as described in **Chapter 3**. The soya oil used is of the crude soya oil type not a processed food supplement; it was obtained from a commercial source. The Co/Mo, Pt/Al and Ni/Al catalysts were purchased from Sigma Aldrich; catalyst loading was 20 wt.% metal on support. All sample work up and analysis methods are described in **Chapter 3**. Analysis of the microalgae strains investigated can be found in **APPENDIX A**.

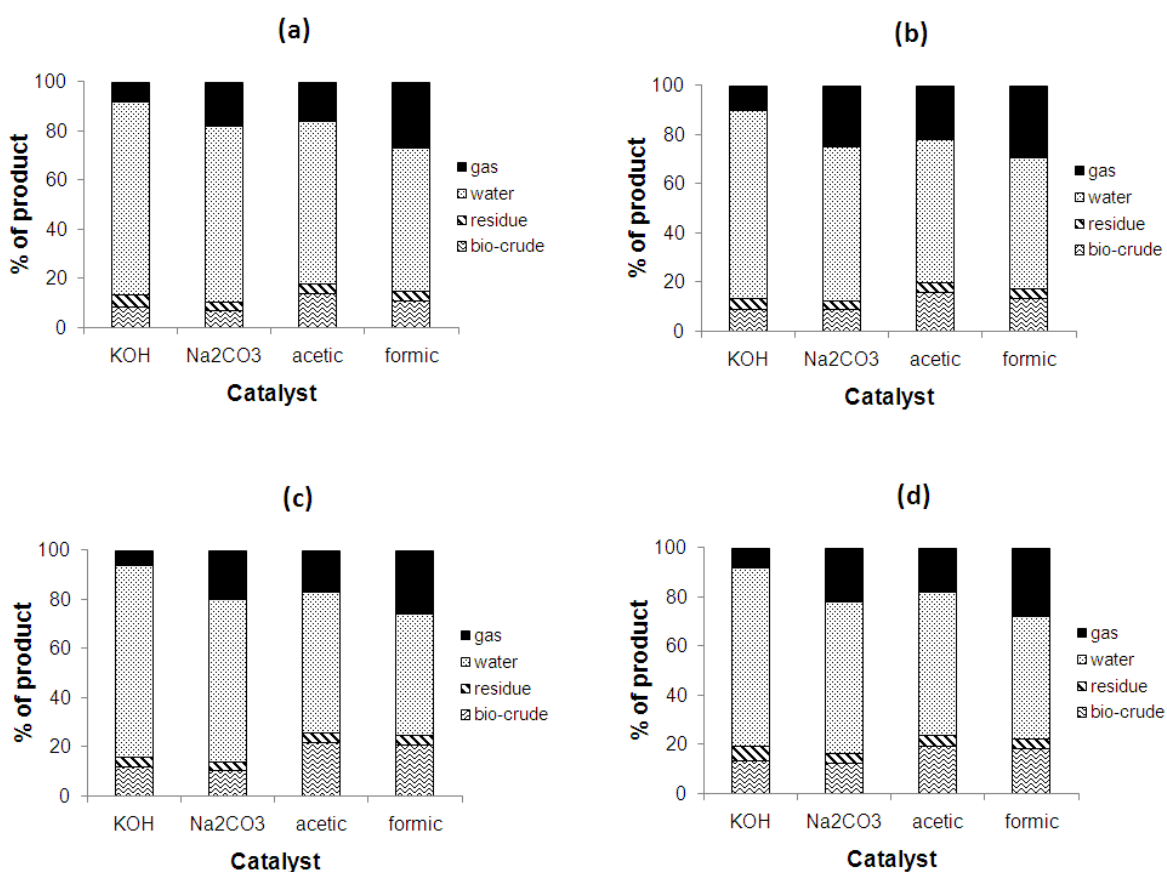
## 6.3 Homogenous Catalysis

### 6.3.1 Liquefaction yields

The product distribution obtained from catalytic liquefaction of microalgae for one hour at 300°C and 350°C are shown in **Figure 6.1** for *Spirulina* and *Chlorella* respectively. Maximum conversion of biomass to bio-crude using an alkali catalyst (KOH) at 350°C were 9 wt.% and 13.6 wt.% for *Spirulina* and *Chlorella* respectively. The yields of residue are relatively constant and range from 4-5 wt.% for both *Spirulina* and *Chlorella*. The residue typically contains 20-30 wt.% carbon with the remainder being mainly inorganic mineral matter. The mass balance indicates that the material dissolved in the water phase and gaseous phase are the major products. The gaseous fraction accounts for approximately 18-20 wt.% using Na<sub>2</sub>CO<sub>3</sub> and 6-10 wt.% using KOH with the gaseous phase containing largely CO<sub>2</sub>.

The yields of bio-crude are higher using the organic acids compared to using alkali catalyst. *Chlorella* shows a higher oil yield than *Spirulina* correlating with its higher lipid content. Acetic acid experiments show higher yields than those using formic acid. Maximum yields of 19.5 wt.% and 15.7 wt.% are achieved using *Spirulina* and *Chlorella* respectively. In both cases however, the organic acid is consumed and so is acting as a reagent rather than a catalyst. This is significant as the organic acids increase the oil yield by this mechanism compared to the alkali catalysts. The gaseous fraction is higher for formic acid and accounts for approximately 30 wt.%. For acetic acid the gaseous fraction is lower and accounts for 16-22 wt.%. The yields of bio-crude obtained follow the trend CH<sub>3</sub>COOH>HCOOH>KOH>Na<sub>2</sub>CO<sub>3</sub>. The yields reported are low due largely to the mass

balance including the catalyst mass. The yields of bio-crude on an organic basis are listed in **Tables 6.1 and 6.2**. When expressed on an organic basis, the  $\text{Na}_2\text{CO}_3$  catalyst provides the highest yields of bio-crude of 27.3 wt.% and 20.0 wt.% for *Chlorella* and *Spirulina* respectively. In this case the yields of bio-crude follow the trend  $\text{Na}_2\text{CO}_3 > \text{CH}_3\text{COOH} > \text{KOH} > \text{HCOOH}$ .



**Figure 6.1:** Yields of products from hydrothermal processing for (a) *Spirulina* at 300°C (b) *Spirulina* at 350°C (c) *Chlorella* at 300°C (d) *Chlorella* at 350°C.

### 6.3.2 Bio-crude Analysis

The ultimate analysis of the bio-crude produced at 300°C and 350°C using both organic acids and alkali catalysts are listed in **Tables 6.1 and 6.2** respectively. Under alkali conditions, the bio-crude

has an average elemental composition of 74.4 wt.% C, 11.5 wt.% H, 4.7 wt.% N, 0.2 wt.% S and 9.2 wt.% O. The HHV falls within the range 33.4-39.9 MJ/kg. This represents a lower oxygen content and higher HHV compared to the average microalgae bio-crude produced from non-catalytic HTL, presented in **Chapter 5**. Using organic acids, the bio-crude has an average elemental composition of 70.8 wt.% C, 9.4 wt.% H, 5.3 wt.% N, 0.65 wt.% S and 13.85 wt.% O and the HHV falls within the range 33.3-35.1 MJ/kg, similar to the average composition of non-catalytic HTL presented in **Table 5.1**. The lower HHV is attributed to the higher oxygen content in the oil. The use of organic acids however, results in a bio-crude with visually improved pour behaviour. The fraction of sulphur in the bio-crude was found to increase with the use of the organic acids by approximately three fold compared to the alkali catalysts. It was also higher for *Spirulina* than for *Chlorella* and was typically 0.6 wt.% for *Chlorella* and 0.9 wt.% for *Spirulina*. The use of alkali catalysts and *Chlorella* resulted in only trace amounts of sulphur at all conditions. It appears that the alkali catalysts are able to reduce the nitrogen content in the oil compared to organic acids. The oxygen content for these catalysts is also lower. Comparing these results to the data in **Table 5.1** from HTL of the same strains without the use of catalysts, the use of organic acids results in higher nitrogen and oxygen contents compared to no catalysts. Alkali catalysts appear to reduce the nitrogen content in the bio-crude by around 1 wt.% and the oxygen content by 2-5 wt.%. However a decrease of yields is also observed with the use of alkali catalysts.

**Table 6.1:** Ultimate Analysis in wt.% and HHV of bio-crude at 300°C

Conditions	C	H	N	S	O*	HHV (MJ/kg)	Bio-crude yield (wt.% db)
<i>Spirulina</i>							
1M Na <sub>2</sub> CO <sub>3</sub>	73.1	11.4	5.0	0.4	10.1	37.8	14.1
1M KOH	71.7	10.2	6.0	0.4	11.7	35.7	12.8
1M HCOOH	72.4	9.3	7.1	0.6	10.6	34.7	16.0
1M CH <sub>3</sub> COOH	69.5	9.7	7.1	0.6	13.1	34.1	22.0
<i>Chlorella</i>							
1M Na <sub>2</sub> CO <sub>3</sub>	73.7	10.8	4.6	0	10.9	37.2	21.9

1M KOH	72.1	10.1	4.6	0	13.2	35.7	18.6
1M HCOOH	72.1	9.5	6.4	0.5	11.5	35.0	30.7
1M CH <sub>3</sub> COOH	70.8	9.4	5.3	0.4	14.1	34.2	35.2

\*by difference

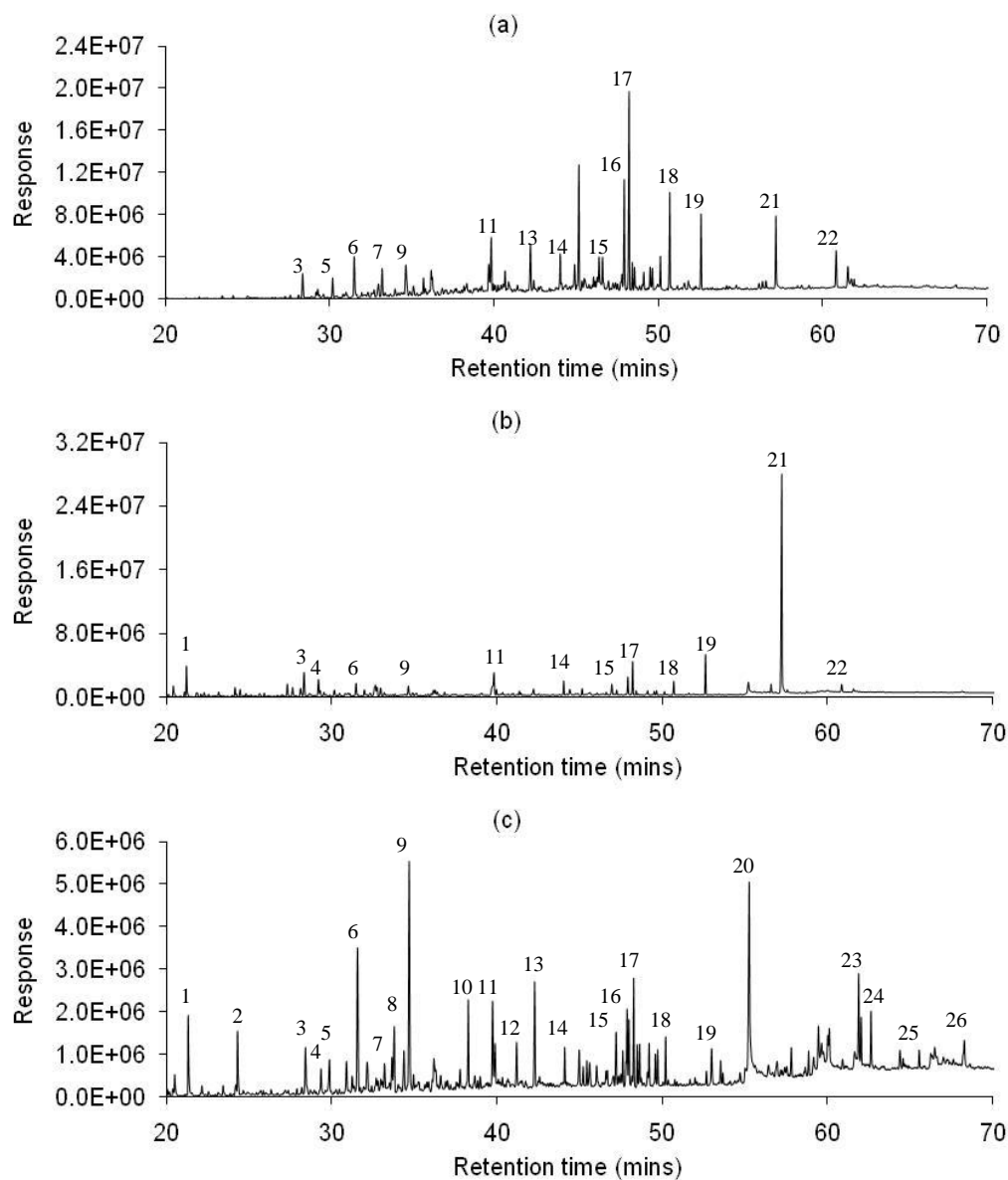
**Table 6.2:** Ultimate Analysis in wt.% and HHV of bio-crude at 350°C

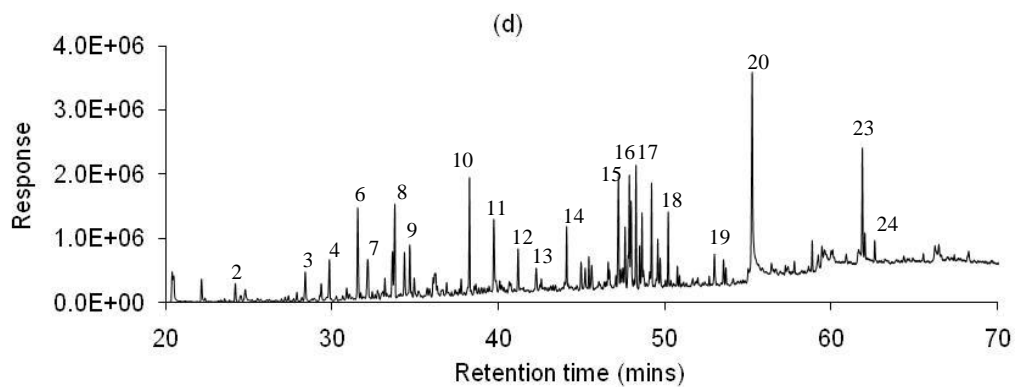
Conditions	C	H	N	S	O*	HHV (MJ/kg)	Bio-crude yield (wt. %db)
<i>Spirulina</i>							
1M Na <sub>2</sub> CO <sub>3</sub>	75.4	10.8	4.6	0.5	8.7	34.8	19.5
1M KOH	74.6	11.4	5.1	0.5	8.5	33.4	14.8
1M HCOOH	72.7	9.76	5.7	0.9	10.9	35.6	21.1
1M CH <sub>3</sub> COOH	71.7	9.73	6.1	0.9	11.6	35.1	27.1
<i>Chlorella</i>							
1M Na <sub>2</sub> CO <sub>3</sub>	73.6	10.7	4.9	0.0	10.7	37.1	26.0
1M KOH	74.0	12.9	4.3	0.0	8.9	39.9	21.3
1M HCOOH	70.8	9.4	5.3	0.6	13.9	35.1	26.6
1M CH <sub>3</sub> COOH	69.6	9.1	5.0	0.5	15.8	33.2	31.3

\*by difference

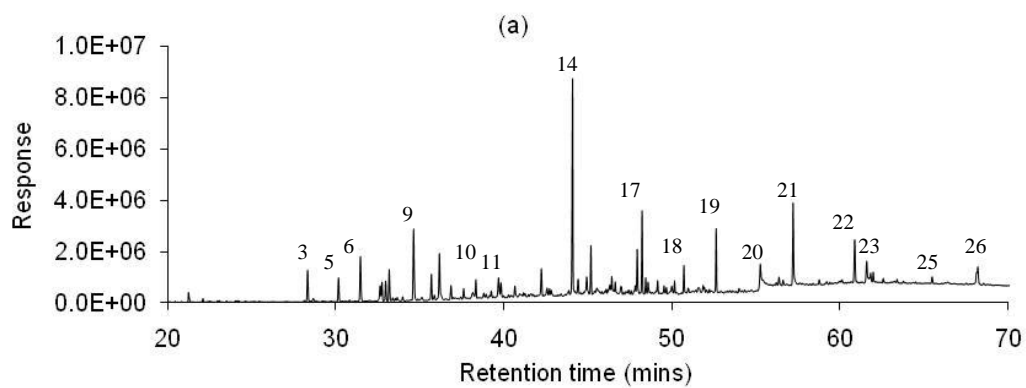
The bio-crude was analysed by GC/MS and the main compounds were identified. Typical chromatograms obtained for *Chlorella* and *Spirulina* are shown in **Figure 6.2** and **Figure 6.3** respectively. Compound identification of the main peaks has been performed using a NIST mass spectral database and are labelled on the chromatograms. **Table 6.3** lists the main compounds identified which include mono aromatics such as toluene, ethyl benzene and styrene, substituted phenols, nitrogen heterocycles such as pyrroles and indole derivatives and long chain alkanes. Indole and pyrrole derivatives are likely products from the protein fraction. Higher nitrogen content of the starting microalgae led to increased amounts of nitrogen heterocycles being observed in the

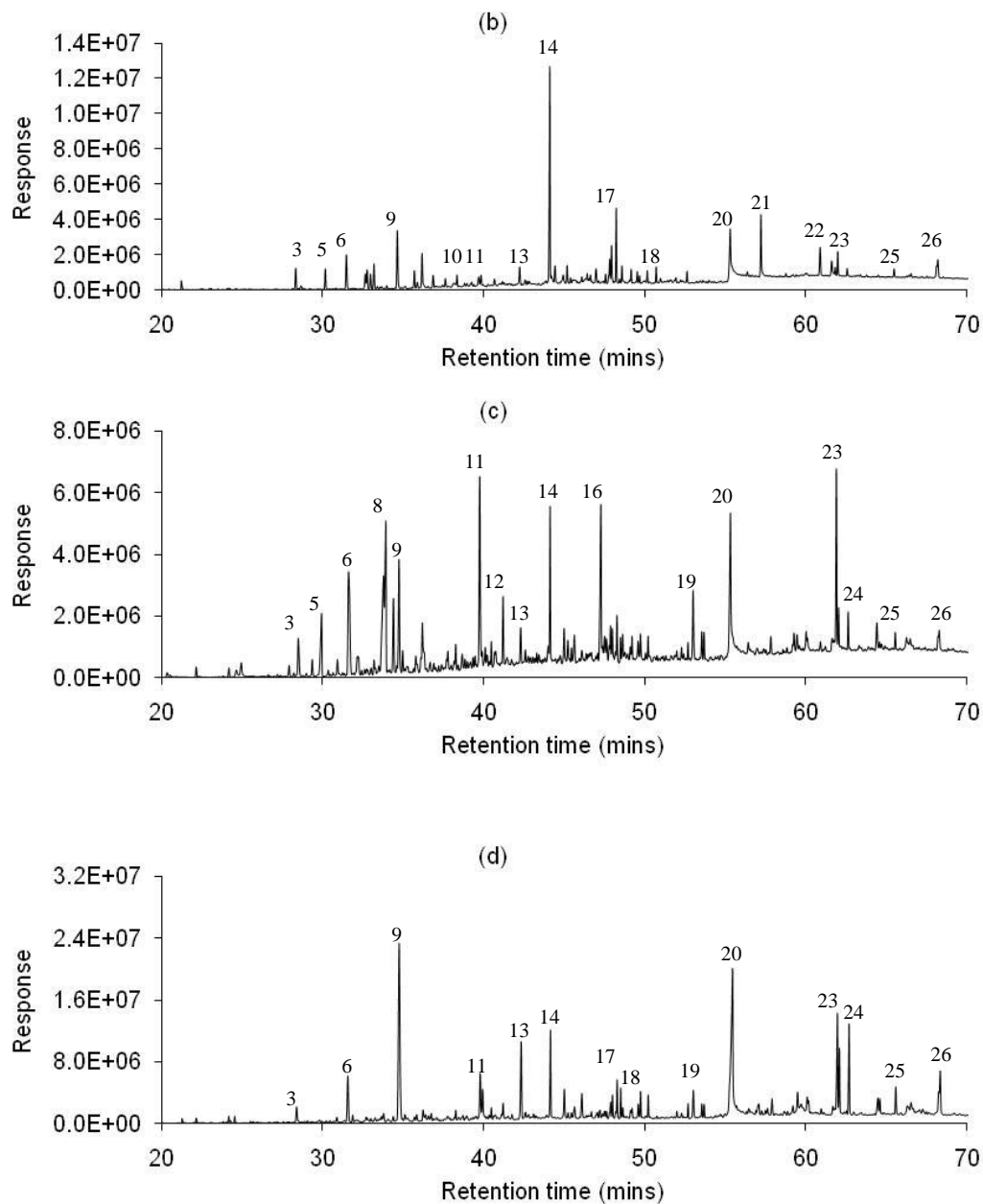
bio-crude. The higher protein containing *Spirulina* produces a higher proportion of pyrroles and indoles in the bio-crude. **Figures 6.2 and 6.3** indicate that similar compounds are observed for KOH and  $\text{Na}_2\text{CO}_3$  catalysed processes although there is a larger distribution of lower molecular weight material using  $\text{Na}_2\text{CO}_3$ . The chromatograms show a significant change in product distribution using organic acids in particular the presence of larger amounts of phenols, fatty acids such as hexadecanoic acid (palmitic acid,  $\text{CH}_3(\text{CH}_2)_{14}\text{COOH}$ ) and fatty acid amides such as hexadecanamide (palmitamide,  $\text{CH}_3(\text{CH}_2)_{14}\text{CONH}_2$ ).





**Figure 6.2.** GC/MS of bio-crude from *Chlorella* at 350°C for (a) 1M Na<sub>2</sub>CO<sub>3</sub> (b) 1M KOH (c) 1M acetic acid and (d) 1M formic acid.





**Figure 6.3.** GC/MS of bio-crude from *Spirulina* at 350°C for (a) 1M  $\text{Na}_2\text{CO}_3$  (b) 1M KOH (c) 1M acetic acid and (d) 1M formic acid.



**Table 6.3:** Compounds identified in bio-crude from HTL of microalgae

No.	Compound	No.	Compound
1	1, butyl pyrrolidine	14	Heptadecane
2	1, pentyl piperidine	15	2, phenylethyl acetamide
3	phenol	16	3,7,11 trimethyl 1-docadanol
4	acetamide	17	hexadecane tetramethyl
5	phenylethyl alcohol	18	1, 3 heptadecyn-1-ol
6	4, methyl phenol	19	piperidine derivative
7	piperidine-2,5-dione	20	n-hexadecanoic acid
8	n- methyl butylacetamide	21	phytol
9	4, ethyl phenol	22	indole derivative
10	1, pentadecene	23	hexadecamide
11	1, butyl 2-pyrrolidinone	24	unknown aliphatic amide
12	hydroxyl ethyl succinimide	25	fatty acid derivative
13	1, methyl indole	26	stearic acid derivative

The boiling point distribution of the bio-crudes has been estimated using thermal gravimetric analysis (TGA) in nitrogen. TGA applied in simulated distillation is regarded as a miniature “distillation” and, although some thermal degradation is likely, it provides an estimate of the boiling range of heavy oils. The TGA curves indicate that the use of organic acids significantly reduces the boiling point range of the bio-crude compared to using an alkali catalyst and this is particularly noticeable for *Spirulina*. This similarly agrees with the GC–MS data shown in **Figures 6.2** and **6.3** which indicates a larger distribution of lower molecular weight compounds using organic acids. **Table 6.4** lists the boiling point distribution of the bio-crudes and indicates that they still contain a large amount of high boiling material. The results indicate that there is about 30–40 wt.% of the bio-crude with a boiling point <250°C. The GC/MS analysis therefore only represents a fraction of the bio- crude as much of the material is of higher molecular weight. Larger naphtha, diesel and kerosene fractions are produced when using the organic acid additives. The lighter

fractions are favoured by formic acid > acetic acid > Na<sub>2</sub>CO<sub>3</sub> > KOH. Particularly noticeable is the reduction of heavy tar (>370°C) for the organic acids compared to the alkali catalyst.

**Table 6.4:** Boiling point distribution of bio-crudes at 350°C

Distillate Range	Boiling point of oil (wt.%)				Boiling point of oil (wt.%)			
	<i>Chlorella</i>				<i>Spirulina</i>			
	KOH	Na <sub>2</sub> CO <sub>3</sub>	CH <sub>3</sub> COOH	HCOOH	KOH	Na <sub>2</sub> C O <sub>3</sub>	CH <sub>3</sub> COOH	HCOOH
40-200°C	21.6	22.2	20.8	15.9	15.1	17.3	28.4	24.2
200-250°C	18.4	9.8	16.1	18.1	19.4	18.3	19.5	20.4
250-300°C	17.1	7.9	16.8	23.0	18.6	16.4	12.9	18.0
300-370°C	12.3	9.2	12.4	16.9	15.4	14.5	12.7	10.3
>370°C	18.0	41.8	28.2	18.0	19.5	18.9	14.6	11.4

### 6.3.3 Aqueous phase analysis

Ion exchange chromatography of the aqueous fractions identified the presence of anions PO<sub>4</sub><sup>3-</sup>, CH<sub>3</sub>COO<sup>-</sup> and Cl<sup>-</sup> and the cations K<sup>+</sup>, Na<sup>+</sup>, Mg<sup>2+</sup>, NH<sub>4</sub><sup>+</sup>, and Ca<sup>2+</sup>. When using alkali catalysts, the nitrogen is mainly in the form of NH<sub>4</sub><sup>+</sup>. The experiments using KOH as catalyst result in a large amount of K<sup>+</sup> in the aqueous phase. Similarly the experiments using a Na<sub>2</sub>CO<sub>3</sub> catalyst result in a large concentration of Na<sup>+</sup>. Acetate levels in the water phase are relatively similar regardless of catalyst type and range from 7,500- 11,000 mg/l. These values are in the same range as shown in **Table 5.3** without the use of catalyst for *Chlorella OZ*.

The phosphate levels in the aqueous phase range from 600-2500 mg/l, while algae derived sodium and potassium range from 700- 1100 mg/l. Liquefaction in organic acids results in similar levels of K<sup>+</sup> and Na<sup>+</sup> in the resulting process water. The levels of PO<sub>4</sub><sup>3-</sup> however are approximately 3 fold higher when using organic acids. Acetate and formate levels are reduced to about 7500-11000 mg/l indicating that the organic acids are being consumed under hydrothermal conditions.

The total organic carbon (TOC) in the aqueous phase is also shown in **Table 6.5** together with the pH. TOC analysis indicates that a significant proportion of the organic products are water soluble. The choice of catalyst influences the amount of carbon dissolved in the water phase. For KOH, increasing the temperature reduces the TOC although this is not observed for Na<sub>2</sub>CO<sub>3</sub>. With organic acids, the total organic carbon decreases slightly with temperature for *Spirulina* while it is inconsistent for *Chlorella*. The concentration of dissolved carbon in the aqueous phase ranges from 15,000-40,000 mg/l. Especially the use of KOH at 300°C results in exceptionally high TOC levels, around 4 times higher than when no catalyst is used (see **Table 5.3**). The pH of the aqueous phase is typically between 9-10 with the exception of acetic acid in which the water phase remains slightly acidic at typically 6.5-6.8. Using formic acid results in pH values of 9.0 and 8.8 for *Spirulina* and *Chlorella* respectively. The levels of ammonium are lowest with the use of formic acid for both strains. For *Spirulina*, increasing the reaction temperature leads to a reduction in ammonium levels with alkali catalysts, but the amount increases when organic acids are used. The opposite of this effect is observed for *Chlorella*. The values are generally in the same range to samples processed without catalysts, expect when formic acid is used which results in lower ammonium levels.

**Table 6.5:** TOC, pH, ammonium, phosphate and potassium content of the aqueous phase.

Algae	Catalyst	Temperature (°C)	TOC (mg/l)	NH <sub>4</sub> <sup>+</sup> (mg/l)	PO <sub>4</sub> <sup>3-</sup> (mg/l)	K <sup>+</sup> (mg/l)	pH
<i>Spirulina</i>							
	Na <sub>2</sub> CO <sub>3</sub>	300	11370	5963	926	1111	10.2
	Na <sub>2</sub> CO <sub>3</sub>	350	13852	5630	926	1111	9.4
	KOH	300	37704	4037	741	19259	11.3
	KOH	350	29556	3926	630	19630	10.8
	HCOOH	300	28519	1519	1926	889	9.0
	HCOOH	350	20111	1889	1519	852	9.0
	CH <sub>3</sub> COOH	300	30630	4778	2259	667	6.8
	CH <sub>3</sub> COOH	350	26222	5519	3037	667	6.5
<i>Chlorella</i>							
	Na <sub>2</sub> CO <sub>3</sub>	300	26296	3259	2222	667	9.8
	Na <sub>2</sub> CO <sub>3</sub>	350	27000	4556	2593	630	9.9
	KOH	300	42444	4333	1481	18519	10.0
	KOH	350	25630	4741	1667	19259	9.7
	HCOOH	300	17037	1778	2556	741	8.8

HCOOH	350	20111	1704	2407	741	8.8
CH <sub>3</sub> COOH	300	29074	4444	2593	741	6.6
CH <sub>3</sub> COOH	350	27000	3148	2407	704	6.8

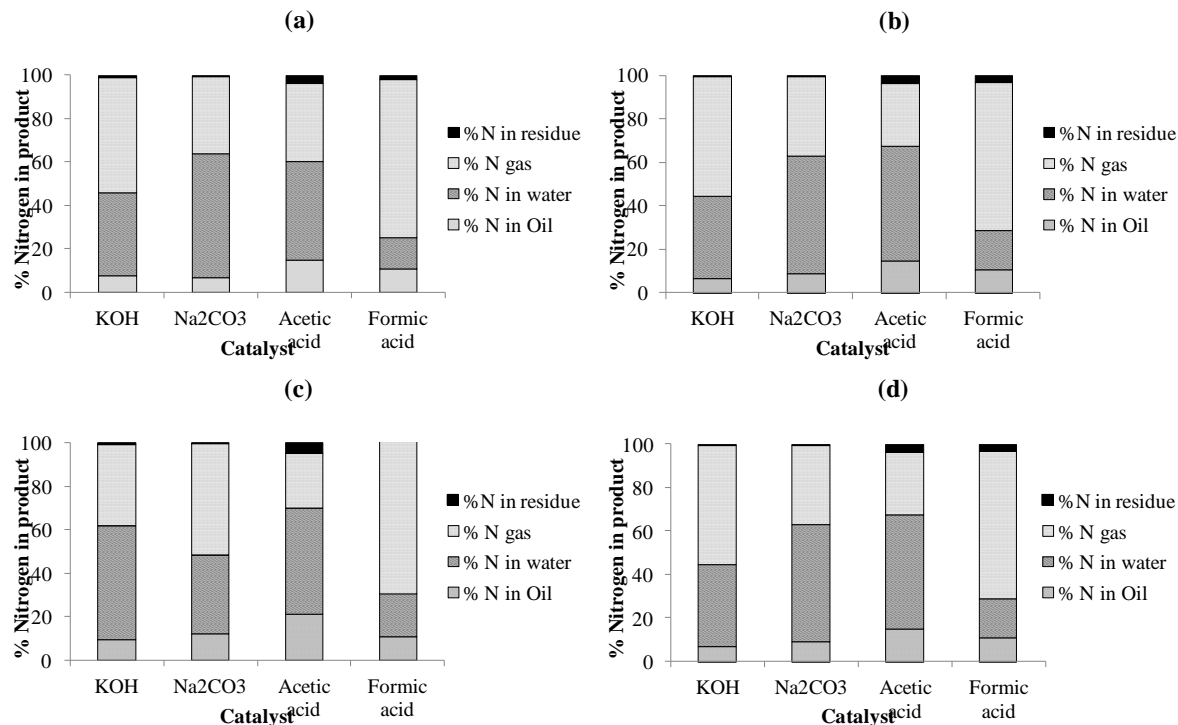
#### 6.3.4 Nitrogen balance in product streams

The ammonium concentrations in the aqueous phase vary with temperature and catalyst type and are listed in **Table 6.5**. When using alkali catalysts, the ammonium concentration varies from 3500-6000 mg/l for *Spirulina* (representing 38-56 wt.% of the feed nitrogen) and 3300-4800 mg/l for *Chlorella* (representing 35-49 wt.% of the feed nitrogen). With *Spirulina* the higher the temperature, the lower the ammonium content of the aqueous phase but this is not the case for *Chlorella*. For liquefaction in formic acid, the ammonium concentration is significantly lower, in the range 1500-2200 mg/l for *Spirulina* (representing 15-17 wt.% of the feed nitrogen) and 1300-1850 mg/l for *Chlorella* (representing 18-19% of the feed nitrogen). The remaining nitrogen is distributed between the bio-crude and the gaseous phase.

The amount of nitrogen in the bio-crude is relatively constant for alkali catalysed experiments ranging from 4-6 wt.% and includes heterocyclic compounds such as pyrrolidinones and indoles, and fatty acid amides. The bio-crudes produced using organic acids contain a higher nitrogen content (up to 7 wt.%). The removal of the nitrogen in the bio-crude is crucial if it is to be used as a fuel so as to minimise NO<sub>x</sub> formation during combustion. The remaining nitrogen in the gaseous phase consists of NO<sub>2</sub>, N<sub>2</sub>O, HCN and NH<sub>3</sub>. A nitrogen mass balance has been performed for the different liquefaction conditions based on the N content of the aqueous phase, solid residue and the bio-crude with the N in the gaseous phase being determined by difference.

**Figure 6.4** illustrates the elemental nitrogen partitioning between the product phases during liquefaction of *Spirulina* and *Chlorella* in alkali and organic acids. The significance of the concentration of ammonium in the aqueous phase is related to the potential for nutrient recycling. The results indicate that in the presence of alkali the higher the liquefaction temperature, the lower the nitrogen content in the aqueous phase. Using organic acids results in higher levels of nitrogen in the bio-crude and a slight increase in the nitrogen content of the residue. Processing in formic acid results in approximately 70 wt.% of the nitrogen partitioning into the gaseous phase lowering levels of nitrogen in the water phase. This could be a drawback if nutrient recycling is important. Na<sub>2</sub>CO<sub>3</sub> produces the bio-crude with the lowest nitrogen content. This trend is similarly observed for

*Chlorella*. Measurement of the pH after processing indicates that the formic acid and acetic acid have decomposed to varying degrees thus increasing the pH from the initial feed. With the exception of acetic acid, which remains slightly acidic (pH 5.5-6.8), the aqueous phase is basic following extraction (pH 9-10). This would agree with the observed results suggesting that the ammonia content in the gaseous phase increases following the order  $\text{CHOOH} > \text{KOH} > \text{Na}_2\text{CO}_3 > \text{CH}_3\text{COOH}$ .



**Figure 6.4:** Distribution of nitrogen in the product streams from (a) *Spirulina* at 300°C, (b) *Spirulina* at 350°C, (c) *Chlorella* at 300°C, (d) *Chlorella* at 350°C.

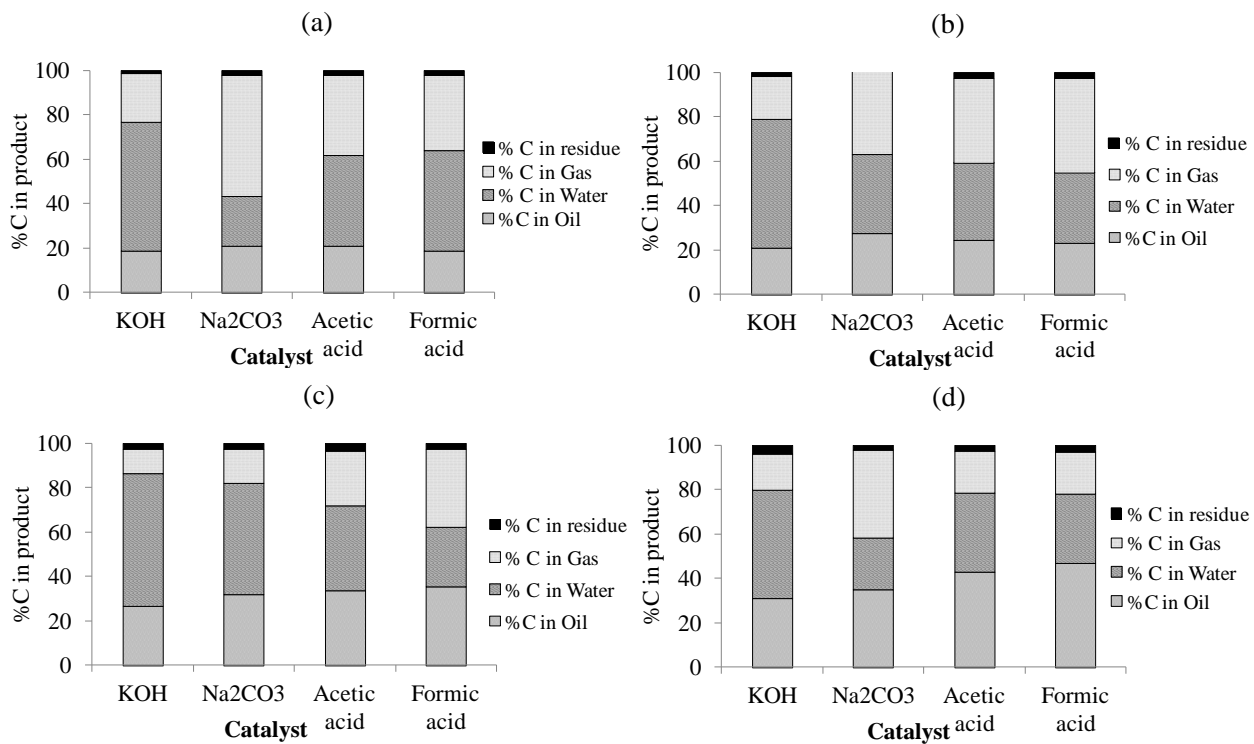
### 6.3.5 Role of catalyst

The formic acid appears to decompose during liquefaction. This is supported by the change in pH, the reduced presence of formate in the water phase and the formation of hydrogen, CO<sub>2</sub> and CO. Experiments also show that when using formic acid, water appears to be consumed. The acetic acid also decomposes but to a lesser extent. The consumption of both the acetic acid and formic acid during liquefaction has been estimated to be over 90% by determining the amount of formate and acetate remaining in the aqueous phase by ion chromatography. Formic acid is well known to decompose to CO<sub>2</sub> and H<sub>2</sub> although acetic acid is more stable under hydrothermal conditions [123].

The pressure measured once the reactor has cooled using alkali is relatively low (max 1-2 bar). Using organic acids, a higher pressure is produced (5 -6 bar acetic acid, 10-14 bar formic acid). In general the higher the temperature, the larger the gaseous fraction.

Watanabe et al. reported a positive effect of oil formation from glucose using formic acid and a cobalt catalyst [124]. In this case the formic acid was added as a hydrogenating agent. In the current investigation, no increase in hydrogen content of the bio-crude is observed. In fact, overall there is an increase in oxygen content. The nitrogen content of the bio-crude is also consistently higher using organic acids than using alkali catalyst. This suggests that the hydrogen generated from formic acid is not incorporated into the oils to a significant degree, although the reducing atmosphere is likely to be influencing reactions pathways. There may be more hydration reactions occurring rather than decarboxylation leading to a reduction in hydrogen content of the oil. The presence of organic acids improve the boiling range of the bio-crude but do not increase the HHV, in fact a slightly lower HHV is observed. In situ hydrogenation may be possible using formic acid with the addition of metal catalysts and will be the focus of continued work.

Using a combination of the TOC of the aqueous phase and the CHNS content of the bio-crude and residues, an elemental carbon balance can be calculated and is shown in **Figure 6.5** for *Spirulina* and *Chlorella* at 350°C. The solid residue is typically low in carbon (20-30 %) and contains the mineral component from the microalgae and therefore doesn't contribute significantly to the carbon balance. For *Spirulina*, there does not appear to be as much difference in C-distribution to the bio-crude between the different catalysts. However for *Chlorella*, the use of the acid catalysts increases the carbon portioning to the bio-crude. *Chlorella* contains a higher lipid content than *Spirulina* which may undergo selective reaction with the organic acids, particularly for acetic acid. This suggests that the use of organic acids and higher lipid content microalgae will have a positive impact on bio-crude formation and is addressed in the next Chapter.



**Figure 6.5:** Carbon balance between product phases for (a) *Spirulina* at 300°C, (b) *Spirulina* at 350°C, (c) *Chlorella* at 300°C, (d) *Chlorella* at 350°C.

## 6.4 Heterogeneous Catalysis

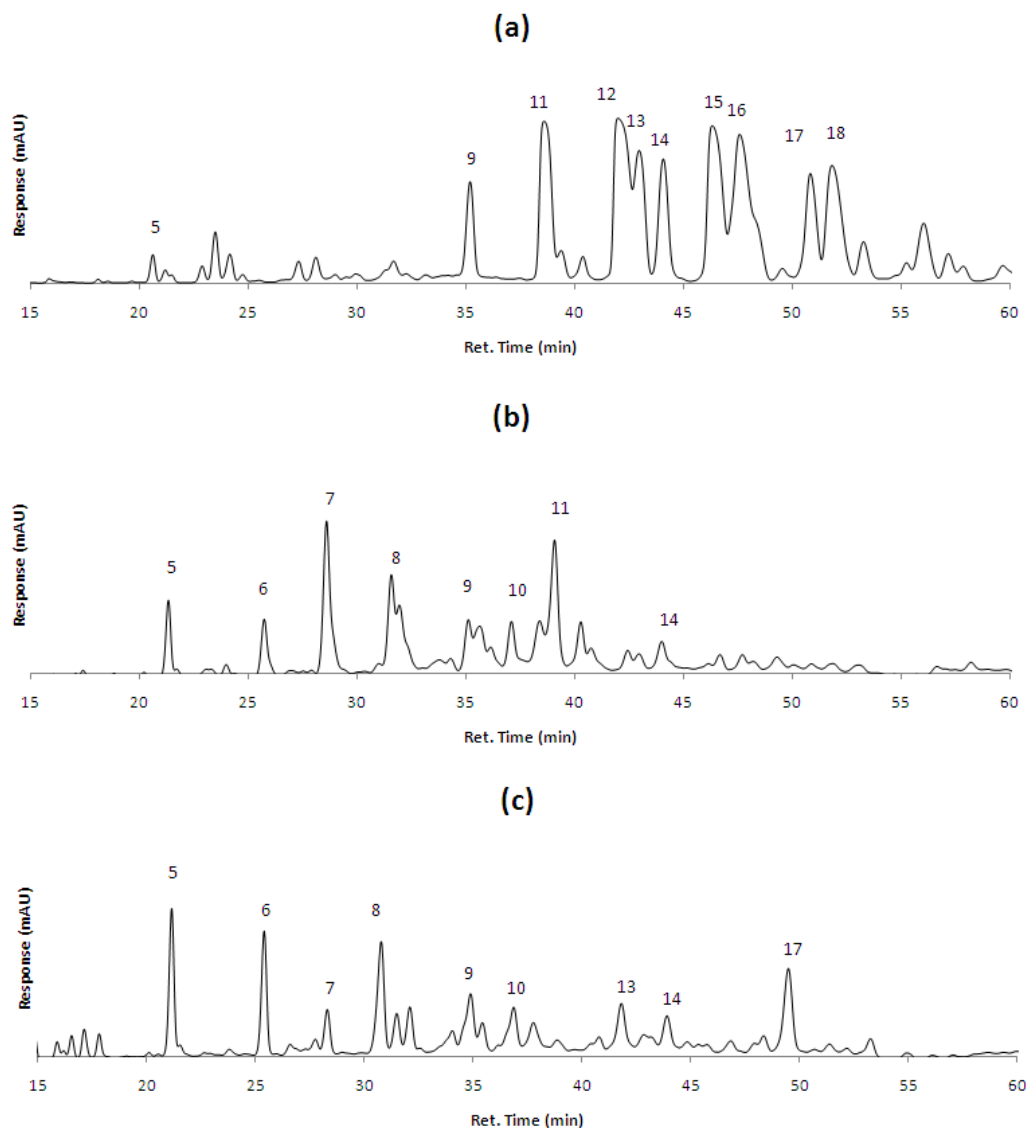
### 6.4.1 Lipid Profiles

Extraction of the lipids has been performed by two methods, firstly the Bligh and Dyer method, which is the standard method to determine the total lipid content of biomass such as microalgae, and secondly using a modified version of the Bligh and Dyer method. The first method uses a 2:1 methanol/chloroform solvent mixture and the modified method uses hexane. The results for the total lipid content using the standard method are found to be in good agreement with results from literature, while the results for the hexane method were found to be lower. Thermogravimetric analysis of the extracts showed that the hexane method preferentially extracted the lower molecular weight free fatty acid fraction and not the triglycerides (TAGs), resulting in the lower lipid yields. GC-MS analysis provided evidence for the formation of fatty acid methyl esters (FAME) from the Bligh and Dyer extraction although this has not been reported before. The esterification reactions at these moderate conditions are expected to only esterify the free fatty acids (FFA) and not the TAGs and does therefore not affect the distribution based on HPLC and GC-MS. The transesterification reactions from the Bligh and Dyer method were more noticeable with *Nannochloropsis* than *Chlorella*; this is most likely due to the larger amounts of alkali salts catalysing esterification. Due to this mechanism the hexane extract which did not affect the FFA is used for the analysis of the FFA summarised in **Table 6.6**. The GC-MS chromatograms for the lipid extracted by the modified Bligh and Dyer method from *Chlorella* and *Nannochloropsis* using the Stabilwax column are not included, but the data is presented in **Table 6.6**. This column allows separation of the free fatty acids (FFA) from the lipid extract but does not separate the tri-, di- and mono-glycerides due to their higher boiling point. The free fatty acids identified include hexadecanoic, pentadecanoic and oleic acid. For both algae the most abundant free fatty acid is oleic acid followed by palmitic acid. *Nannochloropsis* has relatively high amounts of phytol which is a common acyclic diterpene alcohol which is produced from the hydrolysis of chlorophyll [68] but this is lower for *Chlorella* and not detected for soya oil. The triglycerides (TAGs) were separated from the same extract by non-aqueous reverse phase HPLC. Separation by this method occurs by the partition number (PN) of different triglycerides shown in **Eqn. 6.1** and was first reported by Firestone (1994) [111].

$$PN = \text{Carbon Number} - (2 \times \text{Number of Double Bonds}) \quad \text{Eqn. 6.1}$$



Therefore lower carbon chain length and large number of double bonds result in a lower PN. The chromatogram of the soya oil was compared to various chromatograms from the literature using the same method and the peaks could be identified and are in good agreement [125-127]. **Figure 6.6** shows the triglyceride profiles for the soy oil and microalgae lipids and indicates a significantly different profile. The profiles also vary between the two microalgae. It is evident that the microalgae lipids are generally of lower partition number which means they are of lower carbon number or have more double bonds. Microalgae are well known to be a good source of polyunsaturated fatty acids with multiple double bonds [128]. Typical fatty acids that make up these kinds of triglycerides are the  $\omega$ -3 fatty acids such as eicosapentaenoic acid, docosahexaenoic acid and stearidonic acid which all have partition numbers of 10. The other  $\omega$ -3 fatty acids that result in low partition numbers are eicosatetraenoic acid and docosapentaenoic acid with PNs of 12. Even though the peaks 5-8 were not identified, their partition numbers are known and suggest the presence of the above fatty acids. Unsaturated lipids when transesterified to FAME have an increased tendency towards oxidation which increases tenfold when the double bond equivalent increases by one [129]. This makes the fuels problematic for storage due to deterioration by oxidation. If the emerging microalgae industry focuses on biodiesel production, storage and deterioration problems could become an issue due to the large number of double bonds in the algal lipids. GC-MS data of the hydrothermal liquefaction of soya oil shows that the double bonds of fatty acids are largely hydrogenated resulting in a higher quality fuel. This is seen as a major advantage of hydrothermal processing and may be useful also in upgrading plant oils.



**Figure 6.6:** TAG HPLC chromatograms of (a) Soya oil, (b) *Chlorella* and (c) *Nannochloropsis*

**Table 6.6** shows a semi-quantitative analysis of the free fatty acids and triglycerides. The amount of fractions of free fatty acids and triglycerides of the total lipids was determined by a combination of HPLC and TGA. The free fatty acids can be identified in the HPLC method, but, due to the very low PN of free fatty acids, they elute early and are not well resolved. All samples have been analysed in duplicate and the average values are reported. The response of the UV detection is not expected to be linear for the different TAGs therefore this is semi-quantitative data but this allows an estimation of the fractions of TAGs. About 75 % of the TAG from soy oil could be identified with the largest TAGs present being PLL, LLL and LLLn which is in agreement with results from the literature [125-127]. The main FFA found in soybean oil is oleic acid followed by palmitic

acid. Around 60% of the *Chlorella* lipids and 50 % of the *Nannochloropsis* lipids were identified. The largest fractions for *Chlorella* were TAGs with the PN 34, 36 and 38, which indicate high number of double bonds such as found in polyunsaturated fatty acids or a diglyceride of palmitic acid. *Nannochloropsis* showed significant amounts of higher PN TAGs, such as OLLn, PLLn and OOL, making up % of the total TAGs together. There are also larger amounts of the low PN TAGs present in *Nannochloropsis*. Most reports of microalgae derived lipids have concentrated on the fatty acid analysis following conversion to FAME (e.g. [31]). This study has analysed the fatty acid composition in the TAGs directly by HPLC and the free fatty acids by GC-MS. The method presented here gives insight into the fatty acid structural composition of triglycerides and fatty acids from microalgae; previous work published has analysed the FAMEs produced from the free fatty acids and triglycerides to obtain a total fatty acid analysis but not distinguishing their origin. The results from the literature are in agreement with the results presented here on total fatty acid composition, but here there is additional information presented on the actual triglyceride structures [130-132]. Tonon et al. reported similar amounts of low PN  $\omega$ -3 fatty acids derived from the TAG fraction which was separated prior to transesterification as are reported above for *Nannochloropsis* [131]. Two other papers analysing the total fatty acids but not stating if the fatty acids are derived from FFA or TAG are in broad agreement to the results found in this study for *Chlorella vulgaris* [130, 132].

**Table 6.6:** Retention times, PN, quantification and structures of FFA and TAG of the lipid samples

	Peak Number	Retention time (min)	<i>Chlorella</i>	<i>Nannochloropsis</i>	<i>Soya Oil</i>	Partition Number	Possible structure
GC-MS	1	29.2	2.0	8.2	-	-	<i>Phytol</i>
	2	33.7	15.7	14.5	11.1	16	<i>P</i>
	3	36.2	1.8	0.0	5.6	15	<i>Pentadecanoic acid</i>
	4	36.6	11.8	24.0	33.2	16	<i>O</i>
<b>% Fatty Acids identified</b>			31.3	46.6	49.9		
HPLC	5	21.2	3.4	4.6	2.7	30	<i>EPA,ALA, DHA, C</i>
	6	25.6	3.5	4.1	-	32	<i>EPA,ALA, DHA, SDA, ETA, DPA</i>
	7	28.6	11.3	1.7	-	34	<i>EPA,ALA, DHA, SDA, ETA, DPA, ETE, Po</i>
	8	31.5	11.9	4.9	2.8	36	<i>NI</i>
	9	35.1	8.5	2.6	5.9	38	<i>LLnLn</i>
	10	36.9	4.0	2.7	-	38/40	<i>NI</i>
	11	38.4	8.7	-	9.7	40	<i>LLLn</i>
	12	41.8	-	-	10.5	42	<i>LLL</i>
	13	42.4	-	8.0	6.0	44	<i>OLLn</i>
	14	43.9	-	7.6	5.3	44	<i>PLLn</i>
	15	46.2	-	-	9.4	44	<i>OLL</i>
	16	47.5	7.0	-	11.6	46	<i>PLL</i>
	17	5.1	-	9.7	4.6	46	<i>OOL</i>
	18	51.6	-	-	6.7	48	<i>POL</i>
<b>% TAGs identified</b>			58.3	46.0	75.2		

EPA=Eicosapentaenoic acid (20:5); ALA= $\alpha$ -Linolenic acid (18:3); DHA=Docosahexaenoic acid (22:6); C=Capric acid (10:0);

SDA=Stearidonic acid (18:4); ETA=Eicosatetraenoic acid (20:4); DPA= Docosapentaenoic acid (22:5); ETE= Eicosatetraenoic acid

(20:3); Po= Palmitoleic acid (16:1); NI= Not Identified; L=Linoleic acid (18:2); Ln=Linolenic acid (18:3); O=Oleic Acid (18:1);

P=Palmitic acid (16:0)

### 6.4.3 HTL Results

The yields of bio-crude from the liquefaction of the microalgae and soya oil with and without the addition of heterogeneous catalysts are shown in **Table 6.7**. Three heterogeneous catalysts were investigated included an alumina supported Co/Mo catalyst, an alumina/silica supported Ni catalyst and an alumina supported Pt catalyst. Cobalt-Molybdenum catalysts are typical hydrotreatment catalysts and are used for hydrodesulphurisation of petroleum and could therefore be effective in removing heteroatoms S, N and O from bio-crude. The Pt catalyst was chosen due to its high activity in reducing oxygenates to hydrocarbons and the Ni catalyst has previously been shown to be a strong catalyst in hydrothermal gasification [85]. All catalysts were introduced in stainless steel baskets in concentrations of 20 wt.% based on algae loading. The yields for the microalgae feedstock are much lower than the model lipid, soya oil. This is expected and similar results have been shown before for sunflower oil [77]. The carbohydrate fraction of microalgae is only converted to bio-crude with an efficiency of around 5-10 wt.%, and the proteins around 20 wt.%, in water [77]. The use of Co/Mo catalyst results in an increase of the bio-crude yields of soya oil and *Chlorella* by 12 and 3 wt.% respectively, while the yields for *Nannochloropsis* decreased by around 10 wt.%. Most of the material that does not produce bio-crude has been shown to be in the water phase; therefore the Co/Mo catalyst must reduce the amount of water soluble organics from *Chlorella* and soya oil as no increase in the gas fraction was observed. The lower result of *Nannochloropsis* may be due to the large amounts of alkali metals present either promoting alternative pathways or poisoning the catalyst. The yields using the Co/Mo catalyst are lower than those reported by Duan and Savage for this catalyst and they did not observe a decrease in yield with *Nannochloropsis* [85]. Their experimental setup was somewhat different as they were using a stirred reactor and a higher catalyst loading of 50 wt.%. The use of the Ni/Al catalyst resulted in lower bio-crude yields for all conditions. This is attributed to the increased decarboxylation and gas formation observed; this increase in gas formation was not observed by Duan and Savage (2010) using a Ni catalyst or any of the other heterogeneous catalysts they investigated. The residual gas pressures in the reactor were consistently higher with the use of Ni/Al, and the maximum pressure was up to 20 bar higher using the Ni/Al catalyst compared to the uncatalysed setup. Previous research has shown that the gas formed contains N<sub>2</sub> and CO<sub>2</sub> [47], the amount of CO<sub>2</sub> formed can shed light on the extent of decarboxylation although is not available for the current study. The Pt/Al catalyst resulted in a 12 wt.% increase in bio-crude for soya oil, reaching a maximum of 95.5 wt.%. Again the water soluble organic fraction is reduced with the use of this catalyst. This would suggest that the use of Pt/Al promotes the highest recovery of lipids of the catalysts studied. For *Chlorella*

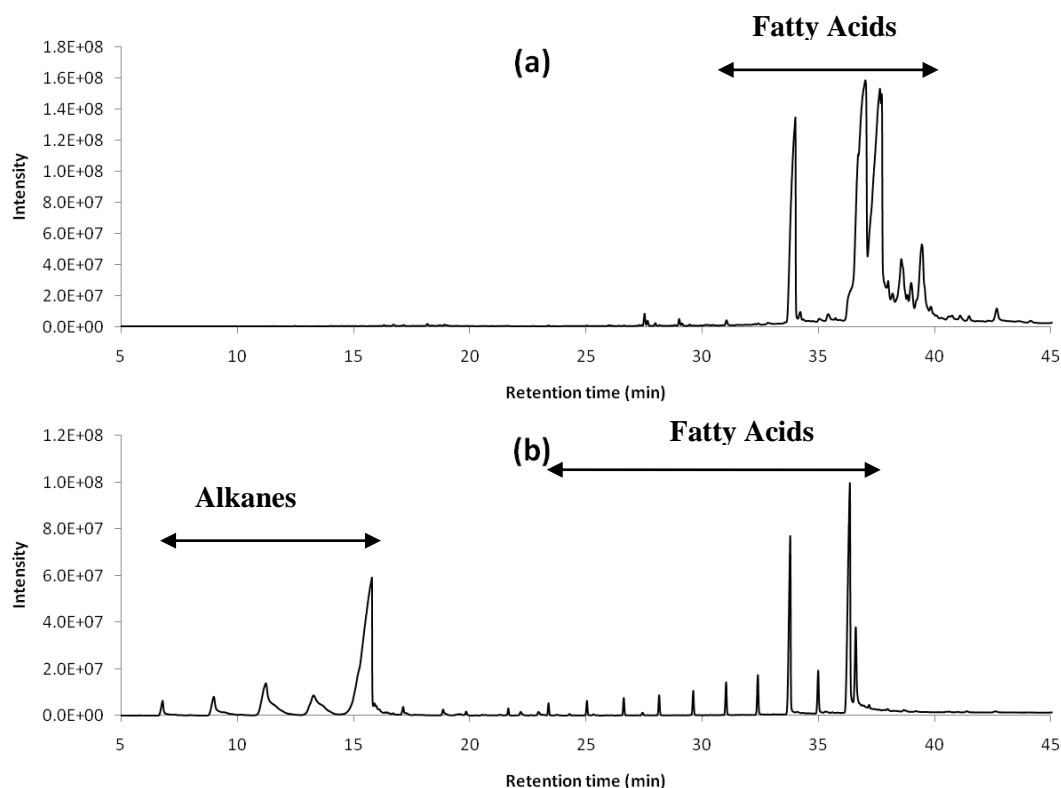
the bio-crude yield was also increased slightly with the Pt/Al catalyst but again for *Nannochloropsis* this is not the case. This observation deserves further examination and will be the focus of future research.

**Table 6.7:** Bio-crude yields from hydrothermal liquefaction

<i>Oil Yields (wt.% daf)</i>	<i>Catalyst</i>			
	<i>H<sub>2</sub>O</i>	<i>Co/Mo</i>	<i>Ni/Al</i>	<i>Pt/Al</i>
<i>Nannochloropsis oc.</i>	34.3	25.5	18.1	30.2
<i>Chlorella vulgaris</i>	35.8	38.7	30.0	38.9
<i>Soya Oil</i>	82.1	93.9	37.7	95.5

#### 6.4.4 Influence of hydrothermal treatment on lipids

**Figure 6.7** shows the GC-MS chromatograms of (a) soya oil processed without the use of a catalyst and (b) soya oil processed with the use of the Ni/Al catalyst. The Stabilwax column's maximum temperature is 260°C, therefore only a portion of the bio-crude can be analysed by this method. The use of the Ni/Al catalyst shows that alkanes were successfully produced by further deoxygenation of the fatty acids from the triglycerides. Duan and Savage also reported the production of alkanes in supercritical water by upgrading a microalgae bio-crude using a Pt/C catalyst [85]. The alkanes produced in this work range from pentadecane to nonadecane. A step-wise decomposition of the fatty acids is also shown compared to the chromatogram of the non-catalysed reaction. The fatty acids produced range from dodecanoic acid to hexadecanoic acid. Using just water (i.e. non catalysed) higher molecular weight fatty acids are present such as hexadecanoic acid and oleic acid. GC-MS analysis of this oil shows that the majority of the double carbon bonds present are hydrogenated during hydrothermal processing. The role of water as a hydrogen source has extensively been reviewed by Akiya et al. 2002. Hydrogen may be formed by hydrolysis or via the water gas shift reaction of CO generated from oxygenated molecules [133]. The large amounts of linoleic acid present in the unprocessed soya oil (see **Table 6.6**), which have two C=C bonds are hydrogenated resulting in increased saturation. The most abundant fatty acids observed after liquefaction have zero or one C=C bond (hexadecanoic and oleic acid). This is significant as this effects the fate of the FAME biodiesel produced from the fatty acids. Additional C=C bonds have negative effects on the oxidative behaviour of biodiesel [129].



**Figure 6.7:** GC-MS chromatograms of (a) soya oil processed in water only and (b) processed with Ni/Al<sub>2</sub>O<sub>3</sub> catalyst.

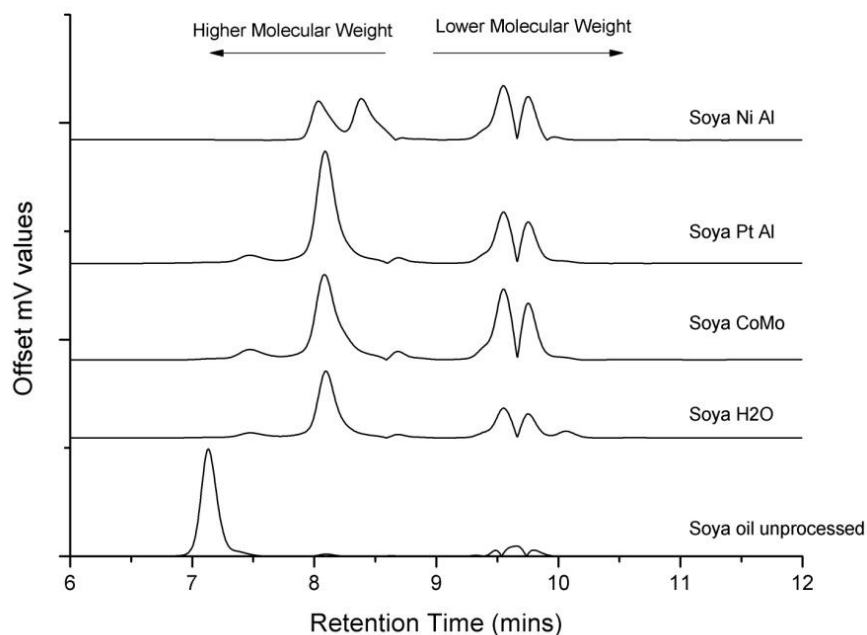
**Figure 6.8** shows the size exclusion chromatography results for the bio-crudes and the unprocessed sample of soya oil. It can be seen that the unprocessed soya oil has a much higher molecular weight distribution than the liquefied samples, around 85 % of the total sample is found in the first high molecular weight peak (>1000 Dalton). The remainder eluted at around 8 minutes and around 10 minutes. The first peak illustrates the triglycerides, while the second peak represents the fatty acid fraction which is relatively small as was shown by HPLC and TGA. **Figure 6.8** shows the soya oil liquefied without a catalyst: the triglyceride peak is completely broken down but there is a small peak at around 7.5 minutes which is most likely from the di- and monoglycerides. The largest peak at 8 minutes represents the fatty acids which are the decomposition products of the triglycerides. The small amount of material between 9 and 10 minutes is unidentified, but it is known that their number average molar mass (Mn) is around 100; therefore it is most likely that this is glycerol which has a molecular mass (MW) of 92. Previous research has stated that the decomposition

products of triglycerides are free fatty acids and glycerol [121]. **Figure 6.8** also shows the results for the Ni/Al catalyst. Again the peak for fatty acids can be seen but just after, a peak for alkanes is found. It is shown that about half the fatty acids are successfully broken down to alkanes using the Ni/Al catalyst. GC-MS shows that there are some relatively long chain alkanes produced, which explains the relatively early elution of the alkane peak. Processing soya oil with the Co/Mo catalyst resulted in there being more di- and monoglycerides left after liquefaction. The majority of the product contains fatty acids with only 3 % low molecular weight alkanes. Around half of the bio-crude is below 200 Dalton (da) at this condition. The Pt/Al catalyst does not show significant differences to the Co/Mo catalyst which explains the similar bio-crude yields in **Table 6.7**. The Pt/Al catalyst produces the largest amounts of fatty acids, at 57 % with the rest as glycerol. These results are in agreement with results from the literature which claim the major products of triglyceride break down are fatty acid compounds [119-120]. This research has shown that there are significant amounts of triglycerides broken down further into compounds of lower molecular mass than 200 dalton (Da). This is presented in **Table 6.8**, where the average molecular masses of the different bio-crudes are presented alongside the mass fraction, above 200 Da. It can be seen that the average molecular mass is reduced drastically by hydrothermal processing from around 500 Da to around 200 Da. The use of Ni/Al resulted in the lowest average molecular number while the Pt/Al catalyst gave the highest average molecular number followed by the results achieved using no catalyst. The heavier molecular mass (>200 Da) material is reduced by around 20-30 % by hydrothermal treatment, most with the use of the Ni/Al catalyst and least with the Pt/Al catalyst.

**Table 6.8:** number average molar mass (Mn) and weight fraction over 200 dalton of bio-crudes and Soya oil

<i>Condition</i>	<i>Av. Mn</i>	<i>wt. % &gt; 200 Da</i>
<i>Soya oil</i>	511	88
<i>Soya + H<sub>2</sub>O</i>	196	63
<i>Soya + Ni/Al</i>	170	54
<i>Soya + Co/Mo</i>	183	55
<i>Soya + Pt/Al</i>	205	66



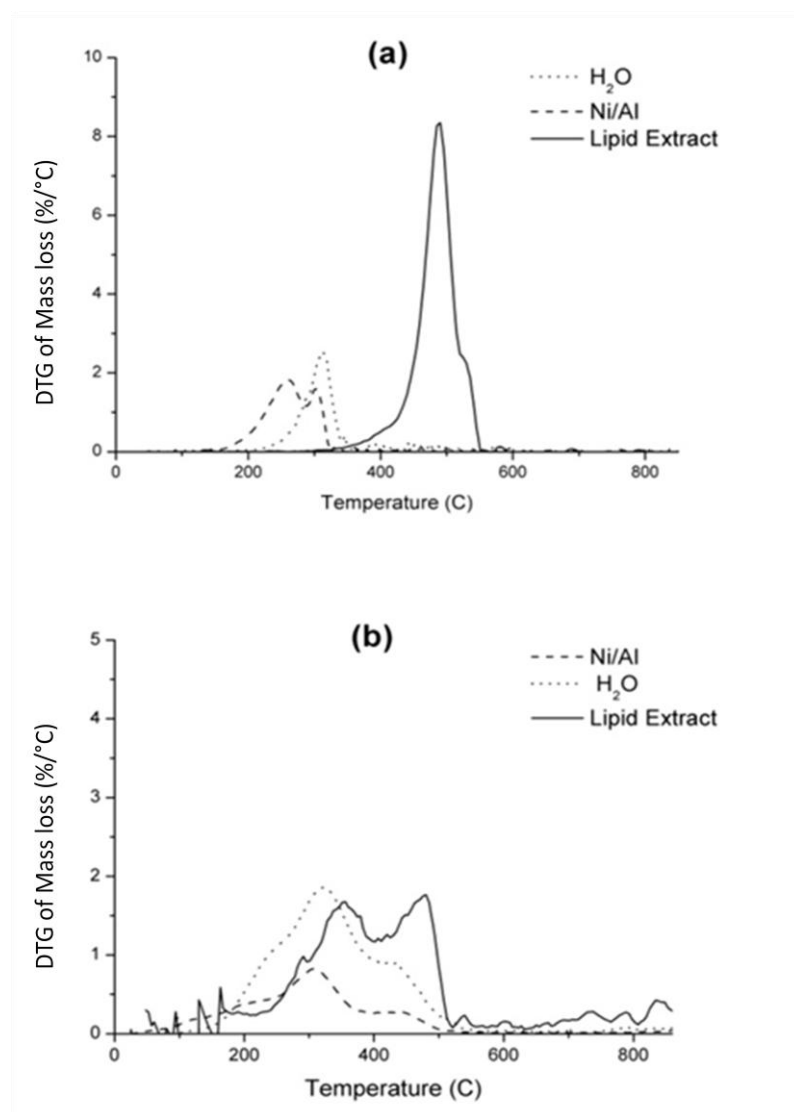


**Figure 6.8:** HPLC-SEC chromatograms of soya oil hydrothermally processed in Ni/Al<sub>2</sub>O<sub>3</sub>, Pt/Al<sub>2</sub>O<sub>3</sub>, Co/Mo/Al<sub>2</sub>O<sub>3</sub>, Water and unprocessed soya oil.

**Figure 6.9 (b)** shows a simulated distillation of the extracted lipids from *Chlorella*, the bio-crude produced in the absence of any catalysts and the bio-crude produced in the presence of the Ni/Al catalyst. The triglycerides from microalgae are shown to have boiling points beyond 260°C, so they cannot be separated using the Stabilwax column which has a maximum temperature of 260°C. It can be seen that the unprocessed lipids have a higher boiling point range than the hydrothermally treated lipids. The peak of the bio-crude at 320°C represents the fatty acids. This peak is also present in the extracted lipids although it also contains tri-, di- and mono-glycerides. The larger molecular weight triglycerides devolatilise slowly and material is still devolatilising up to 900°C, while the majority of bio-crude has devolatilised by 550°C. The distillation of the Ni/Al processed bio-crude shows a broader boiling point range at the lower temperatures indicating further breakdown of the free fatty acids.

**Figure 6.9(a)** shows the simulated distillation of the unprocessed soya oil, the hydrothermally treated soya oil with and without the Ni/Al catalyst. It can be seen that the unprocessed sample has one very distinct peak at around 500°C where the TAGs devolatilise. There is little mass devolatilising earlier or later. The hydrothermally treated sample without catalyst also shows only one distinct peak, this time at around 280°C; this represents the fatty acids produced by

hydrothermal liquefaction. The use of the Ni/Al catalyst results in an additional peak of the lower molecular weight alkanes formed from the decarboxylation taking place, producing alkanes from fatty acids. These have boiling points of around 250°C but there is a distinct shoulder towards lower temperatures due to the various chain length alkanes produced, devolatilising at different temperatures. Integration of the peaks of the Ni/Al processed sample in **Figure 6.9 (a)** results in about 60 wt.% material boiling in the alkane range and 30 wt.% boiling in the fatty acid range. There is also a small amount of material (< 5 wt.%) of heavier molecular weight material present devolatilising after 380°C.



**Figure 6.9:** DTG boiling point profile curves from TGA analysis of lipids and bio-crudes without catalyst and Ni/Al catalyst of (a) soya oil and (b) *Chlorella*.

#### 6.4.5 Elemental analysis of bio-crude

**Table 6.9** shows the elemental analysis of the bio-crudes produced from microalgae and the model lipid. The results indicate that the use of catalysts consistently improved the HHV of the bio-crudes. This is due to the fact that more deoxygenation takes place when using a catalyst, compared to the use of water alone resulting in a simultaneous increase in C. For the microalgae, the Co/Mo and Pt/Al catalyst had the highest effect on deoxygenation; while deoxygenation is highest with the use of the Ni/Al catalyst for soya oil. This suggests that lipids are de-oxygenated favourably with the Ni/Al catalyst while proteins and/or carbohydrates are deoxygenated better with the use of Co/Mo and Pt/Al catalysts. This deserves further investigation and may lead to different choices of catalysts being suitable for microalgae with different biochemical compositions. With the Co/Mo catalyst the oxygen content of *Chlorella* was reduced by another 4 wt.% while for *Nannochloropsis* this was 9 wt.%. The Ni/Al catalyst also increased the deoxygenation reactions, but slightly less for the microalgae, while it performed exceptionally well for the liquefaction of soya oil: the remaining oxygen content was only 5.1 wt.%. The use of heterogeneous catalysts also reduced the amount of nitrogen in the bio-crudes but the reduction is not high, with a maximum reduction of a further 0.5 wt.%. The use of catalysts also resulted in an increase of carbon content of the bio-crude with up to 9 wt.% for *Nannochloropsis* with Ni/Al. The HHV were highest with the use of Pt/Al catalysts for microalgae and highest for the soya oil with the Ni/Al catalyst. It is evident that the use of all heterogeneous catalysts investigated result in additional deoxygenation of the microalgae bio-crude; however this only occurs for the Ni/Al catalyst for the model lipid. Therefore the Co/Mo and Pt catalysts are selectively deoxygenating the carbohydrate and protein fraction or one of them. This is also backed up by the fact that no alkanes are seen on the GC-MS chromatograms of the algal bio-crudes with these catalysts. This observation will have to be addressed in future work as this study concentrates on the lipid fraction and the potential of in-situ alkane production. The higher yields of *Chlorella* and the model lipids with simultaneous increase in HHV and reduction of N and O, suggest that the production of a bio-refinery ready bio-crude high in hydrocarbons is possible by catalysed hydrothermal liquefaction of microalgae. Analysis of the catalyst after liquefaction by atomic absorption spectroscopy indicates however, that some leaching of the metals is apparent; this will be investigated further in future work.

**Table 6.9:** Elemental analysis in wt.% of the bio-crudes and HHV

Condition	Catalyst	C	H	N	S	O*	HHV (MJ/kg)
<i>Chlorella</i>							
	H <sub>2</sub> O	70.7	8.6	5.9	0.0	14.8	35.1
	Co/Mo	75.2	8.3	5.7	0.0	10.7	36.2
	Ni/Al	75.4	6.7	5.4	0.0	12.6	34.5
	Pt/Al	74.8	9.7	5.6	0.6	9.3	37.9
<i>Nannochloropsis</i>							
	H <sub>2</sub> O	68.1	8.8	4.1	0.0	19.0	34.5
	Co/Mo	77.0	8.9	4.6	0.0	9.4	37.6
	Ni/Al	76.8	9.4	3.6	0.0	10.2	38.2
	Pt/Al	74.0	10.2	3.6	0.1	12.0	38.2
<i>Soya Oil</i>							
	H <sub>2</sub> O	76.0	10.8	0.7	0.0	12.5	35.7
	Co/Mo	77.6	10.4	0.6	0.0	11.5	39.7
	Ni/Al	82.5	12.0	0.3	0.0	5.1	42.0
	Pt/Al	73.3	10.5	0.6	0.0	15.6	38.2

\*by difference

## 6.5 Conclusions

The first part of the Chapter showed that during homogeneous catalytic HTL, the yields of bio-crude on an organic (*daf*) basis are higher in the presence of organic acids compared to alkali catalysts. The yields are higher as the temperature increases and are higher for *Chlorella* than for *Spirulina*. This leads to the conclusion that the higher the lipid content of the algae, the higher the yield of bio-crude obtained. The heating value of the bio-crude is higher using the alkali catalysts however there is a noticeable reduction in the boiling point range and improvement of flow properties when using organic acids. The molecular weight and boiling point of the bio-crudes are still relatively high. The nitrogen content of the bio-crude (4-6 wt.%) is significantly higher than a petroleum crude oil and further reduction would be required before the bio-crude could be used as a fuel. The use of organic acids does not reduce the nitrogen content in the bio-crudes. The majority of the fuel nitrogen is concentrated in the aqueous phase as ammonium, and this may represent suitable nitrogen recycle to sustain algal growth. The potential for utilising the aqueous phase to recycle nutrients, is hypothesised to be an advantage of HTL and is investigated in **Chapter 8**. The nitrogen distribution is influenced by the choice of catalyst and when using alkali, more nitrogen goes into the water phase. Formic acid decomposes to produce CO, CO<sub>2</sub> and hydrogen under

hydrothermal conditions. Acetic acid produces methane and hydrocarbon fragments and suggests that the reactor exhibits catalytic wall effects. No evidence for hydrogenation of the bio-crude was observed using formic acid. *In-situ* hydrogenation and upgrading of bio-crudes may be possible using organic acids but it is likely that additional catalysts will be required.

The current work on homogeneous catalysts has shed light on the chemical classes of compounds formed in the bio-crude and the overall elemental balance of carbon and nitrogen. The bio-crudes contain mono-aromatics such as toluene, ethyl-benzene and styrene; substituted phenols; nitrogen heterocycles such as pyrrolidinones and indoles; fatty acids and fatty acid amides. Typically about 40% of the bio-crude has a boiling point <250°C the remainder being higher molecular weight material. An understanding of the chemical nature of this high molecular weight material is required to assist the development of routes for improving bio-crude quality and is the focus of further research.

The results of the second part of the Chapter show that the majority of lipids decompose to fatty acids, and the majority of carbon double bonds are hydrogenated. The use of heterogeneous catalysts was shown to deoxygenate the bio-crude by a further 5-10 wt.%, which resulted in an oxygen removal of up to 67 wt.% for the microalgae feedstock and 64 wt.% for soya oil. The Co/Mo and Pt/Al catalyst were shown to reduce the amount of water soluble organic material and, by this mechanism, to increase the bio-crude yields from lipids. The molecular weight distribution illustrated that molecular weight is reduced significantly by hydrothermal processing and can be further decreased by the use of heterogeneous catalysts. The use of the Ni/Al catalyst successfully deoxygenated around 60 wt.% of the fatty acids from hydrothermal processing of soya oil to various chain length alkanes. The high metal content of *Nannochloropsis* appears to have inhibited the increased bio-crude formation reactions from the Co/Mo and Pt/Al catalysts, but this observation requires further investigation.

## 7. CHAPTER VII - Investigation of bio-crude formation pathways

### 7.1 Introduction

Hydrothermal liquefaction involves the reaction of biomass in water at high temperature and pressure with or without added catalyst as shown in **Chapters 6** and **5** respectively. During liquefaction biomass feedstocks are broken down to small molecules which are reactive and can re-polymerize into oily compounds [36]. The main reaction steps during liquefaction have been summarised by Garcia Alba et al. as follows [37];

1. Hydrolysis of macromolecules (lipids, proteins and carbohydrates) into smaller fragments;
2. Conversion of these fragments by, for example, dehydration into smaller compounds;
3. Rearrangement via condensation, cyclisation, and polymerization producing new oil-like components.

In most cases, the yields of bio-crude are 10-15 wt.% higher than the lipid content of the microalgae suggesting that oil is also derived from the carbohydrate and protein fractions. Most studies to date have used  $\text{Na}_2\text{CO}_3$  as an alkali catalyst. The energy balance and  $\text{CO}_2$  mitigating effect of hydrothermal liquefaction of microalgae is improved as the lipid content increases [79]. Microalgae generally consist of carbohydrates, proteins and lipids. Decomposition reactions in hydrothermal media of model compounds have previously been reported and include glucose and amino acids; however the relevance of the behaviour to the hydrothermal processing of microalgae has not been discussed.

An extensive investigation of the influence of the biochemical composition of different microalgae strains on its liquefaction behaviour has not been performed. The current Chapter investigates the influence of biochemical content of algae on liquefaction yields and product distribution. A range of biopolymers commonly found in microalgae have been investigated under hydrothermal conditions to understand the liquefaction reactions. Seven model compounds have been liquefied under hydrothermal conditions at  $350^\circ\text{C}$  without a catalyst or in the presence of formic acid or sodium carbonate. The model components include the amino acids, asparagine and glutamine, the animal protein, albumin, a plant protein derived from soya, starch and glucose as model carbohydrates and sunflower oil as a model lipid. The results have been correlated with those obtained from the liquefaction of three microalgae and one cyanobacteria processed under the same conditions. The fate of nitrogen from the protein fraction of algae is of particular interest as it is undesirable in the

bio-crude. The nature of the bio-crudes is also of interest and composition determined by GC/MS and elemental analysis is compared for model compounds and microalgae. Product distribution calculations are performed to investigate the distribution of nitrogen and carbon between the different product phases. The aim of this work is to understand the relationship between microalgae composition and hydrothermal liquefaction behaviour, bio-crude yields and composition of product streams.

## 7.2 Methodology

HTL experiments were carried out in the 75 ml Parr high pressure reactors as described in **Chapter 3**. All sample work up and analysis methods are also covered in this Chapter.

## 7.3 Results and Discussion

### 7.3.1 Liquefaction Results

**Table 7.1** lists the proximate and ultimate analysis of the samples investigated. Some of this data is already presented in **Chapter 4** and also found in the data sheets in **APPENDIX A** but is presented here as a comparison of the microalgae to the model compounds. The proximate composition of the microalgae vary widely, in particular the ash content which is higher for the marine strains than the fresh water strains. The ultimate analysis (dry ash free) is relatively constant although an increase in carbon content correlates with the increasing lipid content as listed in **Table 4.2**. *Nannochloropsis* and *Porphyridium* show very high ash contents of around 25 wt.% (db) and this lowers the HHV. The two protein samples are the only model compounds which have significant ash content, the moisture content of the model compounds varies from 0 to 8.5 wt.%. The two amino acids have the highest nitrogen contents followed by the protein samples. The two carbohydrate model compounds are very high in oxygen and have heating values comparable to microalgae. The microalgae and cyanobacteria selected, exhibit a range of biochemical content ranging from high protein to high lipid. The biochemical composition of the algae strains is illustrated in **Table 4.2** in **Chapter 4**. The protein content varies between 42-65 wt.% (daf). *Spirulina* has the highest nitrogen content

correlating with its high protein fraction. The carbohydrate content varies between 8 and 40 wt.% (daf). *Porphyridium* has the highest carbohydrate fraction correlating with the highest oxygen content. The lipid fraction varies from 5-32 wt.% (daf) and is highest for *Nannochloropsis*.

**Table 7.1:** Proximate and ultimate analysis, HHV of the model compounds and microalgae

Compound	Proximate (wt.%)		Ultimate (wt.% daf)					HHV (MJ/kg)
	Ash	Moisture	C	H	N	S	O*	
<i>Albumin</i>	5.3	8.5	44.6	6.4	12.6	0.2	36.4	23.3
<i>Soya Protein</i>	3.6	5.2	46.9	6.5	13.6	0	33.1	24.2
<i>Asparagine</i>	0	5.1	32.2	6.6	18.7	0	42.5	19.3
<i>Glutamine</i>	0	4.2	40.5	6.7	19.1	0	33.7	22.3
<i>Glucose</i>	0	0	34.4	5.9	0	0	59.8	19.2
<i>Starch</i>	0.1	10.3	38.5	6	0	0	55.5	20.7
<i>Sunflower oil</i>	0	0	63.2	9.5	0.1	0	27.3	33.6
<i>Chlorella</i>	7	5.9	52.6	7.1	8.2	0.5	32.2	23.2
<i>Nannochloropsis</i>	26.4	7.15	57.8	8	8.6	NA	25.7	17.9
<i>Porphyridium</i>	24.4	5.1	51.3	7.6	8	NA	33.1	14.7
<i>Spirulina</i>	7.6	7.8	55.7	6.8	11.2	0.8	26.4	21.2

The yields of bio-crude and other products from the hydrothermal liquefaction of the seven model compounds and microalgae are illustrated in **Figure 7.1a-c**. Processing without catalyst is illustrated in sub-figure (a), (b) shows the processing with  $\text{Na}_2\text{CO}_3$  and (c) using formic acid. The protein (albumin and soya protein) show oil yields between 18 and 6 wt.%, with the yields for the soya protein being consistently higher for all three conditions. The mechanism of oil formation from proteins is a result of the C-N peptide bond between the carboxyl and amine groups of the amino acids hydrolysing which are the building blocks of proteins. The amino acids formed by this

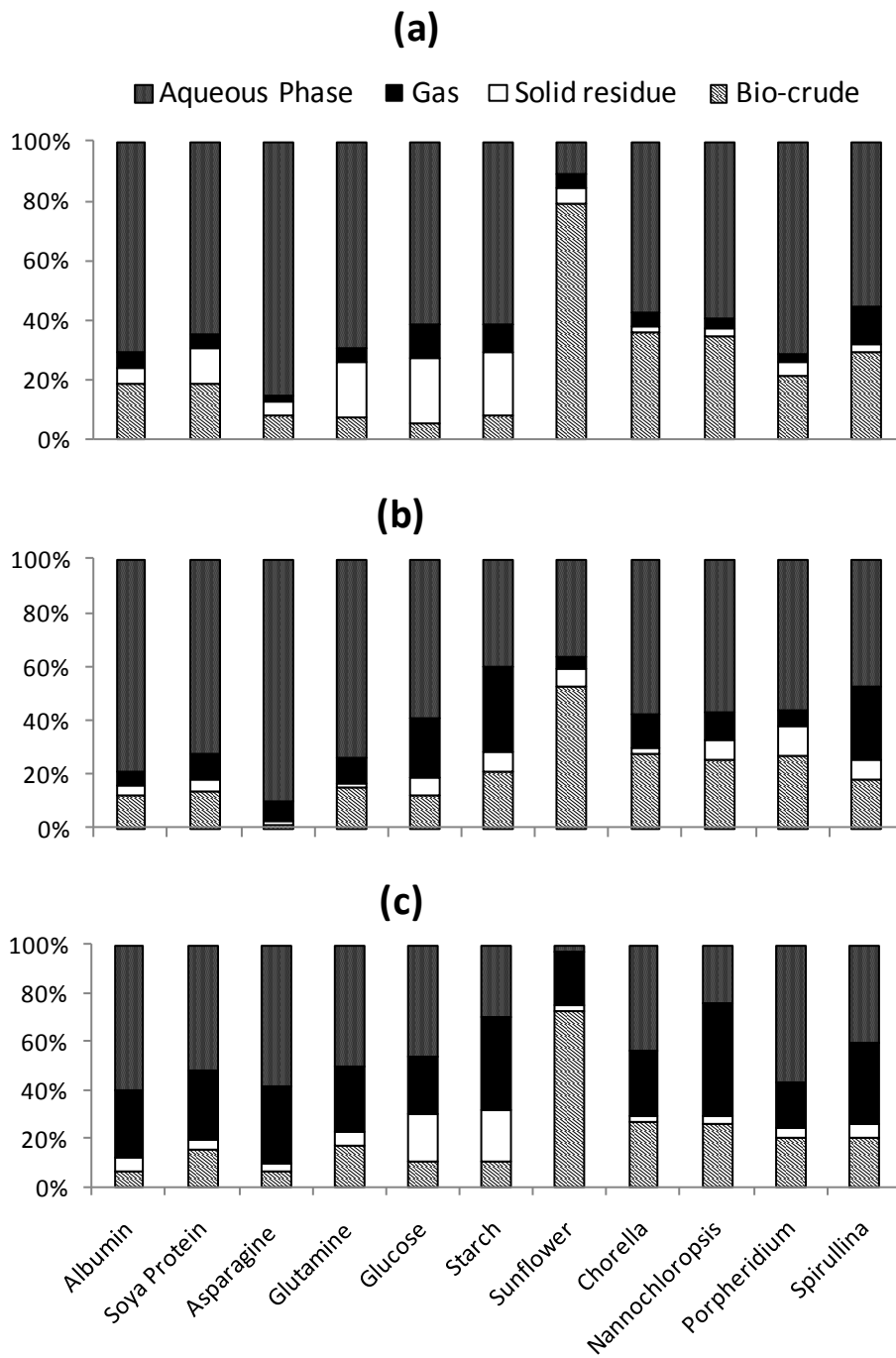


process subsequently degrade by decarboxylation and deamination [35]. The long residence times in this study and relatively severe conditions will allow the small organic materials produced by decarboxylation and deamination of the protein to re-polymerize by Fischer-Tropsch type reactions to longer chain hydrocarbons and aromatic ring-type structures such as phenols and nitrogen heterocycles indole or pyrroles which are the source of bio-crude from liquefaction of protein.

Bio-crude yields are generally highest using water without the addition of catalyst or reagents. **Figure 7.1(c)** clearly shows that the gas phase fraction is highest with the use of formic acid and makes up around 28 wt.% and is consistent with previous data on liquefaction of microalgae in formic acid discussed in **Chapter 6**. The bulk of the product is distributed in the aqueous phase for all conditions and ranges from 52 to 79 wt.%. The amino acids glutamine and asparagine produce lower oil yields than the proteins, most likely due to the lower amount of carbon available for the formation of hydrocarbon type compounds as can be seen in **Table 7.1**. The yields for glutamine are considerably higher than those of asparagine which contradicts the results reported by Dote et al. who observed higher yields for asparagine (1.3 wt.% asparagine, 0.6 wt.% glutamine [134]). Yields of bio-crude were significantly higher for both than those previously reported and reached 4-5 wt.%. The different behaviour of the two amino acids in base and acidic conditions is most likely due to their different solubilities in these kinds of media. Asparagine is not soluble in water but soluble in acid and base media at standard conditions. Glutamine on the other hand is soluble in water and base/acid media [135]. In hot compressed water the dielectric constant changes from 78.5 at standard condition to around 15 at the conditions of this study [39]. The different solubilities in water medium could therefore be the cause of the different liquefaction behaviour. The carbohydrates, starch and glucose, exhibit an increase in solid residue compared to protein, although when using  $\text{Na}_2\text{CO}_3$  the residue reduces. The overall bio-crude yield is lower due to large amounts of the carbohydrates breaking down to polar water soluble organics and not to non-polar hydrocarbon type structures. Srokol et al. reported the breakdown of glucose under similar hydrothermal conditions resulting in the formation of formic acid, acetic acid, lactic acid, acrylic acid, 2-furaldehyde and 1,2,4-benzenetriol. [136] Most of these are polar organics that would dissolve in the water phase and not contribute to the bio-crude yield. The aldehydes and aromatic structures are likely precursors of other larger hydrocarbons that make up the bio-crude fraction following re-polymerization. The alkali catalyst  $\text{Na}_2\text{CO}_3$  has a beneficial influence on oil formation from carbohydrates which is not observed for the proteins as can be seen in **Figure 7.1 (b)**. The residue fraction is larger using  $\text{H}_2\text{O}$  and  $\text{HCOOH}$  (~20 %) (**Figure 7(a), (c)** respectively), but this is reduced to around 6 wt.% with  $\text{Na}_2\text{CO}_3$ . The gaseous fraction is also higher with  $\text{Na}_2\text{CO}_3$  than for

water representing an increase in decarboxylation of the carbohydrates; no increase in gas formation is seen using HCOOH. This does not occur for proteins and suggests  $\text{Na}_2\text{CO}_3$  is selectively promoting decarboxylation of carbohydrates, leading to a lower fraction of product in the water phase than for proteins and amino acids.

Liquefaction of the triglyceride from sunflower oil shows much higher oil yields, ranging from 80 wt.% > 73 wt.% > 53 wt.% for water, formic acid and sodium carbonate respectively. Whilst it is realised that the lipids from microalgae will differ to those of sunflower oil, it is a good approximation for understanding general hydrothermal chemistry. In water, yields are highest and reach 80 wt.% (**Figure 7.1(a)**), the remainder is distributed between the remaining phases with 10 wt.% in the aqueous phase and 5 wt.% for the other two phases. Using formic acid results in the majority of the non-oil phase product being concentrated in the gas phase (**Figure 7.1(c)**).  $\text{Na}_2\text{CO}_3$  has a detrimental effect on oil formation and leads to an increase in solid residue as can be seen in **Figure 7.1(b)**. This observation is attributed to the process of saponification reactions of the lipids in the presence of  $\text{Na}_2\text{CO}_3$  which remained in the residue during filtration. From the liquefaction results of the model compounds it can be concluded that high lipid containing algae should not be processed using  $\text{Na}_2\text{CO}_3$  as a catalyst, while it is favourable for algae with high carbohydrate fraction. High protein containing algae are likely to be most efficiently liquefied without the use of a catalyst; the same applies for high lipid containing algae.



**Figure 7.1:** Yields of products from hydrothermal processing under (a) water, (b) sodium carbonate, (c) formic acid

**Figure 7.1** also shows the results from hydrothermal liquefaction of the three microalgae and the cyanobacteria *Spirulina* at the same conditions as the model compounds. The bio-crude yields are generally higher than for the model compounds (apart from sunflower oil); this means that the oil yields from the different algae are not only derived from the lipid fraction but also from the protein and carbohydrate fractions. The highest oil yields are for *Chlorella* and *Nannochloropsis* which are virtually identical at all conditions and are highest without the use of catalyst (**Figure 7.1 (a)**). Protein was converted to bio-crude most efficiently without a catalyst and this would confirm the observation that the higher protein containing algae *Chlorella* and *Nannochloropsis* have higher oil yields without the use of catalyst. This conclusion is confirmed by the liquefaction behaviour of *Spirulina* which has a protein content of 65 wt.%, the bio-crude yield is over 10 % higher without the use of a catalyst (29 wt.% compared to 17-18 wt.% with catalysts, **Figure 7.1(a) and (b), (c)** respectively).

*Porphyridium* has the lowest bio-crude yields when processed with water and formic acid. With the use of sodium carbonate the yield is in a typical range at 27.1 wt.% . This indicated that the large carbohydrate fraction (40 wt.%) is converted to bio-crude more effectively when using sodium carbonate. This catalyst also consistently produces the largest solid residue fraction for all algae. This could be due to the observed soap formation when liquefying the model lipid sunflower oil. During the liquefaction of the microalgae, the lipid fraction is likely to behave the same way. The soapy fraction of the reaction products is retained during filtration and increases the solid residue fraction. The gas fraction is consistently highest with the use of formic acid as can be seen in **Figure 7.1(c)**. This is due to formic acid breaking down to CO and H<sub>2</sub> increasing the gas fraction as shown in **Chapter 6** [137]. The largest proportion of the product is found in the water phase, just as observed for the model compounds. This aqueous fraction generally makes up around 50 wt.%, being less when using formic acid where the gas fraction makes up a larger portion. Previous researchers have stated that higher lipid containing algae produce higher bio-crude yields [66] which was also observed in **Chapter 5**. When trying to correlate the oil yields of the different biochemical model compounds to the biochemical composition, and assuming that the behaviour of each of the individual components is additive, a simple formula can be created by the measured oil yield results:

$$\text{bio-crude yield wt.}\% = (\text{protein yield wt.}\% \times \text{protein content wt.}\%) + (\text{carbohydrate yield wt.}\% \times \text{carbohydrate content wt.}\%) + (\text{lipid yield wt.}\% \times \text{lipid content yield wt.}\%)$$

**Eqn. 7.1**

This equation would indicate a linear additive behaviour of the model compound yields to the composition of the microalgae and its yield. Investigation of this was performed with a model mixture using the biochemical components and containing soya protein, starch and sunflower oil. The model microalgae containing 43 wt.% protein, 27.6 wt.% carbohydrate and 28.7 wt.% lipid fractions (daf) was processed in water and a bio-crude yield of 30.1 wt.% was observed. With the above equation the predicted yield for this model compound algae is 31.8 %. This suggests that the individual components are behaving additively with respect to oil formation. The 1.7 wt.% percent difference of the calculated and actual yield is most likely due to losses and lies within an acceptable error margin. This relationship was investigated for the microalgae and appears to fit for the microalgae *Chlorella* and *Nannochloropsis*. However, it does not fit for the cyanobacteria, *Spirulina* or for *Porphyridium*, suggesting the behaviour is more complicated. The yields of *Porphyridium* could be affected by the very high ash content which could have catalytic effects and also changes the biomass/water ratio compared to the other samples.

Nevertheless some important and valuable conclusions can be drawn from the liquefaction behaviour of the microalgae investigated in this study which can be related to the liquefaction behaviour of the model compounds. Firstly, it confirms that the higher the lipid content, the higher the bio-crude yield, agreeing with previous reports and results in **Chapter 5**. It is more suitable to convert high lipid containing algae in water or in a reducing atmosphere such as that produced using formic acid. High protein microalgae are best processed without the use of catalysts, as illustrated by the liquefaction results of model proteins and *Spirulina*. Higher carbohydrate microalgae are best processed using an alkali catalyst as illustrated by the higher yields for starch and *Porphyridium*. From the liquefaction results of the model compounds and the microalgae it was shown that the oil formation follows the trend lipids>proteins>carbohydrates. Lipids form oil yields of 80-55 wt.%, protein 18-11 wt.% and carbohydrates 15-6 wt.%. Each of the biochemical components produce bio-crude under hydrothermal conditions, which behave additively for microalgae.

### 7.3.2 Elemental analysis of bio-crude

**Table 7.2** shows the elemental analysis of the bio-crude from hydrothermal processing of the model compounds and the microalgae. The HHV was calculated using the *Dulong formula* [105]. The protein bio-crudes have an average elemental composition 72 wt.% C, 9 wt.% H and 7 wt.% N. Compared to the original composition this is a considerable upgrade, oxygen and nitrogen fractions

are reduced and the HHV increased. The bio-crudes from the amino acids have a nitrogen content of around 8 wt.% which is slightly higher than those from protein but the amino acid samples had higher starting nitrogen contents of 19 wt.%. The effect of catalysts cannot be seen on the elemental composition of the bio-crudes. The bio-crudes from carbohydrates show only trace amounts of nitrogen as the original samples don't contain nitrogen either. The composition is quiet similar to the other bio-crudes apart from the higher oxygen content which is a result of the high oxygen content of carbohydrates; again no clear effect of the catalysts can be seen. The oxygen content is reduced from 55-60 wt.% to a range of differing bio-crudes with oxygen contents of 9-46 wt.%.

The water processed sunflower oil shows no nitrogen but the highest levels of oxygen although the unprocessed oil has a lower oxygen content than the carbohydrates. Using  $\text{Na}_2\text{CO}_3$  the oxygen levels of unprocessed sunflower oil and hydrothermally treated sunflower oil are identical, using water or formic acid results in the oil having lost 7 wt.% oxygen. Most likely the glycerol structure of the triglyceride is harder to remove than the OH groups of carbohydrates. It also appears that the OH group of glucose is easier to deoxygenate than the oxygen in starch.

The HHVs of the algal bio-crudes fall in the range of 33-39 MJ/kg. With *Nannochloropsis* having the highest average HHV, which is in accordance with its higher lipid content. The nitrogen content is highest for the cyanobacteria *Spirulina* which has the highest protein fraction. It also has the highest carbon content, which is probably also a result of the high protein fraction, the model proteins also resulted in high carbon contents. *Spirulina* also has the lowest oxygen content, just like the proteins had the lowest oxygen content of the model compounds. Regarding the elemental composition of bio-crudes from hydrothermal processing it is more desirable for the bio-crude from hydrothermal liquefaction to have a high carbon and content and low oxygen and nitrogen content. Nitrogen in fuel directly forms  $\text{NO}_x$  compounds which are undesirable for environmental and legislative reasons; therefore this cancels out the advantages of higher carbon and lower oxygen contents.

**Table 7.2:** Ultimate analysis, HHV and energy balances of the bio-crudes of model compounds and microalgae

Condition	Catalyst	C	H	N	S	O*	HHV (MJ/ kg)	Energy Recovery (%)	$\Delta H_c$ of feedstock (MJ/kg)	$\Delta H_c$ of bio-crude (MJ/kg)	ECR
<i>Albumin</i>											
	H <sub>2</sub> O	71.4	9.4	7.7	0	11.5	36.3	29.0	0.0	-8.3	1.7
	Na <sub>2</sub> CO <sub>3</sub>	75.5	9.3	6.1	0	9.1	35.5	18.3	0.0	-10.7	2.6
	HCOOH	70.4	9.5	7.6	0	12.5	36.1	8.6	0.0	-12.6	4.6
<i>Soya Protein</i>											
	H <sub>2</sub> O	73	8.6	6.8	0.3	11.3	35.9	30.5	0.9	-8.3	1.4
	Na <sub>2</sub> CO <sub>3</sub>	74.2	9	5	0.3	11.5	36.8	22.4	0.9	-10.1	2.0
	HCOOH	69.9	9	6.7	0.1	14.3	32.3	19.1	0.9	-9.9	1.9
<i>Asparagine</i>											
	H <sub>2</sub> O	69.7	7.5	7.6	0	15.2	33.3	13.4	-4.0	-12.4	4.4
	Na <sub>2</sub> CO <sub>3</sub>	69.2	7.5	6.9	0	16.4	33	1.6	-4.0	-14.7	37.5
	HCOOH	66.2	7.6	8.9	0	17.3	32.3	8.1	-4.0	-13.1	5.8
<i>Glutamine</i>											
	H <sub>2</sub> O	70.6	7.9	11.9	0	9.6	34.2	10.7	-1.0	-12.5	3.7
	Na <sub>2</sub> CO <sub>3</sub>	68.8	8.2	5.6	0	17.4	34	21.7	-1.0	-9.9	1.8
	HCOOH	68	8	8.9	0	15.2	35.9	18.5	-1.0	-8.9	1.5
<i>Glucose</i>											
	H <sub>2</sub> O	74.1	6.9	0.3	0	18.8	34.1	9.1	-4.1	-13.3	4.3
	Na <sub>2</sub> CO <sub>3</sub>	83	8.4	0	0	8.6	39	25.2	-4.1	-10.2	1.6
	HCOOH	77.6	7.4	0.1	0	14.9	35.9	16.3	-4.1	-11.1	1.9
<i>Starch</i>											
	H <sub>2</sub> O	71.7	7.9	0.3	0	20.1	34.5	13.7	-2.6	-12.2	4.0
	Na <sub>2</sub> CO <sub>3</sub>	68.1	5.5	0.1	0	46.4	23.4	23.6	-2.6	-10.1	2.3
	HCOOH	71.5	6.2	0.2	0	22.1	32.4	13.0	-2.6	-11.7	3.4
<i>Sunflower oil</i>											
	H <sub>2</sub> O	68.7	10.6	0.1	0	20.6	36.9	86.7	10.3	14.1	0.3
	Na <sub>2</sub> CO <sub>3</sub>	63.8	8.9	0.1	0	27.1	33.1	52.2	10.3	2.5	0.4
	HCOOH	68.4	11	0.2	0	20.5	37.3	71.2	10.3	12.2	0.3
<i>Chlorella</i>											
	H <sub>2</sub> O	70.7	8.6	5.9	0	14.8	35.1	54.2	-0.1	-2.4	0.8
	Na <sub>2</sub> CO <sub>3</sub>	73.6	10.7	4.9	0	10.7	37.1	44.2	-0.1	-4.8	1.0

<i>Nannochloropsis</i>	HCOOH	70.8	9.4	5.3	0.6	13.9	33.2	31.7	-0.1	-6.0	1.1
	H <sub>2</sub> O	68.1	8.8	4.1	0	18.9	34.5	66.1	-5.4	-3.2	1.2
	Na <sub>2</sub> CO <sub>3</sub>	69.6	9.2	3.8	0	17.3	35.5	50.0	-5.4	-6.1	1.6
<i>Porphyridium</i>	HCOOH	74.7	10.6	4.3	0	10.4	39	41.1	-5.4	-4.8	1.4
	H <sub>2</sub> O	72.8	8.5	5.4	0.3	13.3	35.7	51.6	-8.6	-7.4	1.6
	Na <sub>2</sub> CO <sub>3</sub>	46.1	5.6	3.2	0.2	13.3	22.8	42.1	-8.6	-8.8	2.0
<i>Spirulina</i>	HCOOH	72.5	9.1	5.7	0.4	13.3	36.3	35.2	-8.6	-7.6	1.7
	H <sub>2</sub> O	73.3	9.2	7	0	10.4	36.8	50.7	-2.1	-4.3	1.0
	Na <sub>2</sub> CO <sub>3</sub>	75.4	10.8	4.6	0.5	8.7	34.8	21.0	-2.1	-4.9	1.1
	HCOOH	72.7	9.8	5.7	1	10.9	35.1	19.3	-2.1	-5.1	1.1

### 7.3.3 Energy Balance

**Table 7.2** also shows three different approaches to energy balances of the liquefaction process. The first one is the energy recovery in % this was calculated with the equation:

$$\text{Energy Recovery (\%)} = \frac{\text{HHV of bio - crude} \times \text{mass of bio - crude}}{\text{HHV of feed} \times \text{mass of feed}} \times 100$$

**Eqn. 7.2**

This equation uses the amount of bio-crude produced and takes its heating value into account. It does not compensate for any processing energy used in the liquefaction reaction. The values for the energy recovery of the model compounds range from very low values below ten for the amino acids, to over 80 % for the sunflower oil. For the proteins and the sunflower oil, water without any catalysts has the best energy recovery rates while for the carbohydrates sodium carbonate has beneficial effects on the energy recovery. This is due to the higher bio-crude yields at these conditions. The values for the algae range from 19-66 %, where the values when using formic acid are consistently lower. This is partially because formic acid has its own heating value (11.03 MJ/kg) and this was compensated for in the calculations. The highest energy recovery values were achieved using only water and no catalyst. These values are about 10 % higher; for *Spirulina* even around 20 %. The best performing algae is *Nannochloropsis* with an energy recovery of 66.1 % using water.



This leads to the conclusion that higher lipid containing algae can achieve better energy recoveries. The low lipid, high protein cyanobacteria *Spirulina* results in the lowest recovery rate.

The column “ $\Delta H_c$  of feedstock (MJ)” in **Table 7.2** describes the heat of combustion available when burning or co-firing the feedstock without HTL, the method was adapted from Heilmann et al.,[138]. For this purpose it was assumed that the algae would be received as a slurry of 1kg of biomass to 9 kg of water. The energy for the drying of the water and subsequent combustion of the algae was calculated and compared in the next column ( $\Delta H_c$  of bio-crude (MJ)) to the energy needed to liquefy the algae prior to combustion but avoiding the drying process. The energy for achieving a slurry of 1 kg biomass to 9 kg water was ignored as this would be equal for both processes and this is a comparative calculation. From steam tables the amount of energy needed to remove 9 kg of water from the 10 kg slurry was found to be:  $H_{\text{steam@373 K}} - H_{293 \text{ K}} = 2.68 \text{ MJ/kg} - 0.084 \text{ MJ/kg} = 2.60 \text{ MJ/kg}$ . For 9 kg the energy required is  $9 \text{ kg} \times 2.60 \text{ MJ/kg} = 23.4 \text{ MJ}$ . The heat of combustion of the dry algae minus this value is the net energy balance for the combustion.

For the liquefaction the same slurry has to be heated to 350°C, under pressure without vaporization. From steam tables the enthalpy of saturated liquid water at 350°C is 1.67 MJ/kg, and again 0.084 MJ/kg at 20°C. The heat capacity of the algae present was assumed to be about half that of water therefore:  $\Delta H = 1.59 \text{ MJ/kg} \times 9 \text{ kg} + 0.5 \times 1.59 \text{ MJ/kg} \times 1 \text{ kg} = 15.1 \text{ MJ}$ . The energy available from the bio-crude produced is calculated as the yield per kg multiplied with the HHV of the bio-crude. Subtracting the available energy from combustion with the energy required for liquefaction, results in the overall net energy balance of the liquefaction process.

The results for the model compounds are not as relevant for practical applications as this biomass is not usually present as a slurry. Nevertheless it is possible to see which biochemical compounds are most desirable for the energy balance of microalgae. It can be seen that both proteins and the sunflower oil have positive energy balances following removal of the water with subsequent combustion. But sunflower oil is the only component that also has a positive energy balance for combustion following liquefaction. The carbohydrates have negative energy balances for both conditions and are worse following liquefaction due to their low bio-crude yields, although considerable upgrading of the HHV is achieved. Therefore from these model compound results it is advantageous to have microalgae with high lipid, protein contents and low carbohydrate from an energy balance standpoint. More interesting are the results for the microalgae. It can be seen that all the algae have a net energy loss when directly combusted as dry biomass. The values range from -0.1 MJ for *Chlorella* to -8.6 MJ for *Porphyridium*, the differences are a direct effect of the different

heating values of the feed algae. The energy balance for combusting the bio-crude from liquefaction also shows a net energy loss; for *Chlorella* and *Spirulina* the loss is even larger than for combustion without liquefaction. At these conditions the simplified energy balance would suggest that the liquefaction process has no advantages over conventional co-firing or direct combustion of algae. But it has to be considered that a valuable liquid fuel and potential valuable chemicals are also produced from liquefaction of algae. So from an economical standpoint the process could have a more favourable balance. *Nannochloropsis* and *Porphyridium* on the other hand show more favourable results for liquefaction. For both algae an improvement over conventional combustion is seen apart from when using sodium carbonate. The balance still shows a net loss but the loss is not as high as when burning the dry algae. The better performance is due to the low heating values of the two algae in dry unprocessed form. Both algae have high ash content which results in low heating values but would also be undesirable for direct combustion due to fouling and slagging. The energy balance is poor at these conditions for the microalgae however if liquefaction is performed at 300°C rather than 350°C the bio-crude yields only decrease by around 3 wt.% [139] but the energy required for liquefaction is reduced by 22 %. Therefore lower liquefaction temperatures could be more advantageous from an energy balance standpoint even though less bio-crude is produced. Heilmann et al. produced a char product for co-firing from microalgae by hydrothermal processing at 190-210°C and achieved a positive energy balance for this compared to a negative one if pre-drying and subsequent combustion was assumed. [138]

**Table 7.2** also shows an energy consumption ratio (ECR) adapted from Sawayama et al.'s method which is calculated as:

$$ECR = \frac{m_w \times C_{pw} (\Delta T) + (1 - m_w) \times C_{ps} (\Delta T)}{(1 - m_w) \times m_o \times Y \times r_1 \times r_2} \times (Y \times HHV)^{-1}$$

**Eqn. 7.3** [66]

Where  $m_w$  is the initial moisture mass fraction of the biomass and  $m_o$  is the mass fraction of organic matter in the dry algae.  $C_{pw}$  (4.18 kJ/kg.K) and  $C_{ps}$  (1.25 kJ/kg.K) the average specific heats of water and dry algae,  $\Delta T$  the temperature differential from ambient (298 K) to reaction temperature (623 K),  $Y$  the bio-crude yield,  $r_1$  the efficiency of available combustion energy (0.5),  $r_2$  the efficiency of heat recovery (0.6) and  $HHV$  the heating value of the bio-crude in MJ/kg [66]. A value above 1 means that the energy balance is negative, below 1 means there is a net energy gain. It can be seen from the results in **Table 7.2** that all of the model compounds apart from Sunflower oil have a negative energy consumption ratio when this calculation method is used. Sunflower oil has a

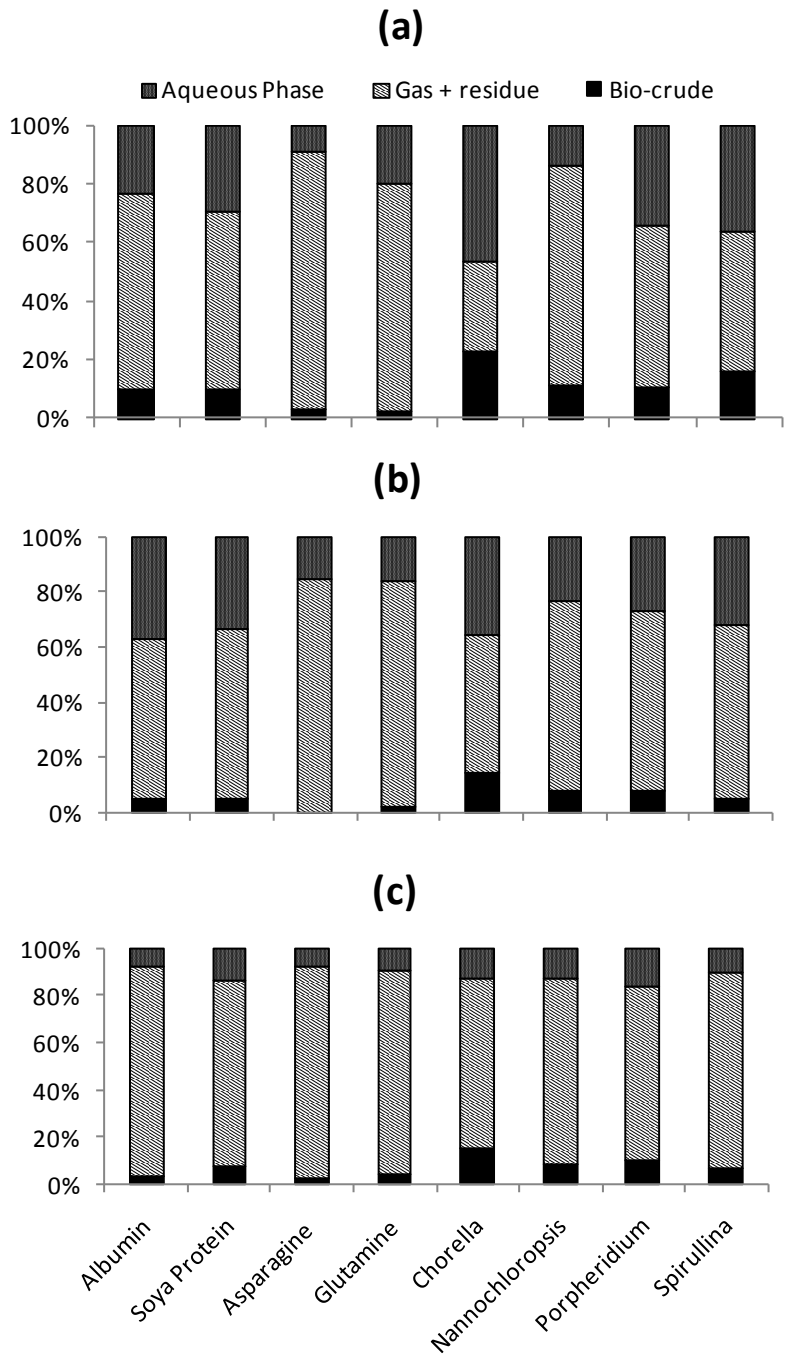
remarkably good energy consumption ratio, due to its high yields and HHV. For the algae liquefaction only *Chlorella* without catalyst has a positive energy consumption ratio. The energy balance of *Spirulina* is 1 or close to 1 indicating that the same amount of energy is used for liquefaction as is gained from the bio-crude. *Porphyridium* performs the least well with up to twice the amount of energy needed for liquefaction than is produced from the oil. The results are considerably lower than those reported by Sawayama et al. [66]. This is due to the heating values and yields in their research being much higher. Concluding it can be said that the high lipid containing algae *Nannochloropsis* has the best energy recovery, which is a calculation based on the heating values and yields. The comparison of direct combustion with pre-drying to combustion post liquefaction shows the most favourable results for the same algae at the same condition but *Porphyridium* also shows improvements for these calculations, while the other two species don't indicate any advantage of liquefaction from solely a heat balance standpoint. The energy consumption ratio calculations result in *Chlorella* without catalyst as the only net energy producing condition. The differing results are due to the ECR calculations taking into account the organic content of the algae for its calculations, resulting in the low ash content microalgae performing better than the high ash content microalgae *Nannochloropsis* and *Porphyridium*, which showed better results for the energy recovery and heat balance comparisons. None of the energy balance calculations take into account the dissolved organics in the water phase or the gas species, CO, CH<sub>4</sub> and H<sub>2</sub> which all have calorific values which would improve the energy balance if they could be recovered.

#### 7.3.4 Nitrogen balance in product streams

The nitrogen distribution of the model compounds in the product streams is illustrated in **Figure 7.2**. Sub-figure **(a)** presents the liquefaction results without catalyst, **(b)** presents the results from processing under sodium carbonate and **(c)** with formic acid. The aqueous fraction was determined by elemental nitrogen contained in ammonium in the water phase and the bio-crude portion by elemental analysis. The gas and residue fraction was combined and determined by difference. From previous research it is known that the nitrogen fraction in the residue is very low not exceeding 5 wt% as shown in **Chapter 6**. The balances for the carbohydrates and sunflower oil are not presented as there are only trace amounts of nitrogen present. The largest fraction of nitrogen was found in the gas phase especially for the amino acids. With the protein samples, 20-30 wt.% of nitrogen is in the

water phase when using water and sodium carbonate, formic acid results in only about 10 wt.% of nitrogen in the gas phase as seen in **Figure 7.2 (a), (b) and (c)** respectively. The amino acids only result in about 10-20 wt.% of nitrogen in the water phase. The nitrogen fraction in the oil for protein is between 4 and 10 wt.%, this is considerably higher than for the amino acids (0.3 – 3.7 wt.%). This confirms Dote et al.'s results [140]. Therefore it is beneficial to break down proteins to amino acids during or prior to hydrothermal liquefaction to obtain a lower nitrogen containing oil.

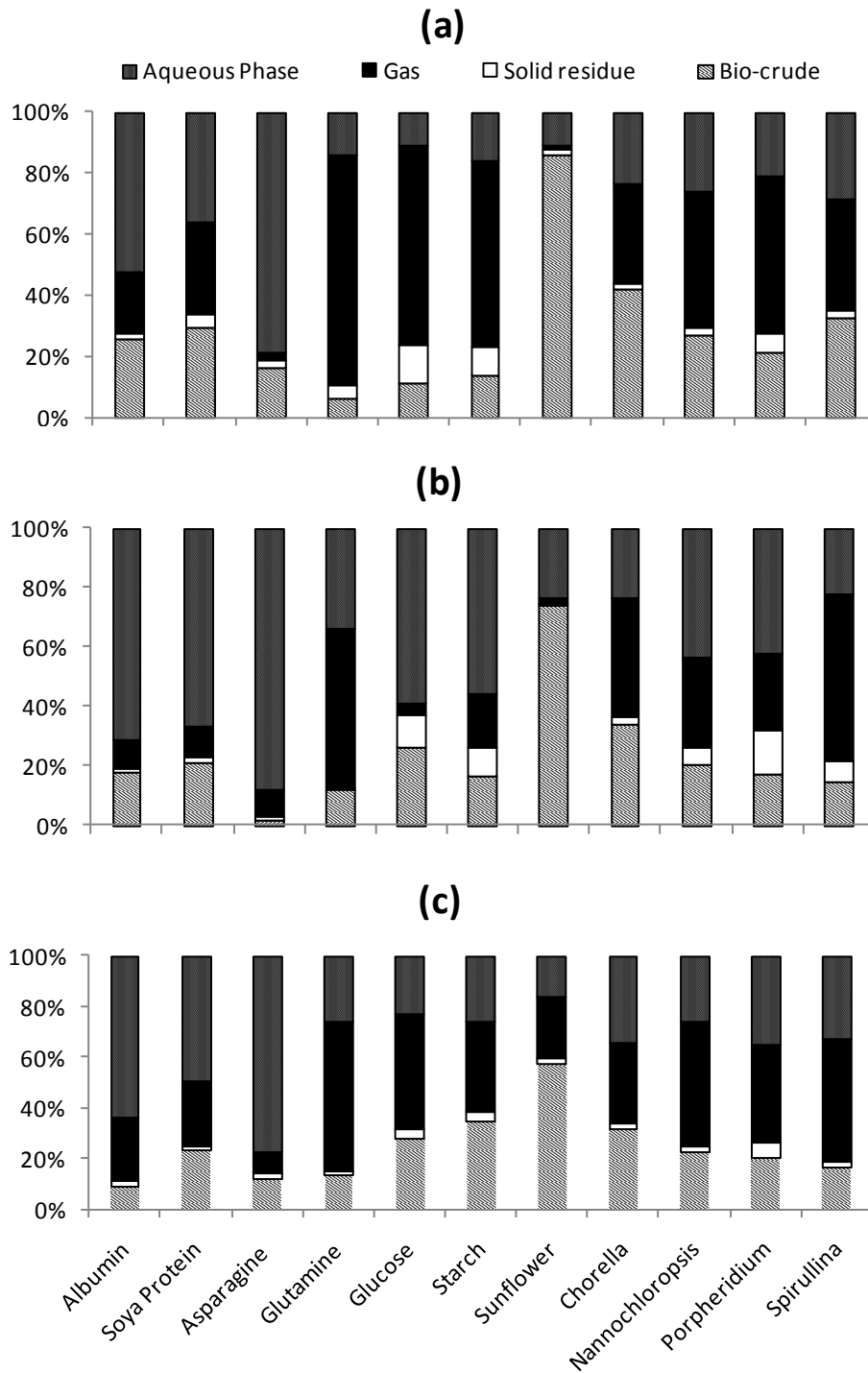
The nitrogen product distribution of the algal bio-crudes is also illustrated in **Figure 7.2a-c**. The nitrogen fraction resulting in the bio-crude is considerably larger than for the nitrogen containing model compounds. **Figure 7.2 (a)** shows that using no catalyst results in the nitrogen partition in the bio-crude being higher than when using catalysts. *Chlorella* has the highest nitrogen fractions in the oil fraction, with water 22 wt.% of the nitrogen ends up in the bio-crude. Sodium carbonate aids the nitrogen not resulting in the oil phase; processing *Spirulina* with Na<sub>2</sub>CO<sub>3</sub> resulted in only 4.5 wt.% of the nitrogen in the bio-crude as seen in **Figure 7.2 (b)**. Again the largest fraction is in the gas and solids, which is a disadvantage when the water is being recycled as a growing media for algae. Amino acids produce lower bio-crude yields than proteins and glutamine considerably more than asparagines (1-8 wt.% compared to 7-17 wt.%). The advantage of the breakdown of proteins to amino acids prior or during liquefaction is that much less nitrogen is fractionated in the bio-crude as is shown by the nitrogen balance of amino acid liquefaction compared to that of proteins. Pre-treatment of high protein algae by hydrolysis is an option that deserves further investigation as this would reduce the amount of nitrogen in the bio-crude. On the other hand a negative effect on bio-crude formation can be expected.



**Figure 7.2:** Distribution of nitrogen in the product streams from hydrothermal processing under (a) water, (b) sodium carbonate, (c) formic acid

### 7.3.5 Carbon balance in product streams

The distribution of carbon in the product phases was calculated using the TOC values from the water phase, estimation from the TGA analysis of the solid residues, and the elemental analysis of the oil and the gas phase by difference. The distribution is illustrated in **Figure 7.3a-c**, again **Figure 7.3 (a)** illustrates using only water, **(b)** sodium carbonate and **(c)** formic acid. The protein samples show most of the carbon in the water phase, around 20% in the oil phase, only small amounts (<5%) in the residue and the remaining carbon in the gas phase. Using formic acid results in there being less carbon in the bio-crude as a larger fraction is found in the gas phase. Using water results in the largest fraction being in the bio-crude and the least in the water phase. Surprisingly the two amino acids behave quite differently concerning their carbon distribution. Glutamine shows the majority of carbon being in the gas phase while asparagine has around 80 wt.% in the water phase; this is most likely due to the different solubilities. Also the catalysts have different effects on the carbon distribution; asparagine results in the highest levels of carbon in the bio-crude without a catalyst (**Figure 7.3(a)**) and for glutamine this is observed with formic acid (**Figure 7.3(c)**). The carbohydrates show larger amounts of carbon in the solid residue which is a result of the increased solid formations from carbohydrates. Carbohydrates also produce relatively high gas yields (**Figure 7.1**); therefore the carbon in the gas phase is significant. The amount of carbon in the oil is higher using catalysts, which is the opposite effect observed for proteins, where the carbon in the oil is highest using water (**Figure 7.3(a)**). The model lipid sunflower oil shows the majority of carbon in the oil, with the highest values for water followed by  $\text{Na}_2\text{CO}_3$  and formic acid. Formic acid shows significant amounts of carbon in the gas phase while the other two conditions show the remaining carbon in the water phase. The carbon distribution in the product phases for the microalgae shows similar trends. The largest fraction of carbon for all algae is in the oil phase when not using any catalyst and the least when using  $\text{Na}_2\text{CO}_3$ . *Chlorella* shows the highest values of carbon in the oil phase and *Porphyridium* the lowest. The solid fraction is generally low apart from *Porphyridium* which results in a large solid fraction but the carbon fraction of the solids is generally low (20-30 wt.%). The effect of catalysts on carbon in gas or water phase is not apparent.



**Figure 7.3:** Distribution of carbon in the product streams from hydrothermal processing under (a) water, (b) sodium carbonate, (c) formic acid

### 7.3.6 GC/MS analysis of the bio-crude

A fraction of the bio-crudes produced from hydrothermal liquefaction was analysed by GC/MS. The final temperature of the GC temperature program was 250°C, at this temperature only half of the oil sample is volatilised as the rest has a higher molecular weight. This was estimated by performing a simulated distillation of the oils using TGA in a nitrogen atmosphere. Using water and sodium carbonate results in half of the oil mass volatilising after 250°C. Processing under formic acid results in around 30 wt.% of the bio-crude volatilising after 250°C, between the different feedstocks these values hardly vary. Therefore formic acid has a positive effect on pour behaviour of the obtained oils and lowers the overall molecular weight as previously shown in **Chapter 6**. The chromatograms are not included but the main compounds identified are discussed and presented in **Table 7.3**.

The soya protein and albumin show very similar chromatographic fingerprints, processing in water and formic acid are similar with a small difference being observed when processing in sodium carbonate as can be seen in **Table 7.3**. The most abundant compounds for all conditions observed are phenols and indoles. All three conditions show the nitrogen heterocycle indole with larger amounts being present using water and formic acid. These conditions also show the heterocyclic amine piperidine and pyrrolidinone which were not found when using sodium carbonate as a catalyst. For the carbohydrates the compounds identified in the bio-crude from glucose do not vary significantly to those found in the bio-crude from starch. Processing with Na<sub>2</sub>CO<sub>3</sub> produced the cyclic ketones, cyclopentanone and cyclohexanone as well as phenols. The amino acid asparagine processed in Na<sub>2</sub>CO<sub>3</sub> results in large amounts of phenols and some indole compounds, however when using water and formic acid, the indoles are reduced and pyrrolidones and cyclic ketones are observed. The sunflower oil processed in water and formic acid results in the decomposition of the triglycerides to produce fatty acids, namely hexadecanoic acid, tetradecanoic acid and oleic acid. Under Na<sub>2</sub>CO<sub>3</sub> the resulting oil contained alkenes, enols and enones mainly the 6- and 7-chain lengths.

The GC/MS analysis of bio-crude from *Chlorella* with Na<sub>2</sub>CO<sub>3</sub> indicates the presence of phenols and piperidine derived compounds but also the alkanes hepta- and hexadecane. Water and HCOOH processing results in similar compounds but additionally aliphatic amides such as dimethyldecanamide, dodecamine and the fatty acid octanoic acid. *Nannochloropsis*, which has a high lipid content, resulted in the bio-crude containing large amounts of fatty acids and heterocycles



such as indole. Processing with  $\text{Na}_2\text{CO}_3$  indicates the presence of the acyclic alcohol phytol, phenol derivatives and hexadecane. *Porphyridium* produces large amounts of indole using  $\text{Na}_2\text{CO}_3$  but also phenolic compounds and phytol. No phytol could be identified using  $\text{H}_2\text{O}$  and  $\text{HCOOH}$  but pyrrolidinone compounds are present. The high protein containing cyanobacteria *Spirulina* resulted in a higher proportion of protein derived pyrroles and indoles but also some hepta- and hexadecane. Under water and formic acid processing, there are aliphatic amides present. *Porphyridium* liquefied with  $\text{Na}_2\text{CO}_3$  only resulted in phenolic and indole compounds and phytol, where the indole peaks were by far the largest. Without catalyst additional pyrrole derived compounds are observed. Processing in  $\text{HCOOH}$  again results in the formation of the aliphatic amide hexadecamide and the fatty acid tetradecanoic acid. The use of sodium carbonate results in a larger fraction of high molecular weight material, this is observed from both GC/MS and simulated distillation experiments by TGA. The higher the protein contents of the algal feedstock, the higher the fraction of nitrogen heterocycles, pyrroles and indoles in the bio-crude. Using sodium carbonate increases the formation of phenolic compounds and also increases the breakdown of lipids to alkanes while water and formic acid resulted in the lipids breaking down to fatty acids. The use of  $\text{HCOOH}$  produces an increase in fatty acid amides. **Table 7.3** shows some distinct clusters of compounds for the different model compounds, especially proteins and carbohydrates. The protein cluster is also present for the algae which all consist of a significant amount of proteins. The lipid cluster can also be seen for the high lipid algae *Nannochloropsis*. Surprisingly the high carbohydrate containing algae *Prophyridium* shows no compounds associated with carbohydrates, this is due to the carbohydrate fraction only producing about 7% bio-crude. Therefore the compounds derived from lipids and proteins are predominant in the GC-MS chromatograms and **Table 7.3**.

**Table 7.3:** Most abundant GC-MS identified compounds in the bio-crudes from liquefaction at different conditions

Bio-crude condition	Albumin			Soya Protein			Asparagine			Glucose			Starch			Sunflower oil			Chlorella			Nannochloropsis			Porphyridium			Spirulina									
	H <sub>2</sub> O	Na <sub>2</sub> CO <sub>3</sub>	HCOOH	H <sub>2</sub> O	Na <sub>2</sub> CO <sub>3</sub>	HCOOH	H <sub>2</sub> O	Na <sub>2</sub> CO <sub>3</sub>	HCOOH	H <sub>2</sub> O	Na <sub>2</sub> CO <sub>3</sub>	HCOOH	H <sub>2</sub> O	Na <sub>2</sub> CO <sub>3</sub>	HCOOH	H <sub>2</sub> O	Na <sub>2</sub> CO <sub>3</sub>	HCOOH	H <sub>2</sub> O	Na <sub>2</sub> CO <sub>3</sub>	HCOOH	H <sub>2</sub> O	Na <sub>2</sub> CO <sub>3</sub>	HCOOH	H <sub>2</sub> O	Na <sub>2</sub> CO <sub>3</sub>	HCOOH										
<i>Phenols</i>	x	x	x	x	x	x	x			x									x	x	x	x	x	x	x	x	x	x	x	x	x	x					
<i>Phytol</i>																																					
<i>Indole</i>	x	x	x	x	x	x	x																														
<i>Pyrrols</i>	x		x	x		x	x																														
<i>Piperidine</i>	x			x		x																															
<i>Hexadecamide</i>																																					
<i>Cyclohexylamine</i>																																					
<i>Hexadecane</i>																																					
<i>Heptadecane</i>																																					
<i>Pentadecene</i>																																					
<i>Octanoic acid</i>																																					
<i>Cyclohexanone</i>																																					
<i>Cyclopentanone</i>																																					
<i>Benzene</i>																																					
<i>Indenone</i>																																					
<i>Ethanone</i>																																					
<i>Tetradecanoic Acid</i>																																					
<i>Oleic Acid</i>																																					
<i>Hexadecanoic Acid</i>																																					

## 7.4 Conclusions

From the liquefaction results of the model compounds and the microalgae it was shown that the bio-crude formation follows the trend lipids>proteins>carbohydrates. Lipids form oil yields of 80-55 wt.%, protein 18-11 wt.% and carbohydrates 15-6 wt.%. Both proteins and lipids were converted to bio-crude most efficiently without the use of catalysts while carbohydrates are best processed using  $\text{Na}_2\text{CO}_3$ . This is shown by the liquefaction of the model compounds and also fits with the results of the high protein and high lipid microalgae, *Spirulina* and *Nannochloropsis* respectively. Amino acids produce lower bio-crude yields than proteins and glutamine considerably more than asparagines (1-8 wt.% compared to 7-17 wt.%). The advantage of the breakdown of proteins to amino acids prior or during liquefaction is that much less nitrogen is found in the bio-crude as is shown by the nitrogen balance of amino acid liquefaction compared to that of proteins. Pre-treatment of high protein algae by hydrolysis is an option that deserves further investigation as this would reduce the amount of nitrogen in the bio-crude. On the other hand a negative effect on oil formation can be expected.

It was shown that carbohydrates are best hydrothermally liquefied using sodium carbonate as this increased the bio-crude yields significantly for the model compounds as well as the high carbohydrate containing microalgae *Porphyridium*.  $\text{Na}_2\text{CO}_3$  selectively increases the decarboxylation of carbohydrates. Very high lipid containing algae are best processed using no catalyst as this gives the highest bio-crude yields and  $\text{Na}_2\text{CO}_3$  should not be used as this results in soap formation which increases the solid residue.

It was further shown that the different biochemical compositions of microalgae behave additively, which means higher oil yields than lipid contents can be achieved by hydrothermal liquefaction. This is a distinct advantage of hydrothermal liquefaction compared to conventional physical extraction methods. The high lipid containing algae *Nannochloropsis* showed the highest bio-crude yields correlating to its higher lipid content. The cyanobacteria *Spirulina* showed 10 % greater bio-crude yields compared to processing with catalysts. This is because of the very high protein content (65 wt.%); it was proven that proteins exhibit higher bio-crude yields without catalysts. The high carbohydrate containing microalgae *Porphyridium* performed best using  $\text{Na}_2\text{CO}_3$  which further proves the point of carbohydrates best being processed using  $\text{Na}_2\text{CO}_3$ .

GC/MS results showed that formic acid and water liquefaction produce very similar bio-crude components. Proteins produce large amounts of nitrogen heterocycles, pyrroles and indoles,

carbohydrates produce cyclic ketones as well as phenols while lipids are converted to fatty acids. High protein containing algae therefore were shown to produce larger amounts of nitrogen compounds.  $\text{Na}_2\text{CO}_3$  was shown to produce more large molecular weight compounds and phenolic compounds.

## 8. CHAPTER VIII - Nutrient Recycling from HTL process water

### 8.1 Introduction

As shown in previous **Chapters 5-7** HTL is an ideal route for the conversion of high moisture content biomass such as microalgae, as a drying step of the feedstock is not necessary. Results have shown that a bio-crude with a high heating value can be produced from the HTL of microalgae, although the oxygen content and nitrogen content are typically still higher than crude oil [47, 68, 77]. An additional benefit of the hydrothermal processing routes is the potential to recycle process water which is rich in nutrients such as nitrogen and phosphorous and elements such as Fe, Ca, Mg, K, as well as other mineral matter and polar organics (see **Chapter 5-6**) [47]. One of the challenges previously identified concerning HTL of microalgae is the large amount of organic carbon in the process water [77]. This represents a loss of carbon efficiency and reduces the bio-crude yields. It is expected that the organic carbon in the process water of HTL can act as a substrate for mixotrophic growth of microalgae. This can lead to increased biomass yields and higher carbon efficiency. Bhatnagar et al. showed that strains of *Chlamydomonas*, *Chlorella* and *Scenedesmus* were able to grow mixotrophically in various sources of process water high in TOC, which led to higher biomass yields [141]. The potential for nutrient recycling is thought to be essential for the economic development of large scale microalgae cultivation. Nutrient recycling potential has largely been focussed on conversion by anaerobic digestion [142] and only limited studies have evaluated hydrothermal processing routes. Tsukahara *et al*, (2001) demonstrated the potential for nutrient recycling on *Chlorella vulgaris* by low temperature gasification of microalgae [98] and more recently Jena et al. (2010) have shown that it is possible to cultivate microalgae in the process water following HTL of the freshwater microalgae *Chlorella minutissima* [48] although they used a different strain for cultivation than for the HTL experiments. Each of these options, whether anaerobic digestion or hydrothermal processing have their associated problems, but it is recognised that integration of microalgae cultivation with some sort of nutrient recycle is essential. This investigation reports the potential of recycling the process water from HTL of four different algae strains and two different HTL processing temperatures.

It is envisioned that a final industrial process could be integrated into a closed loop concept with integrated nutrient recycling as presented in **Chapter 1**. In the current Chapter the aim was to demonstrate the feasibility of a potential closed loop HTL system with nutrient recycling. In the

current laboratory study the cultivation systems were simple, small scale 500 ml conical flasks and HTL was performed in batch 75 or 660 ml high pressure reactors. The purpose of the current research is to demonstrate the feasibility of using the process water for nutrient recycling on laboratory scale. However, in an industrial system a more sophisticated cultivation and processing system would be required. A continuous HTL reactor would also be desirable and the use of solvents to separate the phases would then be avoidable due to self separation of the bio-crude, this is addressed in **Chapter 10**.

## 8.2 Methodology

For the hydrothermal liquefaction experiments at 350°C approximately 3g (*Chlorella* and *Scenedesmus*) of microalgae were added to a 75ml Parr high pressure reactor with 27 ml of distilled water. The top temperature was held for 1 hour, after which compressed air was blown onto the reactor to cool it to room temperature at approximately 20 °C/min. The experiments at 300°C for *Chlorogloeopsis*, *Spirulina* and *Chlorella* were processed at the same ratios (~24g biomass/220 ml H<sub>2</sub>O) and times but in a 660 ml Parr reactor. Both Parr reactors are constructed of 316 Stainless Steel with an elemental composition of 65 wt.% Fe, 12 wt.% Ni, 17 wt.% Cr, 2.5 wt.% Mo, 2.0 wt.% Mn and 1 wt.% Si. The experiments at 350°C were carried out in duplicate and average values are reported however due to limited availability of microalgae biomass the experiments at 300°C in the larger reactors were only carried out once.

## 8.3 Results and Discussion

### 8.3.1 HTL Results

The microalgae strains investigated in the current Chapter are *Chlorella vulgaris*, *Spirulina platensis*, *Scenedesmus dimorphus* and *Chlorogloeopsis fritschii*. Analysis of these feedstocks can be found in **Chapter 4** and the data sheets in **APPENDIX A**. The microalgae were chosen to provide a range of different biochemical contents to study the change in aqueous phase composition and subsequent nutrient recycling. It is known that the biochemical composition affects the HTL

behaviour (see **Chapter 7**) but the nutrient recycling potential has not been investigated. The two cyanobacteria *Chlorogloeopsis* and *Spirulina* have very low lipid contents, 10-20 wt.% lower than the microalgae strains. *Spirulina* has the highest protein content which corresponds to its highest nitrogen content. There is also a range of carbohydrates present which is especially high for *Chlorogloeopsis* (44 wt.%). The oxygen content of all strains was typically around 30 wt.%. The oxygen and the nitrogen components are the two elements primarily removed during HTL.

Following HTL the bio-crude was weighed and analysed. The elemental composition and the calculated Higher Heating Value (HHV) of the bio-crudes are shown in **Table 8.1**. The reactions performed at 300°C were processed in a 660 ml Parr reactor while the reactions at 350°C were processed in a smaller 75 ml reactor. The bio-crude yields range from 27 wt.% for *Scenedesmus* at 350°C to 47 wt.% for *Chlorella* at 300°C. The high bio-crude yields of *Chlorella* are due to its higher lipid content. At higher temperatures, more decomposition to polar organics is observed which result in a higher TOC content in the water phase and a reduction in polar organics in the bio-crude. As shown by the TOC results of *Chlorella OZ* processed at 300 and 350°C in **Chapter 5**. At higher temperatures, the oxygen content of the bio-crude is also lower. The oxygen content varies significantly for the bio-crude derived from the different algae strains, being highest for *Chlorogloeopsis* which corresponds to the lowest HHV. The nitrogen content of the two cyanobacteria *Chlorogloeopsis* and *Spirulina* are highest as a large fraction of the bio-crude originates from the protein fraction as shown in **Chapter 7**. The nitrogen content of the *Chlorella* bio-crude is higher at 350°C as more protein is broken down than at the lower temperatures.

**Table 8.1:** Influence of temperature and biomass species on bio-crude composition, higher heating value, and yield.

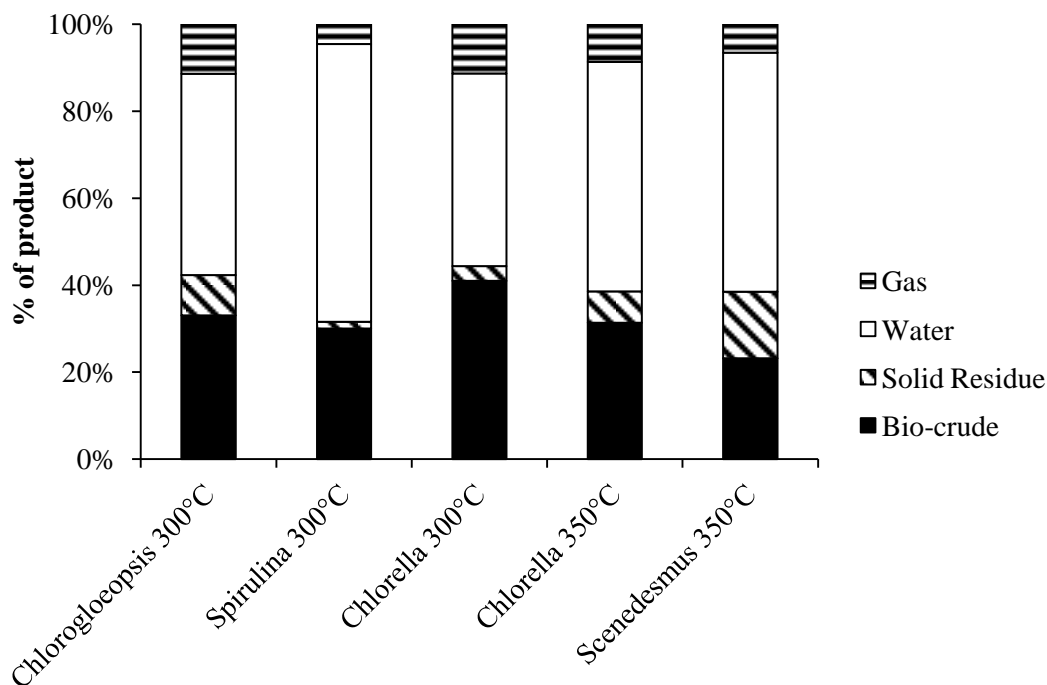
Strain	Temp. (°C)	Elemental Composition of Bio-crude (wt.% daf)					HHV (MJ/kg)	Bio-crude yield (wt.% daf)
		C	H	N	S	O*		
<i>Chlorogloeopsis</i>	300	66.5	7.2	6.8	0.4	19.0	32.0	38.6
<i>Spirulina</i>	300	72.7	8.8	6.3	0.6	11.5	36.1	35.5
<i>Chlorella</i>	300	75.9	9.0	5.3	0.4	9.3	37.5	46.6
<i>Chlorella</i>	350	70.7	8.6	5.9	0.0	14.8	35.1	35.8±0.3
<i>Scenedesmus</i>	350	73.0	8.2	5.7	0.5	12.6	33.6	27.1±0.8

\*by difference; daf = dry ash free; HHV= Higher Heating Value; elemental analysis in duplicate, yields in duplicate and single for 300°C experiments

The product distribution following HTL is shown in **Figure 8.1**. The gas yields are relatively low and consist mainly of CO<sub>2</sub>. The data is presented on an as received basis which explains the lower bio-crude yields than the dry ash free yields presented in **Table 8.1**. The product yields of bio-crude range from 23 to 41 wt.% for *Scenedesmus* and *Chlorella* 300°C respectively. The solid residue is highest for *Scenedesmus* which exhibits the highest ash content. The solid residue consists mainly of the mineral matter but also small amounts of carbon and nitrogen [47]. The largest fraction is shown to be the process water ranging from 46 wt.% for *Chlorella* at 300°C to 68 wt.% for *Spirulina*. This clearly represents a major loss if this fraction was not recovered. The amount of carbon and nitrogen in the product phases is distributed similarly to results shown previously in **Chapter 7**. Up to 40 wt.% of carbon and 50 wt.% of nitrogen accumulate in the process water, resulting in low carbon recovery efficiencies; this was shown in the previous **Chapter 7** where a mass balance on C and N in the product phases was carried out on the HTL of four microalgae strains at the same conditions [77]. Therefore the feasibility of recycling the process water for algae cultivation is investigated to recover the nitrogen and carbon lost to the water phase. In **Chapter 5**



the water phase has also been shown to be rich in  $\text{PO}_4^{3-}$ ,  $\text{NH}_4^+$  and K, compounds essential for algal growth.



**Figure 8.1:** Product distribution from the hydrothermal liquefaction of the different microalgae strains at 300°C and 350°C

### 8.3.2 Analysis of Process Water

Due to the large fraction of product distributed in the process water, its composition was examined to determine the suitability of using this as a source of nutrients for microalgae cultivation. **Table 8.2** lists the main components identified in the water phase as determined by ion exchange chromatography, photometry and ICP-OES. In addition, the water phase is known to contain nitrogen heterocycles such as pyrroles, indoles and phenols from the decomposition of the protein component [47]. The process water was analysed for total phenol content by photometry as these compounds are toxic to certain algae and can inhibit growth. Scragg reported that the growth of *Chlorella vulgaris* was inhibited with concentrations of 400 mg/l, but even at concentrations of 100 and 200 mg/l the growth rate was reduced [101].

**Table 8.2** shows that for all species except nitrate, concentrations in the process water are much higher than those in the standard growth media 3N-BBM+V. In particular, concentrations of K,  $\text{NH}_4^+$ , acetate and  $\text{PO}_4^{3-}$  are very high, orders of magnitude higher than those found in the media. These three nutrients are important to algal growth and are one of the main economic constraints. Acetate is of particular interest because it could potentially act as a substrate for mixotrophic growth, increasing productivity and recycling carbon [141]. In order to reach levels of nutrients similar to the standard media, the process water must be substantially diluted as shown by Jena et al. [48]. It is important to note that the nitrogen source in the media is in the form of nitrate, whereas in the process water the nitrogen is mainly present as ammonium. Microalgae are able to use both sources of nitrogen, and it has been suggested that neither actually provide an advantage to growth [143]. The total amount of nitrogen ranges from 3000-8000 mg/l, *Scenedesmus* and *Chlorogloeopsis* have the lowest amounts due to the low nitrogen content in the algae, *Spirulina* on the other hand has the highest value corresponding to its high protein and nitrogen content. Concerning the nitrogen concentrations compared to the three fold nitrogen BBM media, the process water should be diluted between 25 and 65× its original volume to achieve the same nitrogen levels. For a standard BBM medium the dilutions would be 75-200 times its original volume.

Nickel concentrations are of particular importance due to the inhibitory effects on microalgae, particularly for *Chlorella vulgaris* which was observed to be inhibited by nickel levels as low as 0.85 µg/l [100]. Nickel is present in very small amounts in the algae but it is also added to the process water by leaching of the reactor walls during HTL. A study was carried out in a Hastelloy 75 ml reactor with only distilled water led to a nickel concentration of 41 mg/l and 2.5 mg/l Fe at the same conditions [144]. It is expected that the leaching of nickel from 316 Stainless Steel as used in this study is less because of the lower nickel content of this steel alloy. This is preliminary confirmed by the nickel analysis in **Table 8.2** ranging from 0 to 4 mg/l. The difference in Ni concentrations in the two *Chlorella* process waters is due to the more severe processing conditions leading to additional Ni leaching to the process water. *Scenedesmus* process water has a higher Ni concentration due to the higher Ni content of the algae feedstock. Haiduc et al. realized the significance of the nickel leaching effect in their study on hydrothermal gasification of microalgae [88]. They state that when a continuous system with nutrient recycling is used nickel concentrations would accumulate over time leading to growth inhibition. In the growth trials Haiduc et al. carried out, the media was doped with nickel and all concentrations (1-25 mg/l) had adverse effects on algae growth. They came to the conclusion that reactor wall corrosion, metal leaching and nickel

concentrations in the process water need to be monitored closely. They suggest that levels of 25 mg/l should not be exceeded by either additional dilution or removal of the metal toxicant.

**Table 8.2:** Nutrient analysis of the process water compared to standard growth media 3N-BBM+V

(mg/l)	<i>Chlorogloeopsis</i> 300°C	<i>Spirulina</i> 300°C	<i>Chlorella</i> 300°C	<i>Chlorella</i> 350°C	<i>S. dimorphus</i> 350°C	3N- BBM+V*
<i>pH</i>	8.9	8.9	9	9.2	8.4	6.8
<i>TOC</i>	9060	15123	11373	13764	11119	-
<i>Total N</i>	5636	8136	6636	6888	3139	124
<i>NH<sub>4</sub><sup>+</sup></i>	4748	6295	5673	5920	5280	-
<i>PO<sub>4</sub><sup>3-</sup></i>	280	2159	3109	1121	1470	153
<i>K</i>	303	1506	1460	1419	1150	63
<i>Acetate</i>	2146	7131	4106	5378	1290	-
<i>NO<sub>3</sub><sup>-</sup></i>	508	194	329	237	192	547
<i>Ni</i>	3.8	0	0.1	0.4	0.8	-
<i>Phenols</i>	178	98	108	158	80	-

\*composition of 3N-BBM+V calculated based on prepared media composition; no replicate of analysis available for process waters

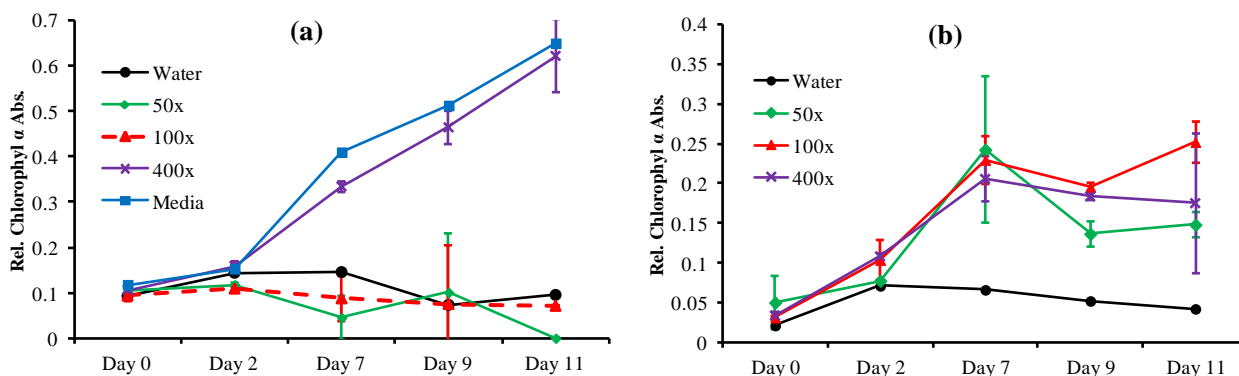
The amount of phenols in the process water could also pose a problem due to their known inhibition affect on algae growth [101]. Phenols are typically present at concentrations of 100-200 mg/l, without dilution of the water phase this would most likely inhibit algal growth. The pH of the process water is more alkaline for all conditions compared to the 3N-BBM media. This is due to the large amounts of ammonium present. The TOC analysis shows that there are significant levels of organic carbon in the process water. The mass balance in **Figure 8.1** showed large amounts of the product distributed to the process water and **Chapter 7** it was shown that this fraction contains large amounts of carbon [77]. The highest values of TOC (*Spirulina*, ~15000 mg/l TOC) in the process water correspond to the highest fraction of product in the entire mass balance in **Figure 8.1**. High

TOC levels are beneficial if the microalgae are capable of using this carbon for mixotrophic growth although ideally it would be beneficial if the bio-crude yields were higher. The organic content of the process water is largely dependent upon the biochemical content of the microalgae as was shown in **Chapter 7** where model proteins, carbohydrates and lipids were processed under the same conditions [77]. In general, the higher the protein content, the higher the phenol and nitrogen heterocycles present in the oil [47]. Phenol and alkyl phenols are also present in the water as well as pyrrolidinones, piperidines, pyrroles and indoles [145].

### 8.3.3 Cultivation Trials

Due to the high concentration of the major nutrients in the process water compared to the media, it was necessary to dilute the process water with distilled water before cultivation. Jena et al. (2010) used similar dilutions for growth trials with the recovered aqueous phase from the HTL of *Spirulina*. They found that a tenfold dilution was too strong and no growth occurred [48]. The growth trials for this study were performed on dilutions of 50×, 100×, and 400× of the original process water. Trials were also performed in the standard media for comparison as well as a distilled water control. Growth was determined by chlorophyll a absorbance as described in **Chapter 3**. The cyanobacterium *Chlorogloeopsis* exhibits a very strong cell wall so that the acetone could not extract the chlorophyll a from the cells. Due to this there is no data available for the growth trials over time of *Chlorogloeopsis* but the final growth was determined. **Figure 8.2(a+b)** shows the chlorophyll a absorbance of growth trials for *Spirulina* and *Chlorella* grown in the recovered aqueous phase from HTL at 300°C. The chlorophyll a absorbance of *Spirulina* for the distilled water, 50× and 100× dilutions showed that no algae growth occurred at these conditions (**Figure 8.2(a)**). The 400× dilution of the process water and the standard media have positive chlorophyll a absorbance indicating growth was occurring. The values follow the same trend of steadily increasing growth after day two and show similar growth although the standard media absorbance is slightly higher. It appears that *Spirulina* is not able to grow in the stronger 50× and 100× dilutions, due to inhibitory effects, which may be attributed to the presence of metals such as nickel and organics such as phenols. According to Belkin and Boussiba (1991) the ammonia uptake at the observed concentrations should not pose a problem for *Spirulina*, especially at the pH levels measured (8.9 pH) [146]. The growth of *Chlorella* is plotted in **Figure 8.2(b)**. The growth in the process water dilutions showed growth in all three dilutions while no growth occurred in the

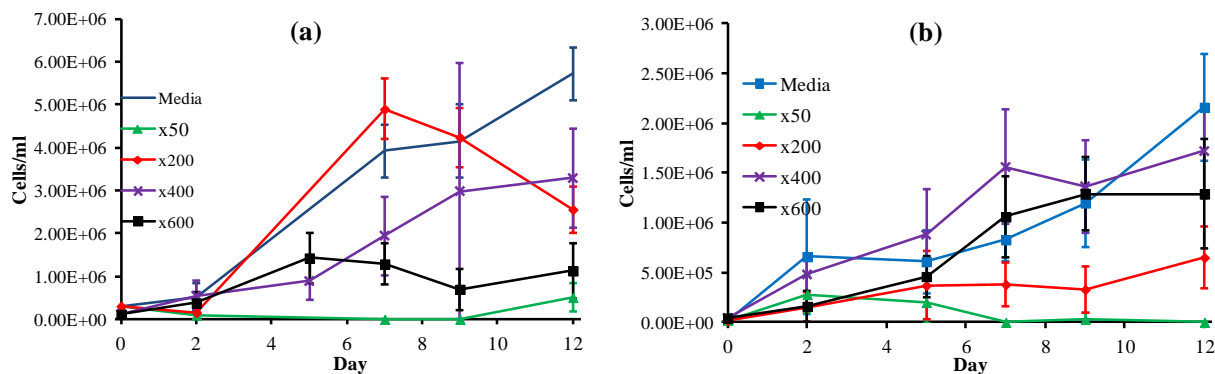
distilled water control. A fourfold increase in biomass concentration was observed in the first 7 days, and then a reduction in concentration is observed for all three trials. It appears that there are not sufficient nutrients available past day 7 for further growth. The 100× dilution exhibits a small final increase in absorbance resulting in the highest relative biomass concentration.



**Figure 8.2:** Growth of algae in process water dilutions of (a) *Spirulina* 300°C (b) *Chlorella* 300°C determined by chlorophyll a absorbance

The growth trials of the HTL process water from *Chlorella* and *Scenedesmus* at 350°C was carried out in the same manner but the dilutions chosen were 50×, 200×, 400× and 600× the original volume. The cultivation trials are compared to the growth in respective standard media 3N-BBM+V. These trials were performed in a different laboratory where chlorophyll a absorbance could not be measured; therefore cell counting using a haemocytometer was used. The correlation between cell count and chlorophyll a absorbance is expected to fit well for mixo- and photo-trophic growing algae as was shown by Bird et al. (1984) [147]. The cell concentration of the growth trials are plotted in **Figure 8.3(a+b)** for *Chlorella* and *Scenedesmus* respectively. Both algae showed no growth in the strongest dilution of 50×. This is most likely due to the high concentration of inhibitors such as nickel, phenols and fatty acids. *Chlorella* grew best in the standard media with a final cell concentration of  $\sim 6.0 \times 10^6$ /ml. Growth in the 400× and 200× dilutions resulted in a similar final cell concentration of around half compared to the media. On day 7 the 200 cell count was very high, higher even than in the media. The 600× dilution showed some growth but the cell count was never above  $1.5 \times 10^6$ /ml indicating insufficient nutrient availability for microalgae growth. It appears that the ideal concentration for cultivation of *Chlorella* in recovered process water lies between 200-400× dilution; there are sufficient nutrients available to support growth and the concentration of inhibitors is not too high. The results from the *Scenedesmus* growth trials are similar; highest cell count occurred for the media with  $2.2 \times 10^6$ /ml. The cell counts for

*Scenedesmus* are much lower due to their larger cell size compared to *Chlorella*. The highest cell concentration for *Scenedesmus* is only 20 % lower than in the media while the highest results for *Chlorella* is 40 % lower. Similarly to *Chlorella* the cell counts on day 7 are higher for the process water dilutions 400× and 600×. Best growth for both algae strains occurred at 400× dilution, but the cell counts of *Scenedesmus* were closer to the media than *Chlorella*. The second highest cell count in process water dilutions for *Scenedesmus* occurred in 600× while it was 200× for *Chlorella*. This suggests that *Scenedesmus* can cope with lower nutrient availability than *Chlorella*. At 200× dilution, *Scenedesmus* struggled to reproduce; an increase in cell count only occurred on the last sampling day indicating that the amount of inhibitors were too large to allow normal cell reproduction.



**Figure 8.3:** Growth of algae in process water dilutions of (a) *Chlorella* 350°C (b) *Scenedesmus* 350°C determined by cell count

Cultures were harvested at 11 and 12 days of growth, respectively for the cultures grown with the process waters from HTL conditions at 300°C and 350°C, centrifuged, dried in a desiccator and weighed to obtain a final biomass yield. The yield is compared to the yield in the respective standard medium and is presented in **Table 8.3**. Again the 300°C samples were investigated for 50×, 100× and 400× while the 350°C samples were grown in 50×, 200×, 400× and 600× dilutions of the original process water. The trials at 300°C led to a significantly higher final biomass concentration due to the higher amount of starting material used to inoculate the growth trials. The purpose of this section is however to compare the process water cultivation to the respective standard media growth. *Chlorogloeopsis* for which no growth data by absorbance is available showed growth in the 100× and 400× dilutions but no growth at the stronger 50× dilution. Again the amount of inhibitors such

as nickel, which is high in this case (**Table 8.2**), potentially inhibited the cells to reproduce. **Table 8.3** shows that at 100× dilution the total biomass production of *Chlorogloeopsis* is only a third compared to the standard medium. For the 400x dilution on the other hand, the yield is increased by a third compared to the media. This indicates that *Chlorogloeopsis* is able to use the organic carbon in the process water to grow mixotrophically. Mixotrophic growth can lead to higher biomass production compared to exclusively phototrophic growth [141]. It appears that the other cyanobacteria *Spirulina* is more sensitive to the growth inhibitors present, as there is no biomass production at the 100× dilution. The potential amount of growth inhibiting fatty acids could be quite high, as the TOC levels are very high for the *Spirulina* process water (**Table 8.2**). It is known that some fatty acids are dissolved in the process water; these are included in the TOC measurement and can act as inhibitors for microalgae growth [102]. **Table 4** shows that at 400× dilution the final growth is similar to the standard media at around 700 mg/l. Both these observations are confirmed by the absorbance data in **Figure 8.2 (a)**.

The process water from *Chlorella* processed at 300°C exhibits growth in all three dilutions investigated, indicating that *Chlorella* is less sensitive to potential growth inhibition. The growth is highest at 100× dilution, being only 15 % less than the 3N-BBM+V media. At the lower and higher dilutions the growth is similar, just under half of the media growth. The absorbance data in **Figure 8.2 (b)** shows the same trend. The growth trials of *Chlorella* and *Scenedesmus* using process waters from the 350°C HTL process were performed for 50×, 200×, 400× and 600× times dilution. Both microalgae strains were able to grow in all dilutions above 50×. It appears that the 50× dilutions are too concentrated for algal growth to occur. *Chlorella* was able to grow in the 50x dilution of 300°C process water but not in the 350°C process water. This is due to the considerably higher concentrations of TOC, phenols and Ni (**Table 8.2**). Additional nickel will leach into the process water from the reactor walls at more severe conditions. At 200× dilution, *Chlorella* was able to grow only about half the amount of cells compared to the media (**Figure 8.3 (a)**) but the final biomass yield was 15 mg/l higher. As shown with *Chlorogloeopsis* this indicates that mixotrophic growth is occurring leading to higher biomass yields. At the higher dilutions the biomass yield is only 60 wt.% and 40 wt.% compared to the standard media for 400× and 600× respectively. The cell count at 400× is actually higher than at 200× but the biomass yield lower, this is attributed to the fact that the TOC levels at 200× are higher leading to increased mixotrophic growth which in turn leads to increased biomass. The biomass yields of *Scenedesmus*, even though they are high in cell numbers are quite poor with a maximum of 48 mg/l at 400× dilution, compared to 117 mg/l for the standard media. This indicates that *Scenedesmus* is not able to use the organic carbon for

mixotrophic growth to the same extent as *Chlorella* and *Chlorogloeopsis*. Additionally the process water of *Scenedesmus* has very low acetate levels which can act as a substrate for mixotrophic growth. The authors acknowledge that the deviance in the data presented in **Table 8.3** is high which is most likely due to the small volumes and resulting mass of algae leading to high estimation of errors. Nevertheless the data presented generally fits with the growth curves in **Figure 8.2 & 8.3** and shows that higher biomass yields can be achieved than in the standard media.

**Table 8.3:** dry weights of harvested algae at the end of growth trials in dilutions of process water and standard media (mg/l)

	Process water dilutions for growth media					
	50×	100×	200×	400×	600×	Media*
<i>Chlorogloeopsis 300°C</i>	no growth	124 ± 10	NA	498 ± 99	NA	386
<i>Spirulina 300°C</i>	no growth	no growth	NA	657 ± 92	NA	706
<i>Chlorella 300°C</i>	449 ± 18	877 ± 280	NA	459 ± 78	NA	1020
<i>Chlorella 350°C</i>	no growth	NA	94 ± 19	47 ± 3	30 ± 3	79
<i>Scenedesmus 350°C</i>	no growth	NA	33 ± 2	48 ± 3	28 ± 1	117

NA = not analysed; \*no replicates carried out, process water trials carried out in duplicate

#### 8.3.4 Analysis of process water after cultivation

Following cultivation in the process water from HTL, the culture was centrifuged and the supernatant was re-analysed for the same nutrient parameters as before. Because *Spirulina* requires high bicarbonate (~15g/l) for growth, all *Spirulina* cultures were supplemented with NaHCO<sub>3</sub>. Due to the large amounts of Na, ion-exchange chromatography could not quantify the minor nutrients present with certainty. Due to this, the data is not presented for the growth trials of *Spirulina* 300°C process water. *Chlorogloeopsis* 50×, *Chlorella* 350°C 50× and *Scenedesmus* 50× data is also not presented as no growth occurred as shown in **Section 8.3.3**.



**Table 8.4** presents a summary of four nutrients at the point of inoculation and of the supernatant after harvest. The data shows that all strains are able to use  $\text{NH}_4^+$  as a source of nitrogen rather than nitrate as it is present in the media. This has previously been reported and is essential if nutrient recycling from HTL is considered, as most of the N is in the form of  $\text{NH}_4^+$  [148]. At the 200× dilution, practically all nutrients are consumed by *Chlorogloeopsis* resulting in the high growth observed in **Table 8.3**. Growth does not seem to be inhibited by a lack of  $\text{PO}_4^{3-}$  at this condition. At 100× the nutrient uptake appears to be significant for all four nutrients, especially acetate, which is readily consumed. From this it could have been expected that the final biomass yield would be slightly higher. *Chlorella* 300°C shows similar trends with  $\text{NH}_4^+$  and acetate readily consumed at all dilutions, especially at 400× dilution it is apparent that there were insufficient nutrients available for further growth. This is confirmed by the dip in cell production in **Figure 8.2(b)** after day 7 when the nutrients are all consumed. The data leads to the conclusion that the limiting nutrients for *Chlorella* are nitrogen and K. There is still  $\text{PO}_4^{3-}$  present after cultivation and acetate is not necessary, as *Chlorella* only consumes this in mixotrophic or heterotrophic growth. The uptake of nutrients for *Chlorella* 350°C is different to *Chlorella* 300°C, as there is no apparent limiting source of nutrients.  $\text{NH}_4^+$ , K and  $\text{PO}_4^{3-}$  are all still present in ample concentrations after cultivation although around half of the nutrients in each dilution have been consumed. Only acetate is entirely consumed which leads to the higher biomass yields presented in **Section 3.4**. From the nutrient uptake it cannot be determined why there is a fall in biomass productivity of *Chlorella* at the 200× dilution after day 7 (**Figure 8.3(a)**). *Scenedesmus* process water at 350°C is relatively low in acetate which could be the reason why a lower biomass yield is observed compared to *Chlorogloeopsis* and *Chlorella* which both readily used acetate as a substrate for mixotrophic growth. At 200× and 400× *Scenedesmus* seems to run out of nitrogen but K and  $\text{PO}_4^{3-}$  seem to be present in ample concentrations.

**Table 8.4:** Nutrient analysis of the culture medium before and after cultivation trials in different dilutions of process water. All units in mg/l, no replicates carried out

	<i>Media</i>	<i>Spent</i>	<i>Media</i>	<i>Spent</i>	<i>Media</i>	<i>Spent</i>	<i>Media</i>	<i>Spent</i>
<i>Chlorogloeopsis 300°C</i>	$NH_4^+$ (mg/l)		K (mg/l)		Acetate (mg/l)		$PO_4^{3-}$ (mg/l)	
100×	58.7	9.6	13.5	1.6	105.2	0.3	4.4	2.2
400×	30.4	0.4	4.3	0.2	21.5	0.8	0	0
<hr/>								
<i>Chlorella 300°C</i>								
50×	64.9	5.6	13	0.5	129.9	3.34	119.5	96.4
100×	53.1	0.9	11.8	0.3	32.2	1.49	54.6	45.3
400×	13.4	0	4.4	0.2	0	0	15.3	13
<hr/>								
<i>Chlorella 350°C</i>								
200×	28.4	18.4	7.3	3.3	20.5	0.9	8.3	2.5
400×	23.8	11.7	3.4	1.8	10.3	0	4.1	5.7
600×	15.9	8.2	2.3	1.1	5.7	0.8	7.5	4.1
<hr/>								
<i>Scenedesmus 350°C</i>								
200×	26.4	17	5.8	4.4	6.5	0	14	7.4
400×	13.2	0	2.9	2.5	3.2	0	4.1	3.7
600×	8.8	0	1.9	1.1	2.2	0.7	4.2	2.5

## 8.5 Conclusions

The water phase resulting from the HTL of microalgae was shown to be high in all required nutrients for algae growth, orders of magnitude higher than in standard growth media. Levels of nitrogen were shown to be 75-200 times higher compared to a standard BBM medium. TOC levels were in the range of 9000-15000 mg/l of which between 5 and 20 wt.% present as acetate. The growth trials in the recycled process water show that heavy dilution of the water phase is necessary

to avoid the effects of growth inhibitors such as phenols, fatty acids and nickel. All algae strains were able to grow in the recycled water but different optimum dilutions were observed. All strains were able to use acetate as a substrate for mixotrophic growth and  $\text{NH}_4^+$  as a source of nitrogen. *Chlorogloeopsis* at 400× and *Chlorella* 350°C at 200× dilutions achieved higher biomass yields than in their respective media probably by growing mixotrophically. The analysis of the spent water after cultivation showed that choosing the right dilution for each specific case is necessary to achieve optimum growing conditions. The analysis also revealed that the majority of acetate and ammonium were removed by algal growth. It was demonstrated that the optimum dilution is strain dependent but ranges between 200-400×. By recycling the organic carbon in the water phase both the carbon efficiency and the biomass yields can be improved. Recycling of nutrients from the HTL process water additionally decreases the financial strain on nutrient input for cultivation and the carbon footprint.

## 9. CHAPTER IX - Py-GC-MS for analysis of microalgae

### 9.1 Introduction

Microalgae have a vast range of applications in different industries. One of the most researched areas is currently the bio-fuels industry due to the ability of microalgae to produce lipids. Extracted lipids are most commonly converted to fatty acid methyl esters for bio-diesel production. Microalgal lipids also have applications within nutrition and health industries due to the high concentration of polyunsaturated fatty acids present. Polyunsaturated fatty acids are essential for human health and cannot be synthesized in the human body. In the nutritional industries, microalgae are also used as a source of high-value compounds such as proteins and pigments, particularly the carotenoids beta-carotene and astaxanthin. Microalgae are currently cultivated on a commercial scale for extraction of these compounds [22]. *Dunaliella salina* (19/30) and *Haematococcus pluviialis* are produced on a large scale for beta-carotene and astaxanthin production respectively [18].

Extraction and analysis of these compounds is a time-consuming process requiring specialist equipment. Pigment analysis is most commonly performed using HPLC following extraction with an organic solvent such as acetone. Proteins are often analysed by the J. Waterborge method [106] which involves the use of a folin reagent, subsequent absorbance measurements at 720 nm and comparison to a protein standard absorbance at this wavelength. Alternately, an approximation method using the elemental composition of microalgae and nitrogen conversion factor could be performed [113].

Total lipids are most commonly quantified by the Bligh-Dyer method, which involves extraction of lipids using a chloroform-methanol mixture and subsequent gravimetric quantification. The extracted lipids can be analysed directly by HPLC or by GC-MS analysis after transesterification to FAMES. Alternatively, a higher throughput technique for total lipids is the Red-Nile dye method which dyes lipids red, enabling spectrometric analysis. Total carbohydrates are commonly measured using a method developed by Sol M. Gerchakov, this involves hydrolysis using H<sub>2</sub>SO<sub>4</sub> with phenol being used as a colorimetric indicator for sugars [107]. Alternatively total carbohydrates can be determined by hydrolysis of the carbohydrates to mono-saccharides with subsequent analysis by HPLC [113].

All methods mentioned involve time-consuming sample preparation, dry feedstock and are specific to the analyte to be determined. This can pose problems as microalgae accumulate certain biochemical components at different stages of their growth, resulting in vast amounts of sampling and analyses. For example, lipid synthesis occurs during the growth period when nutrients, (particularly nitrogen) become depleted. The varying proportions of different biochemical components during the growth cycle are also accompanied with a change in growth rate, which must be taken into account when a maximum biomass harvest is desired. Once growth has stabilised this can be exploited to re-inoculate fresh cultures or the biomass can be harvested at this point. Furthermore it is desirable to know the proportion of the different biochemical components at any given time during growth to maximise recovery of specific components. The maximum amount of sought-after compounds usually does not correspond with the maximum cell density or growth rate.

Growth and accumulation of microalgae has a vast range of influences such as nutrient availability/composition, pH, light intensity, light cycle duration, temperature, mixing, CO<sub>2</sub>, and O<sub>2</sub> concentrations. When producing high-value compounds it is essential to optimise these conditions to achieve the highest yields. This remains true within bio-fuel production, however, in some applications, such as water remediation or algae production for hydrothermal processing, the nutrient removal and total biomass yield respectively, are more important.

When the biochemical composition of microalgae is of particular importance, a vast amount of analysis is required to identify different components at different growth conditions. This is usually a tremendously costly and time-consuming process. The aim of the current Chapter was to develop an analytical method for multiple biochemical components using a single, simple technique with minimal pre-treatment. Pyrolysis Gas Chromatography Mass Spectrometry (Py-GC-MS) was explored as a technique to rapidly estimate growth rates and identify the change in microalgae composition over time, in different media and varying growth conditions. Analytical pyrolysis has previously been used to study the seasonal variation of seaweed as a bioenergy feedstock by Adams et al. [46]. Marker compounds were assigned to carbohydrate, lipid, protein and phenolic origins of the macroalgae to enable qualitative comparison of the composition of macroalgae over its yearly growth cycle. A similar technique is explored in the current Chapter for microalgae.

## 9.2 Methodology

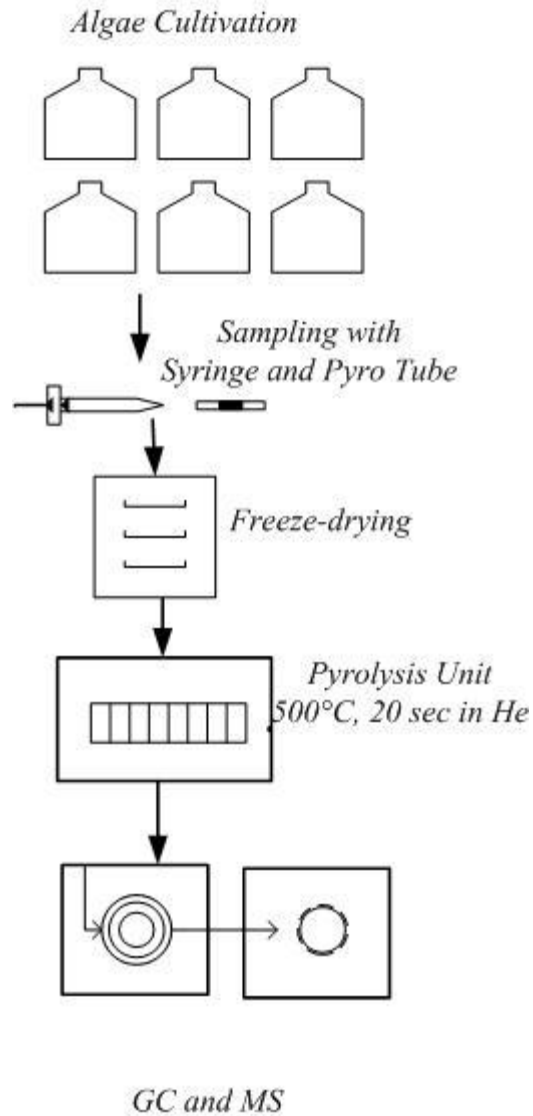
### 9.2.1 Sample preparation

Microalgae biomass samples were prepared for analysis using either a wet or dry method. For the dry method, quartz tubes of 25 mm length and 0.5 mm inner diameter were cleaned in the flame of a Bunsen burner. Quartz wool was packed inside one end of the tube and approximately 2-3 mg of sample placed inside the tube. Another piece of quartz wool was used to cap the top of the tube. The samples were pyrolysed as described in **Chapter 3** and weighed before and after analysis.

For the wet method the same quartz tubes were used. Tubes were half-filled with quartz wool and cleaned in a flame. A 10 ml syringe was used to collect microalgae cell culture directly from the growth flasks. An adapter, built in house, was used to filter the microalgae cells through the quartz wool. The quartz tube was subsequently freeze dried and weighed. From the difference in tube weight, before and after freeze-drying, a volumetric weight of microalgae per 10 ml could be calculated. This was used to determine the microalgae growth rates. **Figure 9.1** shows an image of the prepared tube before and after trapping of microalgae culture directly from the cultivation vessel. The effluent from the pyro tube did not show any visible traces of microalgae cells. The lyophilised sample was finally analysed by the dry Py-GC-MS method. A schematic of the wet method is presented in **Figure 9.2**.



**Figure 9.1:** Image of an empty pyro tube and a tube with trapped algae cells



**Figure 9.2:** Schematic methodology of the wet Py-GC-MS analysis technique.

### 9.2.2 Microalgae and growth trial analysis

For analysis of dry feedstock samples, microalgae were grown as specified in **Table 3.1** in **Chapter 3** unless stated otherwise. For growth trial analysis, samples of *Chlorella vulgaris*, *Botryococcus braunii* and *Haematococcus pluvialis* were grown in house with varying growth media. *Chlorella vulgaris* was grown in 500 ml conical flasks at 16 h light 8 h dark cycles. Growth in the media 3N-BBM+V, was compared to growth in dilutions of hydrothermal processing process water. Dilutions

of process water from hydrothermal gasification (HTG) of the same algae were performed at 50, 200 and 400 dilution. Trials were also carried out using 200, 300 and 400 times dilutions of the process water from hydrothermal liquefaction (as presented in **Chapter 8**). Samples were taken 12 days after inoculation of the cultures. *Botryococcus braunii* was grown in a 500 ml round bottom flask with the same lighting conditions as *Chlorella vulgaris* in a modified BBM+V media with half the nitrogen of the original recipe.

Wet samples were taken every other day for 25 days for *Botryococcus braunii*. *Haematococcus pluvialis* was grown in 3N-BBM+V media and compared to 3N-BBM+V media with 0.25 g/l acetate and a media containing 0.15 g/l NaNO<sub>3</sub> instead of 0.75 g/l as in the 3N recipe. *Navicula sp.* was grown in an unknown growth media with varying silicate concentrations: 100%, 50% and 25% its original value. Samples were collected after 10, 13 and 15 days for the 100% Si sample and after 10 days for the others. All *Navicula sp.* growth trials were conducted at the University of Sheffield, UK.

Model compounds to simulate the different biochemical components included bovine serum albumin, starch, palmitic acid, beta-carotene and astaxanthin and were purchased from Sigma-Aldrich. Chlorophyll *a* was extracted from commercially available fresh spinach. Approximately 100 g of spinach was mixed vigorously for 30 min in 90% acetone and filtered, acetone and water was left to evaporate and the separate chlorophyll *a* (green) and chlorophyll *b* (yellow) layers on the side of the beaker were collected.

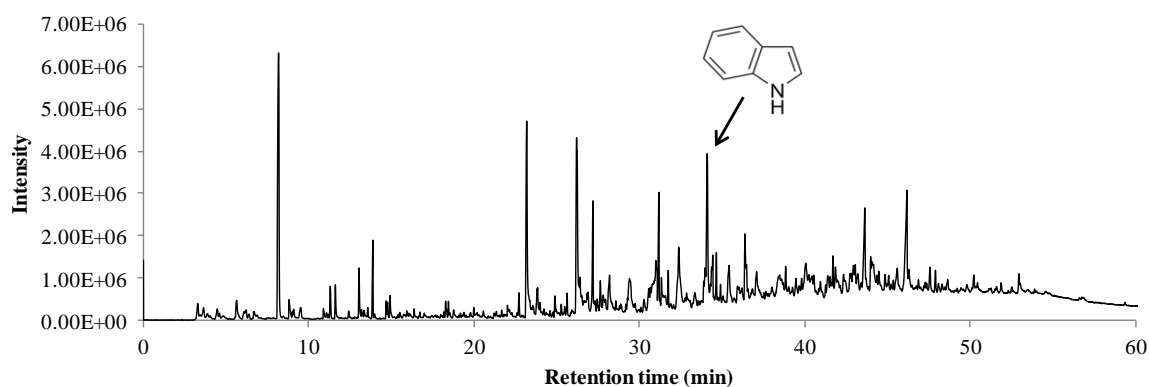
## 9.3 Results

### 9.3.1 Py-GC-MS of Model Compounds

Model compounds were pyrolysed at 500°C and the chromatograms were investigated to identify unique pyrolysis marker compounds. Peaks specific to model compounds, which did not appear on chromatograms of other compounds, were selected. These peaks were subsequently identified in the chromatograms of microalgae. By comparing peak sizes of the unique marker compounds, the amount of each respective model compound present in the microalgae samples could be calculated.



The chromatogram of the pyrolysis products from bovine serum is plotted in **Figure 9.3**. The marker compound selected to represent the protein fraction from microalgae is indole. This was selected as it was not found in any other of the structural model compounds identified and had a relatively large peak area in the pyrolysis chromatogram. The total percentage area of the indole peak is 3.86 %, and as an absolute value was found to be  $15.4 \times 10^7$  / mg sample of protein. Toluene was also found to be a major product of bovine serum pyrolysis but this compound was also detected as a pyrolysis product of pigments.

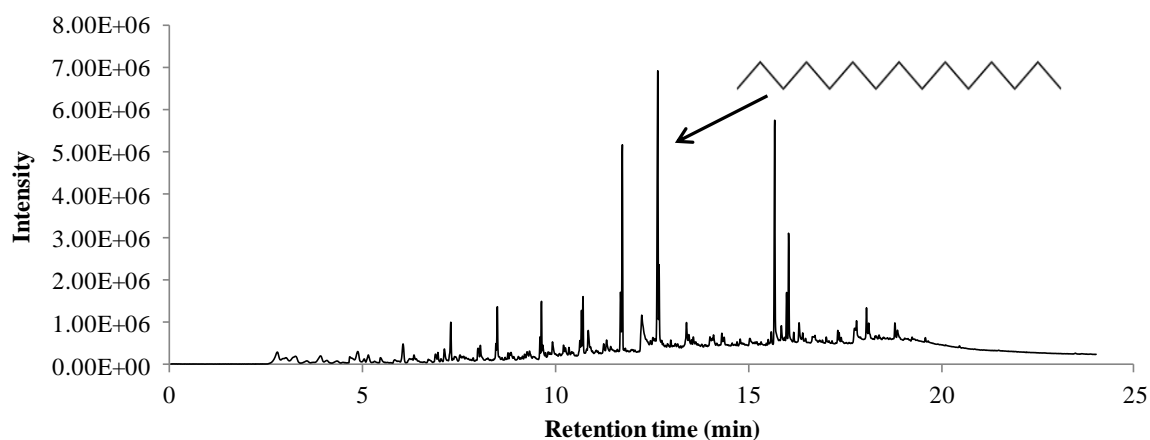


**Figure 9.3:** Total ion chromatogram of bovine serum at 500°C

Palmitic acid (C16:0) is the most abundant fatty acid in nature and was chosen as a model compound for microalgal lipids. Its pyrolysis chromatogram is plotted in **Figure 9.4** with a faster GC oven ramp rate used for this specific chromatogram. Nevertheless the compound could be identified with a high degree of certainty from its mass spec and was found in the chromatograms of microalgae at the standard GC oven ramp rate. Using palmitic acid is an oversimplification as the fatty acid profiles of microalgae lipids are much more complex than a single fatty acid. The majority of lipids are typically present as triglycerides and some free fatty acids as discussed in **Chapter 6**. Sunflower oil and palm oil were additionally pyrolysed to compare pyrolysis products from triglycerides and fatty acids. The main products detected from both types of lipid were alkanes. Pyrolysis of a fatty acid with a particular chain length led to the formation of alkanes with varying chain lengths. Most alkanes detected in chromatograms were consistently one carbon link shorter than the original fatty acid. Alkanes with 2 or 3 fewer carbon links were also found in decreasing quantity as can be seen in **Figure 9.4**.

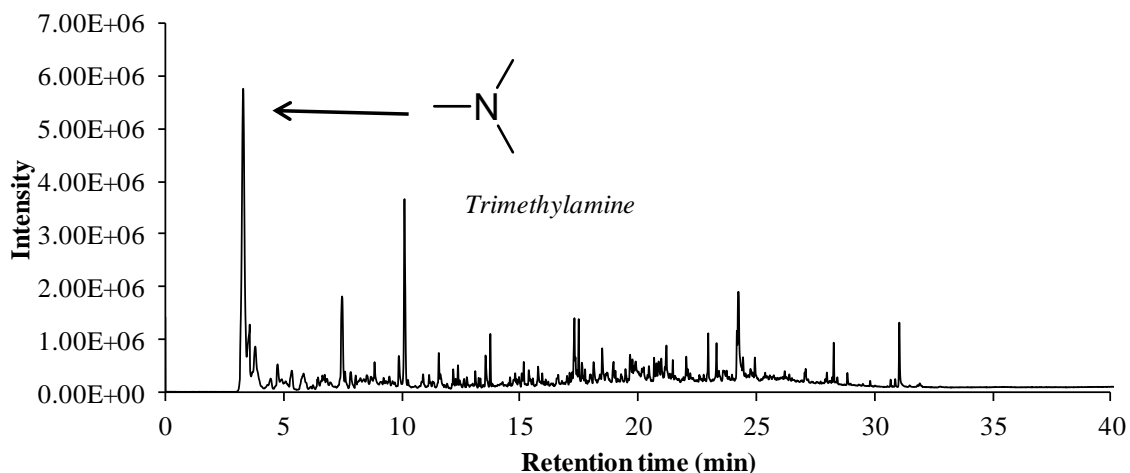
The quantification of respective fatty acid chain lengths was, therefore, extremely difficult. An assumption was made to estimate the lipid content of the microalgae biomass. The quantification of

a certain alkane enabled the abundance of the next longer chain length fatty acid present in the microalgae to be approximated. The chain length chosen for this approximation was microalgae strain-specific and typically the most abundant alkane was chosen for the calculations. A drawback of this approach is that pigments can also produce alkanes at the pyrolysis conditions used, although they are produced in much lower concentrations than those derived from lipids. The approximation is therefore not fully quantitative but provides a reasonable estimation of the lipid content of algae.



**Figure 9.4:** Total ion chromatogram of the model lipid compound palmitic acid.

The standard used for determining chlorophyll *a* content in algae was prepared from spinach. The most abundant compound identified was *di-methyl-Methylamine*. Its peak area was quantified as 38.1 % of the total chromatogram. Assuming a high-purity chlorophyll extract, this corresponds to an absolute area of *di-methyl-Methylamine* to chlorophyll *a* of  $7.3 \times 10^8$  / mg. The chromatogram of chlorophyll *a* is plotted in **Figure 9.5**.



**Figure 9.5:** Total ion chromatogram of the Chlorophyll *a* extract.

For the analysis of carbohydrates, starch was used as a model compound. This is again a simplification for total microalgae carbohydrates as not all microalgae carbohydrates are starch. Carbohydrates in microalgae serve two main functions: as a structural component of the cell wall and as storage carbohydrates for energy. Carbohydrates are made up of varying components including simple sugars (mono-saccharides) and their polymers (di- and poly-saccharides). Different algal species tend to accumulate different types of carbohydrates. Cyanobacteria mainly synthesize glycogen ( $\alpha$ -1,4 linked glucans), red algae synthesize floridean starch (hybrid of starch and glycogen) and green algae synthesize amylopectin-like polysaccharides (starch) [149]. This leads to a different profile of mono-saccharides when hydrolysed carbohydrates are analysed. The most abundant sugars found in algae are glucose, rhamnose, xylose and mannose [149]. There are typically also small amounts of cellulose and alginates present, therefore, using starch as a model compound for total microalgal carbohydrates likely leads to an underestimation.

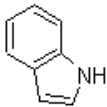
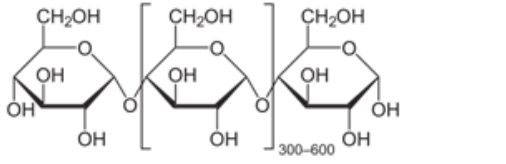
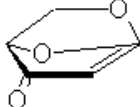
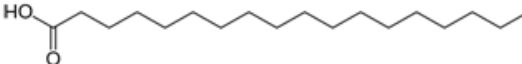

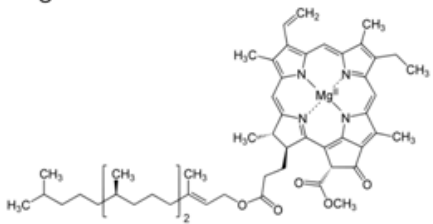
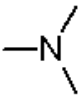
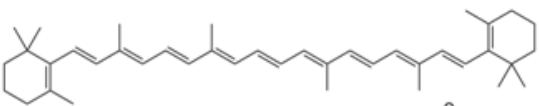
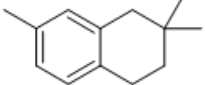
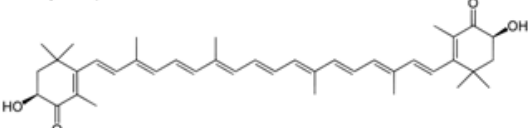
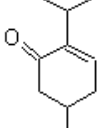
The determination of a marker compound for starch proved to be difficult. The potential marker compounds identified were not always detected in the chromatograms of algae where carbohydrate pyrolysis products were expected. These expectations stemmed from the total carbohydrate analysis by the Sol M. Gerchakov method in **Chapter 3**. Levoglucosenone was chosen as a marker compound as it was found in the majority of microalgae samples and not in any other model compounds investigated. Furfural and 1,2 cyclopentanedione were also likely candidates but could not be identified in all strains investigated. Further work is required to investigate the different carbohydrates present in microalgae. This will be carried out by pyrolysing additional carbohydrate standards, monosaccharides and polysaccharides. The pyrolysis products will then be compared to

microalgae with different carbohydrate profiles. It is hypothesised that hydrolysis of the microalgae carbohydrates and subsequent analysis by HPLC to determine the proportions of each monosaccharide will help to identify the carbohydrate-derived pyrolysis products. In the current work, levoglucosenone was chosen as the marker compound for carbohydrates as it had the best correlation with the actual carbohydrate content of the microalgae samples.

Following analyses of the main biochemical components, additional standards were analysed to identify compounds of high commercial value. These included the pigments beta-carotene and astaxanthin, as they are extracted from microalgae on a commercial scale due to their health benefits. Concentrations of these pigments in microalgae are typically much lower than the structural biochemical components such as lipids, protein and carbohydrates.

Beta-carotene was pyrolysed and the marker compound identified was tetrahydro-trimethyl-Naphthalene. The structure of the carotenoid, beta-carotene, is very similar to other carotenoids commonly found in microalgae such as lutein, zeaxanthin or astaxanthin. Unfortunately, a standard for lutein or other carotenoids was not available. Therefore the potential of overestimating this compound is present. It was, however, possible to identify a different marker compound for the other carotenoid, astaxanthin. 5-Methyl-2-(1-methylethyl)-2-cyclohexen-1-one was identified as the marker compound for astaxanthin. Further work is required to determine the validity of these assumptions. Ideally, all pigments typically found in microalgae should be pyrolysed and the pyrolysis fragments investigated. For the current work the assumptions are justifiable as the algae strains analysed are typically high in these specific pigments and have negligible amounts of other carotenoids. This was confirmed by HPLC pigment analysis as shown in **Chapter 4** and the data sheets in **APPENDIX A**. A summary of the marker compounds, their structure and origin is presented in **Table 9.1**.

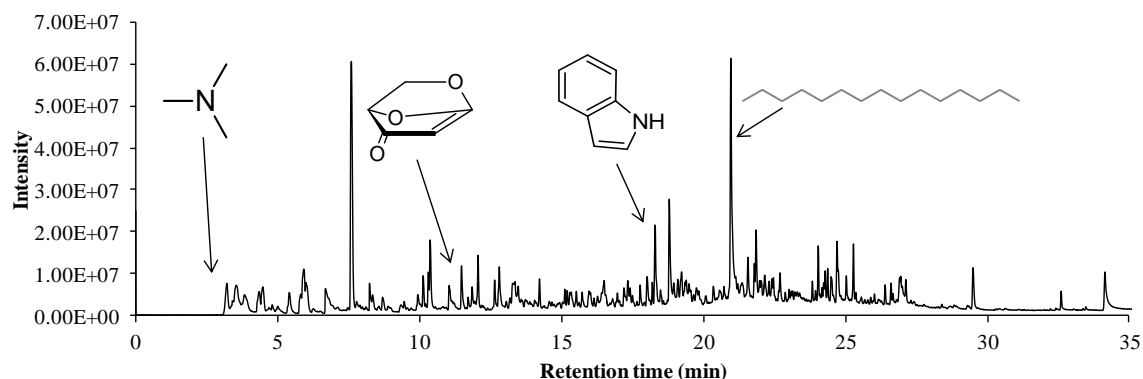
**Table 9.1:** Pyrolysis marker compounds identified from pyrolysis of microalgae model compounds.

Biochemical Component		Pyrolysis marker compound	
Name	Structure	Name	Structure
Protein	not available	Indole	
Starch		Levoglucosenone	
Lipid		Alkanes	
Chlorophyll a		Trimethylamine	
Beta carotene		Tetrahydro-trimethyl-Naphthalene	
Astaxanthin		5-Methyl-2-(1-methylethyl)-2-cyclohexen-1-one	

### 9.3.2 Py-GC-MS of microalgae

**Figure 9.6** shows a typical chromatogram of microalgae. Specifically, the plot shows the chromatogram of *Chlorella vulgaris* grown in 3N-BBM media, pyrolysed at 500°C. The four main marker compounds, previously identified from model compounds, are indicated. Marker compound peaks appear considerably smaller for microalgae compared to the respective model compound chromatograms. The areas of marker compound peaks were calculated as an absolute area by dividing peak area by the mass of sample pyrolysed. These area/mg values are then compared to other samples allowing comparison of specific compound concentrations. The most accurate results are obtained when different samples of one strain are compared to each other rather than comparing different strains. This is due to the variance in carbohydrate, lipid and amino acid composition of different microalgae strains which can potentially affect the pyrolysis behaviour. The change in

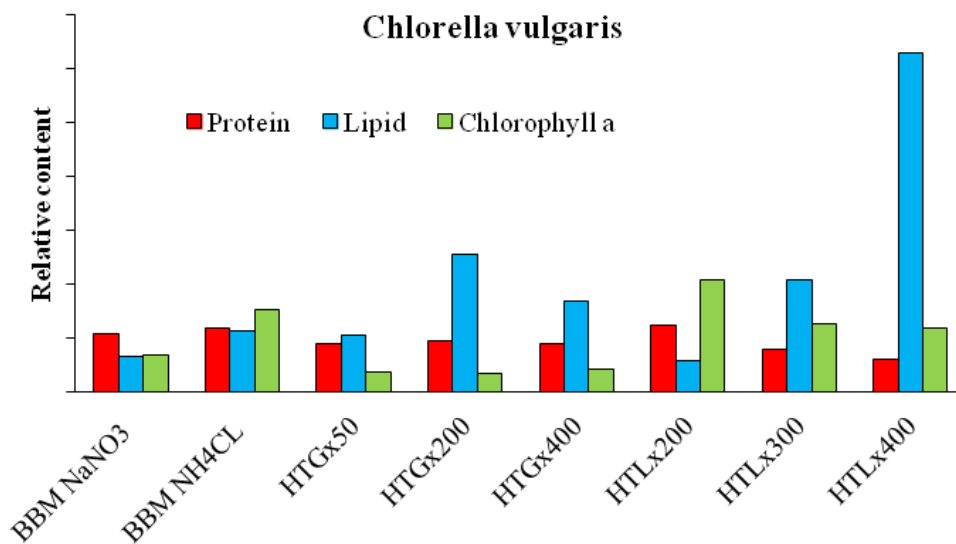
pyrolysis chromatograms of different algae strains becomes apparent when observing the chromatograms plotted in **Chapter 4** and for each algae strain in the data sheets in **APPENDIX A**.



**Figure 9.6:** Chromatogram of *Chlorella vulgaris* with marker compounds indicated.

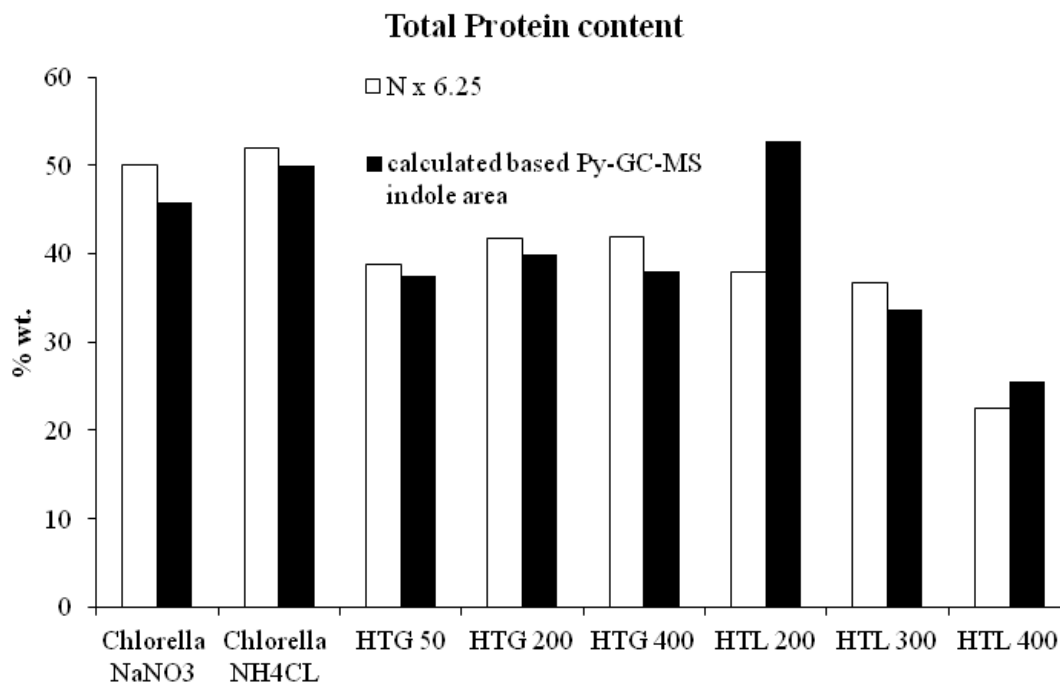
A total of eight samples of *Chlorella vulgaris* were prepared in different growth media. Two standard 3-N-BBM+V media were prepared using nitrogen sources,  $\text{NaNO}_3$  and  $\text{NH}_4\text{Cl}$ . Three samples were grown in the recovered process water from hydrothermal gasification, in dilutions of 50, 200 and 400 times the original volume. The hydrothermal gasification experiments were carried out purely for the purpose of producing process waters to grow and analyse algae from different growing condition. Additionally, three dilutions of process water from hydrothermal liquefaction were set up in dilutions of 200, 300 and 400 $\times$ . Each sample was investigated for chlorophyll *a*, total protein and lipid content. **Figure 9.7** shows that the protein content is highest for samples with the lowest lipid contents. In this case, the lowest lipid contents are observed for the two standard media and the HTL 200 $\times$  sample. This is due to the high concentration of nitrogen in these growth media. It is known that high nitrogen levels lead to low lipid and high protein accumulation in microalgae [150-151]. The lipid content of the algae was highest in the HTL 400 $\times$  dilution process water, representing the media with the lowest nitrogen levels, which led to nitrogen starvation of the algae. The second highest lipid concentration was found in the HTG 200 $\times$  sample, representing another low nitrogen containing media. The reason for the lower lipid level at the 400 $\times$  HTG dilution is unclear; however the trend of nitrogen in the water and lipid levels observed fits well for the remaining samples. The actual lipid content was not measured but the results are in agreement with expectations based on literature. The chlorophyll *a* levels were found to be high in the  $\text{NH}_4\text{Cl}$  and

HTL 200× sample. Chlorophyll *a* levels were not confirmed for these samples by HPLC but visual inspection of the freeze dried algae confirmed the observed trends. Further work is required to validate the data presented in **Figure 9.7** by comparing the observations to results from traditional analysis methods. The data presented is only plotted at relative levels and a full quantitative analysis would be desirable. The lipid data requires validation by either the Bligh-Dyer extraction or Red-Nile lipid staining method. The chlorophyll *a* concentrations can be confirmed via HPLC.



**Figure 9.7:** Calculated protein, lipid and chlorophyll *a* content of *Chlorella* strains grown in different dilutions of process water from HTL/HTG.

The protein contents plotted in **Figure 9.7** are on a relative scale. Quantitative protein contents of microalgae were calculated using the area/mg peak observed for the pure protein sample. The results are plotted in **Figure 9.8** and compared to the protein content calculated using the nitrogen conversion factor 6.25. This is a common method in biochemical analysis of microalgae [113]. The results show that the trend of calculated protein contents, based on the pyrolysis product indole agrees well with the standard method. Apart from sample HTL 200×, there is a 5% deviation for all results. The discrepancy for this sample is unknown but could be due to measurement or sample handling errors. Further work is required to fully confirm the current method; a number of replicate analyses and comparison to protein analysis by the Waterborg method are expected to achieve this.

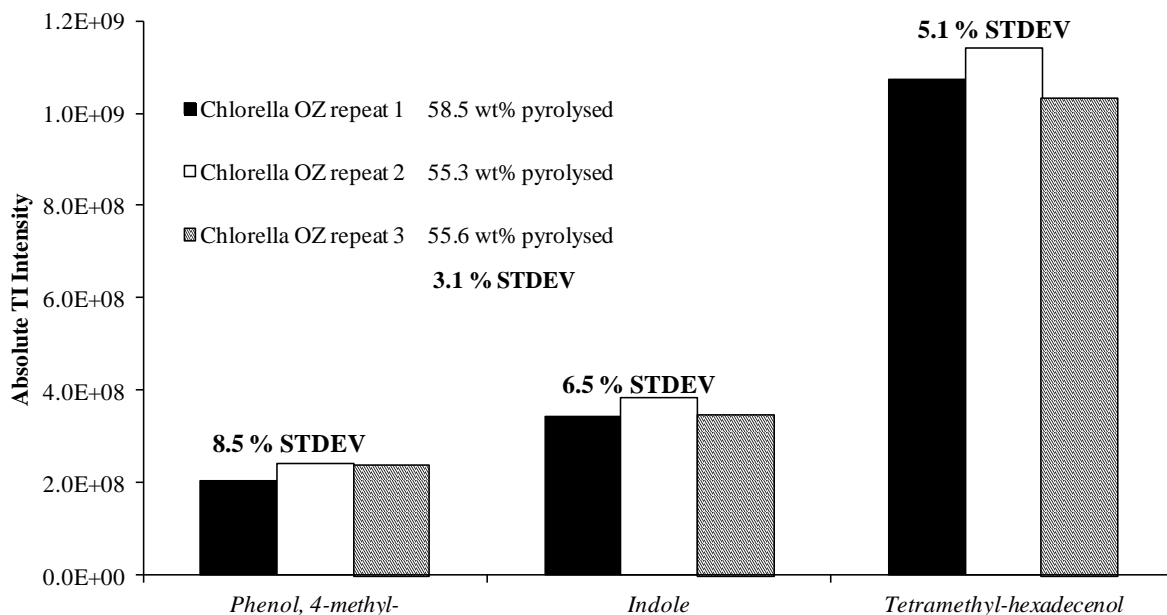


**Figure 9.8:** Protein content of the different *Chlorella* strains by analysis of *Indole* peak areas and by the nitrogen to protein conversion factor of 6.25.

For the majority of analyses in this Chapter each sample was only pyrolysed once since a limited amount of sample was available. To investigate the variability of the pyrolysis procedure a bulk sample of *Chlorella OZ* was pyrolysed three times at identical conditions. **Figure 9.9** shows a plot of three selected peaks repeated in triplicate. A representative peak for the carbohydrate, protein and lipid fraction was chosen to demonstrate the experimental variability of the different biochemical components. Phenol, 4-methyl represents the carbohydrate fraction and is shown to have a percentage deviation of 8.5 %. Errors are expected to be introduced mainly from sample handling and weighing. The protein representative peak, Indole, was detected with a deviation of 6.5 % and the lipid peak Tetramethyl-hexadecanol with 5.1 %. On average of the three compounds this results in a standard deviation of 6.7 %. It is expected that other analysis presented in the current Chapter fall approximately in this margin of error. Additional work is required to investigate if different algae samples result in higher or lower deviations. The value of 6.7 % is in a similar range of the protein analysis deviation presented in **Figure 9.8**. The amount of sample pyrolysed for each repeat was calculated and is presented in **Figure 9.9**. An average of 56.5 wt.% of the microalgae sample was pyrolysed which was achieved with a deviation of 3.1%. Since this value is lower than the deviation of the peak areas it could be that the samples were not entirely homogeneous.



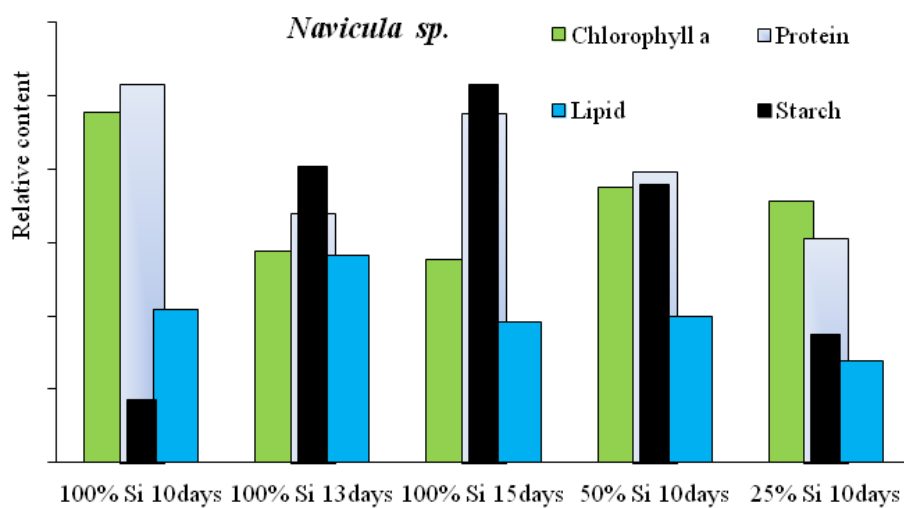
Nevertheless the standard deviations presented are in an acceptable range for the objectives of the current work where the main aim is to see differences between samples rather than full quantitative values.



**Figure 9.9:** Peak areas and percentage standard deviation of three peaks of triplicate repeats of *Chlorella OZ* pyrolysis products.

A strain of *Navicula* was grown at the University of Sheffield in varying concentrations of silicate (100%, 50% and 25 % Si) for 10 days. Additionally, the 100% silicate samples were also harvested after 13 and 15 days. *Navicula* is a diatom which requires silicate for its growth. The results presented in **Figure 9.10** show that decreasing silicate levels lead to a decrease in protein and starch content and an increase in chlorophyll *a* content. The lipid content does not appear to be influenced by Si concentrations of 50% but a decrease is observed at 25%. At 100% Si concentrations, longer cultivation periods led to a decrease of chlorophyll *a* content and an increase in starch content. The lipid content increased at 13 days but a further two days of growth led to lower lipid levels than present after 10 days. The protein content decreased from 10 to 13 days and increased back to the original value after 15 days. CHNS analysis and the nitrogen to protein conversion factor confirm these trends of protein levels from Py-GC-MS analysis (see **Table 9.2**). The lipid and starch contents cannot currently be confirmed as these analyses are still outstanding. The chlorophyll *a* data is confirmed by visual inspection of the different cells as presented in **Figure 9.11**. The results from **Figure 9.7** and **9.10** demonstrate how the novel Py-GC-MS technique can be a powerful method to quickly determine the change in biochemical composition when different culture

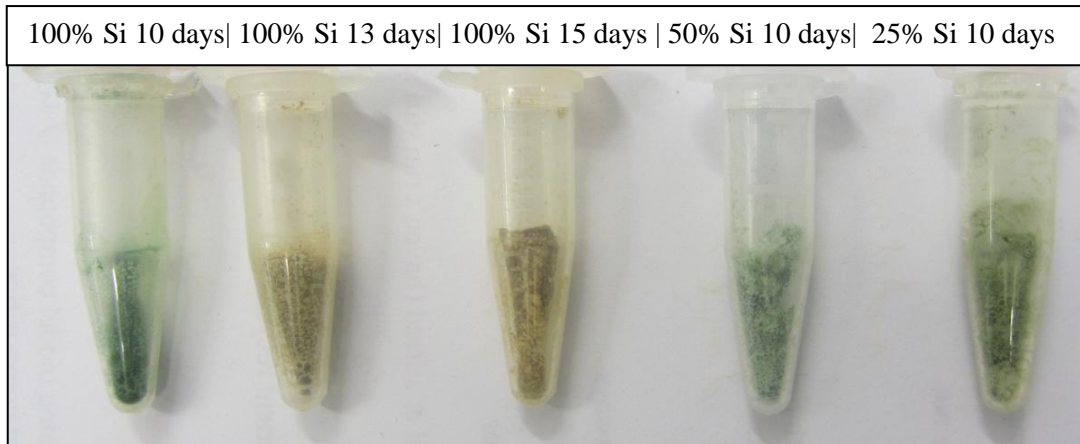
conditions are used. Additional work is required to validate the different parameters and allow fully quantitative analysis.



**Figure 9.10:** Py-GC-MS analysis of *Navicula sp.* strains for Chlorophyll a, protein, lipid and starch grown in different concentration of silicate.

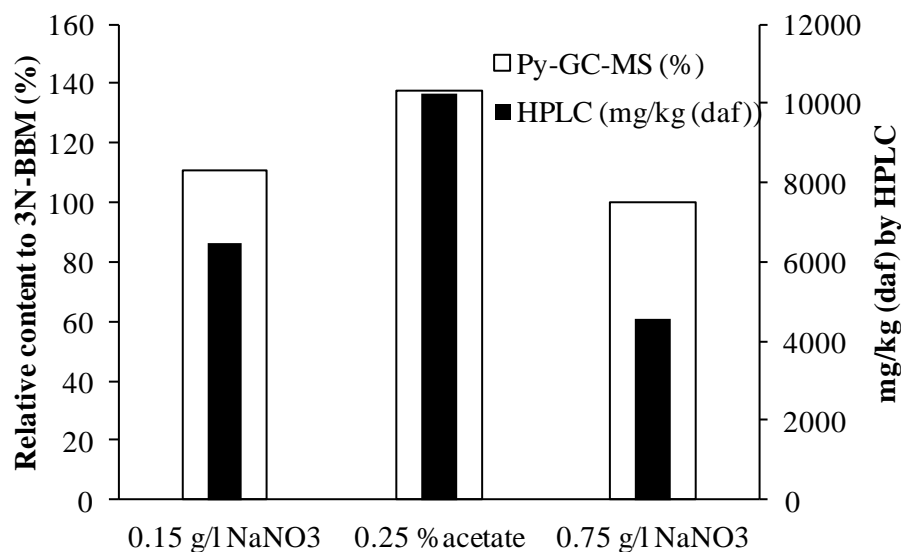
**Table 9.2:** Elemental Analysis of *Navicula sp.* strains.

Condition	% (wt. daf)			
	C	H	N	O
<i>100% Si 10 days</i>	31.3	5.0	4.6	59.1
<i>100% Si 13 days</i>	31.6	5.2	3.0	60.2
<i>100% 15 days</i>	32.3	5.2	3.1	59.5
<i>50% Si 10 days</i>	21.5	3.8	3.1	71.6
<i>25% Si 10 days</i>	30.6	5.1	2.5	61.8



**Figure 9.11:** Photograph of *Navicula sp.* grown in 100% silicate for 10 days, 13 days, 15 days, 50% silicate 10 days and 25 % silicate 10 days.

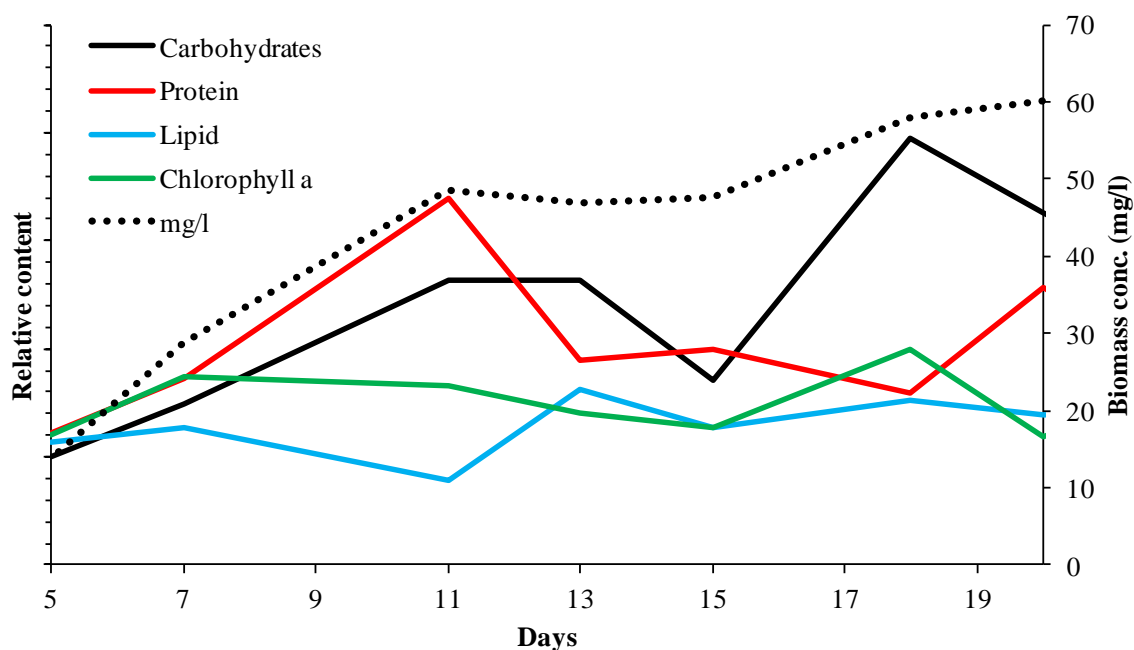
The astaxanthin content of *Haematococcus* was determined in 3N-BBM media and compared to BBM with reduced N levels and BBM with added acetate. The results show that the astaxanthin levels increased when nitrogen content was reduced and acetate added as a substrate for mixotrophic growth. This effect has previously been reported in a study by Choi et al. [152]. The results based on Py-GC-MS show that the astaxanthin content increases by 10% when the culture is subjected to reduced nitrogen concentrations compared to the standard media. Introducing acetate led to an increase of 38 % astaxanthin content in *Haematococcus*. The results based on the peak area of 5-Methyl-2-(1-methylethyl)-2-cyclohexen-1-one by Py-GC-MS of the different strains were compared to the conventional astaxanthin determination method based on HPLC. **Figure 9.12** shows the same general trend, however, slight differences between the methods are observed. The increase under reduced nitrogen conditions, based on HPLC, is found to be 30% compared to 10 % by Py-GC-MS. The acetate-doped media led to a 55% increase in astaxanthin compared to a 38% increase observed using the novel analysis method. Although there are differences in the absolute values measured between the two methods, the general trend is the same. This is significant in this kind of analysis, when quick screening of different growth conditions is required with small sample amounts available. Furthermore, the novel method allows simultaneous analysis of protein, carbohydrates, protein, lipids and chlorophyll *a* content. The HPLC method requires at least 200 mg of dry sample, involves organic solvent extraction and subsequent analysis by HPLC. This results in a labour intensive process and necessitates larger cultivation trials to achieve the required sample mass.



**Figure 9.12:** Astaxanthin levels detected in *Haematococcus pluvialis* grown in different media by Py-GC-MS and HPLC.

*Botryococcus braunii* was grown for 20 days in BBM+V with half the nitrogen content of the original recipe. Samples were taken every other day using the custom built sampling system described in **Section 9.2.1**. The samples were freeze-dried and the growth of the microalgae estimated on a mass/volumetric basis by weighing the mass trapped in the filtering system. Approximately 0.1 mg of sample was sufficient to obtain a high-resolution chromatogram when the GC system was set up for splitless injection. Chromatograms obtained every two days allowed an estimation of the biochemical composition of the microalgae over its growth cycle which is plotted in **Figure 9.13** with the total biomass concentration. As anticipated, the growth is highest in the initial 5-6 days of sampling when exponential growth is typical. The growth starts levelling off at around 12 days and a slight increase observed towards the end of the growth cycle. The biochemical composition was monitored over the growth cycle and showed a decrease in lipid content during the high-growth phase. When growth slowed down, the lipid content increased, most likely due to nitrogen limitation in the growth media. During the strong growth period, the protein content initially increases but reduces as lipid content rises. Towards the end of the cycle, an increase of protein content was observed. The carbohydrate content shows a similar trend to the protein content with a slight lag of around 2 days. Near the end of the experiment, the carbohydrate content increased significantly, most likely due to accumulation of storage carbohydrates as a result of low nutrient availability.

The method proposed in this Chapter enables the determination of an optimum harvest time for recovery of desired microalgal components. If the aim is to recover the maximum amount of lipids and least protein, as is likely in biofuel applications, day 13 would be ideal as the lipid content is highest and the nitrogen content low. If a high protein feedstock is required, the microalgae should be harvested two days earlier when the protein content is at its maximum. The current example demonstrates the exceptional potential of the new method to determine full biochemical analysis of microalgae over its growth cycle, reducing capital cost, sample preparation, analysis time and allows for smaller growth trials.



**Figure 9.13:** Analysis of *B. braunii* grown in  $\frac{1}{2}$  N BBM+V media over 20 days by Py-GC-MS.

## 9.4 Conclusions

By pyrolysing model compounds, unique marker compounds for biochemical components could be identified using GC-MS. The marker compounds were subsequently detected in chromatograms of microalgae and concentrations calculated based on absolute peak areas. Py-GC-MS of *Chlorella vulgaris*, grown in process water dilutions from HT processing, demonstrated the method's ability to determine protein, lipid and chlorophyll *a* levels. The calculated protein content was compared to the actual protein content and results were within 5 % discrepancy. Chlorophyll *a* levels were

determined semi-quantitatively but visual inspection confirmed results for both *Chlorella* and *Navicula*. The results for lipid and carbohydrate content of the microalgae strains are in agreement with expectations based on published literature. Further work is required to fully validate the method for lipids and carbohydrates. The method was shown to be suitable for high value compounds such as astaxanthin. It is likely that the method could be applied to a wide range of microalgal compounds but further work is required to identify suitable marker compounds.

The proposed novel sampling method is a unique way to assess microalgal growth and composition for optimum harvest times for various applications. The technique can simultaneously determine the concentration of the three main biochemical complements, lipids, carbohydrates and proteins. Furthermore, levels of chlorophyll *a*, beta-carotene and astaxanthin could be detected in the same analysis. Traditional analytical methods would require separate measurements of each analyte and involve pre-treatment and extraction steps, therefore, the proposed method could reduce analysis time and costs associated with investigations into microalgae growth.

## 10. CHAPTER X - HTL Reactor Systems

### 10.1 Introduction

Most of the research on HTL has been performed in batch reactors as demonstrated in **Chapter 5, 6, and 7**. However, continuous operation is required in order to make the bio-crude production process more economically feasible and chemically controllable. Heat recovery from a continuous process enhances the overall energy efficiency. Some researchers have studied HTL on continuous or semi-continuous reaction systems for simple water soluble monosaccharide model compounds such as glucose [136, 153]. However, only a small number of reports of continuous HTL biomass reaction systems have been published, these reports deal with lignocellulosic feedstocks and do not include aquatic biomass. Hammerschmidt et al. [154] investigated the hydrothermal processing of food sludge feedstocks with solid concentrations of 6.5, 7.7 and 12 wt.%. A homogeneous potassium carbonate and heterogeneous zirconium oxide catalysts were used at processing temperatures of up to 350°C and residence times of 5-10 minutes in a 0.11 continuous reactor. Makishima et al. [155] investigated the hemicellulose fraction recovered from corn cob in a continuous HTL reactor at 200°C for 10 minutes, up to 15 wt.% solid concentration. Ocfemia et al. [156] processed swine manure in a continuous HTL reactor with a throughput of 48 kg manure slurry per day. At a processing temperature of 305°C and a residence time of 80 minutes, a bio-oil with a HHV of 31 MJ/kg could be produced. The reactor was successfully operated for 16 hours continuously.

Batch HTL of microalgae is relatively well-studied and has received increased interest in recent years. Most studies use small 10-1000 ml batch reaction vessels with slow heating rates and long residence times (~1 hour) such as those presented in **Chapters 5-7**. The results show that a high quality bio-crude suitable for further refining can be produced with a similar nature to petroleum crude oil. Typically, bio-crude yields of around 30 wt.% (daf) are obtained with HHVs of 30-35 MJ/kg. Typical slurry solid concentrations of the batch experiments carried out on microalgae vary from 5-50 wt.%. The higher the solids content the more efficient the energy recovery becomes as the ratio of water heated compared to biomass decreases.

The aim of the current Chapter is to demonstrate, at pilot scale, the technical feasibility of continuous HTL processing of microalgae. Two strains of microalgae were studied in steady flow under a range of conditions and the process performance and products are discussed.

## 10.2 Methodology

The strains of *Chlorella OZ* and *Spirulina OZ* were used in the current Chapter. The methodology concerning the continuous HTL plant is described in **Chapter 3**. The characterization of the microalgae strain can be found in **APPENDIX A** but significant parameters influencing the experiments are also presented in this Chapter. The sample work up and analysis procedures are covered in **Chapter 3**.

## 10.3 Continuous reactor HTL

The experimental work on the continuous flow hydrothermal reactor was carried out at the University of Sydney, Australia as a collaborative effort as part of the World University Network Program. A detailed description of the reactor design is provided in **Chapter 3, Section 3.2.3**. In brief, the reactor consisted of a coiled 2 l volume Swagelok piped reactor within a heated fluidised sand bath. The flow rates were adjusted from 15-30 l/hour leading to residence times within the reactor of 3 to 5 min at temperatures of 250 to 350°C. Residence times could not be increased beyond 5 min due to the design of the reactor. The initial work only investigated microalgae slurry concentrations of 1 %wt. for *Chlorella OZ* and *Spirulina OZ*. On-going work will also include the investigation of higher solids loading, one initial results from processing at 10 wt.% slurry is included in **Section 10.4**.

### 10.3.1 Microalgae Feedstock Analysis

The feedstocks investigated were two commercially available microalgae, *Chlorella* and *Spirulina*. The analysis of the feedstock is presented in **Table 10.1**; the biochemical composition was provided by the supplier, all other data was analysed in the laboratory. Both strains had similar ash (<8 wt.%) and moisture (<6 wt.%) contents, those of *Spirulina* being marginally higher. The HHV of the algal biomass was in the range of 24-25 MJ/Kg; *Chlorella* contains slightly higher amounts of oxygen (27.5 wt.%) and lower levels of carbon and hydrogen leading to a lower HHV. The lipid contents of both strains are low (<10 wt.%) as the microalgae were grown as food supplements rich in protein rather than as feedstocks for biofuels (for which a higher lipid content is beneficial). As presented in



**Table 10.1**, the protein content of the microalgae was in the range of 42-68 wt.%, *Spirulina* contained a larger fraction of protein leading to the higher nitrogen content of 12.1 wt.%.

Metal analysis by ICP shows the main constituents of the ash fraction to be K, Mg and Ca. The presence of potassium has been reported to be significant, as it can be used as a catalyst in hydrothermal media. For example, potassium carbonate can result in lower solid residue when processing wood in HTL, [157] while potassium hydroxide can increase water-gas shift reactions during hydrothermal gasification [158]. K, Fe and Mg are also minor nutrients required for microalgae growth, hence in order to recycle the process water post HTL for algae cultivation, it is desirable that these nutrients report to the water phase. Nickel on the other hand, also present in the algal biomass and possibly deriving via leaching from reactor walls during HTL [144], acts as a growth inhibitor and therefore needs to be considered.

The chloride content was also measured. Chloride poses a risk to pressure vessels constructed from austenitic stainless steels under HTL conditions because of the possible occurrence of chloride stress corrosion cracking, even at ppm levels of the ion. It is monitored routinely at the pilot plant facility as part of the University of Sydney's materials evaluation protocol – it is expected that the choice of reactor material will be especially important when processing marine algal strains because of the high chloride loading that will arise.

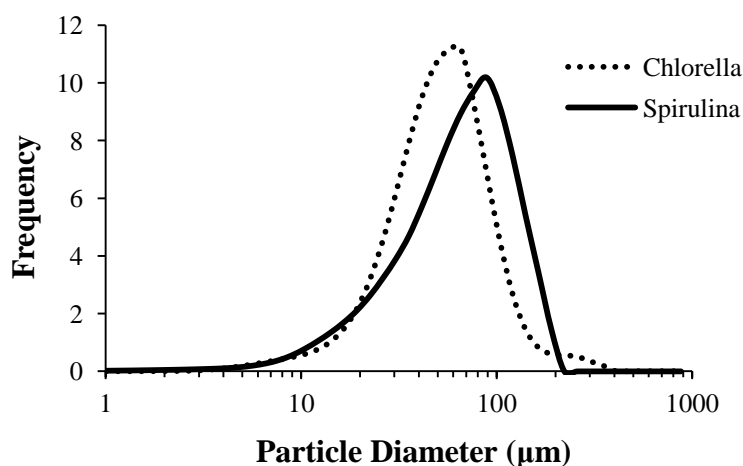
**Table 10.1:** Analysis of microalgae feedstock.

	<i>Chlorella</i>	<i>Spirulina</i>	(mg/kg db)	<i>Chlorella</i>	<i>Spirulina</i>
<i>Proximate analysis (wt.%)</i>			<i>Al</i>	25	402
Ash	6.0	7.6	<i>Ca</i>	1922	7782
Moisture	5.2	5.7	<i>Cl</i>	3946	4433
<i>Elemental composition (wt.% daf)</i>			<i>Cu</i>	6	8
<i>C</i>	53.5	53.7	<i>Fe</i>	846	879
<i>H</i>	7.4	7.7	<i>K</i>	11705	13899
<i>N</i>	11.0	12.1	<i>Mg</i>	3288	4256
<i>S</i>	0.5	0.6	<i>Mn</i>	57	56
<i>O*</i>	27.5	25.9	<i>Na</i>	860	4732
<i>Biochemical content (wt.% daf)</i>			<i>Ni</i>	0.7	2.6
<i>Carbohydrates</i>	15-25	11	<i>Zn</i>	21	27
<i>Protein</i>	53-60	65-70			
<i>Lipids</i>	3-5	8			
<i>HHV (MJ/kg)</i>	24.3	24.9			

daf= dry ash free; db=dry basis \*=by difference.

The microalgae were in addition analysed for their particle size distributions as these were expected to have an influence on the reactor performance. In particular the needle control valve and the back pressure regulator were expected to be influenced by particulate matter and potentially blocked if the particle size flowing through was too large. This can be avoided if the reaction conditions are severe enough to break down the algae cell structure to smaller fragments.

**Figure 10.1** shows the size distributions of the two strains. *Chlorella* has a narrower distribution and a smaller average particulate size. The average particle size  $D(v, 0.5)$  of *Chlorella* and *Spirulina* are 48.4 and 62.2  $\mu\text{m}$  respectively. Since the larger *Spirulina* algae were associated with less difficulty in controlling the reactor press (discussed above in section 3.1), it is apparent that the initial particle size of the algae feed is less important than the behaviour of the cells and how easily they can be broken down to smaller fragments in the reactor. The viscosity of the 1 wt.% algae slurries was found to be  $\sim 0.9$  mPa.s at 40 °C which is noticeably higher than that of water at the same temperature (0.65 mPa.s).



**Figure 10.1:** Size distribution of dehydrated microalgae.

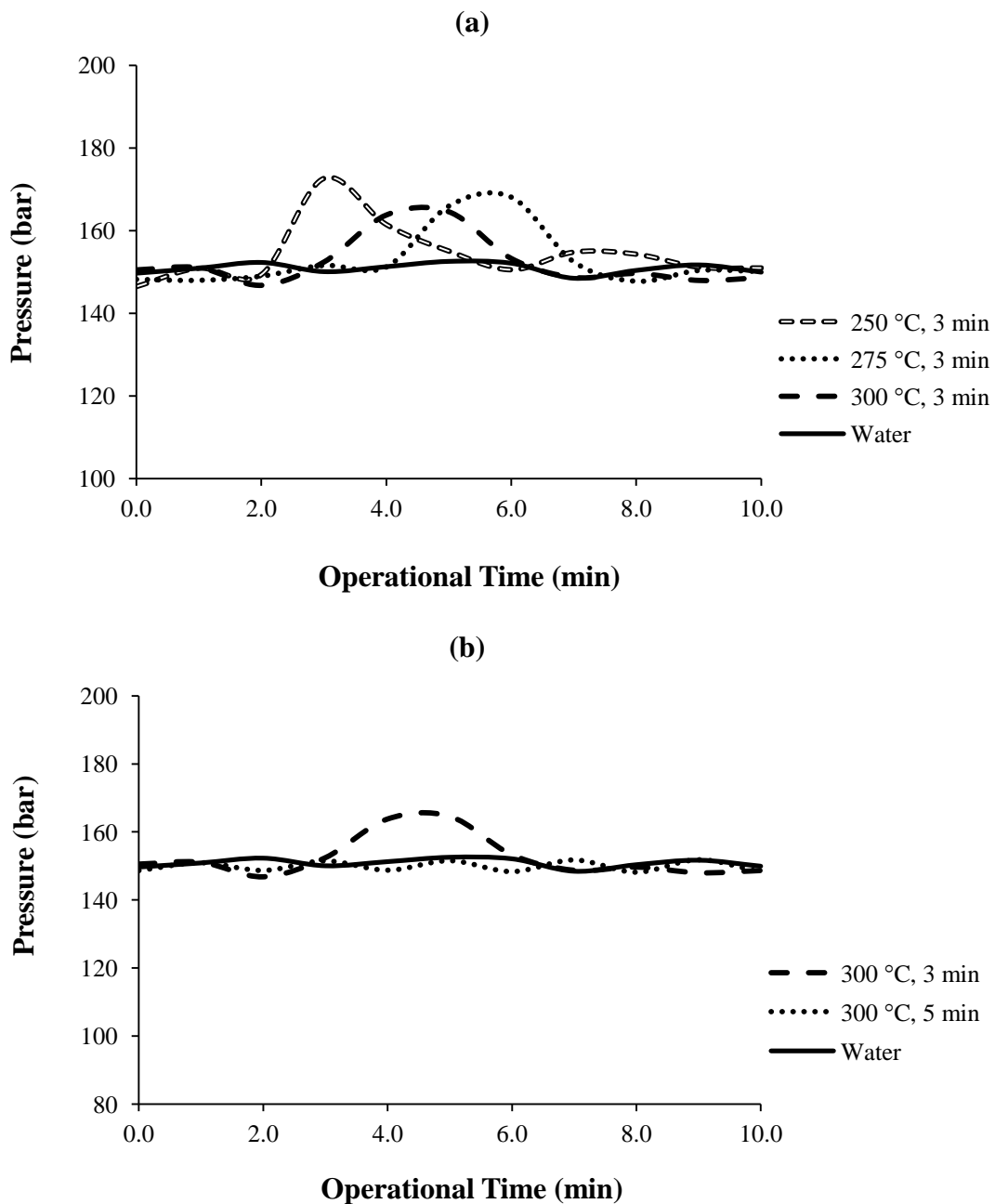
### 10.3.2 Reactor Performance

The performance of the continuous flow HTL reactor with respect to pressure, temperature and flow rate was examined. The results obtained from the experiments indicate that the maximum pressure deviation from the set value occurred at the lowest temperature and shortest residence time (highest flow rate) investigated. The pressure control significantly improved with higher processing

temperatures and longer residence times inside the reactor, this being the case with both algal strains. **Figure 10.1 (a)** shows the pressure-time history when processing *Spirulina* at different temperatures while **Figure 10.1 (b)** highlights the effect of longer residence time on the controllability of the system pressure.

It is believed that the more severe process conditions result in a more pronounced conversion of the algal solids. This was observed for both strains where the solid yields from HTL consistently decreased with increasing temperature and residence time, as discussed in detail in **Section 10.3.3**. The solids observed in the product stream clearly have a tendency to at least partially block the orifice of the control valve, leading to poor pressure control (orifice clearance while valve is fully open:  $\sim 19 \mu\text{m}$ ); it can be seen from **Figure 10.2 (a)** that the higher experimental temperatures correspond to smaller pressure fluctuations. Additionally, increasing the residence time from 3 to 5 minutes at  $300^\circ\text{C}$  for *Spirulina* further decreased the solids yield and resulted in an improvement in pressure control. In fact, as depicted in **Figure 10.2(b)** the pressure controllability was similar to that of clean water which is attributed to the more pronounced conversion of algae solids to bio-crude and/or breakdown to water soluble material at the higher temperatures and residence times examined. Another observation supporting this conclusion is the fact that the control was better for *Spirulina* than for *Chlorella* which coincides with the lower amounts of solids observed when processing *Spirulina*.

It should be noted that because the pressures in the system are always substantially greater than saturation, these pressure fluctuations are not accompanied by temperature fluctuations and are unlikely to have any significant impact on the course of the HTL reactions.



**Figure 10.2:** Pressure control for *Spirulina* at 150 bar **(a)** varying experimental temperatures for a residence time of 3 minutes **(b)** varying residence times of 3 and 5 minutes at 300°C.

The reactor temperature and biomass slurry feeding rate were also recorded during each run. The average temperature of the fluidised bed heater was at all times within  $\pm 3^\circ\text{C}$  from the set point (250, 275 and 300°C). The biomass slurry is expected to reach temperature within 10 °C of the desired temperature inside the first set of the four helical reactor coils immersed in the bed heater. The overall residence time inside the reactor coils was determined by measuring the biomass slurry

feeding rate and correcting for the change in density of the solvent in going from room temperature to the nominal reaction conditions. The slurry feeding rate was maintained to within  $\pm 4\%$  from each of the flow rates investigated in this study (15-30 l/hr).

### 10.3.3 HTL Results

The results obtained from processing *Chlorella* and *Spirulina* in the continuous reactor at different temperatures and residence times are presented in **Figure 10.3**. The highest bio-crude yields were obtained at the highest temperature of 300 °C and longest residence time investigated, overall, higher temperatures and longer residence times increased the yields. This is in agreement with batch HTL experiments on microalgae [67]. It has to be mentioned that the solids to water ratio was very low in this study. A ratio of 1 wt.% was employed initially to ensure no blocking within the reactor pipelines which could result in a dangerous pressure build-up. This ratio is considerably lower than in batch reactions investigated previously in this thesis where concentrations of 10 wt.% were used. This aspect has to be considered when comparing results to batch experiments such as in **Chapter 5** on the same algae strain. The initial aim of the work in this Chapter was to assess the feasibility of processing algae slurries in the continuous reactor. On-going work will investigate higher solids loadings.

The maximum bio-crude yields were 13.2 and 16.4 wt.% for *Chlorella* and *Spirulina* respectively. The yields increased by 4-7 wt.% as a result of a 50 °C increase in temperature (from 250 to 300 °C) and a 2 minutes longer residence time (from 3 to 5 minutes). At the mildest processing range (250 °C and 3 minutes) the bio-crude produced from the two strains varied between 3-8% as only the lipids present in the algae are extracted, while under more severe processing conditions other components including proteins and carbohydrates are also liquefied and become part of the bio-crude. The higher bio-crude yields obtained from *Spirulina* is most likely due to its higher initial lipid content. Results presented in **Chapter 7** previously showed that higher lipid content microalgae give rise to greater bio-crude yields in a batch reactor system.

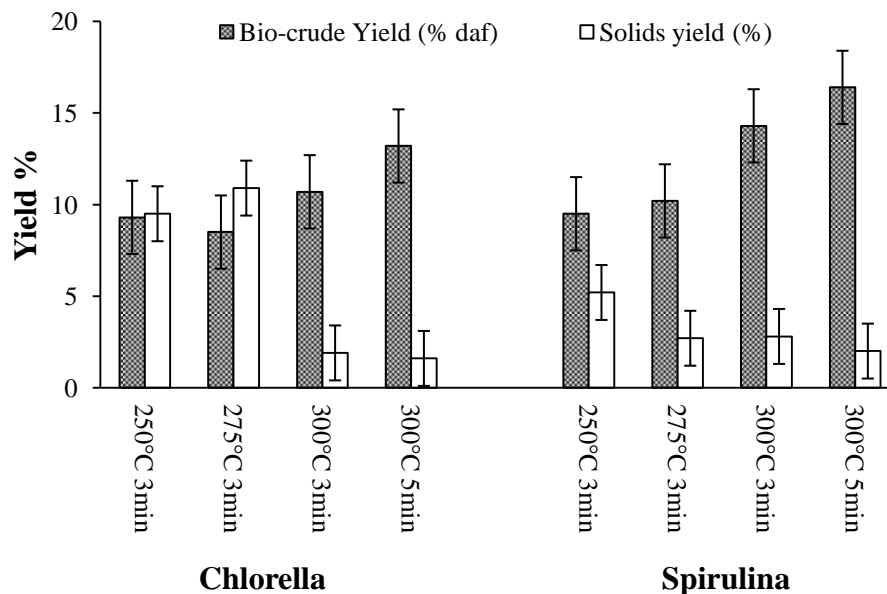
Garcia Alba et al. [37] achieved much higher bio-crude yields in a batch reactor – for example, with a 5 minutes residence time at 300 °C, the bio-crude yield was found to be 40.5 wt.%, which is considerably higher than herein. Our low measured bio-crude yields were initially attributed to the different method of recovery from the product mixture as well as losses of product to the system. A low solvent ratio was used in the current study as it is expected that in an industrial process the use of solvents is not necessary as the bio-crude can be directly decanted. However, due to the low solid

concentrations used here, the bio-crude fraction was very small compared to the process water. In a 500 ml product mixture sample only 5 g of dry algae were processed leading to small amounts of bio-crude produced per volume of water, therefore the use of a solvent was necessary in order to quantify the bio-crude yields gravimetrically. In reported batch experiments with a 10 wt.% biomass loading, water to solvent ratios of 0.1 to 1.4 were used to extract the bio-crude from the product mixture while in the current study which processed a 1 wt.% biomass concentration, this ratio was 10.

In order to investigate the effects of the low solvent ratio on the bio-crude yields, the experiments were repeated using twice the solvent quantity to recover the bio-crude. The yields were found to be unchanged and consequently it was concluded that the loss of bio-crude to the system is the most likely reason for the lower yields observed. These losses are estimated in the carbon balance carried out in **Section 10.3.6**. Further work is required to quantify the gas produced from the continuous flow HTL reactor as well as to investigate the bio-crude recovery with no solvents while processing higher biomass solid concentrations.

Increasing the biomass solids concentration has been shown to enhance bio-crude yields in batch experiments [59, 67]. Both these reports also state that the optimum residence time for bio-crude production is 15 minutes and that the yield is lower at shorter residence times. **Figure 10.3** shows that the solids residue from continuous flow HTL decreases as the bio-crude yield increases with more severe processing conditions for both strains. This indicates that the residence times studied were not long enough to completely break down the particulate matter and convert it to bio-crude by repolymerisation. The solids fractions for *Spirulina* are lower than for *Chlorella* which is consistent with the reactor performance data presented above, namely that *Spirulina* is more readily broken down.

Temperatures higher than 300 °C are expected to further increase the bio-crude yields as indicated by Jena et al. [67] who showed the highest yield from *Spirulina* to be obtained at 350 °C while Garcia et al. [37] achieved the highest yield at 375 °C from *Desmodesmus sp.* Therefore, the potential for higher bio-crude yields on the continuous flow plant exists.



**Figure 10.3:** Yields of products for the different hydrothermal liquefaction experiments.  
\* *daf*=dry ash free.

#### 10.3.4 SEM Analysis

Scanning electron microscopy (SEM) was utilised in order to investigate the visual appearance of the algae cells and the solids residue component after liquefaction in the continuous flow reactor. It is expected that the reactor performance and the bio-crude yields obtained are linked to the algae cell structure being increasingly disrupted with more severe processing conditions. Bio-crude yields were increased with higher temperatures and at the same time the solids residue component was decreased. Additionally, as depicted in **Section 5.3.1**, the reactor performance with respect to pressure fluctuations was significantly improved with higher processing temperatures.

The SEM images of *Chlorella* pre- and post-liquefaction are presented in **Figure 10.4 (a-d)**. A fresh *Chlorella* cell with a 3000x magnification prior to processing is shown in **Figure 10.4 (a)**. Using the scale of the image the cell has a diameter of around 55  $\mu\text{m}$  which fits well with the data obtained by particle size distribution. **Figure 10.4 (b)** shows the solid residue obtained at 250°C: it can be seen that the selected residue particle is much larger (~500x250  $\mu\text{m}$ ) than an individual cell, indicating that cells have agglomerated to form a solid compact structure with filamentous strings. The cell walls seem to have broken at these conditions as there is no apparent resemblance to the

original cell. The pronounced agglomeration to a compact structure suggests that reactor performance will be influenced by the large particles present at these conditions.

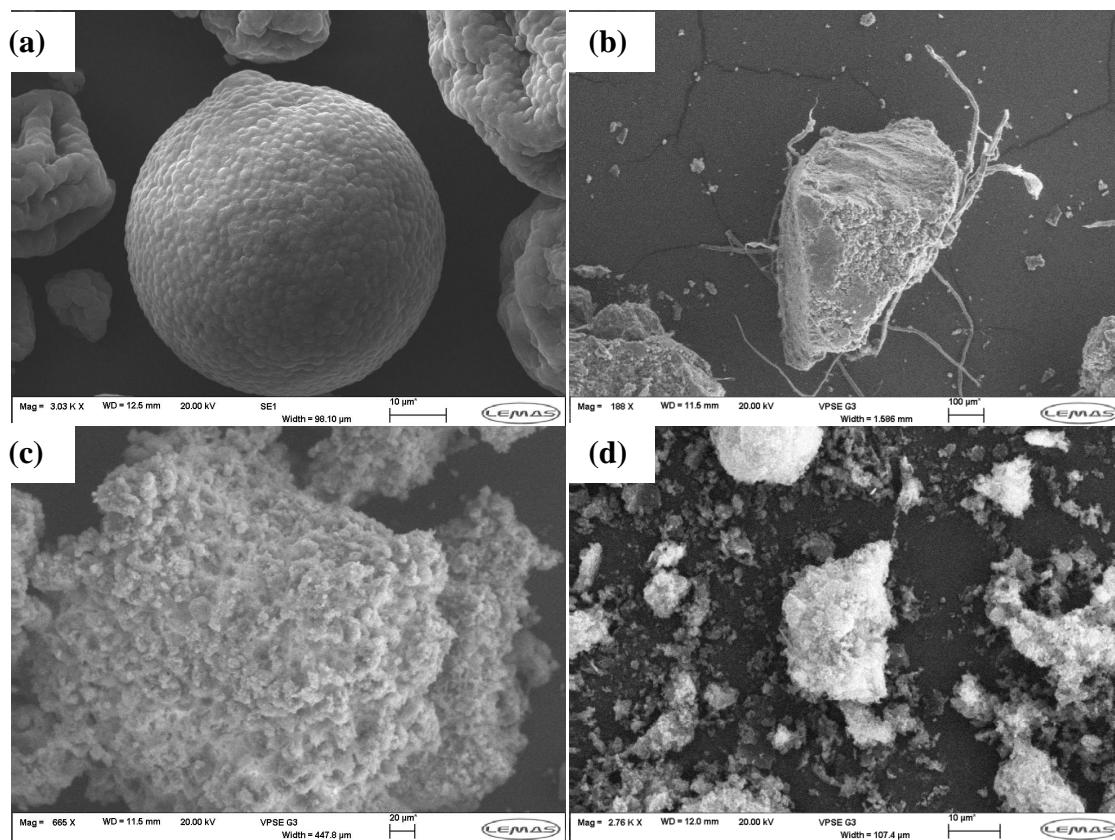
Increasing the temperature by 25 °C to 275 °C with the same residence time leads to the disappearance of the filaments observed at the lower temperature. The overall structure of agglomerated cells remains intact but appears less compact with a less uniform surface morphology. The diameter of the agglomerate is approximately 300 µm, similar to the particle size observed by SEM at 250 °C. In the final image, the solid residue obtained from processing *Chlorella* at 300 °C and a residence time of 3 minutes is presented. The cell structure appears to be completely destroyed; the larger structure seen in **Figure 10.4 (d)** is approximately 10-15 µm, fragments of smaller sizes (<10 µm) can be seen in the background. The conclusion is made that at 300 °C the breakdown of the original cells is largely complete, leading to an improved bio-crude yield and a reduced solids residue giving rise to lower pressure fluctuations.

Garcia Alba et al. [37] performed similar analysis on the cells of *Desmodesmus sp.* after HTL for 5 minutes in batch experiments. The cells of *Desmodesmus sp.* are shown to be considerably smaller ranging from approximately 3-8 µm compared to ~40-80 µm for *Chlorella*. The SEM images presented show the solid residue component post HTL in the temperature range of 175 to 275 °C. It appears that the cells of *Desmodesmus sp.* perform similarly to those of *Chlorella* as they appear to agglomerate to clusters after liquefaction. However, they exhibit filaments in their fresh form which appears to hold the cell clusters together at different processing conditions. In the current study, filaments are not present in the fresh algae and, hence, their origin is unknown. Garcia Alba et al. concluded from their SEM analysis that cell breakage occurred at 250 °C when processed for 5 minutes. Cell breakage also appears to have occurred at the same temperature and comparable residence time in the current study with agglomeration observed at less severe conditions.

It should be considered what type of algae is processed when using a continuous flow reactor of this scale, as their behaviour could drastically influence reactor performance. The point at which agglomeration is overcome should be passed to avoid the high residual solids yield and increased pressure fluctuations. For *Chlorella* this was achieved at 300 °C and 3 minutes residence time in the continuous flow HTL reactor, SEM images for the longer residence time were largely identical and are not presented. It has to be pointed out that Garcia Alba et al. showed that increased residence time led to increased packing density in the agglomerated cell structure. This was not observed in this study which is most likely due to the residence time increase being only 2 minutes compared to



that of 55 minutes in their study. It is also expected that batch reactor configurations may affect this phenomenon differently from those of continuous flow such as the one used here. In addition, it is worthwhile mentioning that commercial processing plants are not expected to encounter such an effect on the reactor performance as higher flowrates and larger valves will be employed that can more readily handle the solid particulates.



**Figure 10.4:** SEM images of *Chlorella* (a) dry unprocessed (b) processed at 250°C 3 min (c) processed at 275°C 3 min (d) processed at 300°C 3 min.

### 10.3.5 Bio-crude Analysis

The recovered bio-crude was analysed for its elemental composition and the data are presented in **Table 10.2**. The oxygen contents ranged from ~21 to 15 wt.%, the lower oxygen levels being obtained at the higher temperatures and longer residence times investigated. The initial oxygen content of the algal biomass feedstock was approximately 30 wt.% signifying a considerable reduction at the most severe conditions examined, 300 °C and 5 minutes. Overall, the more severe

processing conditions result in a greater reduction in the oxygen content, in agreement with results published by Jena et al. [67] on a batch reactor system.

The elemental analyses of the bio-crudes also show an increase in the nitrogen content with the higher temperatures used, indicating an increase in the production of bio-crude from the protein fraction of the algae. These trends are consistent for both strains of microalgae. At 250 °C and 3 minutes residence time, the nitrogen content for bio-crude produced from *Chlorella* was 2.6 wt.%, while that at 300 °C and similar residence time was over 6 wt%. It is important to note here that while the lower processing temperature produced a bio-crude with lower nitrogen content, the yields were also considerably lower.

It has been suggested that to produce a bio-crude with lower levels of nitrogen, the use of heterogeneous catalysts needs to be considered [76, 159]. Another route proposed is to extract the protein fraction of the algae prior to subjecting it to the high temperature HTL process in a biorefinery concept [37]. This route is explored in the subsequent **Chapter 11**.

The HHVs of the bio-crudes ranged from 27 to 32 MJ/kg calculated using the *DuLong formula* as described in **Section 3.13**. This represents a significant increase from the HHV of the algal biomass feedstock (~24 MJ/kg). The observed increase in the HHVs from the biomass to the bio-crude is due to the reduction in oxygen and higher relative carbon contents. The aim should be to reduce the amount of oxygen to increase the HHV, while simultaneously decreasing the levels of nitrogen in order to reduce emissions or refinery processing costs. Petroleum crude oil contains <1 wt.% oxygen and nitrogen and has HHV > 40 MJ/kg which implies that bio-crude produced from microalgae through both batch and continuous flow HTL processes requires upgrading prior to further processing.

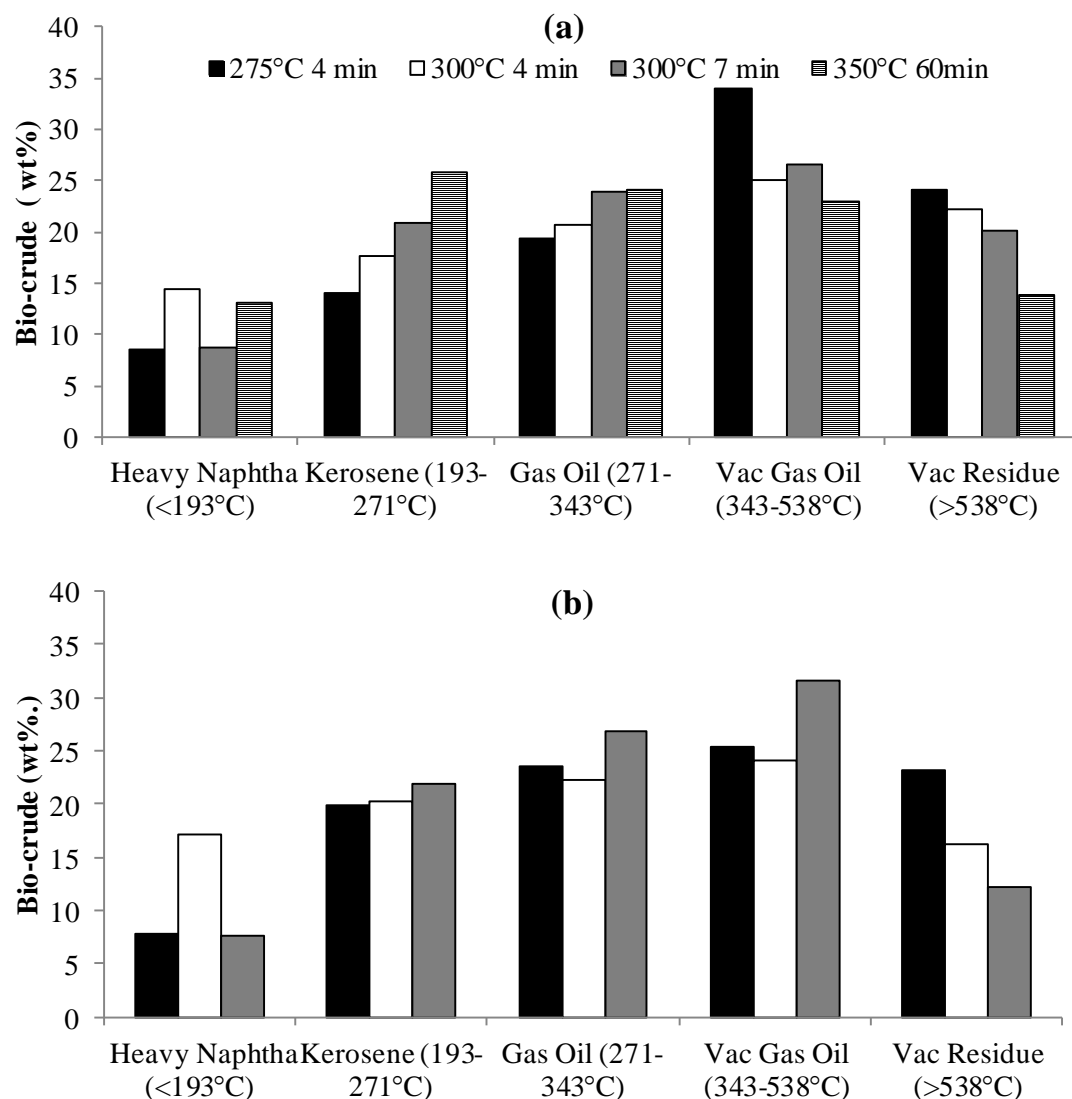
**Table 10.2:** Elemental analysis (wt.%) and Higher Heating Value (HHV) of bio-crudes from hydrothermal liquefaction of *Chlorella* and *Spirulina* at different processing conditions.

<i>Chlorella</i>	<i>Temp.</i>	<i>Res. Time</i>	<i>C</i>	<i>H</i>	<i>N</i>	<i>S</i>	<i>O*</i>	<i>HHV</i> (MJ/kg)
	250°C	3.0	70.3	4.8	2.6	0.4	21.9	26.7
	275°C	3.0	65.9	9	4.3	0.8	20	31.7
	300°C	3.0	64.1	7.8	7.5	1.5	19.1	29.5
	300°C	5.0	67.6	8.2	6.3	2.1	15.8	32.0
<i>Spirulina</i>								
	250°C	3.0	65.8	8.5	3.5	0.5	21.7	30.6
	275°C	3.0	62.3	7.3	6.7	1.1	22.5	27.6
	300°C	3.0	64.3	8.4	7.5	1.3	18.5	30.6
	300°C	5.0	68.3	8.3	6.9	1.1	15.4	32.3

\*=by difference.

To determine the boiling point distribution of the bio-crudes a simulated distillation was carried out by TGA and is presented in **Figure 10.5** for *Chlorella* (a) and *Spirulina* (b). The majority of the bio-crude falls in the distillation range of Vacuum Gas Oil (VGO). Higher processing temperatures and longer residence times resulted in larger amounts of low boiling point material. The greatest yield of the low boiling point fraction, Heavy Naphtha, is obtained at 300 °C and 3 minutes residence time. Generally, the distribution is much more uniform than obtained by Vardon et al. [78] who found the majority of bio-crude to fall in the VGO region (~50 wt.%) for *Spirulina* processed in a batch reactor at 300 °C for 30 minutes. They also found the Heavy Naphtha fraction to be below 5 wt.% and the Kerosene and Gas Oil fraction between 10-15 wt.%.

The bio-crudes obtained from *Chlorella* in the continuous flow HTL reactor are additionally compared to processing *Chlorella* at 350 °C for 60 minutes in a batch reactor from a previous study by Biller et al. [76] (see **Chapter 7**). **Figure 10.5 (a)** shows that the trends observed for the continuous flow system also apply for the higher temperature and longer residence time obtained in the batch process; the residue fraction is further decreased and the lighter fractions increased. The very heavy boiling point material is reduced with increased severity of the processing conditions. The sim-dis data illustrate that the more severe processing conditions are favourable as they lead to an increased yield of lower molecular weight bio-crude fraction.



**Figure 10.5:** Sim-dis by TGA for bio-crudes derived from (a) *Chlorella* and (b) *Spirulina*.

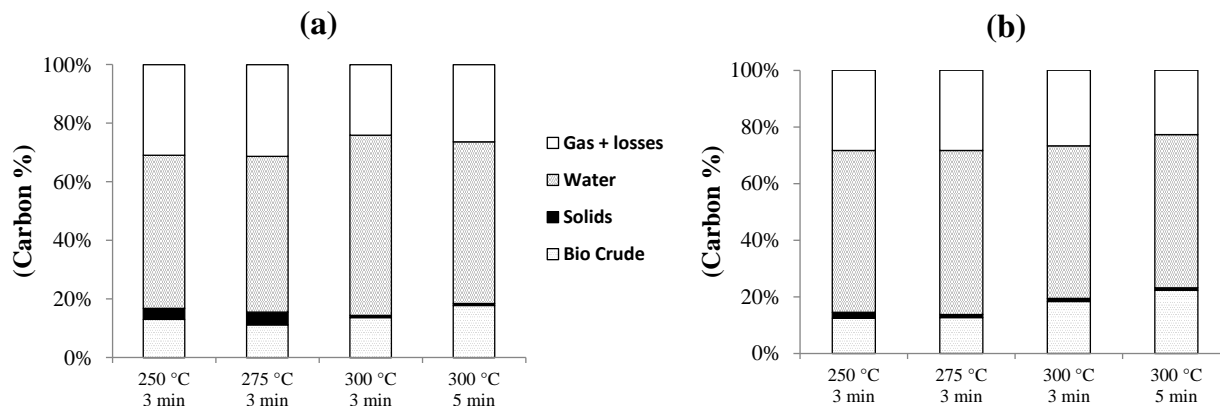
### 10.3.6 Carbon Balance in the product phase

The distribution of carbon in the different product phases was calculated using the elemental composition of the bio-crude and solids residue components along with the carbon content of the process water by TOC analysis. The gas phase was determined by difference, this means that the gas fraction presented here includes any losses to the system as well as those due to the sample workup. The results are presented in **Figure 10.6 (a-b)** for *Chlorella* and *Spirulina* respectively. It can be seen that the carbon recovery to the bio-crude is relatively poor with a maximum of 22 wt.%

for *Spirulina* at 300 °C and 5 minutes residence time. It has been shown by Yu et al. [58] that increasing the reaction time of HTL leads to an improved carbon recovery to the bio-crude component.

A large carbon fraction is found in the *Gas+Losses* phase (20-30 wt.%), this is not surprising as most of the oxygen is removed via decarboxylation and therefore a loss of carbon is unavoidable. Due to the novelty of this work there is very limited experience with losses to the continuous flow HTL process. Since the *Gas+Losses* fraction appears to decrease with higher temperature and longer residence time, it appears that the losses to the system are greater at the lower temperatures investigated in this study. This may indicate carbonisation inside the system including the reactor, heat exchangers, pipes and fittings which would be included as a loss in the calculations. Yu et al. [58] report a carbon recovery to the gas phase of 10 wt.% at 300 °C and 5 wt.% at 250 °C in a batch reactor system with a residence time of 30 minutes. Using this data along with the carbon balance carried out in this study, it is estimated that the losses to the continuous flow system are up to 25 wt.% for the low temperature region (250 °C) whereas those for higher temperatures (300 °C) were lower and are estimated to be around 10 wt.%. This establishes the potential increase in the carbon recovery to the bio-crude if the losses to the system are limited.

Notwithstanding the uncertainties around the extent of losses, it is clear that the greatest fraction, up to 50 wt.%, of carbon reports to the aqueous phase. Most of the carbon in this phase is organic with only about 10 wt.% being inorganic – this was measured using a differential method of organic and inorganic carbon determination (results not presented). This large carbon fraction in the water will impact the economic feasibility of the HTL process; in **Chapter 8** it was suggested using the organic carbon in the aqueous phase as a substrate for mixotrophic growth for microalgae cultivation. Results from the literature have previously shown that the water is also high in nitrogen and phosphorous which are supplementary nutrients required for algae growth [47, 114]. Additionally, the aqueous phase from the current study was analysed for metal content by ICP and showed that there were high levels of K, Na, Ca and other minor nutrients (results not presented). Finally, the carbon fractionation to the solid residue is very small at all conditions investigated and was found to decrease with more severe processing conditions (see **Figure 10.3**).



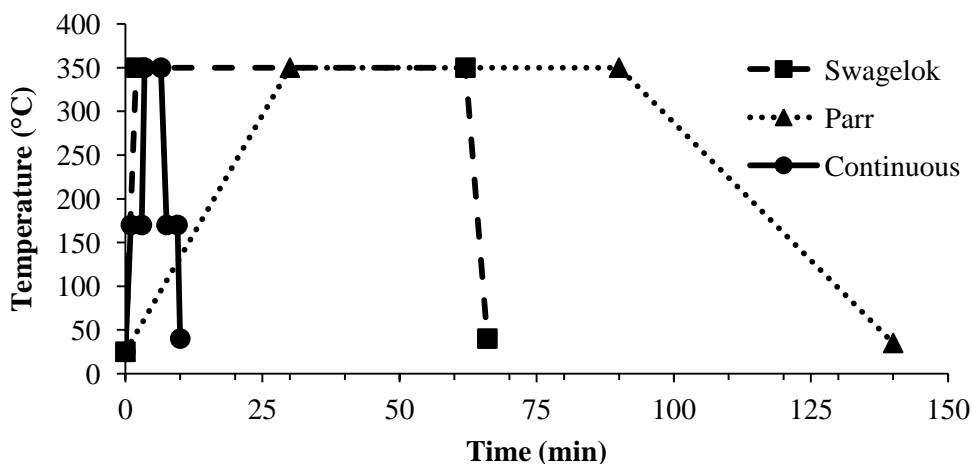
**Figure 10.6:** Carbon balance from the continuous HTL of (a) *Chlorella* and (b) *Spirulina*.

## 10.4 Comparison of reactor types

In Chapter 5 results on HTL of microalgae processed on two different batch reactors are presented. The main differences in the different reactor types are the heating rate and the residence time. The residence time within reactors has been the focus of previous work and is addressed in Chapter 5. The effect of heating rate however on the HTL of microalgae has not been covered in the literature to date. Investigating this possible effect was not one of the aims of the current work. However due to the work carried out in different reactors, limited data is available to examine the effect of heating rate. **Table 10.3** shows the results from processing *Chlorella OZ* for 1 hour at 350°C in the 75 ml Parr reactor and in the custom built 25 ml Swagelok reactors as presented in **Chapter 5**. Results in **Table 10.3** include the results from processing a 10 wt.% slurry in the continuous reactor for 3 min. The sample in the Parr reactor reached final temperature in around 30 min, at which it was held for 1 hour and subsequently required 1 hour to cool back down to ambient temperature. In the Swagelok reactor, the contents reached 350°C within 2 min and after 1 hour were quenched in cold water leading to the contents being cooled within 4 min. **Figure 10.7** depicts the heat profiles applied to the microalgae for the different reactor types. In the continuous reactor heat is applied in a different profile. Details can be found in **Chapter 3**, but briefly; the slurry is heated from ambient to 170°C within a minute. At this temperature the sample is kept for 2 min before it flows into the reactor where it is heated from 170 to 350°C more or less instantly. At 350°C the sample is kept for 3 min before it is cooled in subsequent heat exchanger to 170°C within 1 min. After resting at around 170°C for 2 min the sample is cooled quickly in the second heat exchanger to approximately

40°C. It is apparent that the heating and cooling profile is significantly different to the batch reactor examples.

The results in **Table 10.3** show that the yield in the Swagelok reactor is over 10 wt.% higher compared to the Parr reactor. However the oxygen content is doubled. It is expected that higher yields result in higher oxygen content as most oxygen is removed via decarboxylation during HTL which consequently, unavoidably leads to less carbon available for bio-crude formation and hence lower bio-crude yields. The reason for the different results is not entirely apparent but some hypotheses can be made. At the high temperature of 350°C the large molecules will have depolymerised to low molecular weight compounds which only form bio-crude once cooling occurs by repolymerisation. It is likely that quick cooling by water quenching leads to increased fast repolymerisation of the fragments, resulting in higher bio-crude yields. In the slow cooling example, there is the possibility that decarboxylation continues to occur on newly forming molecules throughout the cooling period. This consequently results in more oxygen and carbon being removed which leads to the overall lower yields but lower oxygen content. Results in **Table 10.3** show that the yield from continuous processing is 2.5 wt.% lower than in the Swagelok reactor and approximately 10 wt.% higher compared to the Parr reactor. The oxygen content was measured as 12 wt.%, which falls in between the values of the other two results. These results support the hypothesis that heating and cooling have significant effects on HTL and deserve considerably more attention than it has received in the research community and published literature to date. Additionally the results suggest that very low residence times and high heating and cooling rates can lead to bio-crude yields similar to those observed for long residence times in batch reactors. This allows higher throughput of microalgae slurries and more favourable energy balances.



**Figure 10.7:** Heat profiles of different reactor types on HTL of 10 wt.% *Chlorella OZ*.

**Table 10.3:** Comparison of bio-crude yields and composition from *Chlorella OZ* at 350°C.

<b>Reactor</b>	<b>Bio-crude yield (wt.% daf)</b>	<b>C</b>	<b>H</b>	<b>N</b>	<b>S</b>	<b>O</b>	<b>HHV (MJ/kg)</b>
		<b>(wt.%)</b>					
<i>Parr</i>	32.3	75.7	9.8	6.5	0	7.8	38.2
<i>Swagelok</i>	44.1	70.4	8.5	6.2	0.5	14.3	33.5
<i>Continuous</i>	41.7	70.7	8.8	7.7	0.8	12.0	33.8

## 10.5 Conclusions

This work demonstrated the successful operation of a continuous flow pilot-scale HTL reactor system – the results provide insight in to the behaviour of processing microalgae in sub-critical conditions. The bio-crude yields reached a maximum of 16.4 wt.% for *Spirulina* at 300°C, 5 minutes residence time and 150 bar. More severe processing conditions are required in order to further enhance the observed yields. It was also indicated from the carbon balance that there are considerable amounts of carbon in the product phases unaccounted for. The extent of products lost to the system due to sticking and carbonisation, which could potentially lead to lower bio-crude yields, requires further investigation in a continuous flow pilot scale HTL reactor.

Overall, more severe processing conditions increased yields, reduced the oxygen content and led to an increased lower molecular weight bio-crude fraction being formed. It was also shown that the higher processing temperatures increased nitrogen levels as more of the protein present in the algae was liquefied and converted to bio-crude. Conversely, the solids residue component consistently decreased with increasing temperatures and residence times. These trends were consistent for both microalgae strains investigated.

The performance of the continuous flow HTL reactor with respect to pressure, temperature and flow rate was also examined. Higher processing temperatures and longer residence times significantly improved the pressure controllability. It was concluded that greater solid yields and larger particles



caused difficulties for the control valve under less severe processing conditions. Flow rate and temperature control on the other hand were not affected with the varying operating conditions.

Finally, comparing different reactor types at the same final operating temperature and slurry concentration, indicates the significant effects of heating rates on HTL. Results suggest that high heating rates can lead to increased bio-crude yields but less decarboxylation. This could have significant impacts on the continuous processing of microalgae in industrial processes.

## 11. CHAPTER XI - Hydrothermal Microwave processing

### 11.1 Introduction

Hydrothermal liquefaction of algae by inductive heating has been investigated in **Chapter 5, 6, 7, 8** and **10** and was shown as a suitable technique to produce a high quality bio-crude from a wet feedstock. Depending on the severity of the reaction conditions, the process is classified as carbonization, liquefaction or gasification with the latter requiring higher temperatures and pressures. Hydrothermal processing does not require a high lipid feedstock as the protein and carbohydrate fraction of algae can also be converted to either a biochar, bio-crude or syngas. Hydrothermal processing of algae has significant potential in the production of microalgae derived biofuels and has been extensively reviewed in **Chapter 1**.

One issue which still requires further research in hydrothermal processing is the extraction of high value compounds prior to biofuel production. The extraction of value added compounds is essential to improve the economics of producing renewable fuels from microalgae and should be considered. Microalgae are a highly promising source of valuable phytochemicals such as pigments, recombinant proteins, mono- and polyunsaturated fats such as omega-3 fats and polysaccharides [18]. Few studies have looked into the extraction of lipids and polysaccharides before further processing into biofuels by hydrothermal processing. Miao et al. have recently investigated the sequential hydrothermal liquefaction of microalgae with extraction of valuable polysaccharides in the first step and subsequent bio-crude production of the residues [73-74]. Vardon et al. investigated the solvent extraction of lipids from *Scenedesmus* prior to hydrothermal liquefaction of the defatted microalgae [75]. Hydrothermal processing is a relatively severe procedure where close control of reaction conditions to achieve specific conversion to desired compounds can be quite difficult.

Microwave processing has been suggested to provide a more controllable method of heating resulting from the rotation of dipolar molecules and vibrations of ions in solution in an electromagnetic field. This mode of heating can reduce residence times, increase reaction rates and provide more accurate control of reaction conditions [160]. Tsubaki et al. showed that the addition of halide salts during the hydrothermal hydrolysis of cellobiose resulted in an increase in hydrolysis of carbohydrates, resulting in a reduction of unwanted side reactions and energy consumption. It is therefore hypothesized that algae, which are naturally high in salts, could prove to be a promising feedstock for microwave processing. Microwave processing could either be used to facilitate

extractions of valuable compounds such as polysaccharides or protein, as recently shown by Budarin et al. [161] or applied as a means to produce a biofuel by microwave-mediated pyrolysis of algae [162].

The current Chapter aims to investigate the use of microwaves for the pre-treatment of microalgae feedstock and for the extraction of value added compounds before further processing to biofuels by hydrothermal liquefaction. The influence of inorganic salts on hydrothermal microwave processing is investigated and the process is evaluated as a technique for extraction of valuable compounds as well as a pre-treatment for the production of biofuels via both hydrothermal liquefaction and flash pyrolysis. During direct hydrothermal liquefaction, proteins in microalgae are broken down to rearranged to produce complex nitrogen containing molecules which are found in the bio-crude as shown in **Chapter 7**. This produces a bio-crude with undesirably high nitrogen content which can lead to complications if the fuel is to be upgraded via hydro treatment/hydrogenation and increased NO<sub>x</sub> emissions during direct combustion. It has previously been shown that proteins can be hydrolysed to water soluble amino acids or extracted as proteins to the water phase during subcritical water treatment [163-164]. If the proteins can be fractionated into the water phase during hydrothermal microwave processing it is expected that a bio-crude of lower nitrogen content can be produced by HTL and flash pyrolysis. Additionally, as shown in **Chapter 7**, the processing of amino acids result in a bio-crude containing a lower nitrogen content than from protein, therefore if the proteins can be decomposed to produce amino acids, this may result in a lower N bio-crude. Du et al. performed work similar to this concept by subcritical water pre-treatment before flash pyrolysis to produce a bio-oil with fewer nitrogen containing compounds [165].

## 11.2 Methodology

Three microalgae strains were investigated; *Nannochloropsis oculata*, *Chlorogloeopsis fritschii* and *Pseudochoricystis ellipsoidea*. All three strains were freeze-dried before use. Samples were prepared by mixing ~1g of freeze-dried microalgae with 10 ml of deionised water to form a slurry. The low ash containing high-lipid fresh water strain (*Pseudochoricystis ellipsoidea*) was mixed with 0.1M NaCl to investigate the effects of inorganic salt content on microwave processing. Samples of each strain were prepared in triplicate for each processing temperature used. Details on the microwave processing can be found in **Chapter 3**. The methods of lipid extraction, hydrothermal processing, flash pyrolysis and TGA are also described in **Chapter 3**.

## 11.3 Results and Discussion

### 11.3.1 Microwave processing

Three strains of algae were investigated for the purpose of the current research; *Nannochloropsis oculata*, the high-lipid strain *Pseudochoricystis ellipsoidea* and the cyanobacteria *Chlorogloeopsis fritschii*. *Nannochloropsis* is a marine strain which was grown in f/2 media and therefore has much higher ash content than the other two fresh water strains, this corresponds to its lower calorific value (CV) of 17.9 MJ/kg as seen in **Table 11.1**. The characterisation of the three algae strains can also be found in **APPENDIX A** but a summary of relevant parameters is presented here to aid discussion throughout the Chapter. *Pseudochoricystis* has the highest CV due to its low ash content and very high lipid content of 67 wt.%. Both *Nannochloropsis* and *Chlorogloeopsis* have a high nitrogen content of around 9 wt.% which corresponds to their high protein content of 57 and 50 wt.% respectively. The most abundant inorganics were also investigated as metals and salts have been shown to absorb microwave irradiation and influence reaction rates during microwave processing [160]. *Nannochloropsis* is shown to have the largest concentration of all inorganic compounds investigated; the concentration of Cl and Na are particularly high. The concentration of Na in *Nannochloropsis* is around 50 fold higher than for *Chlorogloeopsis* and 1500 fold higher for *Pseudochoricystis*. The high lipid strain is exceptionally low in inorganics apart from K which is a third of the level in *Chlorogloeopsis* and a fifth of the concentration present in the *Nannochloropsis*. Due to the low concentrations of salts in *Pseudochoricystis* it was decided to process this strain in a solution of 0.1 M NaCl to investigate the effect of inorganics on the hydrothermal processing of microalgae. The three strains were also analysed for phosphorous content. Phosphorous is an essential nutrient within the cultivation of algae; however it is a finite non-renewable resource extracted from phosphate rock and extraction requires high energy inputs [103], therefore the fate of phosphorous during hydrothermal microwave processing and the possibility of nutrient recycling and/or nutrient extraction is investigated and addressed in this study.

**Table 11.1:** Proximate, ultimate, biochemical and metal analysis of microalgae feedstock.

	<i>Chlorogloeopsis</i>	<i>Nannochloropsis</i>	<i>Pseudochoricystis</i>
H <sub>2</sub> O (wt.%)	10.1	9.2	1.2
Ash (wt.%)	3.6	25.7	1.0
C (wt.% daf)	52.2	57.8	61.3
H (wt.% daf)	7.5	8	9.1
N (wt.% daf)	9.8	8.6	2.1
S (wt.% daf)	0.2	n/d	n/d
O* (wt.% daf)	30.3	25.7	27
HHV (MJ/kg)	18.9	17.9	29.4
Protein (wt.% daf)	50	57	25
Carbohydrate (wt.% daf)	44	8	7
Lipid (wt.% daf)	7	32	67
Cl (mg/kg db)	578	76955	10
Na (mg/kg db)	3905	189271	124
Fe (mg/kg db)	692	714	48
K (mg/kg db)	4844	14989	2899
Mg (mg/kg db)	2693	3295	244
P (mg/kg db)	7847	7806	6256

\*by difference, n/d=not detected, daf=dry, ash free, db= dry basis

Each microalgae sample was processed under hydrothermal microwave conditions at temperatures of 80, 100, 120 and 140°C while *P. ellipsoidea* was also processed in 0.1M NaCl. The recovered solid fraction was analysed for elemental composition and ash content and the results are presented in **Table 11.2**. For *C. fritschii* around 80-84 wt.% of the total solid was recovered indicating that 20% of the mass resulted in the water phase as water soluble products. The gas produced during microwave processing was not quantified but is assumed to be low as comparable conditions during conventional heating by Garcia Alba et al. resulted in gas yields of <3 wt.% at 175°C and residence times of 5 and 60 min [37]. The processing temperature had no significant effect on the mass of solids or the ash content recovered from *C. fritschii*. The ash content was reduced from 3.6 wt.% in the initial biomass to around 2 wt.% in the microwaved samples, indicating that water soluble salts are fractionated to the water phase. The elemental analysis revealed that around 25 wt.% carbon results in the water phase at 80 and 100°C and increased to 31 wt.% at the highest processing temperature of 140°C. Fractionation of the nitrogen content of the algae into the water phase would

be beneficial as this could potentially upgrade the biomass feedstock for further processing and could also be used as a source of nutrients for microalgae cultivation. The feasibility of recycling nitrogen for algae cultivation from hydrothermal processing was demonstrated in **Chapter 8**. Hydrothermal microwave processing of *C. fritschii* led to a maximum recovery of N to the solids of 91.7 wt.% at the lowest temperature and a minimum of 71.8 wt.% at 140°C. This indicates that at higher temperatures the protein and/or chlorophyll derived nitrogen becomes more soluble in water either by breakdown to more soluble compounds such as hydrolysis of protein to amino acids or by breaking cell structures and hence releasing nitrogen compounds to the water phase.

The results for the marine algae *Nannochloropsis* differ significantly to those of microwave-processed *C. fritschii*. A maximum of 50 wt.% of the total mass is recovered in the solid fraction at the lower temperatures of 80 and 100°C, compared to around 80 wt.% for *C. fritschii*. At 120 and 140°C the recovery is even lower with 38 wt.% and 27.8 wt.% respectively. A proposed reason for this is that the high ash content of *Nannochloropsis*, which is comprised mainly of water soluble salts, is recovered to the water phase. The majority of the salts appear to be extracellular as a water control experiment led to 61 wt.% of the mass being recovered by washing out the salts. The salt removal results in significantly lower ash content in the residue than in the original biomass. The ash contents of the residues range from 4 to 6.5 wt.% compared to 25.7 wt.% in the original feedstock. This is beneficial for further processing, as a high ash content can lead to complications such as chloride stress corrosion and fouling and slagging issues in combustion [112]. However it is not only the ash that is removed, the carbon recovery is also much lower compared to *C. fritschii*, the maximum is 48 wt.% at the low processing temperatures and is reduced down to 22 wt.% at 140°C. This represents a large loss of carbon into the water phase. The N content of the recovered solids after hydrothermal microwave processing follows the same trend; maximum recovery in the solid is around 44 wt.% and this decreases to 17 % at 140°C. This indicates that the majority of the nitrogen is fractionated into the water phase.

For *P. ellipsoidea*, the mass recovery is remarkably similar to that of *C. fritschii* at all conditions. The maximum (83.2 wt.%) is seen at the lowest processing temperature and the minimum of 76.8 wt.% at 140°C. The mass recovery when *P. ellipsoidea* is processed in 0.1 M NaCl is only affected slightly with marginally higher recoveries at 80 and 100°C. The carbon recovery ranges from 87.3-82 wt.% when processed in deionised water and 89.4-80.1 wt.% when processed in 0.1M NaCl. This represents the highest carbon recovery of the three strains investigated. The ash content of *P. ellipsoidea* is not significantly affected up to 120°C, however at 140°C the ash content is below the detection limit of TGA analysis, indicating that processing at 140°C removes the ash content

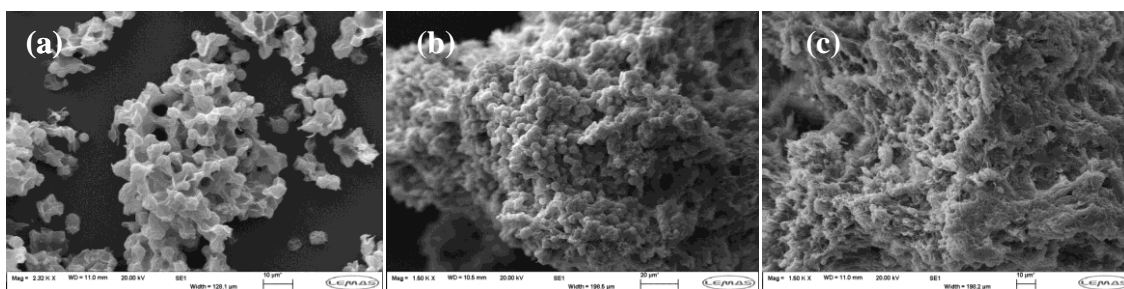
completely. The nitrogen content of the solid algal residue is reduced up to 41 wt.% when processed in deionised water and 48 wt.% when processed in 0.1 M NaCl at a temperature of 140°C. For *P. ellipsoidea* microwave pre-treatment appears to be more beneficial compared to the other strains. Over 80 wt.% of the carbon is recovered and over half the nitrogen is removed, improving the quality of the biomass feedstock for biofuel production by HTL and simultaneously extracting polysaccharides and amino acids to the water phase. This has also been shown to be possible in the low temperature hydrothermal treatment of *Chlorella sorokiniana* by Chakraborty et al. [73].

The hydrothermal microwave pre-treatment is shown to effectively remove a large fraction of the ash and nitrogen from *Nannochloropsis* but at the same time removing undesirably high amounts of carbon. The nitrogen removal from *C. fritschii* is lower but still significant, therefore the advantages and disadvantages of hydrothermal pre-treatment will need to be assessed based on overall mass and energy balances as well the benefits it has on product quality. The influence pre-treatment has on product quality is described in the following sections.

**Table 11.2:** Ash content and % carbon and nitrogen recovered to the solid microalgae residue following HMP.

<i>C. fritschii</i>	80°C	100°C	120°C	140°C
Mass % recovered	83.8	84.0	80.3	82.3
C wt.% recovered	75.6	75.6	73.1	68.9
N wt.% recovered	91.7	82.8	81.0	71.8
Ash wt.%	2.0	2.2	1.3	3.7
<i>Nannochloropsis</i>				
Mass % recovered	49.0	50.3	38.0	27.8
C wt.% recovered	45.8	47.7	36.9	22.3
N wt.% recovered	44.3	43.1	35.8	17.2
Ash wt.%	4.2	4	5.5	6.5
<i>P. ellipsoidea</i>				
Mass % recovered	83.2	80.1	81.9	76.8
C wt.% recovered	87.3	86.3	86.3	82
N wt.% recovered	67.1	62.5	56.5	48.4
Ash wt.%	0.8	1.1	1.3	0
<i>P. ellipsoidea + 0.1M NaCl</i>				
Mass % recovered	85.0	83.0	78.7	77.1
C wt.% recovered	89.4	88.5	83.9	80.1
N wt.% recovered	79.1	76.1	58.1	40.8
Ash wt.%	0.4	1.5	0.5	0.5

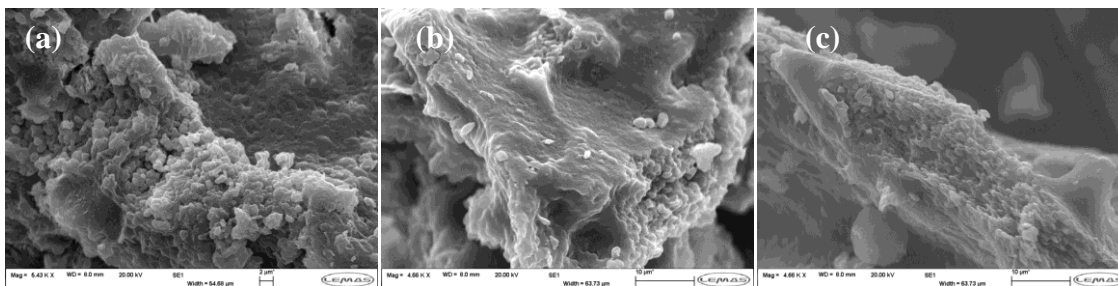
Following hydrothermal microwave treatment the algal biomass was recovered, freeze dried and visually inspected by SEM. The unprocessed cells of *Chlorogloeopsis* are shown in **Figure 11.1a** at a magnification of 2320 $\times$ . The cells are around 2-8  $\mu\text{m}$  in diameter and are clearly identifiable in the unprocessed algae with individual cells linked together by extracellular material. This hormogonia is partly removed even at 80 $^{\circ}\text{C}$  making the individual cells more prominent but no damage has occurred to the actual cell structures. Increasing the temperature leads to increased removal of hormogonia but up to 120 $^{\circ}\text{C}$  does not seem to affect the cells (**Figure 11.1b**). Only at 140 $^{\circ}\text{C}$  are the actual cells broken which can clearly be seen in **Figure 11.1c**. These observations correspond to the mass balance where the loss of carbon and nitrogen were almost identical up to 120 $^{\circ}\text{C}$  but especially the nitrogen was removed at 140 $^{\circ}\text{C}$  where cell wall breakage is observed by SEM leading to increasing amounts of nitrogen in the water phase.



**Figure 11.1:** SEM images of untreated *Chlorogloeopsis* (a) Mag=2320, processed at 120 $^{\circ}\text{C}$  (b) Mag=1500 and 140 $^{\circ}\text{C}$  (c) Mag=1500.

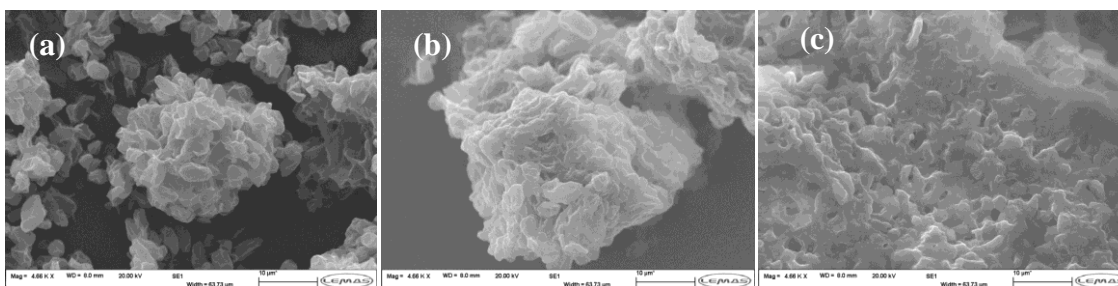
*Nannochloropsis* cells are seen to be very small cells of less than 1  $\mu\text{m}$  (**Figure 11.2a**). Processing *Nannochloropsis* at 80 $^{\circ}\text{C}$  does not seem to affect the cells but leads to more compact clustering of the cells to a solid structure and removal of extracellular material. This effect is also observed at 100 and 120 $^{\circ}\text{C}$ , only at the highest temperature are cells torn from the solid structures and appear to be isolated and in some cases even broken. The large mass loss when microwaving is mostly due to the extracellular material removed, it is also expected that the salt containing ash is removed almost entirely which cannot be seen when inspecting the cells visually.





**Figure 11.2:** SEM images of untreated *Nannochloropsis* (a) Mag=5430, processed at 120°C (b) Mag=4660 and 140°C (c) Mag=4660.

The unprocessed *Pseudochoricystis* shows clear individual cells (~3-8  $\mu\text{m}$  diameter), often agglomerated to larger structures but individual cells are recognisable. When the microwaving temperature is augmented individual cell structures become less prominent and larger, more compact agglomerations of cells appear, possibly of broken cell structures. The extracellular material linking cells together in **Figure 11.3a** appears to have either become compacted or removed leading to the more solid structures and the around 20% loss of mass observed in the mass balance of **Table 11.2**. At 140°C cells are almost entirely morphed to one large structure with individual cells barely recognisable, however if the cells walls are entirely broken is not clear from the image in **Figure 11.3c**. The loss of nitrogen to the water phase observed in the mass balance however indicates that this may occur at least partially.



**Figure 11.3:** SEM images of *Pseudochoricystis* (a) Mag=4660, processed at 120°C (b) Mag=4660 and 140°C (c) Mag=4660.

The supernatant after centrifuging the microwaved samples was analysed for its pH and for anions and cations by ion exchange chromatography as presented in **Table 11.3**. The fate of these is significant for nutrient recycling for further microalgae growth in a closed loop process as proposed

in **Chapter 1**. The levels of Na and Cl are highest in the marine strain *Nannochloropsis* followed by the *Pseudochoricystis* strain processed in 0.1M NaCl while levels are lowest for *Pseudochoricystis*. Levels of ammonia could only be detected in the *Chlorogloeopsis* sample but levels are much lower compared to those observed during hydrothermal liquefaction of the same strain. HTL at 300°C for 1 hour led to concentrations of ammonium of 4750 mg/l compared to around 150 mg/l observed from hydrothermal microwave treatment [114]. This is due to the much less severe conditions employed in the current study. It is not expected that the protein fraction containing the majority of nitrogen is broken down during HMP as significantly as during HTL. This is also the reason why there is no ammonia detected in the other strains. The pH of the process water generally decreases with increasing processing temperature for all strains. This is most likely due to the onset of acid formation by decomposition of simple carbohydrates such as glucose to compounds such as formic, acetic and levulinic acid. Work by Tsubaki et al. showed this effect of increasing organic acid formation from cellobiose under hydrothermal microwave processing resulting in lower pH values at higher processing temperatures and with the addition of halide salts [160]. This effect is also observed in the current work where the pH values of *Pseudochoricystis* processed in sodium chloride are lower compared to the samples processed in deionised water. Interestingly the amount of  $\text{PO}_4^{3-}$  detected in the *Chlorogloeopsis* sample is higher at the lower temperatures and decreases to a third at the highest temperature, leading to the conclusion that if a process water high in  $\text{PO}_4^{3-}$  is required, for nutrient recycling or extraction, that mild processing conditions are favourable. Comparing these results with results published previously on HTL at 300°C for an hour, the concentrations are twice as high in the mild microwave processing [114]. The trend of increasing  $\text{PO}_4^{3-}$  concentrations in the process water is not observed for the marine strain *Nannochloropsis* where the concentrations increase by around 30 % at higher temperatures. The values of around 1000 mg/l  $\text{PO}_4^{3-}$  for *Nannochloropsis* allow the calculation of an elemental phosphorus (P) balance from the values measured in **Table 11.1** and indicate that up to 50 wt.% of the elemental algal P is recovered to the water phase. This value is between 30-40 wt.% for *Chlorogloeopsis* but only around 15-20 wt.% for *Pseudochoricystis*. *Nannochloropsis* is the only strain to exhibit acetate in the water phase, this is the reason the carbon recovery in the solid residue after microwaving is so much lower compared to the other samples. The reason for acetate formation from *Nannochloropsis* and not from the other two strains is not clear but could be due to different type of carbohydrates present in the algae strain. The levels of acetate are comparable to those observed from HTL of different algae presented in **Chapter 8** at more severe conditions of 300°C [114]. Acetate in the water phase can act as a substrate for heterotrophic microalgal growth as previously demonstrated [114, 141].

**Table 11.3:** Analysis of water phase after microwave treatment.

<i>Chlorogloeopsis</i>	(mg/l)	80°C	100°C	120°C	140°C
Na <sup>+</sup>		323	345	357	242
K <sup>+</sup>		174	179	188	140
NH <sub>4</sub> <sup>+</sup>		150	147	136	111
Acetate		47	38	34	57
Cl <sup>-</sup>		-	-	-	-
PO <sub>4</sub> <sup>3-</sup>		850	915	942	303
pH		7.97	7.64	7.73	7.42
<i>Nannochloropsis</i>	(mg/l)				
Na <sup>+</sup>		7662	8077	8325	8400
K <sup>+</sup>		716	772	787	799
NH <sub>4</sub> <sup>+</sup>		-	-	-	-
Acetate		1550	2240	748	2845
Cl <sup>-</sup>		4080	5248	5373	5628
PO <sub>4</sub> <sup>3-</sup>		708	930	778	1133
pH		7.56	7.42	7.66	7.19
<i>Pseudochoricystis</i>	(mg/l)				
Na <sup>+</sup>		110	84	103	104
K <sup>+</sup>		258	238	251	232
NH <sub>4</sub> <sup>+</sup>		-	-	-	-
Acetate		-	-	-	-
Cl <sup>-</sup>		54	27	34	31
PO <sub>4</sub> <sup>3-</sup>		207	118	147	159
pH		6.62	6.44	6.09	5.62
<i>Pseudochoricystis</i> NaCl	(mg/l)				
Na <sup>+</sup>		2122	2286	2183	2295
K <sup>+</sup>		236	262	256	259
NH <sub>4</sub> <sup>+</sup>		-	-	-	-
Acetate		-	-	-	-
Cl <sup>-</sup>		3406	3679	3472	3629
PO <sub>4</sub> <sup>3-</sup>		155	155	130	196
pH		6.71	6.66	5.09	5.54

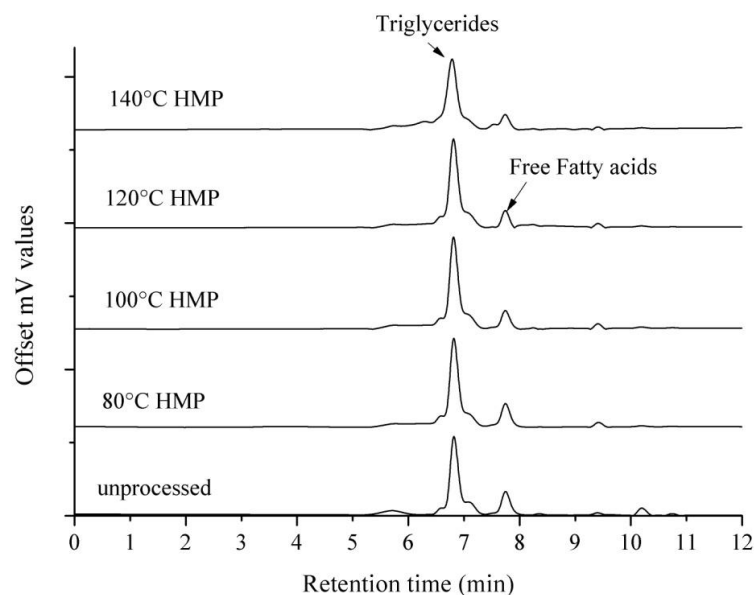
### 11.3.2 Lipid Extraction

Microwave processing has previously been suggested as a technique to facilitate lipid extraction using solvents. Cell disruption by microwaves as seen in **Figure 11.1-3** can lead to much higher recovery of lipids from microalgae than conventional solvent extraction alone. A study by Lee et al. (2010) identified microwave cell disruption as the most simple and efficient disruption method for the recovery of lipids from *Botryococcus sp.*, *Chlorella v.*, and *Scenedesmus sp.*. They investigated autoclaving, bead milling, microwave heating (100°C), sonification and osmotic shock [28]. In the current study simple solvent extraction using dichloromethane was carried out on unprocessed and microwaved samples. The yields of extraction are presented in **Table 11.4**. For all strains, microwaving had a large effect on the recovery of lipids. *Chlorogloeopsis* has a very low lipid content and yields of only 0.5 wt.% were observed when the unprocessed sample was subjected to solvent extraction. The recovery increased up to a maximum of 1.4 wt.% at the highest temperature of 140°C. Higher temperatures led to consistently increasing lipid extraction yields for *Chlorogloeopsis*. Untreated *Nannochloropsis* biomass yielded a 1.6 wt.% lipid recovery; this was increased to a maximum of 11.3 wt.% at 120°C. The microwave operating temperature did not show a strong effect on the lipid yields. The high lipid strain *Pseudochoricystis* had the highest yield of lipids when not subjected to microwave processing of 13.1 wt.%; this could be increased after microwaving to about 30-35 wt.%. Extraction yields increase both slightly with processing temperature for the NaCl processed and deionised water samples. The differences between the two are marginal indicating that the addition of sodium chloride does not have any beneficial effect on lipid extraction. The increase in lipid recovery is apparent for all three strains with 3-7 fold increases even at the lowest temperature investigated of 80°C. These results confirm the findings of Lee et al. who describe microwaving as a low energy intensive method of cell disruption for lipid recovery [28]. Size exclusion chromatography (SEC) was carried out on the samples to investigate if microwaving the samples had any effect on the composition or structures of the lipid fraction. Only minor shifts in profiles towards lower molecular weight compounds were observed indicating that hydrolysis of the lipids is not taking place (data not presented). This is beneficial if the lipids are extracted as polyunsaturated fatty acids, as these fatty acids are of high commercial value.

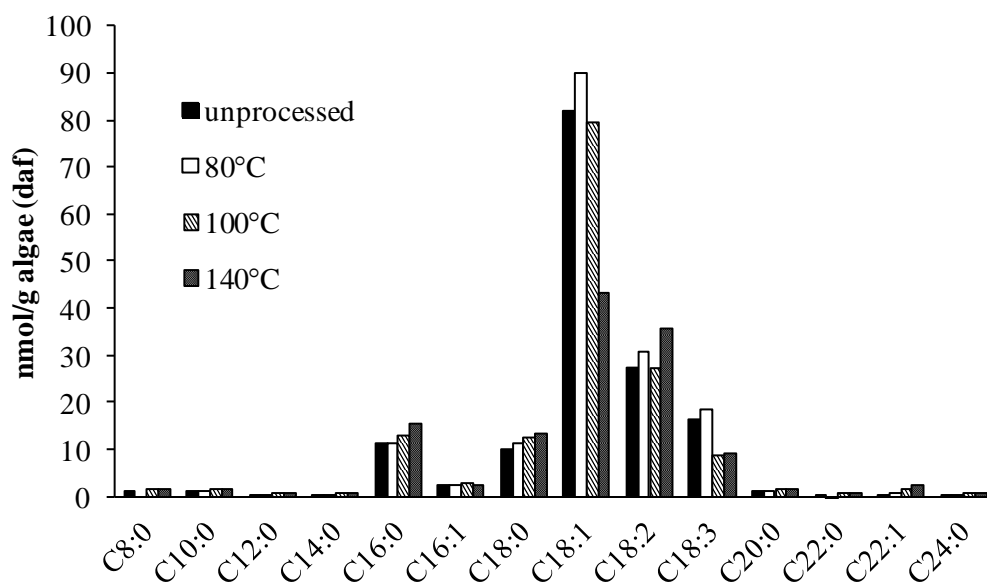
**Table 11.4:** Lipid extraction yields (wt.%) from solvent extraction using DCM

	<i>Chlorogloeopsis</i>	<i>Nannochloropsis</i>	<i>Pseudochoircystis</i>	<i>Pseudochoircystis</i> 0.1M NaCl
<b>unprocessed</b>	0.5	1.6	13.1	13.1
<b>80°C</b>	0.7	10.6	30.6	31.5
<b>100°C</b>	1	10.5	33.2	33.2
<b>120°C</b>	1.2	11.3	31.4	34.4
<b>140°C</b>	1.4	10	37.5	35.3

Size exclusion chromatography (SEC) was carried out on the samples to investigate if microwave processing has any effect on the structures of the lipid fractions. A representative SEC chromatogram of the unprocessed and HMP lipids of *P. ellipsoidea* is plotted in **Figure 11.4**. It is shown that the majority of lipids are present as triglycerides which represent the largest peak at 6.9 min. This peak was identified to be in the range of Mw 1200, the second peak at 7.8 min is of Mw 420 and represents the free fatty acid fraction of the lipids. There are no changes in lipid profiles observed for the different HMP temperatures. This indicates that no significant hydrolysis of triglycerides to free fatty acids is taking place under HMP.

**Figure 11.4:** HPLC-SEC chromatogram of *P.ellipsoidea* indicating the triglyceride and free fatty acid fractions

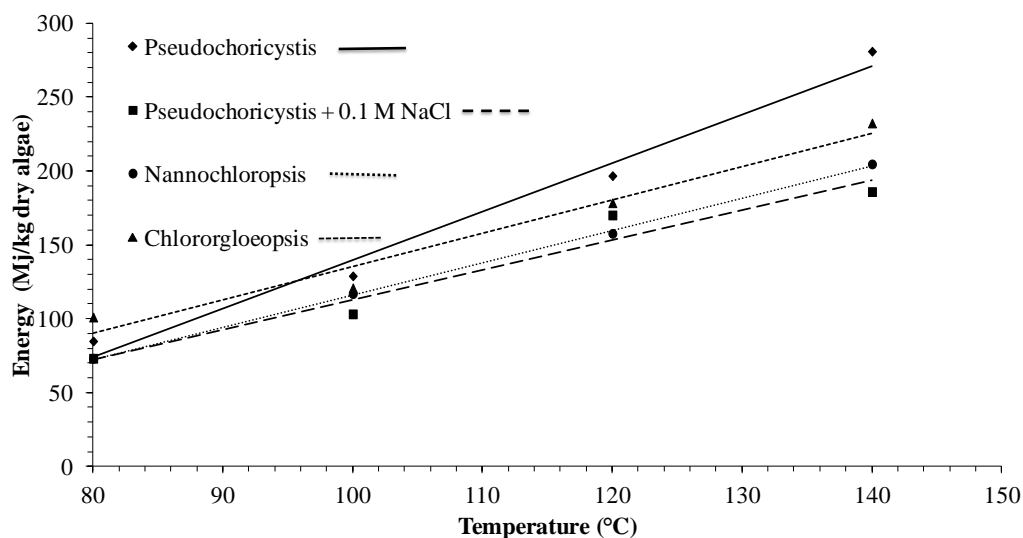
Additionally the lipids were analysed for fatty acid composition after transesterification. **Figure 11.5** plots the distribution of the fatty acids which were included in the calibration standard. It is known that this algae additionally contains significant amounts of C16:2 and C16:3 which were not included in the analysis [166]. The profiles show no change in carbon chain saturation at 80°C HMP. At 100°C around half the C18:3 fatty acids disappear with the remaining fatty acids being present in identical concentrations. At the highest temperature about half the C18:1 fatty acids are also removed and slight increased levels of C18:0 and C18:2 are observed. It is likely that double bonds are removed at the maximum temperature leading to an increase of saturated fatty acids. This leads to the conclusion that polyunsaturated fatty acids can be extracted undamaged with no loss of degree of saturation using HMP at 80°C despite the high sensitivity of omega-3 fatty acids to thermal processing. This is beneficial if the lipids are extracted as polyunsaturated fatty acids, as these fatty acids are of high commercial value. Additionally it was shown in **Table 4** that the extraction efficiency is already greatly improved at the 80°C HMP temperature.



**Figure 11.5:** Distribution of fatty acid methyl esters from unprocessed and HMP samples of *P. ellipsoidea* at 80°C, 100°C and 140°C.

The power required to heat the reactants to the desired temperature and residence time were logged by the microwave reactor and automatically integrated to Wh values to determine the energy used. The Wh were converted to MJ/kg of dry algae to allow comparison to data published in literature and is plotted in **Figure 11.6**. It is apparent that more energy is used at the higher temperatures and the trend lines plotted show that the increase is linear. The increase in energy requirement from 80°C to 140°C is around 230-330 % depending on the sample. The low ash and low halide salt

containing sample *P. ellipsoidea* exhibits the largest increase in energy consumption. This sample also has the largest energy requirement at 100, 120 and 140°C of all samples, indicated by the solid trend line in **Figure 11.6**. The second largest amount of energy is required to heat the *C. fritschii* sample followed by *Nannochloropsis* and the lowest being *P. ellipsoidea* processed in 0.1M NaCl. This trend follows the amount of microwave absorbing inorganics, such as halide salts, present in the sample. The energy requirement to heat *P. ellipsoidea* in pure water to 140°C is 66 % higher than for the sample processed in 0.1M NaCl. This shows that microwave processing of marine algae samples or macroalgae which are also high in ash content is beneficial for two reasons; firstly this technique removes large amounts of the inorganic ash fraction, upgrading the biomass feedstock for further processing. Secondly this approach of heating biomass in salt water takes advantage of the increase in heating by ionic conductance resulting in lower energy requirements to heat the reactants to the desired processing temperature. The values in **Fig. 11.4** range from 70-270 MJ/kg algae while the original feedstock only contains a maximum of 29 MJ/kg. Clearly it appears to be energetically unfeasible to process microalgae using HMP regarding these values. However it has to be considered that this is a laboratory study with the main objective of investigating the effects of HMP rather than energy usage. Continuous processing in the reactor also deserves investigation as this can greatly decrease the applied power. Nevertheless the current study compares favourably to other pre-treatment methods such as sonication (132 MJ/kg algae), high-pressure homogenisation (529 MJ/kg), bead milling (504 MJ/kg) and other microwave processing studies (140-420 MJ/kg) [167].



**Figure 11.6:** Energy requirement to heat samples to desired temperature at constant heating rate and residence time.

### 11.3.3 Hydrothermal processing of pre-treated algae

Hydrothermal microwave processing was evaluated as a pre-treatment technique for the production of a bio-crude by hydrothermal liquefaction. Similar work was carried out previously by Miao et al. where conventional heating was used to hydrothermally pre-treat *Chlorella* before liquefaction for bio-crude production. Their investigation showed positive results as valuable polysaccharides were extracted in the first step, reducing the overall energy requirements and producing a lower amount of unwanted solid residue in the process [74]. In the current work the microwaved residues were subjected to HTL at 300°C for 15 min and compared to unprocessed samples. The results presented in Table 6 show that the yields of bio-crude did not increase significantly for *Nannochloropsis* and *Chlorogloeopsis*. It should be noted that the yields were calculated on a *dry ash free* basis, therefore the yields of *Nannochloropsis* on a *as-received* basis would be much higher for the pre-treated samples than for the untreated sample as this exhibits an ash content of 25 wt.% compared to ~5 wt.% for the microwaved samples (see **Table 11.2**). One of the aims of pre-treating the algae was to reduce the amount of nitrogen in the final product which does not occur to any significant extent for *Chlorogloeopsis* or *Nannochloropsis*. The sample of *Chlorogloeopsis* at 140°C did show a decrease of nitrogen content of almost 1 wt.% however the oxygen content increased leading to a lower HHV. Apart from the higher yields of bio-crude on an *as-received* basis for *Nannochloropsis* microwave pre-treatment for HTL for *Nannochloropsis* and *Chlorogloeopsis* does not appear particularly beneficial. However the results for *Pseudochoricystis* are more positive; the amount of nitrogen in the bio-crude decreases consistently with increasing pre-treatment temperature. This can be expected from the mass balance presented in **Table 11.2**, as more nitrogen is fractionated to the water phase. The nitrogen content is reduced from 1.7 wt.% to 0.6 wt.% at the 140°C. Additionally the yields of bio-crude increase from 33.4 wt.% to a maximum of 49.5 wt.%, this is most likely due to some initial hydrolysis reactions of the algae compounds which are more easily converted to bio-crude during HTL. The HHV was increased by almost 10 MJ/kg as a result of the decreasing amounts of oxygen in the bio-crude. This was reduced from 20 wt.% to 10.5 wt.%. These results show that the bio-crude quality is increased significantly when the *Pseudochoricystis* samples are pre-treated by microwave irradiation with minimum energy requirements.



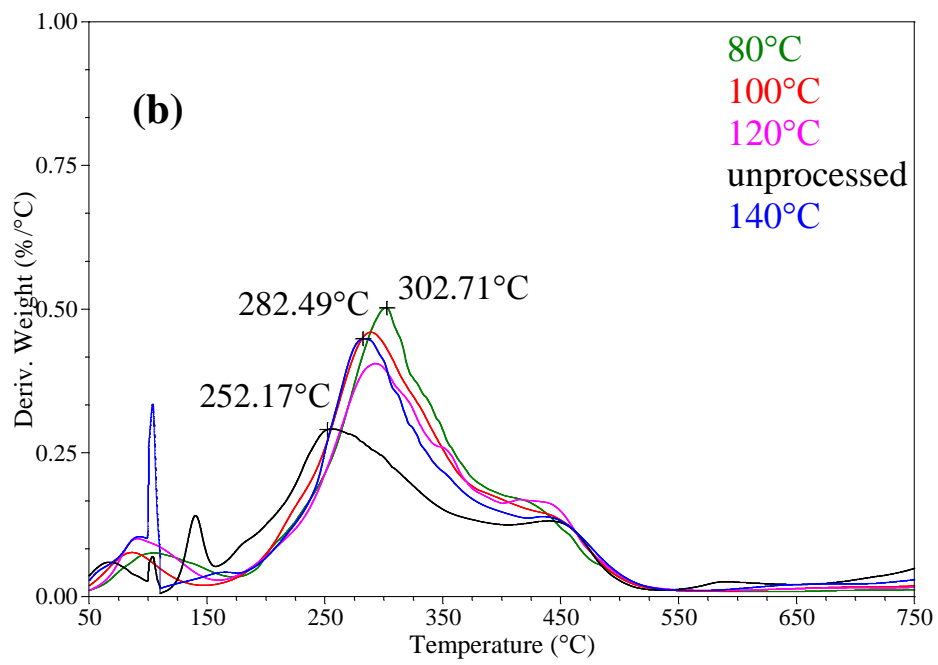
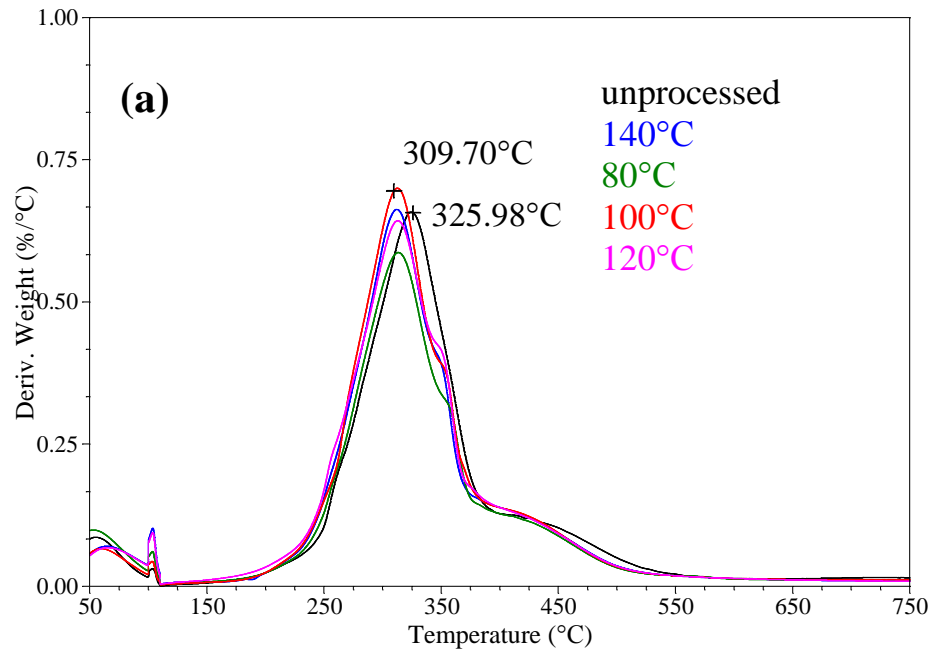
**Table 11.5:** Bio-crude yields, elemental composition and HHV from the hydrothermal liquefaction of pre-treated algae.

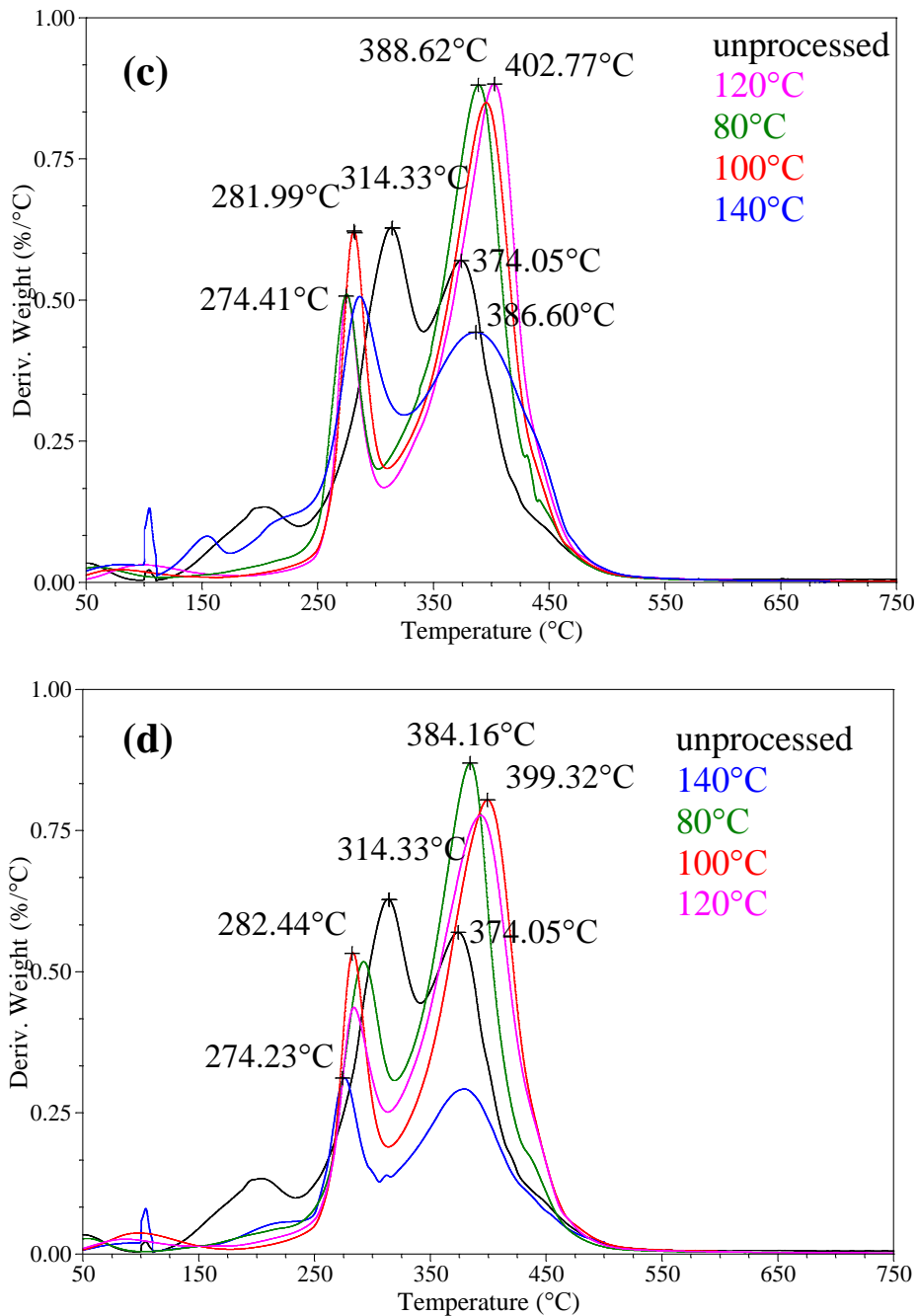
Sample	Bio-crude yield		Ultimate analysis (wt. % daf)					HHV (MJ/kg)
	HMP Temp	(wt. %daf)	C	H	N	S	O	
<i>Nannochloropsis</i>	raw	25.7	72.3	10.6	4.5	0.0	12.6	40.8
	80°C	24.6	73.1	10.2	4.9	0.0	11.9	40.4
	100°C	29.4	67.6	10.2	4.7	0.0	17.5	39.1
	120°C	22.5	70.2	9.1	4.9	0.0	15.8	38.2
	140°C	26.5	73.2	10.8	5.1	0.0	10.9	41.3
<i>Chlorogloeopsis</i>	raw	20.5	69.1	8.9	5.5	0.0	16.5	37.7
	80°C	18.8	68.8	9.1	6.9	0.0	15.2	37.7
	100°C	18.0	67.3	8.8	6.0	0.0	17.9	37.0
	120°C	19.7	65.5	9.1	6.4	0.0	19.0	37.0
	140°C	23.9	63.6	8.1	4.7	0.0	23.6	35.3
<i>Pseudochoricystis</i>	raw	33.4	72.3	6.1	1.7	0.0	19.9	35.0
	80°C	43.0	74.0	11.6	0.8	0.0	13.6	42.9
	100°C	47.4	74.7	11.6	0.9	0.0	12.8	43.1
	120°C	49.5	77.1	11.0	0.8	0.0	11.1	42.9
	140°C	44.1	76.7	12.2	0.6	0.0	10.5	44.4

### 11.3.4 Pyrolysis behaviour

**Figure 11.7 a-d** show the derivatives of the thermo-gravimetric data vs temperature for the three samples investigated plus *Pseudochoricystis* in 0.1M NaCl. The pyrolysis behaviour of *Chlorogloeopsis* (**Figure 11.7(a)**) is not affected significantly when pre-treated under hydrothermal microwave conditions. The main devolatilisation peak only shifts from 326°C to around 310°C, indicating slight upgrading of the biomass. *Nannochloropsis* behaves quite different under these slow pyrolysis conditions; the main devolatilisation peaks are shifted to higher temperatures. This is most likely do to removal of the inorganic ash which has previously been shown to catalyse pyrolysis reactions [168]. The removal of inorganics results in the main devolatilisation peaks occurring at 50°C higher temperatures for 80°C HMP samples compared to unprocessed samples.

The biomass is subsequently upgraded slightly with higher HMP temperatures, lowering the main devolatilisation peaks down to 280°C. The shoulders at the end of the plots of *Chlorogloeopsis* and *Nannochloropsis* at around 450°C represent the lipid fraction of the lipids which have a high boiling point. This has previously been shown to occur for microalgal lipids at this temperature range in **Chapter 6**. *Pseudochoricystis* processed in deionised water exhibits a definitive peak at around 450°C which is due to the large amount of lipids present in this algae sample. The other peaks represent the remaining biochemical components of the microalgae such as protein and carbohydrates. Additionally this specific strain is known to produce aliphatic hydrocarbons which devolatilise at lower temperatures [104]. The peaks at around 200°C most likely represent these hydrocarbons devolatilising. The peaks representing the lipids at around 380°C are not affected significantly by HMP; however their height is increased indicating that the relative amount of lipids to other biochemical components is increased. This is desirable regarding biofuels applications as the lipids and hydrocarbons result in better bio-crude quality from pyrolysis and HTL. The peak of the unprocessed sample at 314°C is lowered to around 275°C following HMP which suggests upgrading of the biomass. The lipid peak of the sample pre-treated at 140°C is considerably smaller, suggesting that hydrolysis of the triglycerides occurs at this temperature. The samples processed in 0.1 M NaCl appear very similar to the deionised water processed samples; therefore the advantages of processing in a salt solution appear to be beneficial for energy consumption reasons but the effects are negligible on the biomass pyrolysis behaviour.





**Figure 11.7:** DTG pyrolysis plots of pre-treated and raw algae in nitrogen at 50-750°C of (a) *Chlorogloeopsis*, (b) *Nannochloropsis*, (c) *Pseudochoricystis* and (d) *Pseudochoricystis* in 0.1M NaCl.

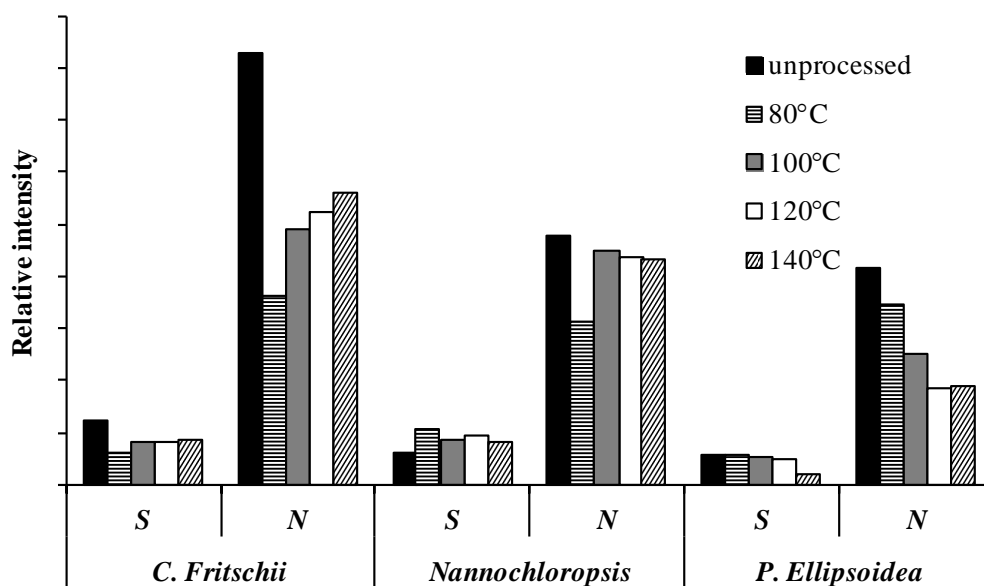
The HMP samples were additionally investigated by flash pyrolysis at 500°C for 20 sec and analysed by a combination of Py-GC-MS/AED. The pyrolysis volatile yields were calculated on a dry ash free basis and are presented in **Table 11.6**. It is shown that the yields of volatile bio-crude for *Chlorogloeopsis* are within approximately 10 % but reach the highest value of 81 wt.% at the highest HMP temperature. At the low HMP temperatures of 80 and 100°C the yields appear 10 % lower compared to the untreated sample. The yields for *Nannochloropsis* are all within a 5% range. However the yields take the ash and moisture content into account (dry ash free basis). On an as received basis the yields would be much higher as the unprocessed sample exhibits 20 wt.% more ash compared to the HMP samples (see **Table 11.2**). The *Pseudochoricystis* yields don't differ significantly between the unprocessed and pre-treated samples, a 5 wt.% increase is seen for all samples indicating slight upgrading of flash pyrolysis behaviour.

**Table 11.7:** Flash Pyrolysis volatiles yields on a dry ash free basis.

<i>Condition</i>	<i>Chlorogloeopsis</i>	<i>Nannochloropsis</i>	<i>Pseudochoricystis</i>
	<i>Yield (wt.% daf)</i>		
raw	76.6	62.6	55.8
80°C	69.9	66.4	59.4
100°C	69.5	60.5	56.0
120°C	72.2	63.2	60.4
140°C	81.0	64.1	59.8

The total amount of nitrogen and sulphur in the flash pyrolysis volatiles from the different samples was detected by GC-AED and is presented in **Figure 11.8**. These two elements can cause problems when pyrolysis oils are upgraded due to catalyst poisoning during hydro-treating and due to increased emissions of NO<sub>x</sub> and SO<sub>x</sub> upon combustion. Therefore the concentrations of these elements should be kept to a minimum. The amounts of each element were calculated by comparing the total areas of the element specific chromatograms from the GC-AED and compared to each other. The amount of nitrogen during flash pyrolysis of *Chlorogloeopsis* is highest of all algae strains but reduces significantly when the strain is subjected to HMP. Surprisingly the lowest amount of nitrogen and sulphur are found at the lowest pre-treatment temperature of 80°C. The

balance on nitrogen in **Table 11.2** for the current data do not explain the cause for this observation. This finding deserves further investigation and is the focus of ongoing work. The N and S content of *Nannochloropsis* bio-crude volatiles show slightly different trends with an observed increase in S content and only a slight decrease in N content. The nitrogen content of the sample at 80°C HMP temperature is lowest for *Chlorogloeopsis*. The samples pre-treated at 100, 120 and 140°C have a similar but slightly lower N content to the untreated sample. *Pseudochoricystis* exhibits the lowest nitrogen content of the unprocessed algae samples which is expected due to the low protein content of this sample. For *Pseudochoricystis* the nitrogen and sulphur contents of the bio-crudes decrease consistently with increasing microwave processing temperature which agrees with the data of nitrogen recovery presented in **Table 11.2**. The results on heteroatom content, derived using Py-GC-MS, suggest that hydrothermal microwave treatment results in bio-crudes from flash pyrolysis with lower nitrogen and sulphur contents.



**Figure 11.8:** Relative amounts of Nitrogen and Sulphur present in the bio-crude from flash pyrolysis detected by Py-GC-AED.

## 11.4 Conclusions

Hydrothermal microwave processing has been demonstrated to be a low energy intensive processing method for wet biomass such as microalgae. The process is especially suited for high ash, marine strains or macroalgae as the inorganic salts act as microwave absorbers allowing further saving on energy input and increased reaction rates. The microalgae doped with 0.1M NaCl and the naturally high ash containing algae *Nannochloropsis* were shown to use considerably less energy to reach reaction temperature compared to samples low in salt. HMP was shown to increase simple lipid recovery by solvent extraction 3-7 fold and showed beneficial effects on the hydrothermal liquefaction behaviour to produce a bio-crude of increased quality. Even at mild processing conditions large amounts of the nutrients such as P and N are recovered for recycling in the water phase and simultaneously upgrading the biomass feedstock. The ash fraction of *Nannochloropsis* was reduced from 26 to around 5 wt.%, improving its suitability as a feedstock for combustion. Moreover the yields of bio-crude from flash pyrolysis and HTL were increased. TGA analysis revealed that the pyrolysis performance of *Pseudochoricystis* and *Chlorogloeopsis* improved by lowering devolatilisation temperatures. The bio-crudes produced from flash pyrolysis were shown to contain less nitrogen and sulphur after hydrothermal microwave processing for all three strains. At the low processing temperatures investigated the extracted compounds such as polysaccharides and fatty acids are undamaged, effectively allowing the simultaneous extraction of bio-products, pre-treatment for bio-fuel production and nutrient recovery or recuperation.

## 12. CHAPTER XII – Conclusions, Implication and Future Work

The introduction of the thesis identifies the current need to diversify our energy sources due to climate change and depletion of fossil fuels. Microalgae are identified as a suitable alternative feedstock for third generation biofuels, due to their fast growth rates and lipid accumulation. However cultivation is still costly, representing the area with the largest uncertainties. Hydrothermal processing is identified as one of the most appropriate conversion routes as it allows processing of wet slurries. HTL has received increasing attention in the published literature, however, while considerable amounts of research has been conducted in batch reactors this is the first to evaluate a continuous system. One of the draw backs identified is the high nitrogen content in the produced bio-crude. Utilisation of homogeneous and heterogeneous catalysts has been investigated with the aim of improving the bio-crude quality. The combination of experimental work performed and an assessment of the literature leads to the conclusion that the products from HTL are highly strain and system specific. The concept of a closed loop system of bio-crude production from microalgae under HTL conditions is introduced. This involves the recovery of nutrients from the process water to grow algae as well as looping the produced CO<sub>2</sub> to the cultivation stage for enhanced algae growth. The residual solid residue is envisioned to be useful as a bio-char fertiliser while the primary product bio-crude can further be upgraded to drop in fuels.

### 12.1 Experimental studies

The characterisation of the microalgae feedstocks gives an overview of their compositions and feasibility as a feedstock for bio-crude production. The large variety of analysis parameters and algae strains presents a significant contribution to the characterisation of microalgae strains commonly used for bioenergy applications.

The hydrothermal liquefaction of algae studies in **Chapter 5** present data on 11 different microalgae strains at constant conditions. This data represents the single largest data set of different strains and their hydrothermal liquefaction performance available to date. The average bio-crude yield was shown to be 33.7 wt.% with a nitrogen content of 4.7 wt.% and an oxygen content of 13.6 wt.%, resulting in a HHV of 36.0 MJ/kg. In terms of HHV and yields these results are a success concerning the overall aim of the thesis to produce a bio-crude from HTL of microalgae. However it is made apparent that the main challenge still outstanding in HTL of microalgae is reducing the



nitrogen content in the bio-crude. The HHV, oxygen content and yields fall into acceptable levels suitable for combustion or upgrading. The variety of strains investigated is significant for future applications and feasibility studies when assessing the viability of a HTL system.

The effect of operating conditions on the HTL of microalgae has been the focus of numerous publications in the literature; therefore this was not a major part of the current work. Experimental data in this thesis and the literature review suggest that the optimum operating temperature and residence time in batch systems lies at around 15 min and 300°C. However, as highlighted by several researchers and herein, operating conditions are highly strain specific and processing system dependant.

Due to some undesirable properties of the produced bio-crude, the use of different catalysts were investigated to reduce the viscosity, oxygen and nitrogen content in **Chapter 6**. The use of organic acid catalysts during HTL results in increased yields of bio-crude compared to alkali catalysts. The heating value of the bio-crudes are higher using the alkali catalysts however there is a noticeable reduction in the boiling point range and improvement of flow properties when using organic acids. The molecular weight and boiling point of the bio-crudes were still relatively high using homogeneous catalysts. The use of organic acids does not reduce the nitrogen content in the bio-crudes. The majority of the fuel nitrogen is concentrated in the aqueous phase as ammonium, and this represents a suitable nitrogen recycle to sustain algal growth. No evidence for hydrogenation of the bio-crude was observed using organic acids. *In-situ* hydrogenation and upgrading of bio-crudes may be possible using organic acids but it is likely that additional catalysts are required. The results in **Chapter 6** show that lower boiling point bio-crudes can be produced but are unsuccessful towards to overall aim of reducing the nitrogen content in the bio-crude in a significant way. Therefore the use of homogeneous catalysts is not deemed a suitable route towards the production for refinery ready or combustible bio-crude.

The results of the second part of **Chapter 6** show that the majority of the lipids decompose to fatty acids, and the majority of the carbon double bonds are hydrogenated during HTL. The use of heterogeneous catalysts was shown to deoxygenate the bio-crude by a further 5-10 wt.%, resulting in an oxygen removal of up to 67 % for the microalgae feedstock and 64 wt.% for soya oil. The Co/Mo and Pt/Al catalyst were shown to reduce the amount of water soluble organic material and by this mechanism increase the bio-crude yields. SEC analysis illustrates that the molecular weight is reduced significantly by hydrothermal processing and can be further decreased by the use of heterogeneous catalysts. The use of the Ni/Al catalyst successfully deoxygenates around 60 wt.% of

the fatty acids from hydrothermal processing of soya oil to smaller chain alkanes. These results suggest there is potential for both improving yields, reducing boiling point range and improving the HHV of bio-crudes using heterogeneous catalysts. However the additional cost of catalysts and the remaining high nitrogen in the bio-crude suggest are still outstanding issues towards the goal of a bio-refinery ready bio-crude.

From the liquefaction results, presented in **Chapter 7**, of model compounds and microalgae it was demonstrated that the bio-crude formation follows the trend lipids>proteins>carbohydrates. Lipids produce bio-crude yields of 80-55 wt.%, protein 18-11 wt.% and carbohydrates 15-6 wt.%. Both proteins and lipids are converted to bio-crude most efficiently without the use of catalysts while carbohydrates are best processed using  $\text{Na}_2\text{CO}_3$ . This is shown by the liquefaction of the model compounds and also agrees with the results of the high protein and high lipid microalgae, *Spirulina* and *Nannochloropsis* respectively. The processing of carbohydrates using sodium carbonate results in significantly increased bio-crude yields for both the model compounds as well as the high carbohydrate containing microalgae *Porphyridium*.  $\text{Na}_2\text{CO}_3$  selectively increases the decarboxylation of carbohydrates. Very high lipid containing algae are best processed using no catalyst as this gives the highest bio-crude yields. Using alkali such as  $\text{Na}_2\text{CO}_3$  for high lipid algae results in saponification reactions.

It was further shown that the different biochemical compositions of microalgae behave additively, which means higher oil yields than lipid contents can be achieved by HTL. This is a distinct advantage compared to conventional physical extraction methods for bio-diesel production. GC-MS results show that formic acid and water liquefaction produce very similar bio-crude components. Proteins produce large amounts of nitrogen heterocycles, pyrroles and indoles, carbohydrates produce cyclic ketones as well as phenols while lipids are converted to fatty acids. High protein containing algae therefore were shown to produce larger amounts of nitrogen compounds. These results are significant in understanding the hydrothermal chemistry of bio-crude production. The objective outlined for this Chapter was met and the results are helpful in achieving the aim of producing bio-crude from microalgae.

Analysis of the HTL water phase in **Chapter 5** and **8** indicates the presence of high levels of nutrients suitable for recycling for algal cultivation. Levels of nitrogen were shown to be 75-200 times higher compared to a standard BBM growth medium. Growth trials in the recycled process water showed that heavy dilution is necessary to avoid the effects of growth inhibitors. The algae strains investigated, were able to grow in the recycled water but different optimum dilutions were

observed. All examined strains were able to use acetate as a substrate for mixotrophic growth and  $\text{NH}_4^+$  as a source of nitrogen and no ammonium toxicity was observed. *Chlorogloeopsis* at 400× and *Chlorella* at 200× dilutions achieved higher biomass yields than in their respective media by growing mixotrophically. The analysis of the spent water after cultivation revealed that the majority of acetate and ammonium was removed by the algae. It was demonstrated that the optimum dilution is strain dependent but ranges between 200-400×. By recycling the organic carbon in the water phase both the carbon efficiency and the biomass yields can be improved. This is one of the first detailed studies proving the feasibility of a closed loop system incorporating nutrient recycling which is a significant step towards the aim of producing sustainable bio-crude from microalgae.

The small scale cultivation trials in **Chapter 8** identified the need for new methods of analysis capable of using small sample amounts. By pyrolysing model compounds using Py-GC-MS, marker compounds were identified for different biochemical components from microalgae allowing subsequent detection of these in real samples and the estimation of the biochemical composition of unknown algae. Py-GC-MS of *Chlorella vulgaris*, grown in process water dilutions from HTL processing, demonstrated the method's ability to determine the level of protein, lipid and chlorophyll *a*. The results generated are in agreement with expectations based on published literature. The method was shown to be applicable for high value compounds such as astaxanthin. It is likely that the method can be applied to a wide range of compounds found in microalgae but further work is required to identify suitable marker compounds.

The work carried out in **Chapter 10** demonstrated the successful operation of a continuous flow pilot-scale HTL reactor system. Overall, more severe processing conditions increased yields, reduced the oxygen content and led to an increase in lower molecular weight bio-crude fraction being formed. It was also shown that the higher processing temperatures increase nitrogen levels as more of the protein present in the algae is liquefied and converted to bio-crude. These results from the continuous system are in agreement with results from batch processing in **Chapter 5**. These results represent the first investigation of HTL microalgae on a continuous system, proving the feasibility of this concept. This is a major step towards the industrial production of microalgae via HTL. Additionally the results demonstrate that heating and cooling rates have a much higher impact on bio-crude yields than previously identified in literature on batch systems. This has a significant impact on the commercialisation of HTL as it is shown that much lower residence times and high heating rates can lead to higher bio-crude yields.

Hydrothermal microwave processing (HMP) was investigated as a low energy intensive pre-treatment method for microalgae. The process is shown to be especially suited for high ash, marine strains or macroalgae as the inorganic salts act as microwave absorbers allowing further saving on energy input and increased reaction rates. The microalgae doped with 0.1M NaCl and the naturally high ash containing algae *Nannochloropsis* were shown to use considerably less energy to reach reaction temperature compared to samples low in salt. HMP was shown to increase simple lipid recovery by solvent extraction and showed beneficial effects on the hydrothermal liquefaction behaviour to produce a bio-crude of increased quality. Even at mild processing conditions large amounts of the nutrients such as P and N are recovered for recycling in the water phase and simultaneously upgrading the biomass feedstock. Moreover the yields of bio-crude from flash pyrolysis and HTL of the pre-treated algae were increased. The bio-crudes produced from flash pyrolysis were shown to contain less nitrogen and sulphur after hydrothermal microwave processing. At the low processing temperatures investigated the extracted compounds such as polysaccharides and fatty acids are undamaged, effectively allowing the simultaneous extraction of bio-products, pre-treatment for bio-fuel production and nutrient recovery or recuperation.

## 12.2 Implications for process development

The experimental data presented within this thesis represents a significant contribution to the research area of hydrothermal liquefaction of microalgae. The wide range of strains investigated at standard conditions shows the average yields and composition of bio-crude produced from HTL. Knowing the HTL products for different algae strains is helpful in the design of future HTL systems and mass and energy balances. The composition of bio-crudes greatly influences its suitability as a fuel for direct use or upgrading to higher quality fuels. The amount of nitrogen and oxygen contained in the bio-crude is the primary consideration for these applications and affects the cost of upgrading and emissions from combustion. The data presented now allows other researchers to calculate more accurate LCA for the entire process. When such a calculation is required for an algae strain which was not investigated in the current study, the results from **Chapter 7** on model compounds allow the extrapolation to a new algae strain based on the biochemical composition. Especially the mass and heat balances presented can aid the techno-economic analysis of future HTL systems.

The use of catalysts was investigated in **Chapter 6** and showed some improvements on the bio-crude quality and yields. The improvements however are not sufficient to increase the quality of the bio-crude to a standard which doesn't require further upgrading. Additionally the reusability, stability and cost of heterogeneous catalysts are areas of uncertainty that deserve more attention. The additional cost most likely doesn't justify the improvements especially if upgrading is possible for the non-catalysed HTL bio-crudes. The use of homogeneous catalysts equally exhibits additional cost and the recovery of catalyst causes a major challenge. Even though these catalysts are cheaper than heterogeneous catalysts their effects do not justify their use in a HTL system. The effect on the process water and its suitability for nutrient recycling is also an area of uncertainty that should be investigated before the employment of catalysts. However the de-oxygenation of lipids using a Ni/Al catalyst shown in **Chapter 6** could be a promising route towards the production of green diesel from lipid rich microalgae or vegetable oils.

For the envisioned closed loop process presented during this work **Chapter 8** presents the most detailed study to date on recycling of nutrients from HTL process water. The feasibility of recycling nutrients is proven for four different algae strains processed at two temperatures. This proof of concept is a major step towards commercialisation which can distinguish HTL from other microalgae biofuel production pathways. The cost of nutrients is a major factor in any industrialised process which can be reduced significantly with the proposed nutrient recycling. The organic carbon in the process water has previously been regarded as a major issue of HTL due to the reduced carbon efficiency of the process and the high cost of water remediation. As presented in the experimental work of the thesis, the majority of the organic carbon was shown to be consumed by mixotrophic algal growth, therefore increasing the carbon efficiency and reducing water remediation costs. The main cost driving nutrients N and P were efficiently recycled by algae in the process water. However a full mass balance on nutrients is required to facilitate a comprehensive LCA of the closed loop HTL process.

A further step towards the goal of a closed loop process for HTL biofuel production is presented in the experimental work on the continuous reactor at the University of Sydney. This represents the first study in literature where a continuous HTL reactor is operated successfully. This is a major step towards the commercialisation of the process. The data presented shows that even at low residence times, high bio-crude can be produced which increases the throughput of the system and improves the energy balance. It is expected that a continuous process is required to achieve a positive energy balance and cost effectiveness in a HTL system. Heat recovery and bio-crude

recovery are greatly improved on such a reactor system. The current work demonstrates that this is technically feasible on a pilot scale.

Hydrothermal microwave processing is demonstrated as a novel technique for extraction of phytochemicals and pre-treatment for bio-fuel applications. The concept has enormous potential for the targeted extraction of valuable compounds from microalgae. The temperature can be controlled accurately allowing efficient extraction of desired compounds. Additionally the energy consumption is low and benefits from microwave absorbing salts within microalgae. The technique could prove useful in an industrial process where high valuable compounds are extracted prior to processing the residue to bio-crude. This is the first contribution to the literature on HMP of microalgae with results presented on lipid and nutrient extraction, energy consumption and further processing. The results are promising especially for high salt containing microalgae which could damage stainless steel reactor systems as investigated in the current work.

Overall the results presented within the thesis lead to the conclusion that the field of algal biomass as a renewable source of energy is still relatively new and unexplored. The potential is large due to the extraordinary growth rates and oil contents that some microalgae strains can achieve. Large amounts of resources are currently being invested into research on the cultivation of microalgae; including PBR design, strain identification/selection, nutrient optimization and harvesting technologies. If strains are identified which are able to grow fast, are resistant to external influences/bacteria and can grow in brackish/salt water and at the same time remediate waste water, the potential of microalgae is enormous. Hydrothermal treatment will most likely find its place in an energy system where algae are used due to its safe and cheap reactant ( $H_2O$ ). Any algal biomass source is expected to be processed wet as the energy required for drying is very high and would make most processes uneconomical. Garcia Alba et al. describe microalgae and HT processing in a biorefinery concept where high valuable compounds are extracted wet pre-HT processing [37], similar to the work presented in the thesis on hydrothermal microwave processing. This then allows HT treatment of the low valuable residue to bio-crude. Any commercial application of HT processing of algae would require the use of a continuous process where heat recovery can be incorporated, increasing the energy efficiency and allowing high throughput. The feasibility of such a system as presented during the current work. The engineering challenges on the processing side are relatively straight forward although high salt content and corrosion could pose problems. Nevertheless the main challenge lies in designing a biorefinery concept where the supply of aquatic biomass is substantial and cheap. If waste water treatment and high value products can be incorporated, the development could be accelerated significantly. Any future advances in this field

also largely depend on future legislation, the price of fossil energy and energy security but if these factors are favourable, HT technology with algal biomass could become reality in the next decade.

### 12.3 Future Work

The characterisation of microalgae feedstock presented in **Chapter 4** is comprehensive but ideally additional parameters should be investigated. The carbohydrate fraction deserves more attention; in particular the structural composition could prove to be significant. Only the total carbohydrate content was examined and no distinction of polysaccharide, di- and mono-saccharides is made. The overall sugar composition is also of interest, especially for the Py-GC-MS work carried out in **Chapter 9**. It would be desirable to know the fatty acid profiles of different microalgae strains in order to examine their fate during HTL. Additionally, fully quantitative analysis of the pigments should be performed.

The thesis describes the hydrothermal liquefaction of different microalgae strains before investigating the effect of operating conditions. Operating conditions are only examined for one algae strain at constant solids loading and heating rates. This parametric study deserves further attention as it was shown that different microalgae strains results in different bio-crude yields and properties. Especially the effect of temperature and residence time should be investigated for a wider range of algae classes such as marine strains, cyanobacteria and diatoms. The work carried out on model compounds should include varying operating conditions. This would shed light on the most favourable process conditions of biochemical components and predictions of optimum processing conditions for different algae strains. The work on model compounds revealed very useful data but additional model compounds such as chlorophyll *a*, complex carbohydrates and fatty acids of different saturations should be investigated. This would allow a more thorough understanding of the hydrothermal chemistry of microalgae.

The catalytic HTL using heterogeneous catalysts showed the potential for deoxygenation and improved bio-crude yields. However the work on this subject deserves more attention. The results indicated that catalysts influence biochemical components differently and this should be investigated by processing model compounds. Transition metal catalysts of Fe, Co, Cu and Ni should be investigated with model compounds and microalgae. There is also a potential of using zeolite catalysts during HTL which deserves investigation.

It could be shown that nutrient recycling using the aqueous phase from HTL is possible but some growth inhibition was observed. The inhibiting compounds need to be identified by doping growth media with e.g. phenols and nickel. Identifying the growth inhibitors is essential in order to be able to remove them from the water phase or alter the process to produce less of the inhibiting compounds. Additionally growth trials need to be scaled up in order to grow enough biomass to run a new HTL experiment. It would be interesting to see how the algae composition changes after a few repeats and the levels of inorganics and inhibitors in the water phase are affected. From these results a comprehensive balance on nutrients could be calculated which would be a step forward towards commercialisation. The growth trials should also be carried out on process water from the continuous reactor.

The new analysis technique using Py-GC-MS is introduced in **Chapter 9** and showed very promising results. Nevertheless there is room for improvement; the method requires full quantification and comparison to conventional analysis techniques. The wet analysis technique from live cultures requires more repeats and the growth rates need to be compared to standard growth estimation methods. The potential of the technique to investigate concentrations of high value compounds was demonstrated and is likely to be applicable to a wider range of compounds. By pyrolysing standards of high value compounds an attempt should be made to expand the technique to additional phytochemicals.

The continuous HTL reactor results show the feasibility of processing microalgae at pilot scale. The main area of uncertainty is the unaccounted carbon lost to the system, this requires investigation. The solids loading was initially only examined at 1 wt.% which is not economical, therefore solids loadings of 10 wt.% and higher need to be assessed. Due to the low solids loading solvents were used to recover the bio-crude. Future work should include recovery of the bio-crude without the use of solvents.

Hydrothermal microwave processing is shown to be a promising new technique for extraction of microalgae components and pre-treatment for biofuel production. To understand the chemical and physical reactions under microwave irradiation in water, model compounds should be processed at varying operating conditions. The development of a continuous system is also desirable as this could greatly reduce the energy demand. There is a high potential of using catalysts in microwave systems due to their high absorbance which could greatly influence reaction pathways.



### 13. References

1. Perry, R.H. and D.W. Green, *Perry's Chemical Engineers' Handbook (7th Edition)*. 1997, McGraw-Hill.
2. *A look back at the U.S. Department of Energy's Aquatic Species Program [electronic resource] : biodiesel from algae / by John Sheehan ... [et al.] ; prepared by the National Renewable Energy Laboratory*. NREL/TP ; 580-24190, ed. J. Sheehan and L. National Renewable Energy. 1998, Golden, Colo. :: National Renewable Energy Laboratory.
3. Gallagher, E., *The Gallagher Review of Biofuels*. Renewable Fuels Agency, 2008. **St Leonards-on-Sea, UK**.
4. (IEA), I.E.A., *CO2 emissions from fuel combustion: highlights (2011 edition)*. 2011, Paris: OECD / IEA.
5. Transport, D.f. (2003) *UK Report to European Commission under Article 4 of the Biofuels Directive (2003/30/EC)*.
6. Transport, D.f., *Renewable Transport Fuels Obligation*. UK, 2011.
7. BP, *BP Statistical Review of World Energy 2012*.
8. Brennan, L. and P. Owende, *Biofuels from microalgae--A review of technologies for production, processing, and extractions of biofuels and co-products*. Renewable and Sustainable Energy Reviews, 2009. **14**(2): p. 557-577.
9. Li, Y., et al., *Biofuels from Microalgae*. Biotechnol. Prog., 2008. **24**: p. 815-820.
10. Schenk, P., et al., *Second Generation Biofuels: High-Efficiency Microalgae for Biodiesel Production*. BioEnergy Research, 2008. **1**(1): p. 20-43.
11. Falkowski, P.G. and J.A. Raven, *Aquatic Photosynthesis: Second Edition*. 2007: Princeton University Press.
12. Stephens, E., et al., *Future prospects of microalgal biofuel production systems*. Trends in Plant Science. **In Press, Corrected Proof**.
13. Wijffels, R.H., M.J. Barbosa, and M.H.M. Eppink, *Microalgae for the production of bulk chemicals and biofuels*. Biofuels, Bioproducts and Biorefining, 2010. **4**(3): p. 287-295.
14. Demirbas, A. and M. Fatih Demirbas, *Importance of algae oil as a source of biodiesel*. Energy Conversion and Management. **In Press, Corrected Proof**.
15. Lee, J.W., *Advanced Biofuels and Bioproducts*. 2012: Springer.
16. Rodolfi, L., et al., *Microalgae for Oil: Strain Selection, Induction of Lipid Synthesis and Outdoor Mass Cultivation in a Low-Cost Photobioreactor*. Biotechnology and Bioengineering, 2008. **102**(1): p. 100-112.
17. Chisti, Y., *Biodiesel from microalgae*. Biotechnology Advances. **25**(3): p. 294-306.
18. Brennan, L., et al., *Phytochemicals from Algae*, in *Biorefinery Co-Products*. 2012, John Wiley & Sons, Ltd. p. 199-240.
19. Spolaore, P., et al., *Commercial applications of microalgae*. Journal of Bioscience and Bioengineering, 2006. **101**(2): p. 87-96.
20. Grobbelaar, J.U., *Algal Nutrition - Mineral Nutrition*, in *Handbook of Microalgal Culture*, R. Amos, Editor. 2007. p. 95-115.
21. Pittman, J.K., A.P. Dean, and O. Osundeko, *The potential of sustainable algal biofuel production using wastewater resources*. Bioresource Technology, 2011. **102**(1): p. 17-25.
22. Borowitzka, M.A., *Commercial production of microalgae: ponds, tanks, tubes and fermenters*. Journal of Biotechnology, 1999. **70**(1-3): p. 313-321.
23. Draaisma, R.B., et al., *Food commodities from microalgae*. Current Opinion in Biotechnology, 2013. **24**(2): p. 169-177.

24. Miao, X. and Q. Wu, *Biodiesel production from heterotrophic microalgal oil*. *Bioresource Technology*, 2006. **97**(6): p. 841-846.
25. Meng, X., et al., *Biodiesel production from oleaginous microorganisms*. *Renewable Energy*, 2009. **34**(1): p. 1-5.
26. Philip T. Pienkos; Al Darzins, *The promise and challenges of microalgal-derived biofuels*. *Biofuels*, *Bioprod. Bioref.*, 2008. **3**: p. 431-440.
27. Bligh, E.G.D., W.J, *A rapid method for total lipid extraction and purification*. *J. Biochem. Physiol.*, 1959. **37**: p. 911-917.
28. Lee, J.-Y., et al., *Comparison of several methods for effective lipid extraction from microalgae*. *Bioresource Technology*, 2010. **101**(1, Supplement 1): p. S75-S77.
29. Xu, L., et al., *Assessment of a dry and a wet route for the production of biofuels from microalgae: Energy balance analysis*. *Bioresource Technology*, 2011. **102**(8): p. 5113-5122.
30. Laird, D.A., et al., *Impact of biochar amendments on the quality of a typical Midwestern agricultural soil*. *Geoderma*, 2010. **158**(3-4): p. 443-449.
31. Levine, R.B., T. Pinnarat, and P.E. Savage, *Biodiesel Production from Wet Algal Biomass through in Situ Lipid Hydrolysis and Supercritical Transesterification*. *Energy & Fuels*, 2010. **24**(9): p. 5235-5243.
32. Patil, P.D., et al., *Optimization of direct conversion of wet algae to biodiesel under supercritical methanol conditions*. *Bioresource Technology*, 2011. **102**(1): p. 118-122.
33. Matsui, T.-o., et al., *Liquefaction of micro-algae with iron catalyst*. *Fuel*, 1997. **76**(11): p. 1043-1048.
34. Ikenaga, N.-o., et al., *Co-liquefaction of Micro Algae with Coal Using Coal Liquefaction Catalysts*. *Energy & Fuels*, 2001. **15**(2): p. 350-355.
35. Peterson, A.A., et al., *Thermochemical biofuel production in hydrothermal media: A review of sub- and supercritical water technologies*. *Energy & Environmental Science*, 2008. **1**(1): p. 32-65.
36. Zhang, L., C. Xu, and P. Champagne, *Overview of recent advances in thermo-chemical conversion of biomass*. *Energy Conversion and Management*, 2010. **51**(5): p. 969-982.
37. Garcia Alba, L., et al., *Hydrothermal Treatment (HTT) of Microalgae: Evaluation of the process as conversion method in an Algae Biorefinery Concept*. *Energy & Fuels*, 2011.
38. Chakinala, A.G., et al., *Catalytic and Non-catalytic Supercritical Water Gasification of Microalgae and Glycerol*. *Industrial & Engineering Chemistry Research*, 2009. **49**(3): p. 1113-1122.
39. Kruse, A. and E. Dinjus, *Hot compressed water as reaction medium and reactant: Properties and synthesis reactions*. *The Journal of Supercritical Fluids*, 2007. **39**(3): p. 362-380.
40. Wagner, W. and A. Pruss, *The IAPWS Formulation 1995 for the Thermodynamic Properties of Ordinary Water Substance for General and Scientific Use*. *Journal of Physical and Chemical Reference Data*, 2002. **31**(2): p. 387-535.
41. Uematsu, M. and E.U. Frank, *Static Dielectric Constant of Water and Steam*. *Journal of Physical and Chemical Reference Data*, 1980. **9**(4): p. 1291-1306.
42. Bandura, A.V. and S.N. Lvov, *The Ionization Constant of Water over Wide Ranges of Temperature and Density*. *Journal of Physical and Chemical Reference Data*, 2006. **35**(1): p. 15-30.
43. Kruse, A. and E. Dinjus, *Hot compressed water as reaction medium and reactant: 2. Degradation reactions*. *The Journal of Supercritical Fluids*, 2007. **41**(3): p. 361-379.
44. Elliott, D.C., *Hydrothermal Processing*, in *Thermochemical Processing of Biomass*. 2011, John Wiley & Sons, Ltd. p. 200-231.
45. Toor, S.S., L. Rosendahl, and A. Rudolf, *Hydrothermal liquefaction of biomass: A review of subcritical water technologies*. *Energy*, 2011. **36**(5): p. 2328-2342.

46. Adams, J.M.M., et al., *Seasonal variation in the chemical composition of the bioenergy feedstock Laminaria digitata for thermochemical conversion*. *Bioresource Technology*, 2011. **102**(1): p. 226-234.
47. Ross, A.B., et al., *Hydrothermal processing of microalgae using alkali and organic acids*. *Fuel*, 2010. **89**(9): p. 2234-2243.
48. Jena, U., et al., *Evaluation of microalgae cultivation using recovered aqueous co-product from thermochemical liquefaction of algal biomass*. *Bioresource Technology*, 2011. **102**(3): p. 3380-3387.
49. Steinbeiss, S., G. Gleixner, and M. Antonietti, *Effect of biochar amendment on soil carbon balance and soil microbial activity*. *Soil Biology and Biochemistry*, 2009. **41**(6): p. 1301-1310.
50. Libra, J.A., et al., *Hydrothermal carbonization of biomass residuals: a comparative review of the chemistry, processes and applications of wet and dry pyrolysis*. *Biofuels*, 2010. **2**(1): p. 71-106.
51. Hu, B., et al., *Engineering Carbon Materials from the Hydrothermal Carbonization Process of Biomass*. *Advanced Materials*, 2010. **22**(7): p. 813-828.
52. Specht, F.B.H., *Die Anwendung hoher Drucke bei chemischen Vorgängen und eine Nachbildung des Entstehungsprozesses der Steinkohle*. Verlag Wilhelm Knapp, Halle an der Saale, 1913: p. 58.
53. Titirici, M.-M., A. Thomas, and M. Antonietti, *Back in the black: hydrothermal carbonization of plant material as an efficient chemical process to treat the CO<sub>2</sub> problem?* *New Journal of Chemistry*, 2007. **31**(6): p. 787-789.
54. Sevilla, M. and A.B. Fuertes, *Chemical and Structural Properties of Carbonaceous Products Obtained by Hydrothermal Carbonization of Saccharides*. *Chemistry – A European Journal*, 2009. **15**(16): p. 4195-4203.
55. Sevilla, M. and A.B. Fuertes, *The production of carbon materials by hydrothermal carbonization of cellulose*. *Carbon*, 2009. **47**(9): p. 2281-2289.
56. Heilmann, S.M., et al., *Hydrothermal carbonization of microalgae*. *Biomass and Bioenergy*, 2010. **34**(6): p. 875-882.
57. Heilmann, S.M., et al., *Hydrothermal carbonization of microalgae II. Fatty acid, char, and algal nutrient products*. *Applied Energy*, 2011. **88**(10): p. 3286-3290.
58. Yu, G., et al., *Distributions of carbon and nitrogen in the products from hydrothermal liquefaction of low-lipid microalgae*. *Energy & Environmental Science*, 2011. **4**(11): p. 4587-4595.
59. Anastasakis, K. and A.B. Ross, *Hydrothermal liquefaction of the brown macro-alga Laminaria Saccharina: Effect of reaction conditions on product distribution and composition*. *Bioresource Technology*, 2011. **102**(7): p. 4876-4883.
60. Duan, P. and P.E. Savage, *Upgrading of crude algal bio-oil in supercritical water*. *Bioresource Technology*, 2011. **102**(2): p. 1899-1906.
61. Duan, P. and P.E. Savage, *Catalytic hydrotreatment of crude algal bio-oil in supercritical water*. *Applied Catalysis B: Environmental*, 2011. **104**(1–2): p. 136-143.
62. Xiu, S. and A. Shahbazi, *Bio-oil production and upgrading research: A review*. *Renewable and Sustainable Energy Reviews*, 2012. **16**(7): p. 4406-4414.
63. Dote, Y., et al., *Recovery of liquid fuel from hydrocarbon-rich microalgae by thermochemical liquefaction*. *Fuel*, 1994. **73**(12): p. 1855-1857.
64. Inoue, S., et al., *Analysis of oil derived from liquefaction of Botryococcus Braunii*. *Biomass and Bioenergy*, 1994. **6**(4): p. 269-274.
65. Minowa, T., et al., *Oil production from algal cells of Dunaliella tertiolecta by direct thermochemical liquefaction*. *Fuel*, 1995. **74**(12): p. 1735-1738.

66. Sawayama, S., T. Minowa, and S.Y. Yokoyama, *Possibility of renewable energy production and CO<sub>2</sub> mitigation by thermochemical liquefaction of microalgae*. Biomass and Bioenergy, 1999. **17**(1): p. 33-39.
67. Jena, U., K.C. Das, and J.R. Kastner, *Effect of operating conditions of thermochemical liquefaction on biocrude production from Spirulina platensis*. Bioresource Technology, 2011. **102**(10): p. 6221-6229.
68. Brown, T.M., P. Duan, and P.E. Savage, *Hydrothermal Liquefaction and Gasification of Nannochloropsis sp.* Energy & Fuels, 2010. **24**(6): p. 3639-3646.
69. Yu, G., et al., *HYDROTHERMAL LIQUEFACTION OF Low LIPID CONTENT MICROALGAE INTO BIO-CRUDE OIL*. 2011, American Society of Agricultural Engineers: St. Joseph, MI, ETATS-UNIS. p. 239-246.
70. Zhou, D., et al., *Hydrothermal Liquefaction of Macroalgae Enteromorpha prolifera to Bio-oil*. Energy & Fuels, 2010. **24**(7): p. 4054-4061.
71. Torri, C., et al., *Hydrothermal Treatment (HTT) of Microalgae: Detailed molecular characterization of HTT oil in view of HTT mechanism elucidation*. Energy & Fuels, 2011.
72. Brown, T.M., P. Duan, and P.E. Savage, *Hydrothermal Liquefaction and Gasification of Nannochloropsis sp.* Energy & Fuels, 2010.
73. Chakraborty, M., et al., *Concomitant extraction of bio-oil and value added polysaccharides from Chlorella sorokiniana using a unique sequential hydrothermal extraction technology*. Fuel, 2012. **95**(0): p. 63-70.
74. Miao, C., M. Chakraborty, and S. Chen, *Impact of reaction conditions on the simultaneous production of polysaccharides and bio-oil from heterotrophically grown Chlorella sorokiniana by a unique sequential hydrothermal liquefaction process*. Bioresource Technology, 2012. **110**(0): p. 617-627.
75. Vardon, D.R., et al., *Thermochemical conversion of raw and defatted algal biomass via hydrothermal liquefaction and slow pyrolysis*. Bioresource Technology, 2012. **109**(0): p. 178-187.
76. Biller, P., R. Riley, and A.B. Ross, *Catalytic hydrothermal processing of microalgae: Decomposition and upgrading of lipids*. Bioresource Technology, 2011. **102**(7): p. 4841-4848.
77. Biller, P. and A.B. Ross, *Potential yields and properties of oil from the hydrothermal liquefaction of microalgae with different biochemical content*. Bioresource Technology, 2011. **102**(1): p. 215-225.
78. Vardon, D.R., et al., *Chemical properties of biocrude oil from the hydrothermal liquefaction of Spirulina algae, swine manure, and digested anaerobic sludge*. Bioresource Technology, 2011. **102**(17): p. 8295-8303.
79. Yang, Y.F., et al., *Analysis of energy conversion characteristics in liquefaction of algae*. Resources, Conservation and Recycling, 2004. **43**(1): p. 21-33.
80. Li, D., et al., *Preparation and characteristics of bio-oil from the marine brown alga Sargassum patens C. Agardh*. Bioresource Technology, (0).
81. Shuping, Z., et al., *Production and characterization of bio-oil from hydrothermal liquefaction of microalgae Dunaliella tertiolecta cake*. Energy, 2010. **35**(12): p. 5406-5411.
82. Zou, S., et al., *Thermochemical Catalytic Liquefaction of the Marine Microalgae Dunaliella tertiolecta and Characterization of Bio-oils*. Energy & Fuels, 2009. **23**(7): p. 3753-3758.
83. Jena, U., K.C. Das, and J.R. Kastner, *Comparison of the effects of Na<sub>2</sub>CO<sub>3</sub>, Ca<sub>3</sub>(PO<sub>4</sub>)<sub>2</sub>, and NiO catalysts on the thermochemical liquefaction of microalga Spirulina platensis*. Applied Energy, (0).
84. Savage, P.E., *A perspective on catalysis in sub- and supercritical water*. The Journal of Supercritical Fluids, 2009. **47**(3): p. 407-414.

85. Duan, P. and P.E. Savage, *Hydrothermal Liquefaction of a Microalga with Heterogeneous Catalysts*. Industrial & Engineering Chemistry Research, 2010; p. null-null.
86. Calzavara, Y., et al., *Evaluation of biomass gasification in supercritical water process for hydrogen production*. Energy Conversion and Management, 2005. **46**(4): p. 615-631.
87. Biller, P., et al., *Nutrient recycling of aqueous phase for microalgae cultivation from the hydrothermal liquefaction process*. Algal Research, (0).
88. Haiduc, A., et al., *SunCHem: an integrated process for the hydrothermal production of methane from microalgae and CO<sub>2</sub> mitigation*. Journal of Applied Phycology, 2009. **21**(5): p. 529-541.
89. Minowa, T. and S. Sawayama, *A novel microalgal system for energy production with nitrogen cycling*. Fuel, 1999. **78**(10): p. 1213-1215.
90. Stucki, S., et al., *Catalytic gasification of algae in supercritical water for biofuel production and carbon capture*. Energy & Environmental Science, 2009. **2**(5): p. 535-541.
91. Guan, Q., P.E. Savage, and C. Wei, *Gasification of alga Nannochloropsis sp. in supercritical water*. The Journal of Supercritical Fluids, (0).
92. Resende, F.L.P. and P.E. Savage, *Effect of Metals on Supercritical Water Gasification of Cellulose and Lignin*. Industrial & Engineering Chemistry Research, 2010. **49**(6): p. 2694-2700.
93. Resende, F.L.P. and P.E. Savage, *Expanded and Updated Results for Supercritical Water Gasification of Cellulose and Lignin in Metal-Free Reactors*. Energy & Fuels, 2009. **23**(12): p. 6213-6221.
94. Schumacher, M., et al., *Hydrothermal conversion of seaweeds in a batch autoclave*. The Journal of Supercritical Fluids, 2011. **58**(1): p. 131-135.
95. Yanik, J., et al., *Biomass gasification in supercritical water: Part 1. Effect of the nature of biomass*. Fuel, 2007. **86**(15): p. 2410-2415.
96. Frank, E., et al., *Life cycle comparison of hydrothermal liquefaction and lipid extraction pathways to renewable diesel from algae*. Mitigation and Adaptation Strategies for Global Change, 2012: p. 1-22.
97. Boer, K., et al., *Extraction and conversion pathways for microalgae to biodiesel: a review focused on energy consumption*. Journal of Applied Phycology, 2012. **24**(6): p. 1681-1698.
98. Tsukahara, K., et al., *Microalgal cultivation in a solution recovered from the low-temperature catalytic gasification of the microalga*. Journal of Bioscience and Bioengineering, 2001. **91**(3): p. 311-313.
99. Bordons, A. and J. Jofre, *Extracellular adsorption of nickel by a strain of Pseudomonas sp.* Enzyme and Microbial Technology, 1987. **9**(12): p. 709-713.
100. Spencer, D.F. and L.H. Nichols, *Free nickel ion inhibits growth of two species of green algae*. Environmental Pollution Series A, Ecological and Biological, 1983. **31**(2): p. 97-104.
101. Scragg, A.H., *The effect of phenol on the growth of Chlorella vulgaris and Chlorella VT-1*. Enzyme and Microbial Technology, 2006. **39**(4): p. 796-799.
102. Bosma, R., et al., *Growth inhibition of Monodus subterraneus by free fatty acids*. Biotechnology and Bioengineering, 2008. **101**(5): p. 1108-1114.
103. Cordell, D., J.-O. Drangert, and S. White, *The story of phosphorus: Global food security and food for thought*. Global Environmental Change, 2009. **19**(2): p. 292-305.
104. Imamura, S., et al., *Genetic transformation of *Pseudochoircystis ellipsoidea*, an aliphatic hydrocarbon-producing green alga*. The Journal of General and Applied Microbiology, 2012. **58**(1): p. 1-10.
105. Corbitt, R.A., *Standard Handbook of Environmental Engineering*. 1998, New York: McGraw-Hill Inc.
106. Waterborge, J., *The Lowery Method for protein quantification in Th Protein Protocols Handbook*, J.M. Walker, Editor. 2002, Human Press: New Jersey.

107. Gerchakov, S.M. and P.G. Hatcher, *Improved Technique for Analysis of Carbohydrates in Sediments*. Limnology and Oceanography, 1972. **17**(6): p. 938-943.
108. Wright, S.W., et al., *Improved HPLC method for the analysis of chlorophylls and carotenoids in marine phytoplankton*. Mar. Ecol. Progr. Ser., 1991. **77**: p. 183-196.
109. van Leeuwe, M.A., et al., *An optimized method for automated analysis of algal pigments by HPLC*. Marine Chemistry, 2006. **102**(3-4): p. 267-275.
110. Barrón, L. and G. Santa-María, *Non-aqueous reverse-phase HPLC analysis of triglycerides*. Chromatographia, 1987. **23**(3): p. 209-214.
111. Firestone, D.J., *Liquid Chromatography Method for Determination of Triglycerides in Vegetable Oils in Terms of Their Partition Numbers: Summary of a Collaborative Study*. Ass. Off. Anal. Chem. Int., 1994(77): p. 954-957.
112. Anastasakis, K., et al., *Predictive fouling behaviour of seaweed ash during combustion*. Proceedings of the bioten conference on biomass, bioenergy and biofuels 2010, 2011: p. 778-785.
113. Laurens, L.M.L., et al., *Algal Biomass Constituent Analysis: Method Uncertainties and Investigation of the Underlying Measuring Chemistries*. Analytical Chemistry, 2012. **84**(4): p. 1879-1887.
114. Biller, P., et al., *Nutrient recycling of aqueous phase for microalgae cultivation from the hydrothermal liquefaction process*. Algal Research, 2012. **1**(1): p. 70-76.
115. Kebelmann, K., et al., *Intermediate pyrolysis and product identification by TGA and Py-GC/MS of green microalgae and their extracted protein and lipid components*. Biomass and Bioenergy, 2013. **49**(0): p. 38-48.
116. Biller, P. and A.B. Ross, *Hydrothermal processing of algal biomass for the production of biofuels and chemicals*. Biofuels, 2012. **3**(5): p. 603-623.
117. Wang, K., et al., *Fast pyrolysis of microalgae remnants in a fluidized bed reactor for bio-oil and biochar production*. Bioresource Technology, (0).
118. Watanabe, M., T. Iida, and H. Inomata, *Decomposition of a long chain saturated fatty acid with some additives in hot compressed water*. Energy Conversion and Management, 2006. **47**(18-19): p. 3344-3350.
119. Holliday, R.L., J.W. King, and G.R. List, *Hydrolysis of Vegetable Oils in Sub- and Supercritical Water*. Industrial & Engineering Chemistry Research, 1997. **36**(3): p. 932-935.
120. W. King, J., R. L. Holliday, and G. R. List, *Hydrolysis of soybean oil . in a subcritical water flow reactor*. Green Chemistry, 1999. **1**(6): p. 261-264.
121. Patil, T.A., et al., *Thermal hydrolysis of vegetable oils and fats. 1. Reaction kinetics*. Industrial & Engineering Chemistry Research, 1988. **27**(5): p. 727-735.
122. Alenezi, R., et al., *Hydrolysis kinetics of sunflower oil under subcritical water conditions*. Chemical Engineering Research and Design, 2009. **87**(6): p. 867-873.
123. Yu, J. and P.E. Savage, *Decomposition of Formic Acid under Hydrothermal Conditions*. Industrial & Engineering Chemistry Research, 1998. **37**(1): p. 2-10.
124. Watanabe, M., F. Bayer, and A. Kruse, *Oil formation from glucose with formic acid and cobalt catalyst in hot-compressed water*. Carbohydrate Research, 2006. **341**(18): p. 2891-2900.
125. Cunha, S.C. and M.B.P.P. Oliveira, *Discrimination of vegetable oils by triacylglycerols evaluation of profile using HPLC/ELSD*. Food Chemistry, 2006. **95**(3): p. 518-524.
126. Deineka, V., L. Deineka, and V. Sorokopudov, *Reverse-phase HPLC in the analysis of plant oils. Monitoring of authenticity and detection of adulteration of sea buckthorne oil*. Pharmaceutical Chemistry Journal, 2009. **43**(1): p. 51-54.
127. Fasciotti, M. and A.D. Pereira Netto, *Optimization and application of methods of triacylglycerol evaluation for characterization of olive oil adulteration by soybean oil with HPLC-APCI-MS-MS*. Talanta, 2010. **81**(3): p. 1116-1125.

128. Medina, A.R., et al., *Downstream processing of algal polyunsaturated fatty acids*. Biotechnology Advances, 1998. **16**(3): p. 517-580.
129. Ogawa, T.K., Shuji; Kosaka, Satoru; and I.M. Tajima, Yamamoto, *Analysis of Oxidative Deterioration of Biodiesel Fuel*, in *SAE Powertrains, Fuels and Lubricants Meeting*. 2008, SAE International, Warrendale, Pennsylvania, USA: Rosemont, Illinois, USA.
130. Isik, O., et al., *Comparison of the fatty acid composition of the freshwater fish larvae Tilapia zillii, the rotifer Brachionus calyciflorus, and the microalgae Scenedesmus abundans, Monoraphidium minimum and Chlorella vulgaris in the algae-rotifer-fish larvae food chains*. Aquaculture, 1999. **174**(3-4): p. 299-311.
131. Tonon, T., et al., *Long chain polyunsaturated fatty acid production and partitioning to triacylglycerols in four microalgae*. Phytochemistry, 2002. **61**(1): p. 15-24.
132. Barker, J.P.M., Ann M.; Kramlich, John C., *Fatty Acid Compositions of Solvent Extracted Lipids from Two Microalgae*, in *SAE AeroTech Congress and Exhibition*. 2009, SAE International, Warrendale, Pennsylvania, USA: Seattle, Washington, USA.
133. Akiya, N. and P.E. Savage, *Roles of water for chemical reactions in high-temperature water*. Chemical Reviews, 2002. **102**(8): p. 2725-2750.
134. Dote, Y., et al., *Distribution of nitrogen to oil products from liquefaction of amino acids*. Bioresource Technology, 1998. **64**(2): p. 157-160.
135. Trevino, S.R., J.M. Scholtz, and C.N. Pace, *Amino Acid Contribution to Protein Solubility: Asp, Glu, and Ser Contribute more Favorably than the other Hydrophilic Amino Acids in RNase Sa*. Journal of Molecular Biology, 2007. **366**(2): p. 449-460.
136. Srokol, Z., et al., *Hydrothermal upgrading of biomass to biofuel; studies on some monosaccharide model compounds*. Carbohydrate Research, 2004. **339**(10): p. 1717-1726.
137. Ross, A.B., et al., *Hydrothermal processing of microalgae using alkali and organic acids*. 2010.
138. Heilmann, S.M., et al., *Hydrothermal carbonization of microalgae*. Biomass and Bioenergy, 2010. **In Press, Corrected Proof**.
139. Ross, A.B., et al., *Hydrothermal processing of microalgae using alkali and organic acids*. Fuel, 2010. **In Press, Corrected Proof**.
140. Dote, Y., et al., *Studies on the direct liquefaction of protein-contained biomass: The distribution of nitrogen in the products*. Biomass and Bioenergy, 1996. **11**(6): p. 491-498.
141. Bhatnagar, A., et al., *Renewable biomass production by mixotrophic algae in the presence of various carbon sources and wastewaters*. Applied Energy, 2011. **88**(10): p. 3425-3431.
142. Sialve, B., N. Bernet, and O. Bernard, *Anaerobic digestion of microalgae as a necessary step to make microalgal biodiesel sustainable*. Biotechnology Advances. **27**(4): p. 409-416.
143. Chen, M., et al., *Effect of nutrients on growth and lipid accumulation in the green algae Dunaliella tertiolecta*. Bioresource Technology. **102**(2): p. 1649-1655.
144. Ross, A.B., P. Biller, and C. Hall. *Catalytic hydrothermal processing of microalgae with integrated nutrient recycling*. in *18th European Biomass Conference and Exhibition*. 2011. Berlin, Germany.
145. Biller, P., R. Riley, and A.B. Ross, *Catalytic hydrothermal processing of microalgae; Decomposition and upgrading of lipids*. Bioresource Technology, 2011.
146. Belkin, S. and S. Boussiba, *High internal pH conveys ammonia resistance in spirulina platensis*. Bioresource Technology, 1991. **38**(2-3): p. 167-169.
147. Bird, D. and J. Kalf, *Empirical relationships between bacterial abundance and chlorophyll concentration in fresh and marine waters*. Canadian Journal of Fisheries and Aquatic Sciences, 1984. **41**(7): p. 1015-1023.
148. Chen, M., et al., *Effect of nutrients on growth and lipid accumulation in the green algae Dunaliella tertiolecta*. Bioresource Technology, 2011. **102**(2): p. 1649-1655.
149. Markou, G., I. Angelidaki, and D. Georgakakis, *Microalgal carbohydrates: an overview of the factors influencing carbohydrates production, and of main bioconversion technologies*

- for production of biofuels. *Applied Microbiology and Biotechnology*, 2012. **96**(3): p. 631-645.
150. Dean, A.P., et al., *Using FTIR spectroscopy for rapid determination of lipid accumulation in response to nitrogen limitation in freshwater microalgae*. *Bioresource Technology*, 2010. **101**(12): p. 4499-4507.
  151. Converti, A., et al., *Effect of temperature and nitrogen concentration on the growth and lipid content of *Nannochloropsis oculata* and *Chlorella vulgaris* for biodiesel production*. *Chemical Engineering and Processing: Process Intensification*, 2009. **48**(6): p. 1146-1151.
  152. Choi, Y., Y.S. Yun, and J. Park, *Evaluation of factors promoting astaxanthin production by a unicellular green alga, *Haematococcus pluvialis*, with fractional factorial design*. *Biotechnology progress*, 2002. **18**(6): p. 1170-1175.
  153. Promdej, C. and Y. Matsumura, *Temperature Effect on Hydrothermal Decomposition of Glucose in Sub- And Supercritical Water*. *Industrial & Engineering Chemistry Research*, 2011. **50**(14): p. 8492-8497.
  154. Hammerschmidt, A., et al., *Catalytic conversion of waste biomass by hydrothermal treatment*. *Fuel*, 2011. **90**(2): p. 555-562.
  155. Makishima, S., et al., *Development of continuous flow type hydrothermal reactor for hemicellulose fraction recovery from corncob*. *Bioresource Technology*, 2009. **100**(11): p. 2842-2848.
  156. Ocfemia, et al., *Hydrothermal processing of swine manure into oil using a continuous reactor system : Development and testing*. 2006, American Society of Agricultural Engineers: St. Joseph, MI, ETATS-UNIS. p. 9.
  157. Karagöz, S., et al., *Hydrothermal upgrading of biomass: Effect of K<sub>2</sub>CO<sub>3</sub> concentration and biomass/water ratio on products distribution*. *Bioresource Technology*, 2006. **97**(1): p. 90-98.
  158. Schmieder, H., et al., *Hydrothermal gasification of biomass and organic wastes*. *The Journal of Supercritical Fluids*, 2000. **17**(2): p. 145-153.
  159. Duan, P. and P.E. Savage, *Hydrothermal Liquefaction of a Microalga with Heterogeneous Catalysts*. *Industrial & Engineering Chemistry Research*, 2010: p. 1899-1906.
  160. Tsubaki, S., et al., *Microwave-assisted hydrothermal hydrolysis of cellobiose and effects of additions of halide salts*. *Bioresource Technology*, 2012. **123**(0): p. 703-706.
  161. Budarin, V., et al., *Microalgae biorefinery concept based on hydrothermal microwave pyrolysis*. *Green Chemistry*, 2012.
  162. Budarin, V.L., et al., *Microwave-mediated pyrolysis of macro-algae*. *Green Chemistry*, 2011. **13**(9): p. 2330-2333.
  163. Lamoolphak, W., et al., *Hydrothermal decomposition of yeast cells for production of proteins and amino acids*. *Journal of Hazardous Materials*, 2006. **137**(3): p. 1643-1648.
  164. Sereewatthanawut, I., et al., *Extraction of protein and amino acids from deoiled rice bran by subcritical water hydrolysis*. *Bioresource Technology*, 2008. **99**(3): p. 555-561.
  165. Du, Z., et al., *Hydrothermal pretreatment of microalgae for production of pyrolytic bio-oil with a low nitrogen content*. *Bioresource Technology*, 2012. **120**(0): p. 13-18.
  166. Satoh, A., et al., *Characterization of the Lipid Accumulation in a New Microalgal Species, *Pseudochoricystis ellipsoidea* (*Trebouxiophyceae*)*. *Journal of the Japan Institute of Energy*, 2010. **89**(9): p. 909-913.
  167. Lee, A.K., D.M. Lewis, and P.J. Ashman, *Disruption of microalgal cells for the extraction of lipids for biofuels: Processes and specific energy requirements*. *Biomass and Bioenergy*, 2012. **46**(0): p. 89-101.
  168. Saddawi, A., J.M. Jones, and A. Williams, *Influence of alkali metals on the kinetics of the thermal decomposition of biomass*. *Fuel Processing Technology*, 2012. **104**(0): p. 189-197.



## 14. Nomenclature

AD	Anaerobic Digestion
ar	as received
amu	Atomic mass unit
BBM	Bold Basal Media
CV	Calorific Value
daf	dry ash free
db	dry basis
FAME	Fatty Acid Methyl Ester
FFA	Free Fatty Acid
GC	Gas Chromatography
GHG	Green House Gas
HPLC	High Pressure Liquid Chromatography
HHV	Higher Heating Value
HT	Hydrothermal
HTC	Hydrothermal Carbonisation
HTG	Hydrothermal Gasification
HTL	Hydrothermal Liquefaction
HMP	Hydrothermal Microwave Processing
ICP-OES	Inductively Coupled Plasma-Optical Emission Spectrometry
IEC	Ion Exchange Chromatography
LCA	Life Cycle Assessment
MS	Mass Spectrometry
MJ	Mega Joule
M	Molar

PN	Partition Number
ppb	parts per billion
ppm	parts per million
Py-GC-MS	Pyrolysis GC-MS
RTFO	Renewable Transport Fuel Obligation
SEM	Scanning Electron Microscope
SEC	Size Exclusion Chromatography
TGA	Thermo Gravimetric Analysis
3N-BBM+V	Three fold Nitrogen-BBM+Vitamin
TIC	Total Inorganic Carbon
TN	Total Nitrogen
TOC	Total Organic Carbon

## DATA SHEET: *Botryococcus braunii*

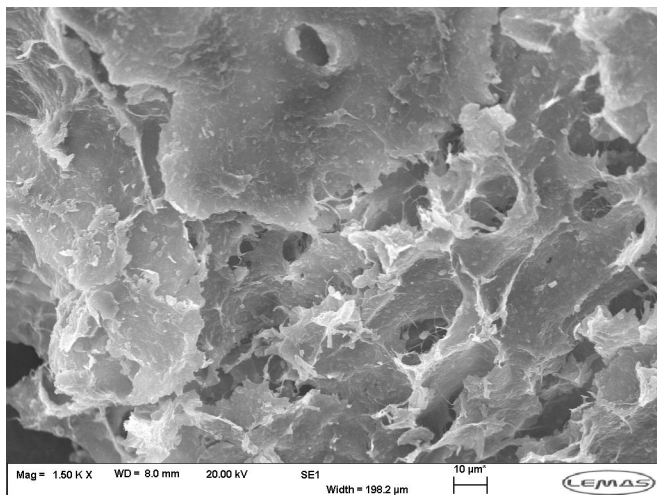
## APPENDIX A

Scientific name	Strain	Source	Growth media
<i>Botryococcus braunii</i>	807/1 Guadeloupe (race B)	Plymouth Marine Laboratory, UK	3N-BBM+V

Proximate Analysis	Gross As Received:
Moisture	6.0 %
Ash	5.4 %
Volatile matter	74.1 %
Fixed carbon	14.5 %
Heat Value (MJ/kg)	24.8

Ultimate Analysis (daf %):	
Carbon	54.3
Oxygen	28.8
Hydrogen	7.3
Nitrogen	9.5
Sulfur	ND

Biochemical (daf %)	
Protein	45
Carbohydrate	NA
Lipid	NA



SEM at 1500 times magnification

Metal Analysis (a/r ppm)	
Al	NA
Ca	NA
Cl	NA
Cu	NA
Fe	NA
K	NA
Mg	NA
Mn	NA
Na	NA
Ni	NA
P	NA
Zn	NA

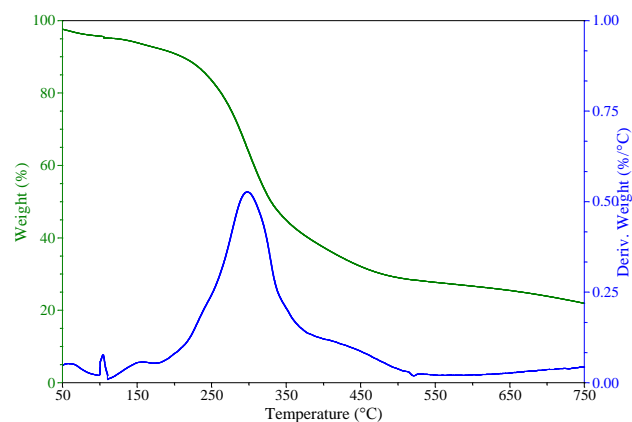
Pigment Analysis (a/r ppm)	
Chlorophyllide a	1116
Chlorophyll C1/C2	471
Fucoxanthin	-
Violaxanthin	941
Astaxanthin	-
Lutein	4763
Zeaxanthin	-
Antheraxanthin	525
Chlorophyll b1	3994
Chlorophyll b2	894
Chlorophyll a	2321
$\alpha$ -carotene	-
$\beta$ -carotene	459

# DATA SHEET: *Botryococcus braunii*

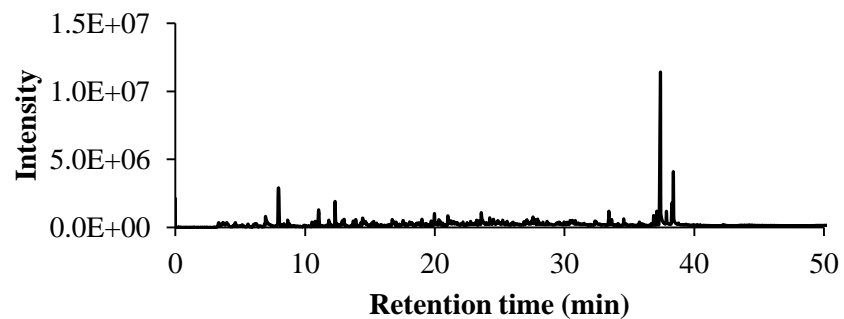
# APPENDIX A

## TGA/DTG in N<sub>2</sub>

Size: 1.2530 mg



## Py-GC-MS at 500°C



Py-GC-MS Analysis		
Retention time	Area %	Compound
7.947	15.68	Toluene
11.047	5.86	o-Xylene
12.315	5.78	Styrene
23.585	2.79	Phenol, 4-methyl-
33.424	2.78	3-Octadecene, (E)-
37.118	3.09	2-Hexadecene, 3,7,11,15-tetramethyl-,
37.398	45.7	3,7,11,15-Tetramethyl-2-hexadecen-1-ol
37.858	2.62	3,7,11,15-Tetramethyl-2-hexadecen-1-ol
38.271	4.66	6,6-Dimethyl-cyclooct-4-enone
38.392	11.04	3,7,11,15-Tetramethyl-2-hexadecen-1-ol

**DATA SHEET: *Chlorella sp.***

**APPENDIX A**

Scientific name	Strain	Source	Growth media
<i>Chlorella sp.</i>	unknown	Naturally Green Ltd, UK	unknown

Proximate Analysis	Gross As Received:
Moisture	5.9 %
Ash	7.0 %
Volatile matter	78.5 %
Fixed carbon	11.3 %
Heat Value (MJ/kg)	23.2

Ultimate Analysis (daf %):	
Carbon	52.6
Oxygen	32.2
Hydrogen	7.1
Nitrogen	8.2
Sulfur	0.5

Biochemical (daf %)	
Protein	55
Carbohydrate	9
Lipid	36

Metal Analysis (a/r ppm)	
Al	13
Ca	3141
Cl	3893
Cu	6
Fe	1179
K	14899
Mg	4028
Mn	44
Na	1108
Ni	1
P	7954
Zn	135

Pigment Analysis (a/r ppm)	
Chlorophyllide a	-
Chlorophyll C1/C2	-
Fucoxanthin	-
Violaxanthin	-
Astaxanthin	-
Lutein	11771
Zeaxanthin	-
Antheraxanthin	-
Chlorophyll b1	14414
Chlorophyll b2	2401
Chlorophyll a	2870
$\alpha$ -carotene	-
$\beta$ -carotene	-

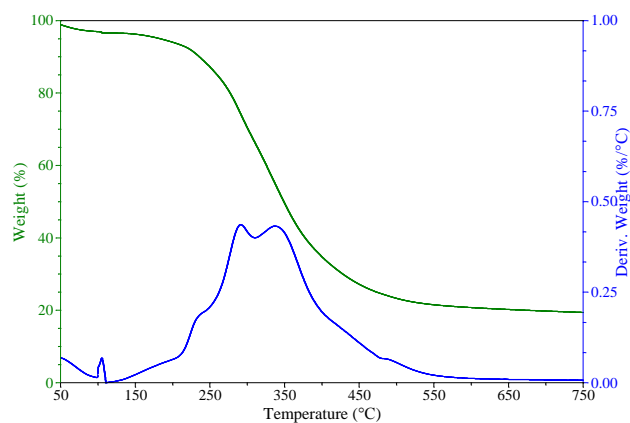
SEM at 1500 times magnification not available

## DATA SHEET: *Chlorella sp.*

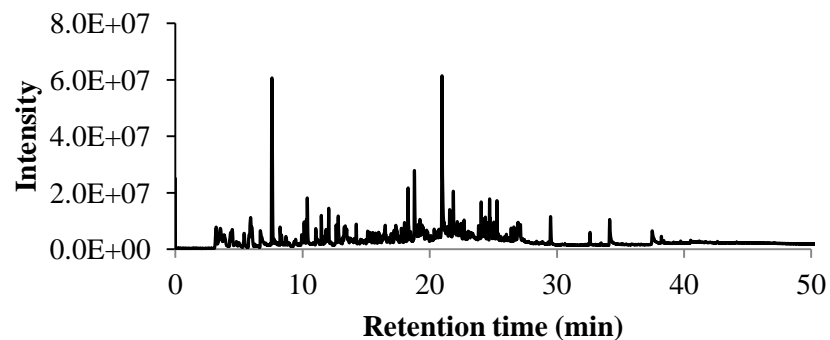
## APPENDIX A

### TGA/DTG plot in N<sub>2</sub>

Size: 4.6650 mg



### Py-GC-MS at 500°C



Py-GC-MS Analysis		
Retention time	Area %	Compound
7.597	33.39	Toluene
10.376	5.88	Benzene, 1,3-dimethyl-
11.479	3.31	Styrene
12.063	3.17	ND
12.811	4.05	1H-Pyrrole, 3-methyl-
18.305	7.56	Thiophene, 2-methoxy-5-methyl-
18.802	9.41	Phenol
20.971	24.58	Phenol, 4-methyl-
21.861	5.08	Benzyl nitrile
24.053	3.57	Naphthalene, 1,2-dihydro-1,1,6-trimethyl-

**DATA SHEET: *Chlorella vulgaris* OZ**

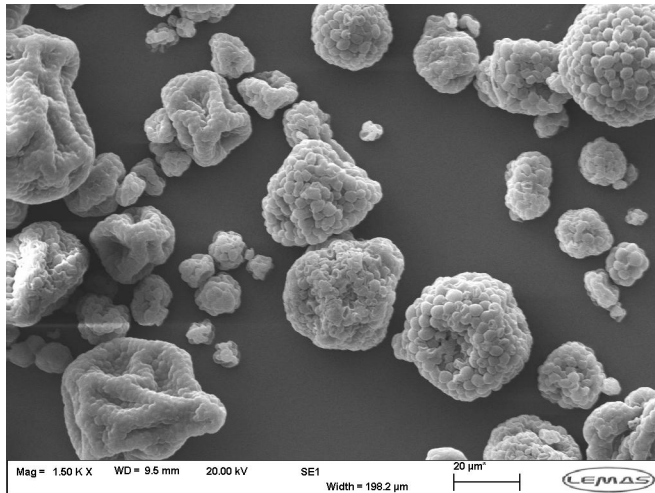
**APPENDIX A**

Scientific name	Strain	Source	Growth media
<i>Chlorella vulgaris</i> OZ	unknown	Synergy Natural, Australia	unknown

Proximate Analysis	Gross As Received:
Moisture	5.2 %
Ash	6.0 %
Volatile matter	76.3 %
Fixed carbon	12.1 %
Heat Value (MJ/kg)	24.3

Ultimate Analysis (daf %):	
Carbon	53.5
Oxygen	27.5
Hydrogen	7.4
Nitrogen	11.0
Sulfur	0.5

Biochemical (daf %)	
Protein	53-60
Carbohydrate	15.-25
Lipid	3-5



**SEM at 1500 times magnification**

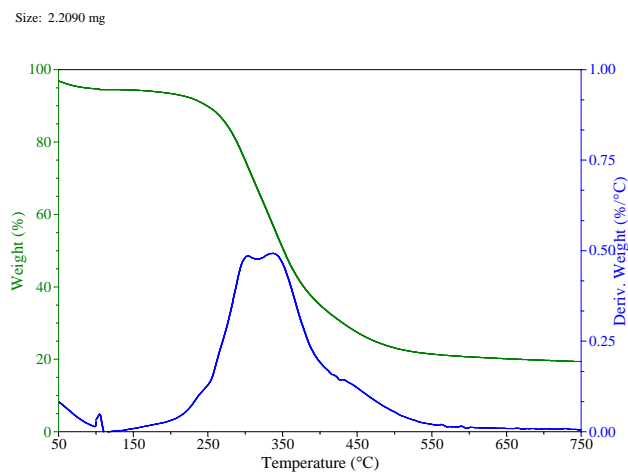
Metal Analysis (a/r ppm)	
Al	25
Ca	1922
Cl	3946
Cu	6
Fe	846
K	11705
Mg	3288
Mn	57
Na	860
Ni	0.7
P	9319
Zn	21

Pigment Analysis (a/r ppm)	
Chlorophyllide a	-
Chlorophyll C1/C2	-
Fucoxanthin	-
Violaxanthin	-
Astaxanthin	-
Lutein	229
Zeaxanthin	-
Antheraxanthin	-
Chlorophyll b1	1396
Chlorophyll b2	511
Chlorophyll a	504
α-carotene	-
β-carotene	-

## DATA SHEET: *Chlorella vulgaris* OZ

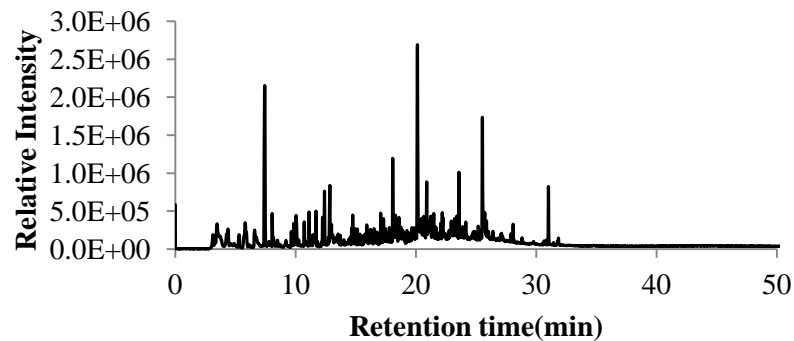
## APPENDIX A

### TGA/DTG plot in N<sub>2</sub>



Py-GC-MS Analysis		
Retention time	Area %	Compound
7.43	29.04	Toluene
11.116	2.78	Styrene
12.398	5.57	1H-Pyrrole, 3-methyl-
12.842	5.71	2-Furanmethanol
18.069	6.79	Phenol
20.121	25.1	Phenol, 4-methyl-
20.892	3.14	Benzyl nitrile
23.568	4.6	Benzenepropanenitrile
25.52	12.62	Indole
31.011	4.65	3,7,11,15-Tetramethyl-2-hexadecen-1-ol

### Py-GC-MS at 500°C





**DATA SHEET: *Dunaliella salina***

**APPENDIX A**

Scientific name	Strain	Source	Growth media
<i>Dunaliella salina</i>	19/18	University of Sheffield, UK	modified f/2, 2.0 M NaCl

Proximate Analysis	Gross As Received:
Moisture	1.5 %
Ash	xx %
Volatile matter	34 %
Fixed carbon	xx
Heat Value (MJ/kg)	NA

Ultimate Analysis (daf %):	
Carbon	NA
Oxygen	NA
Hydrogen	NA
Nitrogen	NA
Sulfur	NA

Biochemical (daf %)	
Protein	NA
Carbohydrate	NA
Lipid	NA

SEM at 1500 times magnification not available

Metal Analysis (a/r ppm)	
Al	NA
Ca	NA
Cl	NA
Cu	NA
Fe	NA
K	NA
Mg	NA
Mn	NA
Na	NA
Ni	NA
P	NA
Zn	NA

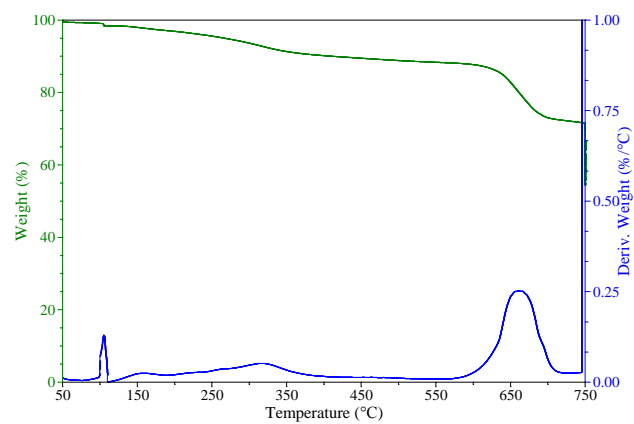
Pigment Analysis (a/r ppm)	
Chlorophyllide a	-
Chlorophyll C1/C2	-
Fucoxanthin	-
Violaxanthin	2818
Astaxanthin	8813
Lutein	-
Zeaxanthin	-
Antheraxanthin	-
Chlorophyll b1	6606
Chlorophyll b2	-
Chlorophyll a	3660
$\alpha$ -carotene	656
$\beta$ -carotene	8088

# DATA SHEET: *Dunaliella salina*

# APPENDIX A

## Thermal Analysis

Size: 2.2870 mg



**DATA SHEET: *Dunaliella salina***

**APPENDIX A**

Scientific name	Strain	Source	Growth media
<i>Dunaliella salina</i>	19/30	University of Sheffield, UK	modified f/2

Proximate Analysis	Gross As Received:
Moisture	3.0 %
Ash	35.1 %
Volatile matter	44.8 %
Fixed carbon	20.4 %
Heat Value (MJ/kg)	NA

Ultimate Analysis (daf %):	
Carbon	NA
Oxygen	NA
Hydrogen	NA
Nitrogen	NA
Sulfur	NA

Biochemical (daf %)	
Protein	NA
Carbohydrate	NA
Lipid	NA

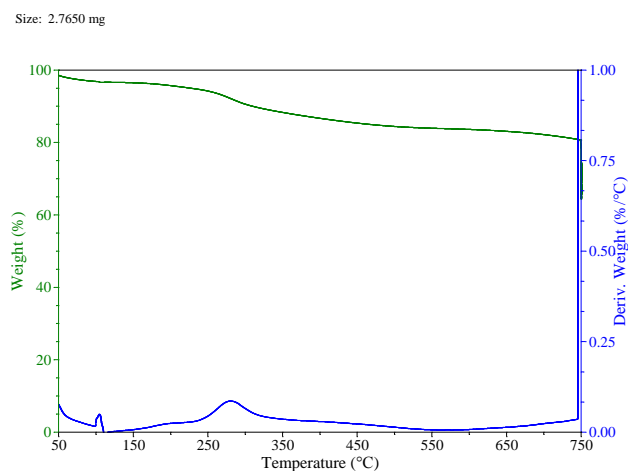
SEM at 1500 times magnification not available

Metal Analysis (a/r ppm)	
Al	NA
Ca	NA
Cl	NA
Cu	NA
Fe	NA
K	NA
Mg	NA
Mn	NA
Na	NA
Ni	NA
P	NA
Zn	NA

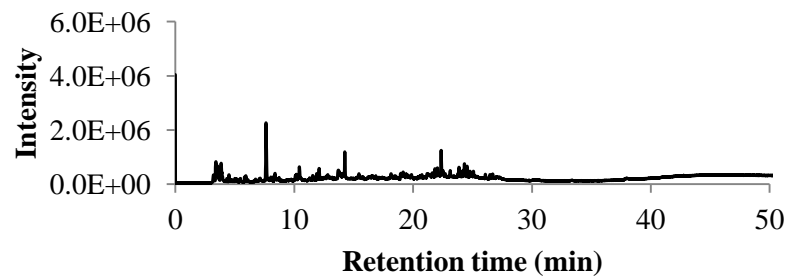
Pigment Analysis (a/r ppm)	
Chlorophyllide a	-
Chlorophyll C1/C2	-
Fucoxanthin	-
Violaxanthin	1647
Astaxanthin	-
Lutein	-
Zeaxanthin	-
Antheraxanthin	-
Chlorophyll b1	-
Chlorophyll b2	-
Chlorophyll a	1177
$\alpha$ -carotene	-
$\beta$ -carotene	-

## DATA SHEET: *Dunaliella salina*

### TGA/DTG plot in N<sub>2</sub>



### Py-GC-MS at 500°C



## APPENDIX A

Py-GC-MS Analysis		
Retention time	Area %	Compound
3.414	14.23	Methylamine, N,N-dimethyl-
3.856	5.58	ND
7.629	36.1	Toluene
		2-(1-Benzyl-2-indolyl)-4-[(4-methoxybenzoyl)hydrazono]-4-phenylbutyric acid
10.436	4.36	ND
11.883	3.24	ND
12.102	4.59	ND
14.257	9.9	D-Limonene
22.366	10.68	2,3;5,6-Diacetone-4-O-methylmannitol
24.324	5.72	5,6-Dihydro-2-iso-propenyl-4,4,6-trimethyl-(4H)-1,3-oxazine
24.547	5.6	Cyclopropane, (1,2-dimethylpropyl)-

**DATA SHEET: *Dunaliella tertiolecta***

**APPENDIX A**

Scientific name	Strain	Source	Growth media
<i>Dunaliella tertiolecta</i>	19/27	CCAP	f/2

Proximate Analysis	Gross As Received:
Moisture	6.8 %
Ash	9.4 %
Volatile matter	77.4 %
Fixed carbon	6.4 %
Heat Value (MJ/kg)	NA

Ultimate Analysis (daf %):	
Carbon	NA
Oxygen	NA
Hydrogen	NA
Nitrogen	NA
Sulfur	NA

Biochemical (daf %)	
Protein	NA
Carbohydrate	NA
Lipid	NA

**SEM at 1500 times magnification not available**

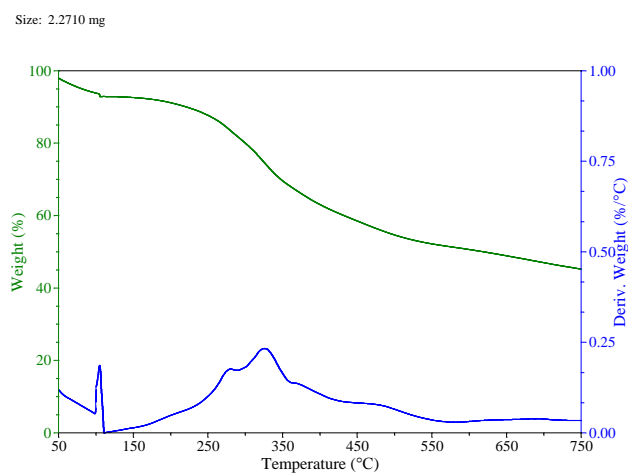
Metal Analysis (a/r ppm)	
Al	NA
Ca	NA
Cl	NA
Cu	NA
Fe	NA
K	NA
Mg	NA
Mn	NA
Na	NA
Ni	NA
P	NA
Zn	NA

Pigment Analysis (a/r ppm)	
Chlorophyllide a	572
Chlorophyll C1/C2	-
Fucoxanthin	-
Violaxanthin	2731
Astaxanthin	-
Lutein	12420
Zeaxanthin	-
Antheraxanthin	-
Chlorophyll b1	10231
Chlorophyll b2	1690
Chlorophyll a	4818
α-carotene	-
β-carotene	2017

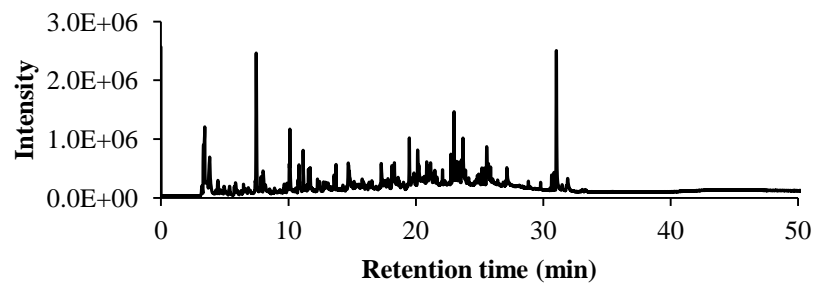
**DATA SHEET: *Dunaliella tertiolecta***

**APPENDIX A**

**TGA/DTG plot in N<sub>2</sub>**



**Py-GC-MS at 500°C**



Py-GC-MS Analysis		
Retention time	Area %	Compound
3.843	4.48	3-Buten-1-ol, 2-methyl-
7.495	24.37	Toluene
11.677	1.69	Cyclotetrasiloxane, octamethyl-
11.745	2.74	Perfluoropropanimidamide,
19.956	45.27	1-Ethyl-2-pyrrolidinone
20.885	4.41	7-Chloro-1,3,4,10-tetrahydro-10-hydroxy-acridinone
22.987	11.55	1-Hexanol, 4-methyl-, (S)-
23.108	2.02	N,N-Dicyclohexyl-benzamide
23.211	1.52	N,N-Dicyclohexyl-acetamide
24.162	1.94	Hexadecane

## DATA SHEET: *Pseudochoricystis ellipsoidea*

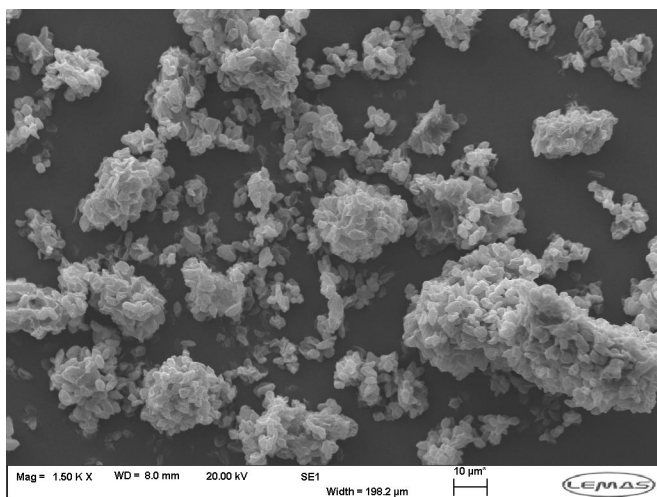
## APPENDIX A

Scientific name	Strain	Source	Growth media
<i>Pseudochoricystis ellipsoidea</i>	MBIC11204	DENSO Corporation, Japan	unknown

Proximate Analysis	Gross As Received:
Moisture	1.2 %
Ash	1.0 %
Volatile matter	90.7 %
Fixed carbon	4.4 %
Heat Value (MJ/kg)	27.0

Ultimate Analysis (daf %):	
Carbon	61.3
Oxygen	27.0
Hydrogen	9.1
Nitrogen	2.1
Sulfur	ND

Biochemical (daf %)	
Protein	25
Carbohydrate	7
Lipid	67



SEM at 1500 times magnification

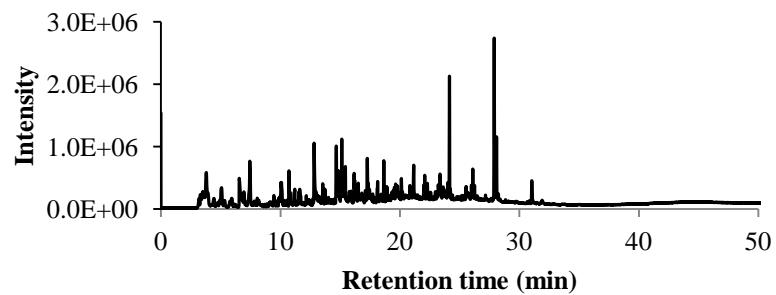
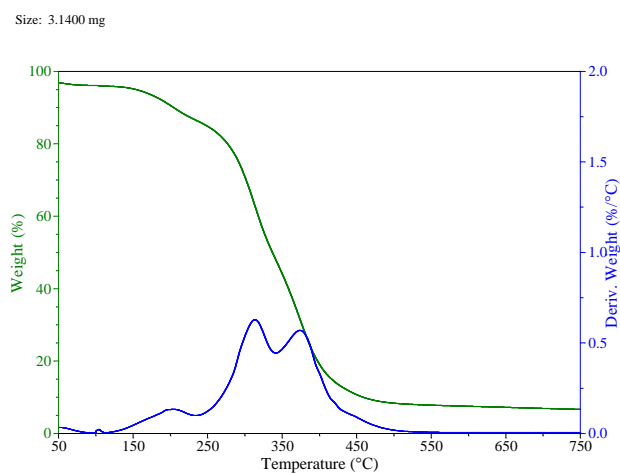
Metal Analysis (a/r ppm)	
Al	0
Ca	209
Cl	10
Cu	11
Fe	48
K	2899
Mg	244
Mn	7
Na	124
Ni	0
P	6256
Zn	11

Pigment Analysis (a/r ppm)	
Chlorophyllide a	-
Chlorophyll C1/C2	-
Fucoxanthin	-
Violaxanthin	-
Astaxanthin	-
Lutein	626
Zeaxanthin	-
Antheraxanthin	48
Chlorophyll b1	197
Chlorophyll b2	-
Chlorophyll a	44
$\alpha$ -carotene	-
$\beta$ -carotene	-

**DATA SHEET: *Pseudochoricystis ellipsoidea***

**APPENDIX A**

**TGA/DTG plot in N<sub>2</sub>**



Py-GC-MS Analysis		
Retention time	Area %	Compound
7.44	7.08	Toluene
12.823	11.56	2-Furanmethanol
14.678	11.23	1,2-Cyclopentanedione
14.841	4.98	ND
15.137	5.74	3-Undecene, (E)-
17.271	5.99	1,2-Cyclopentanedione, 3-methyl-
18.656	4.56	5-Decen-1-ol, (Z)-
24.151	13.37	Pentadecane
27.896	28.04	3-Heptadecene, (Z)-
28.093	7.46	Heptadecane



## DATA SHEET: *Haematococcus pluvialis*

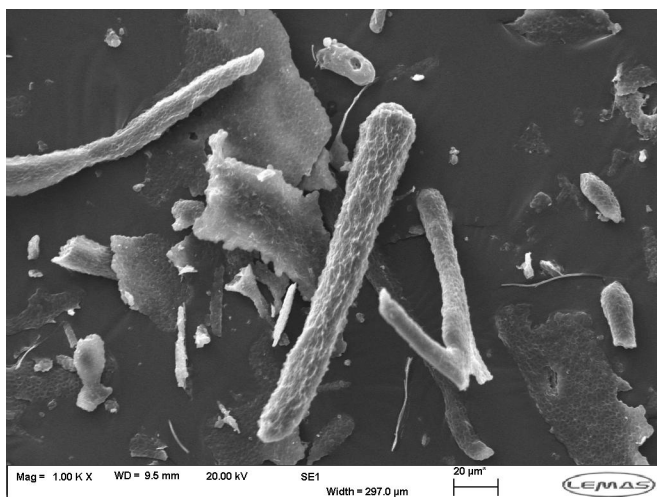
## APPENDIX A

Scientific name	Strain	Source	Growth media
<i>Haematococcus pluvialis</i>	34/1D	CCAP	3N-BBM+V

Proximate Analysis	Gross As Received:
Moisture	8.1 %
Ash	5.7 %
Volatile matter	77.5 %
Fixed carbon	14 %
Heat Value (MJ/kg)	23.9

Ultimate Analysis (daf %):	
Carbon	52.7
Oxygen	31.6
Hydrogen	7.5
Nitrogen	7.8
Sulfur	ND

Biochemical (daf %)	
Protein	37
Carbohydrate	NA
Lipid	NA



SEM at 1500 times magnification not available

Metal Analysis (a/r ppm)	
Al	NA
Ca	NA
Cl	NA
Cu	NA
Fe	NA
K	NA
Mg	NA
Mn	NA
Na	NA
Ni	NA
P	NA
Zn	NA

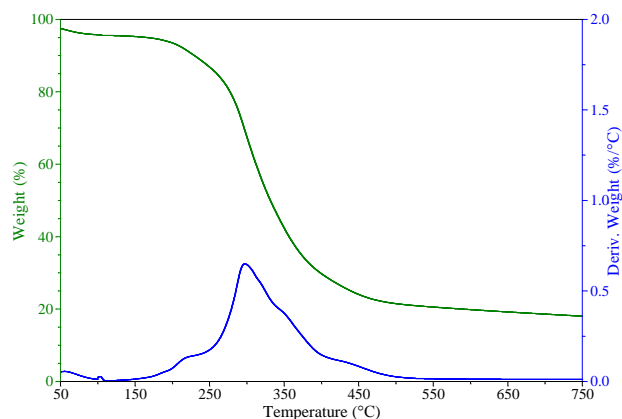
Pigment Analysis (a/r ppm)	
Chlorophyllide a	-
Chlorophyll C1/C2	-
Fucoxanthin	-
Violaxanthin	160
Astaxanthin	3745
Lutein	-
Zeaxanthin	-
Antheraxanthin	-
Chlorophyll b1	1873
Chlorophyll b2	-
Chlorophyll a	928
$\alpha$ -carotene	0
$\beta$ -carotene	690

**DATA SHEET: *Haematococcus pluvialis***

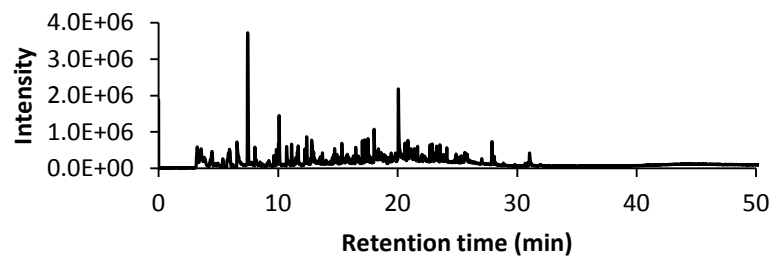
**APPENDIX A**

**TGA/DTG plot in N<sub>2</sub>**

Size: 2.0840 mg



**Py-GC-MS at 500°C**



Py-GC-MS Analysis		
Retention time	Area %	Compound
7.455	40.31	Toluene
9.85	4.04	Ethylbenzene
10.033	3.48	Pyrole
10.09	10.12	o-Xylene
12.394	4.8	1H-Pyrrole, 2-methyl-
17.05	3.37	Pyrrole, 4-ethyl-2-methyl-
17.242	6.88	1,2-Cyclopentanedione, 3-methyl-
18.036	6.32	Phosphonic acid, (p-hydroxyphenyl)-
20.07	15.89	Phenol, 4-methyl-
27.9	4.79	8-Heptadecene

**DATA SHEET: *Miyako***

**APPENDIX A**

Scientific name	Strain	Source	Growth media
<i>unknown</i>	unknown	DENSO Corporation, Japan	unknown

Proximate Analysis	Gross As Received:
Moisture	2.6 %
Ash	2.3 %
Volatile matter	87.4 %
Fixed carbon	6.6 %
Heat Value (MJ/kg)	26.9

Ultimate Analysis (daf %):	
Carbon	60.4
Oxygen	26.7
Hydrogen	9.5
Nitrogen	3.0
Sulfur	0.4

Biochemical (daf %)	
Protein	14
Carbohydrate	NA
Lipid	28

SEM at 1500 times magnification not available

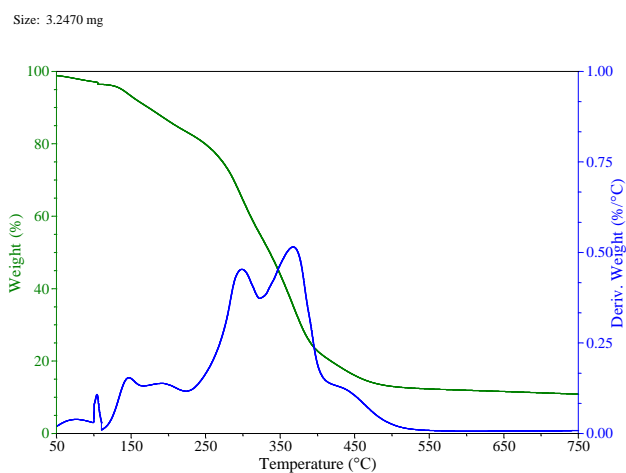
Metal Analysis (a/r ppm)	
Al	263
Ca	645
Cl	250
Cu	133
Fe	464
K	8991
Mg	2448
Mn	27
Na	2696
Ni	7.6
P	6345
Zn	87

Pigment Analysis (a/r ppm)	
Chlorophyllide a	NA
Chlorophyll C1/C2	NA
Fucoxanthin	NA
Violaxanthin	NA
Astaxhanthin	NA
Lutein	NA
Zeaxanthin	NA
Antheraxanthin	NA
Chlorophyll b1	NA
Chlorophyll b2	NA
Chlorophyll a	NA
$\alpha$ -carotene	NA
$\beta$ -carotene	NA

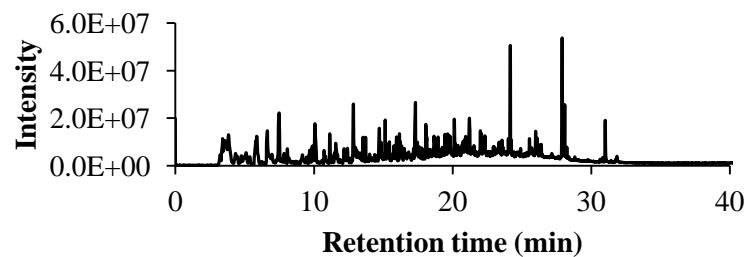
## DATA SHEET: *Miyako*

## APPENDIX A

### TGA/DTG plot in N<sub>2</sub>



### Py-GC-MS at 500°C



Py-GC-MS Analysis		
Retention time	Area %	Compound
7.488	15.56	Toluene
12.846	9.94	2-Furanmethanol
15.14	4.48	3-Undecene, (E)-
17.321	11.7	1,2-Cyclopentanedione, 3-methyl-
22.006	2.57	Pentadecane
24.165	15.65	Pentadecane
27.905	23.6	3-Heptadecene, (Z)-
27.975	3.37	6,9-Heptadecadiene
28.09	7.39	Heptadecane
31.013	5.74	3,7,11,15-Tetramethyl-2-hexadecen-1-ol

## DATA SHEET: *Nannochloropsis oculata*

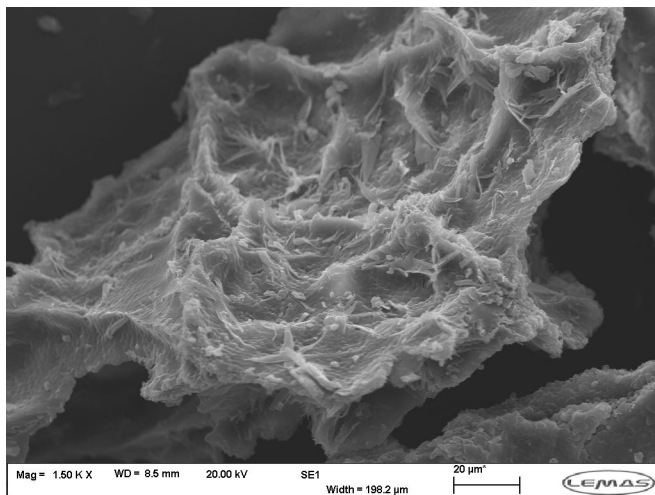
## APPENDIX A

Scientific name	Strain	Source	Growth media
<i>Nannochloropsis oculata</i>	unknown	University of Almeria, Spain	unknown

Proximate Analysis	Gross As Received:
Moisture	7.2 %
Ash	26.4 %
Volatile matter	61.5 %
Fixed carbon	8.4 %
Heat Value (MJ/kg)	17.9

Ultimate Analysis (daf %):	
Carbon	57.8
Oxygen	25.7
Hydrogen	8.0
Nitrogen	8.6
Sulfur	ND

Biochemical (daf %)	
Protein	57
Carbohydrate	8
Lipid	35



SEM at 1500 times magnification

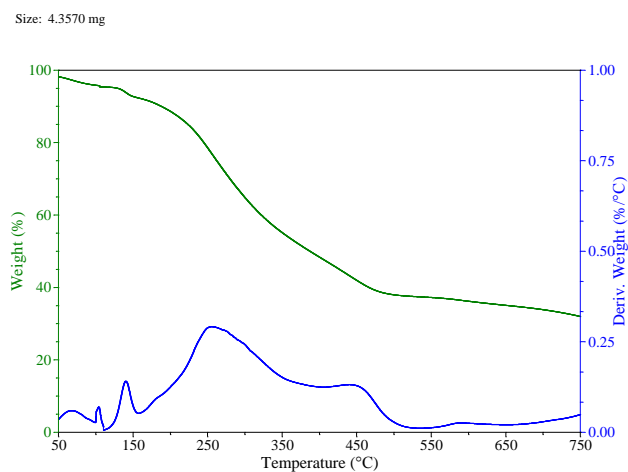
Metal Analysis (a/r ppm)	
Al	0
Ca	700
Cl	76955
Cu	10
Fe	714
K	14989
Mg	3295
Mn	53
Na	189271
Ni	0
P	7806
Zn	18

Pigment Analysis (a/r ppm)	
Chlorophyllide a	-
Chlorophyll C1/C2	-
Fucoxanthin	-
Violaxanthin	1072
Astaxanthin	-
Lutein	401
Zeaxanthin	-
Antheraxanthin	-
Chlorophyll b1	-
Chlorophyll b2	-
Chlorophyll a	535
$\alpha$ -carotene	75
$\beta$ -carotene	204

## DATA SHEET: *Nannochloropsis oculata*

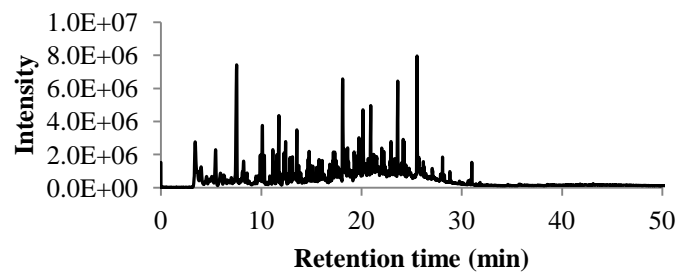
## APPENDIX A

### TGA/DTG plot in N<sub>2</sub>



Py-GC-MS Analysis		
Retention time	Area %	Compound
7.551	26.7	Toluene
11.766	6.97	Pseudosolasodine diacetate
13.556	4.23	Ethanone, 1-(2-furanyl)-
18.124	17.16	Phenol
19.749	2.63	Lyxitol, 1-O-decyl-
20.15	9.29	Phenol, 4-methyl-
20.923	6.4	Benzyl nitrile
23.617	10.91	Benzenepropanenitrile
24.161	2.4	Pentadecane
25.544	13.31	Indole

### Py-GC-MS at 500°C



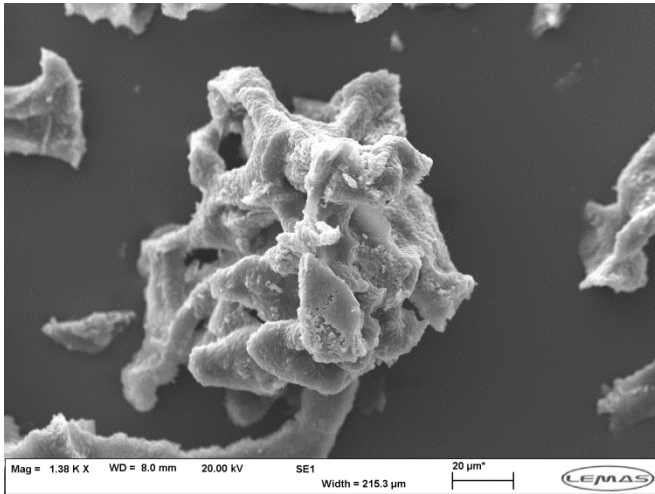
**DATA SHEET: *Navicula sp.***

Scientific name	Strain	Source	APPENDIX A Growth media
<i>Navicula sp.</i>	unknown	University of Sheffield, UK	f/2 with 100% Silicate

Proximate Analysis	Gross As Received:
Moisture	6.7 %
Ash	4.0 %
Volatile matter	80.8 %
Fixed carbon	9.3 %
Heat Value (MJ/kg)	17.5

Ultimate Analysis (daf %):	
Carbon	35.7
Oxygen	52.9
Hydrogen	5.9
Nitrogen	5.6
Sulfur	ND

Biochemical (daf %)	
Protein	27
Carbohydrate	NA
Lipid	NA



SEM at 1500 times magnification not available

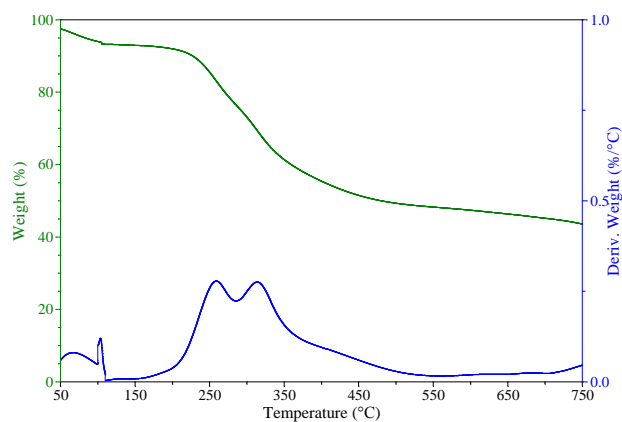
Metal Analysis (a/r ppm)	
Al	NA
Ca	NA
Cl	NA
Cu	NA
Fe	NA
K	NA
Mg	NA
Mn	NA
Na	NA
Ni	NA
P	NA
Zn	NA

Pigment Analysis (a/r ppm)	
Chlorophyllide a	-
Chlorophyll C1/C2	-
Fucoxanthin	294
Violaxanthin	-
Astaxanthin	-
Lutein	-
Zeaxanthin	-
Antheraxanthin	-
Chlorophyll b1	-
Chlorophyll b2	-
Chlorophyll a	1908
α-carotene	476
β-carotene	3268

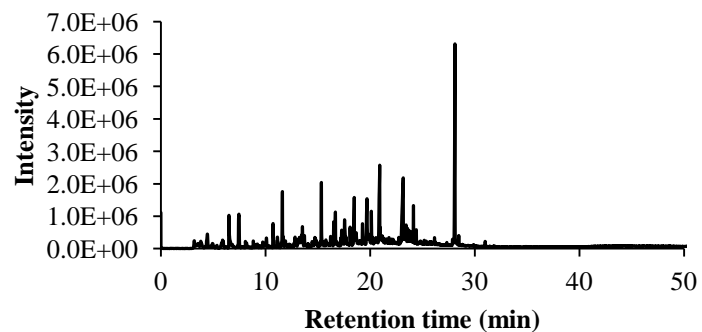
## DATA SHEET: *Navicula sp.*

### TGA/DTG plot in N<sub>2</sub>

Size: 3.8690 mg



### Py-GC-MS at 500°C



## APPENDIX A

Py-GC-MS Analysis		
Retention time	Area %	Compound
7.456	8.93	Alanine, 3-N-carboxy-, N-b
11.613	7.18	Furfural
15.34	7.77	2-Furancarboxaldehyde, 5-methyl-
16.518	2.55	4-Amino-2(1H)-pyridinone
16.683	5.55	Oxazolidine, 2,2-diethyl-3-methyl-
19.698	10.69	Maltol
20.117	3.88	Phenol, 4-methyl-
20.914	14.15	Levogluosenone
24.143	3.94	Pentadecane
28.107	35.36	Ethanol, 2-(octadecyloxy)-



## DATA SHEET: *Chlorogloeopsis fritschii*

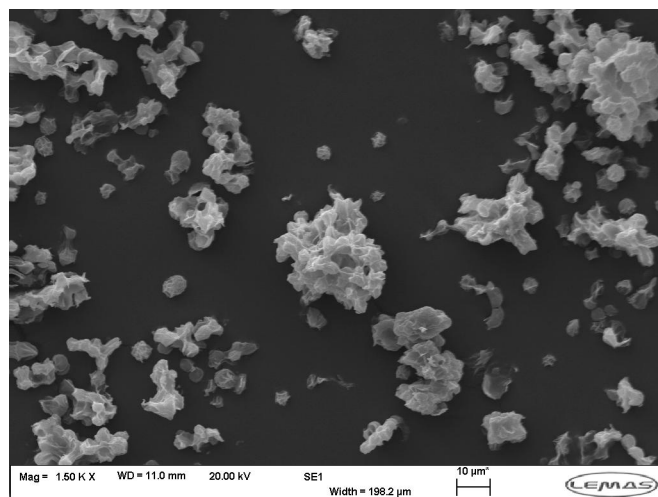
## APPENDIX A

Scientific name	Strain	Source	Growth media
<i>Chlorogloeopsis fritschii</i>	1411/1	Plymouth Marine Laboratory, UK	JM

Proximate Analysis	Gross As Received:
Moisture	6.8 %
Ash	7.6 %
Volatile matter	75.5 %
Fixed carbon	6.6 %
Heat Value (MJ/kg)	23.3

Ultimate Analysis (daf %):	
Carbon	54.4
Oxygen	31.4
Hydrogen	6.9
Nitrogen	7.3
Sulfur	ND

Biochemical (daf %)	
Protein	50
Carbohydrate	44
Lipid	7



SEM at 1500 times magnification

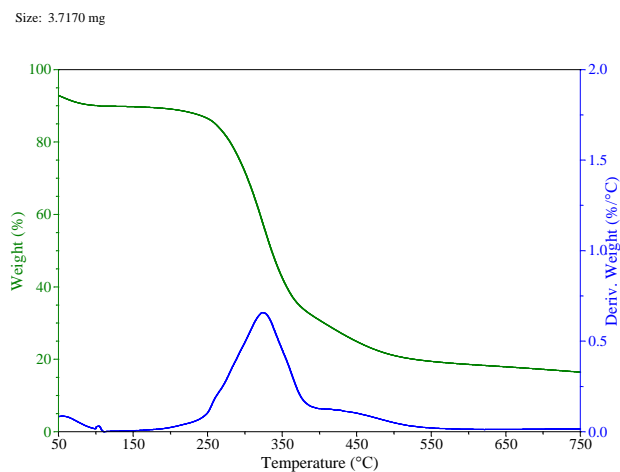
Metal Analysis (a/r ppm)	
Al	0
Ca	4350
Cl	578
Cu	19
Fe	692
K	4844
Mg	2693
Mn	91
Na	3905
Ni	0.4
P	7847
Zn	68

Pigment Analysis (a/r ppm)	
Chlorophyllide a	NA
Chlorophyll C1/C2	NA
Fucoxanthin	NA
Violaxanthin	NA
Astaxanthin	NA
Lutein	NA
Zeaxanthin	NA
Antheraxanthin	NA
Chlorophyll b1	NA
Chlorophyll b2	NA
Chlorophyll a	NA
$\alpha$ -carotene	NA
$\beta$ -carotene	NA

## DATA SHEET: *Chlorogloeopsis fritschii*

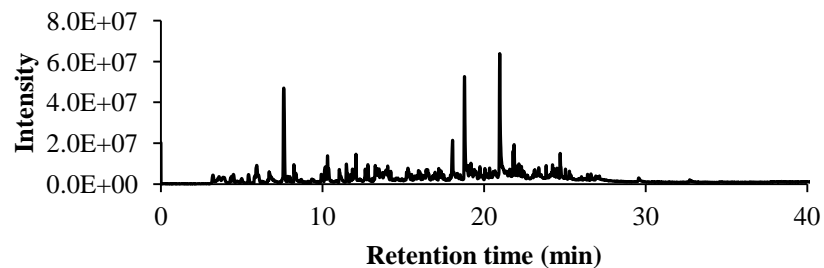
## APPENDIX A

### TGA/DTG plot in N<sub>2</sub>



Py-GC-MS Analysis		
Retention time	Area %	Compound
7.604	24.93	Toluene
10.125	3.14	Ethylbenzene
10.315	2.66	Pyrrole
12.075	2.9	Maytansine
18.056	7.49	1,2-Cyclopentanedione, 3-methyl-
18.794	20.83	Phenol
20.974	27.12	Phenol, 4-methyl-
21.804	3.52	1-Hexene, 2-methyl-
21.865	4.89	Benzyl nitrile
24.717	2.52	Benzenepropanenitrile

### Py-GC-MS at 500°C



## DATA SHEET: *Porphyridium cruentum*

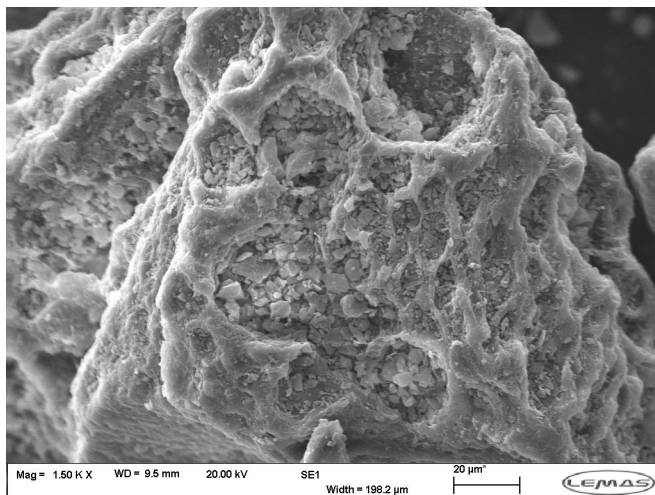
## APPENDIX A

Scientific name	Strain	Source	Growth media
<i>Porphyridium cruentum</i>	unknown	University of Almeria, Spain	unknown

Proximate Analysis	Gross As Received:
Moisture	5.1 %
Ash	24.4 %
Volatile matter	65.5 %
Fixed carbon	5.5 %
Heat Value (MJ/kg)	14.7

Ultimate Analysis (daf %):	
Carbon	51.3
Oxygen	33.1
Hydrogen	7.6
Nitrogen	8.0
Sulfur	ND

Biochemical (daf %)	
Protein	43
Carbohydrate	40
Lipid	17



SEM at 1500 times magnification

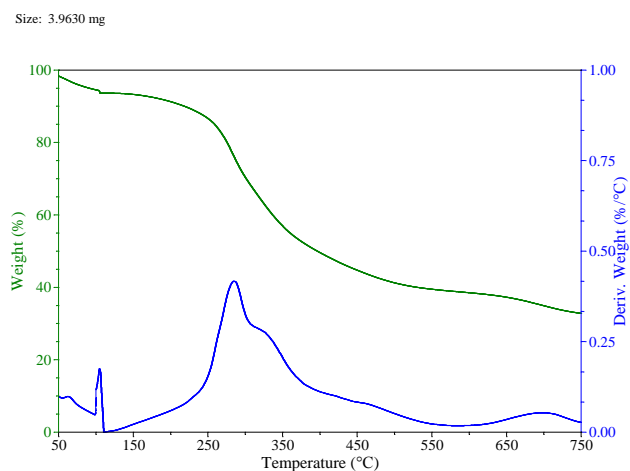
Metal Analysis (a/r ppm)	
Al	0
Ca	39852
Cl	25348
Cu	16
Fe	1815
K	19009
Mg	5085
Mn	116
Na	80400
Ni	2.7
P	8889
Zn	99

Pigment Analysis (a/r ppm)	
Chlorophyllide a	-
Chlorophyll C1/C2	-
Fucoxanthin	57
Violaxanthin	-
Astaxanthin	-
Lutein	-
Zeaxanthin	963
Antheraxanthin	-
Chlorophyll b1	252
Chlorophyll b2	66
Chlorophyll a	196
$\alpha$ -carotene	-
$\beta$ -carotene	-

**DATA SHEET: *Porphyridium cruentum***

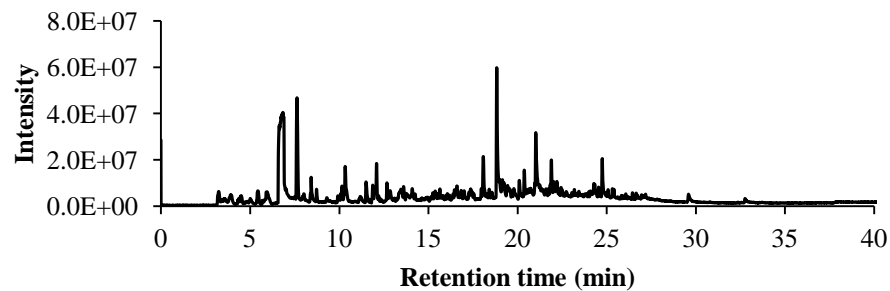
**APPENDIX A**

**TGA/DTG plot in N<sub>2</sub>**



Py-GC-MS Analysis		
Retention time	Area %	Compound
7.635	27.81	Toluene
10.335	4.2	Pyrrole
11.967	3.24	2-Cyclopenten-1-one
12.094	5.46	Tetracontane, 3,5,24-trimethyl-
18.078	7.01	1,2-Cyclopentanedione, 3-methyl-
18.832	25.89	Phenol
20.377	3.98	2-Cyclopenten-1-one, 3-ethyl-2-hydroxy-
21.021	11.57	Phenol, 4-methyl-
21.896	4.55	Benzyl nitrile
24.75	6.29	Benzenepropanenitrile

**Py-GC-MS at 500°C**



## DATA SHEET: *Scenedesmus dimorphus*

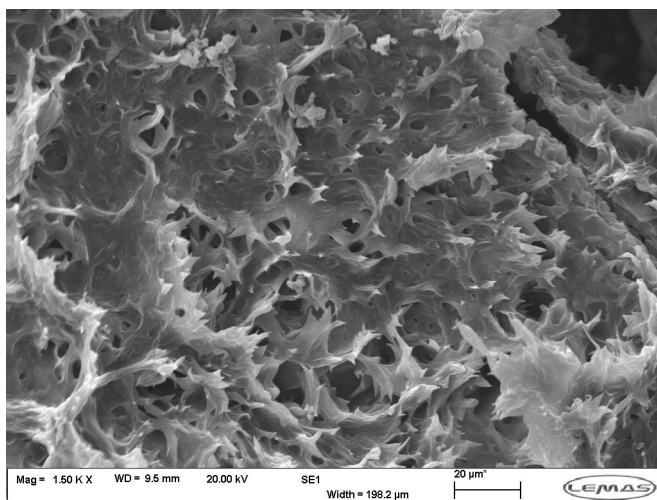
## APPENDIX A

Scientific name	Strain	Source	Growth media
<i>Scenedesmus dimorphus</i>	276/48	CCAP	3N-BBM+V

Proximate Analysis	Gross As Received:
Moisture	1.6 %
Ash	11.8 %
Volatile matter	79.1 %
Fixed carbon	4.1 %
Heat Value (MJ/kg)	18.3

Ultimate Analysis (daf %):	
Carbon	53.4
Oxygen	31.0
Hydrogen	7.8
Nitrogen	7.9
Sulfur	ND

Biochemical (daf %)	
Protein	43
Carbohydrate	16
Lipid	18



SEM at 1500 times magnification

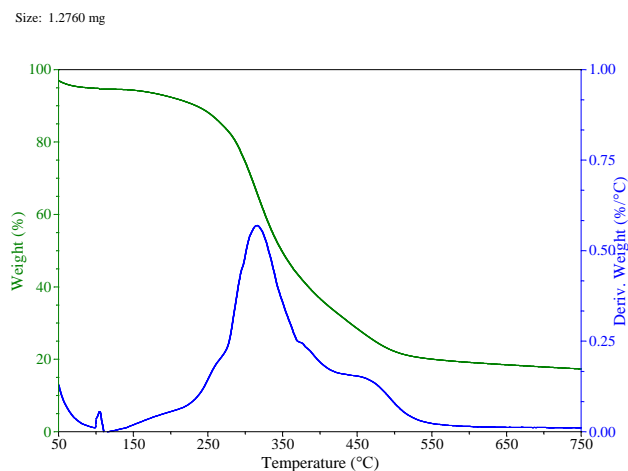
Metal Analysis (a/r ppm)	
Al	200
Ca	151241
Cl	3893
Cu	35
Fe	505
K	8358
Mg	15215
Mn	425
Na	1492
Ni	2.9
P	
Zn	197

Pigment Analysis (a/r ppm)	
Chlorophyllide a	0
Chlorophyll C1/C2	-
Fucoxanthin	411
Violaxanthin	0
Astaxanthin	-
Lutein	2257
Zeaxanthin	-
Antheraxanthin	0
Chlorophyll b1	7452
Chlorophyll b2	601
Chlorophyll a	2070
$\alpha$ -carotene	0
$\beta$ -carotene	648

## DATA SHEET: *Scenedesmus dimorphus*

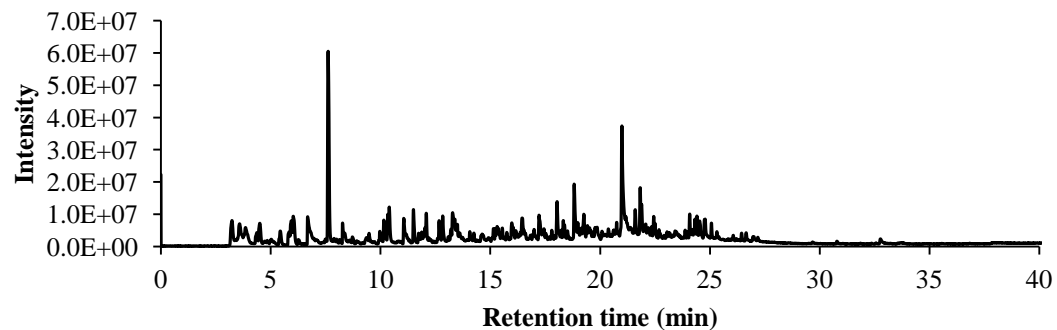
## APPENDIX A

### TGA/DTG plot in N<sub>2</sub>



Py-GC-MS Analysis		
Retention time	Area %	Compound
7.615	40.99	Toluene
10.142	3.79	ND
10.325	3.86	Pyrrole
10.399	4.77	Benzene, 1,3-dimethyl-
18.042	5.25	1,2-Cyclopentanedione, 3-methyl-
18.82	9.41	Phosphonic acid, (p-hydroxyphenyl)-
20.991	20.64	Phenol, 4-methyl-
21.826	5.11	Cyclohexanecarbonitrile, 1-hydroxy-
21.9	3.68	Benzyl nitrile
24.08	2.5	Naphthalene, 1,2-dihydro-1,1,6-trimethyl-

### Py-GC-MS at 500°C



## DATA SHEET: *Spirulina sp.*

## APPENDIX A

Scientific name	Strain	Source	Growth media
<i>Spirulina sp.</i>	unknown	Naturally Green Ltd, UK	unknown

Proximate Analysis	Gross As Received:
Moisture	7.8 %
Ash	7.6 %
Volatile matter	73.7 %
Fixed carbon	12.4 %
Heat Value (MJ/kg)	21.2

Ultimate Analysis (daf %):	
Carbon	55.7
Oxygen	26.4
Hydrogen	6.8
Nitrogen	11.2
Sulfur	0.8

Biochemical (daf %)	
Protein	65
Carbohydrate	20
Lipid	5

Metal Analysis (a/r ppm)	
Al	11
Ca	1015
Cl	3239
Cu	2
Fe	563
K	14994
Mg	2890
Mn	24
Na	15113
Ni	1
P	7138
Zn	35

Pigment Analysis (a/r ppm)	
Chlorophyllide a	-
Chlorophyll C1/C2	-
Fucoxanthin	-
Violaxanthin	2208
Astaxanthin	-
Lutein	-
Zeaxanthin	3752
Antheraxanthin	0
Chlorophyll b1	-
Chlorophyll b2	-
Chlorophyll a	4125
$\alpha$ -carotene	0
$\beta$ -carotene	5656

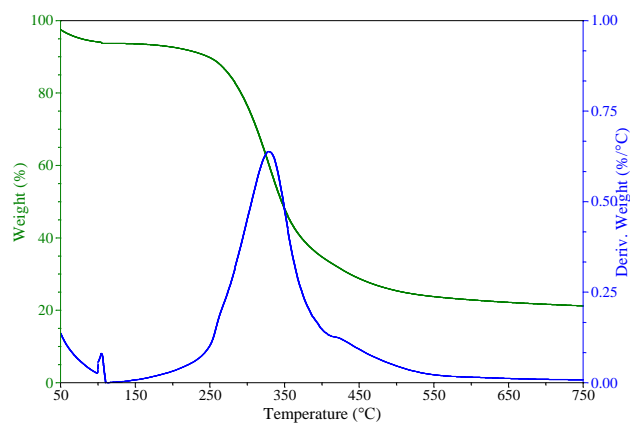
SEM at 1500 times magnification not available

## DATA SHEET: *Spirulina sp.*

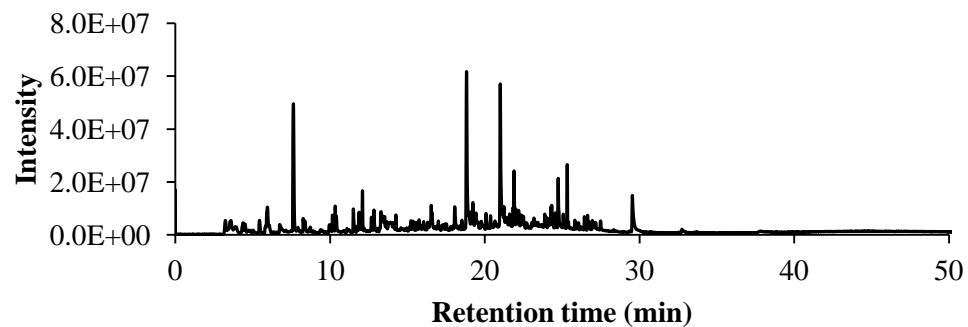
## APPENDIX A

### TGA/DTG plot in N<sub>2</sub>

Size: 2.4810 mg



### Py-GC-MS at 500°C



Py-GC-MS Analysis		
Retention time	Area %	Compound
7.632	24.39	Toluene
11.867	2.48	Propanedinitrile, ethyl(1-oxopropoxy)-
12.094	3.73	Pentanenitrile, 4-methyl-
18.821	25.84	Phosphonic acid, (p-hydroxyphenyl)-
21	20.26	Phenol, 4-methyl-
21.825	2.08	Aziridine, 1-(2-buten-2-yl)-
21.89	6.15	Benzyl nitrile
24.325	2.95	2-Pentene, 2-methyl-
24.742	6.28	Benzenepropanenitrile
25.328	5.84	Pentadecane



## DATA SHEET: *Spirulina sp. OZ*

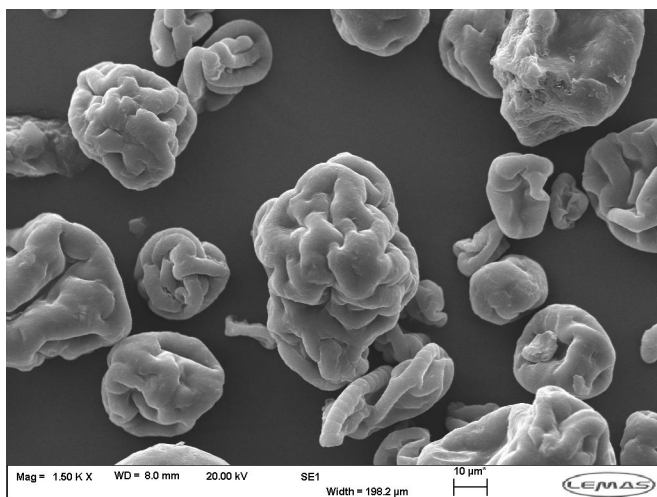
## APPENDIX A

Scientific name	Strain	Source	Growth media
<i>Spirulina sp. OZ</i>	unknown	Synergy Natural, Australia	unknown

Proximate Analysis	Gross As Received:
Moisture	5.7 %
Ash	7.6 %
Volatile matter	71.9 %
Fixed carbon	14.2 %
Heat Value (MJ/kg)	21.2

Ultimate Analysis (daf %):	
Carbon	53.7
Oxygen	25.9
Hydrogen	7.7
Nitrogen	12.1
Sulfur	0.6

Biochemical (daf %)	
Protein	65-70
Carbohydrate	11
Lipid	8



SEM at 1500 times magnification

Metal Analysis (a/r ppm)	
Al	402
Ca	7782
Cl	4433
Cu	8
Fe	879
K	13899
Mg	4256
Mn	56
Na	4732
Ni	2.6
P	8817
Zn	27

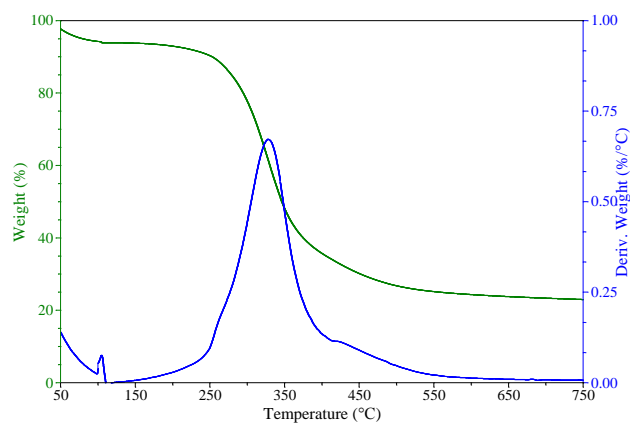
Pigment Analysis (a/r ppm)	
Chlorophyllide a	-
Chlorophyll C1/C2	-
Fucoxanthin	-
Violaxanthin	2691
Astaxanthin	-
Lutein	-
Zeaxanthin	4139
Antheraxanthin	-
Chlorophyll b1	-
Chlorophyll b2	-
Chlorophyll a	5042
$\alpha$ -carotene	-
$\beta$ -carotene	5920

## DATA SHEET: *Spirulina sp. OZ*

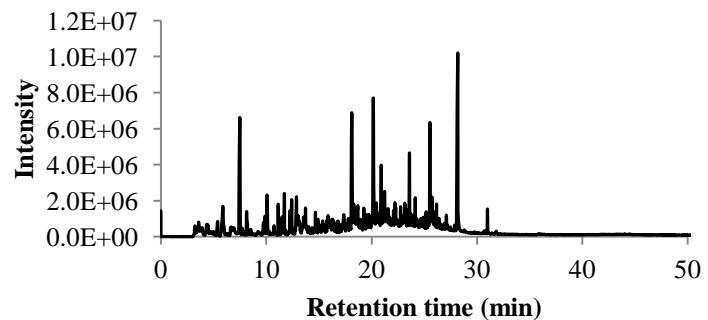
## APPENDIX A

### TGA/DTG plot in N<sub>2</sub>

Size: 2.7600 mg



### Py-GC-MS at 500°C



Py-GC-MS Analysis		
Retention time	Area %	Compound
7.49	17.78	Toluene
10.076	4.41	3-(2-Propenyl)cyclopentene
11.723	2.63	Pentanenitrile, 4-methyl-
12.411	2.89	1H-Pyrrole, 3-methyl-
18.119	17.51	Phenol
20.164	15.65	Phenol, 4-methyl-
20.916	4.07	Benzyl nitrile
23.597	4.44	Benzenepropanenitrile
25.538	7.53	Indole
28.18	23.09	Heptadecane

## DATA SHEET: *Tetraselmis chui*

## APPENDIX A

Scientific name	Strain	Source	Growth media
<i>Tetraselmis chui</i>	8/6	CCAP	f/2

Proximate Analysis	Gross As Received:
Moisture	8.93 %
Ash	29.51 %
Volatile matter	61.75 %
Fixed carbon	13.42 %
Heat Value (MJ/kg)	NA

Ultimate Analysis (daf %):	
Carbon	NA
Oxygen	NA
Hydrogen	NA
Nitrogen	NA
Sulfur	NA

Biochemical (daf %)	
Protein	NA
Carbohydrate	NA
Lipid	NA

SEM at 1500 times magnification not available

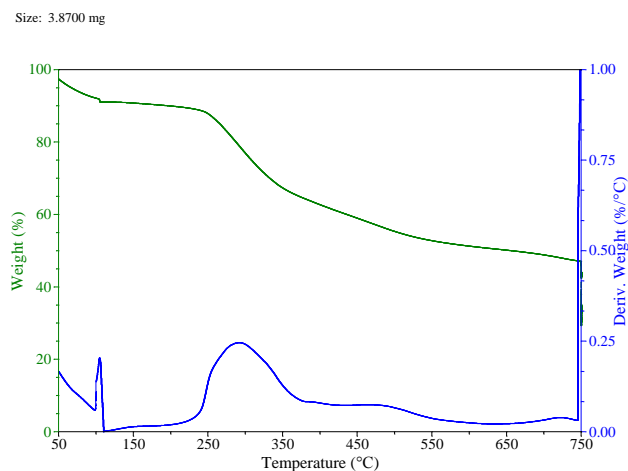
Metal Analysis (a/r ppm)	
Al	NA
Ca	NA
Cl	NA
Cu	NA
Fe	NA
K	NA
Mg	NA
Mn	NA
Na	NA
Ni	NA
P	NA
Zn	NA

Pigment Analysis (a/r ppm)	
Chlorophyllide a	203
Chlorophyll C1/C2	-
Fucoxanthin	-
Violaxanthin	462
Astaxanthin	-
Lutein	2015
Zeaxanthin	-
Antheraxanthin	-
Chlorophyll b1	2129
Chlorophyll b2	489
Chlorophyll a	555
$\alpha$ -carotene	-
$\beta$ -carotene	496

## DATA SHEET: *Tetraselmis chui*

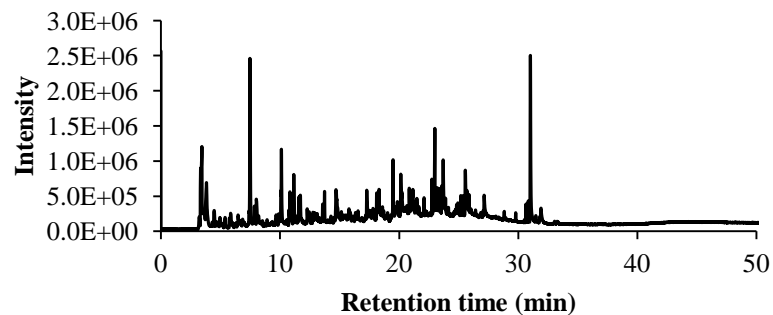
## APPENDIX A

### TGA/DTG plot in N<sub>2</sub>



Py-GC-MS Analysis		
Retention time	Area %	Compound
3.439	18.64	Methylamine, N,N-dimethyl-
7.477	20.21	Toluene
10.118	7.12	Benzene, 1,3-dimethyl-
11.159	4.84	Styrene
18.117	4.37	Phenol
19.491	4.92	ND
23	9.01	1-Hexanol, 4-methyl-, (S)-
23.702	7.26	Pentanamide, 2-(dimethylamino)
25.561	4.53	Indole
31.026	19.1	3,7,11,15-Tetramethyl-2-hexadecen-1-ol

### Py-GC-MS at 500°C



## DATA SHEET: *Zenmyo*

## APPENDIX A

Scientific name	Strain	Source	Growth media
<i>unknown</i>	unknown	DENSO Corporation, Japan	unknown

Proximate Analysis	Gross As Received:
Moisture	4.0 %
Ash	8.8 %
Volatile matter	81.8 %
Fixed carbon	4.4 %
Heat Value (MJ/kg)	19.7

Ultimate Analysis (daf %):	
Carbon	56.7
Oxygen	30.9
Hydrogen	8.7
Nitrogen	3.3
Sulfur	0.3

Biochemical (daf %)	
Protein	16
Carbohydrate	NA
Lipid	18

SEM at 1500 times magnification not available

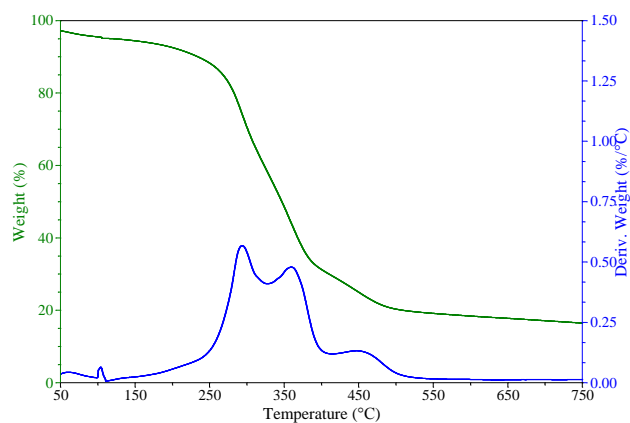
Metal Analysis (a/r ppm)	
Al	25880
Ca	1816
Cl	1144
Cu	31
Fe	1996
K	10937
Mg	1949
Mn	45
Na	6763
Ni	6.3
P	6559
Zn	437

Pigment Analysis (a/r ppm)	
Chlorophyllide a	NA
Chlorophyll C1/C2	NA
Fucoxanthin	NA
Violaxanthin	NA
Astaxhanthin	NA
Lutein	NA
Zeaxanthin	NA
Antheraxanthin	NA
Chlorophyll b1	NA
Chlorophyll b2	NA
Chlorophyll a	NA
$\alpha$ -carotene	NA
$\beta$ -carotene	NA

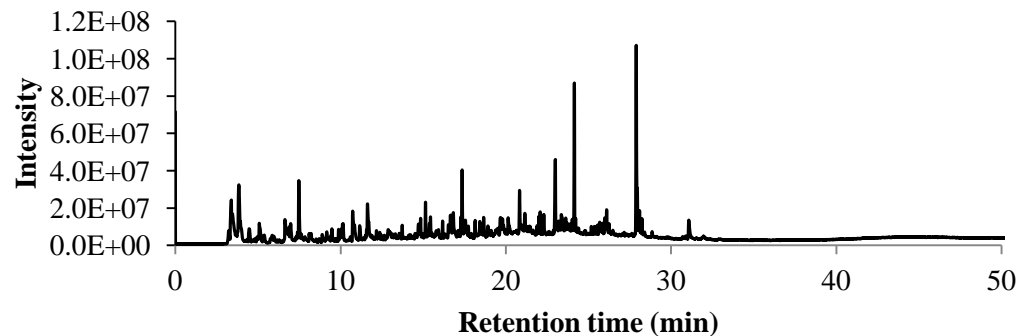
## DATA SHEET: Zenmyo

### TGA/DTG plot in N<sub>2</sub>

Size: 2.6560 mg



### Py-GC-MS at 500°C



## APPENDIX A

Py-GC-MS Analysis		
Retention time	Area %	Compound
3.846	10.9	2-Propenal
7.475	9.42	Toluene
15.141	3.32	3-Undecene, (E)-
17.275	3.79	1,2-Cyclopentanedione, 3-methyl-
17.358	7.92	2- Bromopropionic acid, heptyl ester
20.833	5.08	Levoglucosenone
22.997	10.49	1-Hexanol, 4-methyl-, (S)-
24.149	15.6	Pentadecane
27.893	28.38	3-Heptadecene, (Z)-
27.958	5.1	6,9-Heptadecadiene